Effector delivery and effector characterisation in Dothistroma needle blight of pines

A dissertation presented in partial fulfilment of the

requirements for the degree of

Doctor of Philosophy (Sciences)

in

Genetics/Molecular Plant Pathology

at Massey University, Manawatū, New Zealand

Lukas Hunziker

2018

Abstract

The filamentous fungus *Dothistroma septosporum* causes a serious foliar disease, Dothistroma needle blight (DNB), on *Pinus radiata* in New Zealand and on many pine species worldwide. Potentially correlated to changes in climate, this disease has been on the rise for 20 to 30 years, and current countermeasures often struggle to contain the damage it causes. A molecular approach to combat DNB could be promising. Effectors are small proteins secreted by pathogens to promote host colonisation, and have been a major focus of plant pathologists in recent years. However, effector biology in pathogens of gymnosperms has received little research attention. Here, candidate effectors (CEs) were selected using a series of computational prediction tools, as well as RNAseq data from a compatible *D. septosporum*-–pine interaction. A shortlist of 55 highly *in planta* expressed CEs, predicted to be secreted to the apoplast, was characterised *in silico*. While almost half of them lacked a predicted function, none were exclusive to *D. septosporum*. Seventeen effector candidates of particular interest were taken forward for functional characterisation. Specifically, these proteins were screened for induction of plant defences in the form of cell death in the model plants *Nicotiana benthamiana* and *N. tabacum* using an *Agrobacterium* transient expression assay. Five CEs induced cell death in these plants, suggesting recognition by the plant defence machinery. Of those five, three are similar to previously described proteins. Effector screening methods are not available for pine, thus various approaches to achieve this were trialled. A high-throughput method to collect each protein in the apoplastic wash fluid of *N. benthamiana* was developed. This fluid was applied to *P. radiata* shoots raised from tissue culture to screen for a response, with promising results. Along with an array of *D. septosporum* CEs, these shoots may ultimately be used to screen for resistant pine genotypes. Selection of genotypes at this early stage could speed up DNB resistance screening for pine breeding and the protocol could be transferred to related pathosystems. This research also contributes to the molecular understanding of forest diseases and effectors that may be common among pathogens of distantly related hosts.

Acknowledgements

I extend my utmost gratitude to my supervisor Dr Rosie Bradshaw for the immense support. You know I prefer to use more words than less, but now I am almost out of words. I would not have made the trip to the other side of the globe if I had not had a good feeling about this, and I have not regretted my decision for one second. I usually left our meetings with more confidence than before—because you found the right balance of words. Your dedication to your work is admirable, and I can only hope to keep building the same love for teaching that you have. I greatly value how you maintain attention to detail while not losing sight of the red thread, all amidst this sea of knowledge from your countless projects. I appreciate your patience with the development of my writing style. Further, I have certainly been lucky to have Dr Rebecca McDougal and Dr Carl Mesarich on my team. I am grateful for your guidance, counsel, and sharing of expertise. Hardly any PhD project is 'smooth sailing' throughout—this one was no exception, and I appreciate how all of you helped me get through it, particularly 'calling it' for certain methods and rather discussing new ideas.

I quickly grew fond of the incredibly friendly and helpful staff members of IFS. A special thanks goes out to Dr Dave Wheeler for great virtual machine (Linux) and Python teaching, Dr Pierre-Yves Dupont for advice on phylogenies and some very useful freeware, and of course the IFS admin team—it seems no request was ever too much. I salute my fellow postgrads. This is a magnificent community.

I thank Scion for funding this project and providing plant material, and Cathy Hargreaves and Keiko Gough for the collaboration. In our lab, I cannot thank Melissa and Pranav enough for sharing know-how and discussing issues and findings, but also non-science topics. Simren, it was great to have a 'PhD partner' starting at the same time, I always liked our chats about New Zealand and PhD life. Kutay, I think we helped each other out several times, and I enjoyed our fantasy talks. I will also not forget the generous help of Andre, along with intriguing discussions I had never come across before. Thanks to our latest lab members Silvia and Ellie, you have made these last months more pleasant. I thank all of you for the (sometimes too extensive) coffee breaks and laughs. Lastly I am grateful to our lab manager Carole for always finding and organising materials. I also thank Dr Keehoon Sohn for sharing Golden Gate resources and Jay, Maxim and Toby (all formerly SAE) for explaining the cloning methods.

A doctoral student obviously learns other things than those that make them an expert in a very particular topic. On a more personal level, these four years far away from home may have been the last step to grow up. It has been an in intense journey that I have shared with many people. I thank you all for your friendship, especially Elsa, Mark, Majela, Patry, François, Jason and Sabrina. Gabi and Heather, you above all have made this a second home to me.

I may have failed to express how deeply grateful I am for the ongoing support of my friends and family back home, but this is a start. You are the reason I cannot easily make the decision to keep staying so far away.

With all that said, there has never been the slightest doubt that I dedicate this thesis to my parents. You have my ceaseless gratitude and love.

Acronyms & units

aa	Amino acid
ATTA	*Agrobacterium* transient transformation assay
Avr	Avirulence factor
AWF	Apoplastic wash fluid
bp	Base pair(s)
cDNA	Complementary DNA
CE	Candidate effector
cm	Centimetre
d	Day(s)
dH_2O	Distilled water
DNA	Deoxyribonucleic acid
DNB	Dothistroma needle blight
dNTP	Deoxynucleotide triphosphates
dpi	Day(s) post inoculation
Ecp	Extracellular protein
fmol	femtomol
g	Gram(s)
h	Hour(s)
IP	Invasion pattern
kDa	Kilo-Dalton
kV	Kilovolt
l	Litre(s)
M	Molar (1 M = 1 mol per litre)
μg	Microgram(s)
μl	Microlitre(s)
μM	Micromolar
mg	Milligram(s)
ml	Millilitre(s)
mm	Millimetre(s)
mM	Millimolar
MQ	Milli-Q
ms	Millisecond(s)
min	Minute(s)
ng	Nanogram(s)
n/a	Not applicable
NR	Neutral red
nt	Nucleotides
OD	Optical density
opm	Oscillations per minute
pg	Picogram
PAMP	Pathogen-associated molecular pattern
PCR	Polymerase chain reaction
PRR	Pattern recognition receptor
qPCR	Quantitative PCR
RNA	Ribonucleic acid
RPMK	Reads per million per kilobase
s	Second(s)
SM	Secondary metabolite
v/v	Volume per volume (%)
w/v	Weight per volume (%)

Contents

List of Figures

List of Tables

Chapter 1.

Introduction

1.1. Dothistroma needle blight

Dothistroma needle blight (DNB) is among the most important foliar diseases of pine trees. It affects no less than 109 different host species in 76 countries, and is prevalent across a wide climatic range and elevation level (Fig. 1.1; Drenkhan *et al.*, 2016; Watt *et al.*, 2009). DNB is caused by the filamentous Dothideomycete fungi *Dothistroma septosporum* and *D. pini* (Barnes *et al.*, 2004). These fungi colonise and later kill the needles, causing premature defoliation and reduced growth rates, and in ideal disease conditions (and successive years of infection), death of trees and entire stands (Gibson, 1972).

D. septosporum accounts for the majority of DNB, particularly in North America and across the Southern Hemisphere, where it has caused devastation in plantations of *Pinus radiata* (Bulman *et al.*, 2016). Serious disease outbreaks were limited to these regions until about 20 years ago, when the occurrence and intensity of DNB notably increased (Bradshaw, 2004). Anthropogenic factors, including changes in climate conducive to the dispersal of the fungus, have been implicated (Welsh *et al.*, 2014; Woods *et al.*, 2016). Stronger and more continuous rainfall favours all crucial steps of DNB, including spore dispersal by water splash (Woods *et al.*, 2016). Along with prolonged periods of temperatures enabling maximal disease development, these factors are predicted to develop towards a situation with more DNB in the Northern Hemisphere (Woods *et al.*, 2016).

In New Zealand, forestry is a major industry, with ˜1.7 million hectares of planted forest area (NZ Forest Owners Association, Facts and Figures 2016/2017), directly and

indirectly contributing NZD 3.55 billion to the GDP (˜1.5%). *P. radiata* accounts for 90% of plantation trees. Losses due to DNB of *P. radiata* were estimated at NZD 20 million per year during the 2000s (Watt *et al.*, 2011).

1.1.1. Symptoms

Symptoms of DNB initially appear as yellowish to pale brown spots or bands on needles (Bulman *et al.*, 2013). Within weeks of infection, the 1-3 mm bands turn characteristically red and may remain on the needles (Fig. 1.1) until after the needles die and are cast, founding the common disease name red band needle blight (Bradshaw, 2004). The red colour results from the production of a mycotoxin called dothistromin (Shain & Franich, 1981), which is briefly discussed below. The band colour and frequency can vary, depending on the host species (Barnes *et al.*, 2008). Further symptoms are yellow to brown necrotic tissue alongside the red bands (Bradshaw, 2004; Bulman *et al.*, 2013), flanked by dark green, highly lignified tissue (Franich *et al.*, 1986), and black conidiomata (fruiting bodies) within the red band.

The part of the needle distal to the disease lesion dies, while the remaining tissue turns necrotic and will eventually be cast prematurely; although, in contrast to other needle diseases, dead needles remain on the tree for some time (Bulman *et al.*, 2013). Symptoms typically appear at the base of the crown first and then proceed towards the top of the tree. Until extensive needle loss devastates the crown, it may resemble a lion's tail—as in many other defoliating diseases of pine (Bulman *et al.*, 2013).

1.1.2. Causal species

The causal agents of DNB, the Ascomycetes *D. septosporum* (Dorogin) M. Morelet and *D. pini* Hulbary (Barnes *et al.*, 2004; Fig. 1.2), are very hard to distinguish morphologically (Barnes *et al.*, 2004; Bulman *et al.*, 2013). The taxonomic history was "beset with confusion" up to the publication of the phylogenetic study by Barnes *et al.*, 2004. By sequencing DNA and comparing four specific gene regions, the authors showed that there are two distinct phylogenetic lineages. They redefined them as *D. septosporum*, appearing virtually worldwide, and *D. pini*, so far limited to North Central USA, but also

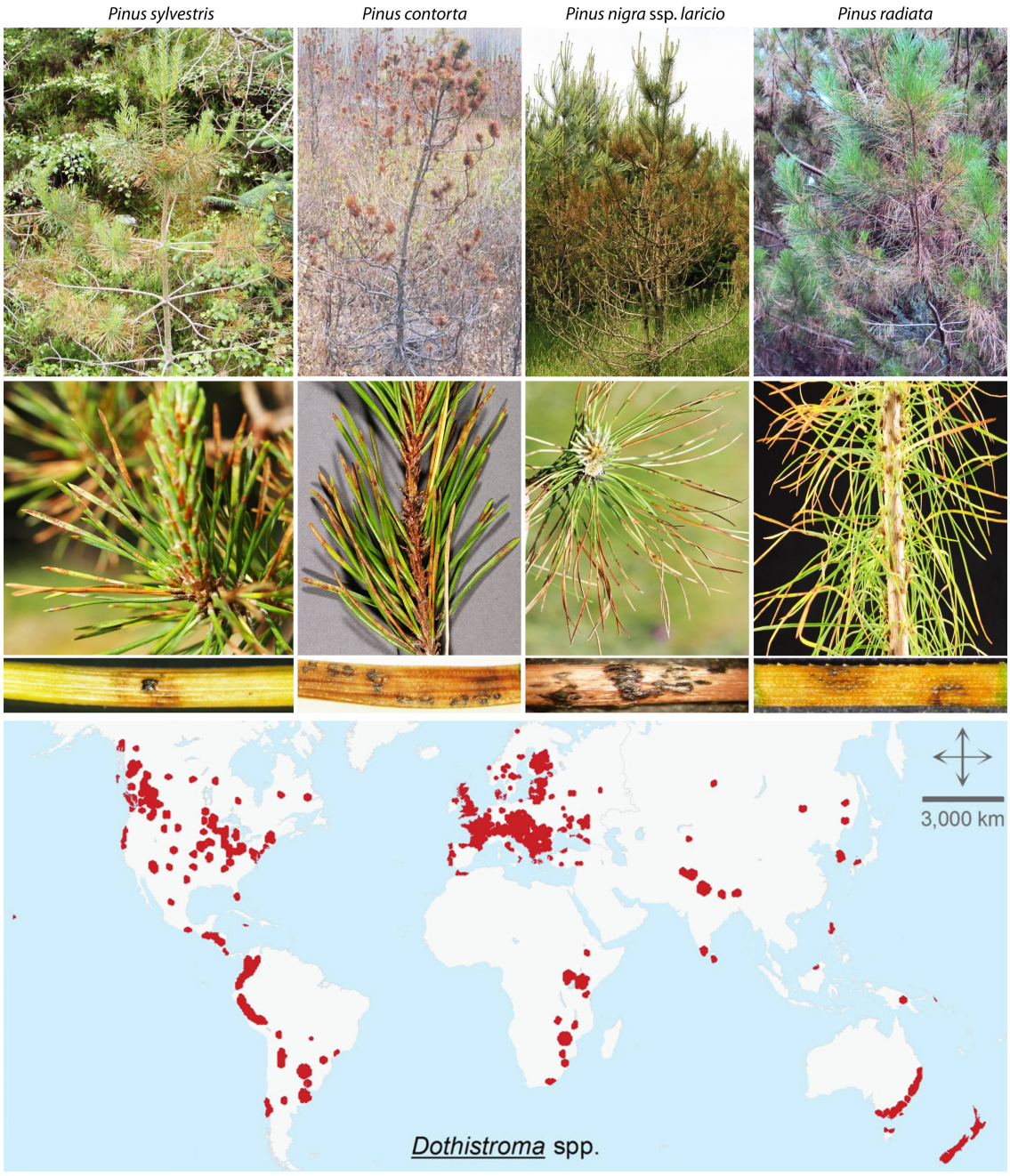

Figure 1.1.: Dothistroma needle blight (DNB) overview. The top panels show different hosts with the disease at an advanced stage with increasing magnification, up to a close-up of needles with characteristic symptoms (reproduced from Fraser *et al.*, 2015 with permission). The map indicates occurrences of DNB (reproduced from Drenkhan *et al.*, 2016 with permission). Presence of *Dothistroma septosporum* or *D. pini* has not been confirmed in all locations. *D. septosporum* is present in north-west North America, throughout Europe, many of the Southern Hemisphere regions and Bhutan and far Eastern Asia; *D. pini* is present in Western, Central and Eastern Europe and Central North America (Drenkhan *et al.*, 2016).

increasingly identified in parts of Eurasia (Barnes *et al.*, 2008; Piou & Ioos, 2013). Very recently, it was discovered that some *Dothistroma* strains currently inhabiting Guatemala are a separate species (Dr Irene Barnes, not published). The sexual stage (teleomorph) of *Dothistroma* was found predominantly in the Northern Hemisphere and Central America, however, sexual names are obsolete following the "one fungus, one name" rule (Drenkhan *et al.*, 2016).

Dothistroma spp. are heterothallic, i.e., individuals carry one of two mating type genes (Groenewald *et al.*, 2007). Presence of both types in a region enables recombination and thus emergence of more virulent and adapted strains (McDonald & Linde, 2002). Interestingly, the teleomorph of *D. septosporum* has not been observed in South Africa and the United Kingdom despite the presence of both mating types and concerted efforts to find it (Groenewald *et al.*, 2007). Further, the major DNB outbreaks in Southern Hemisphere plantations were most likely exclusively caused by *D. septosporum* with one mating type, reproducing asexually. This is consistent with the assumption that the pathogen was introduced in these regions (Groenewald *et al.*, 2007). The main fungal isolate investigated here represents the clonal population of New Zealand (Hirst *et al.*, 1999; Barnes *et al.*, 2014).

1.1.3. Origins, spatial and temporal distribution

It is disputed where *D. septosporum* has its origins and how it has migrated around the world. The pathogen was confirmed in the Himalaya region on a native pine (Barnes *et al.*, 2008), establishing this region as one probable origin; it could be indigenous in north-west North America where it also appears on native hosts, likewise as in high-altitude cloud forests in Central America (Evans, 1984). Within a certain group of examined strains, a Guatemalan isolate was also proposed to be ancestral (Bradshaw *et al.*, 2013). In their most recent population genetics study, Barnes *et al.* (2014) suggest that *D. septosporum* strains have been exchanged between Europe and North America as well as Asia (Bhutan), while the species was introduced into South America and Central Africa and more recently into South Africa, Australia and New Zealand. Additional studies are ongoing, including molecular markers for *D. pini*, and certainly a global population study would

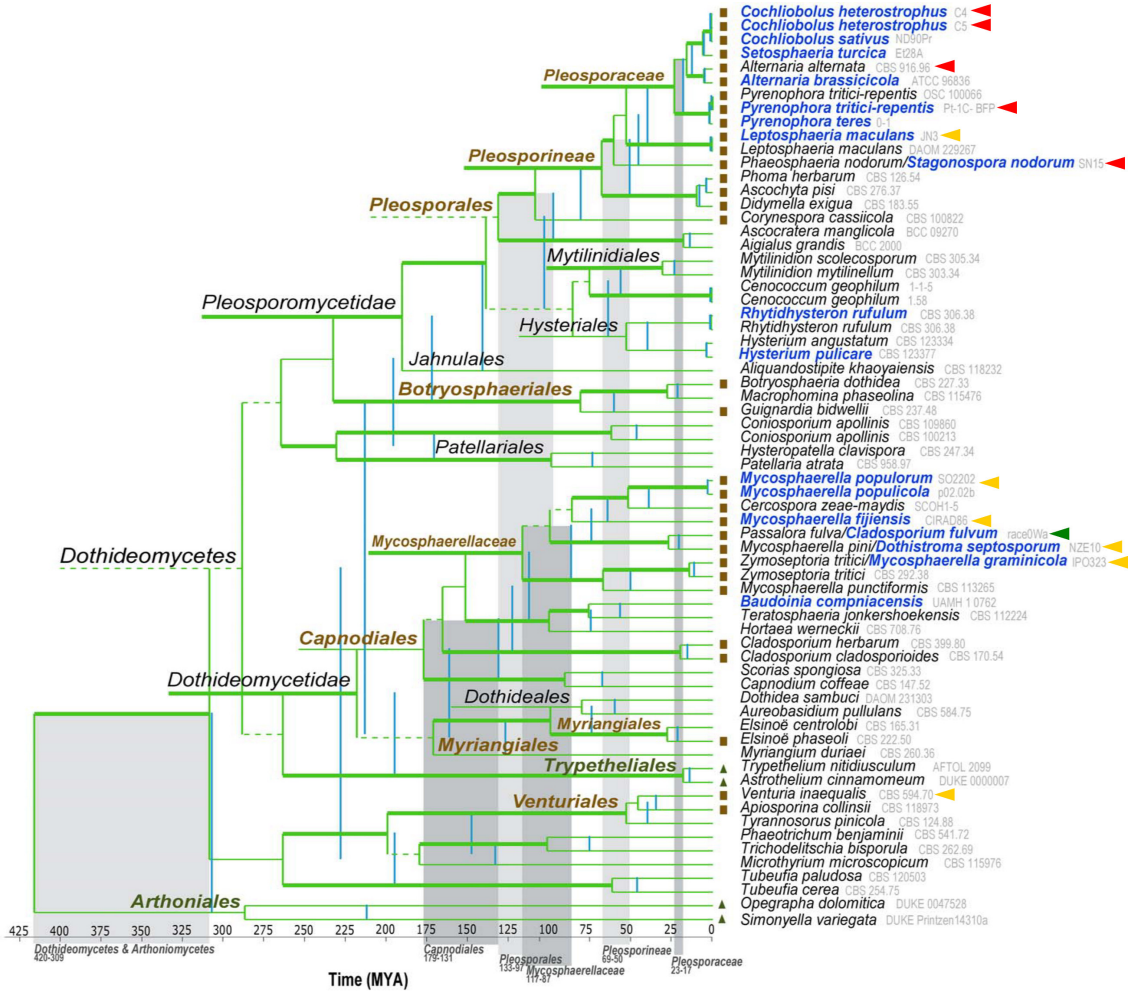

Figure 1.2.: Phylogeny of Dothideomycetes with estimated divergence times based on sequences of three genes (Ohm *et al.*, 2012). The 18 species with a genome sequenced in that study are highlighted in dark blue. Vertical lines in blue and green indicate minimum and maximum ages for specific nodes, respectively. The age ranges for highlighted taxa are indicated by blocks with different shades of gray. Horizontal green lines indicate bootstrap recovery for specific nodes—thickened branches represent more than 70%, normal branches 50–70%, and dashed lines less than 50%. In some cases relevant horizontal lines were stylistically extended to highlight node labels. Only families with multiple genomes are indicated. Orders, suborders and families that contain important plant–pathogenic species are coloured brown and those containing mostly lichenised species are green. Brown squares indicate plant pathogens and green triangles indicate lichenised species. Saprotrophs and fungi with other nutritional modes are not labelled. Figure and legend adapted from Ohm *et al.* (2012). Arrows on the right were added to indicate pathogens of interest in the context of similarities, or differences, to *Dothistroma septosporum* (red, necrotrophic lifestyle, yellow, hemibiotrophic, green, biotrophic).

help elucidate the likely origin of *Dothistroma* (Drenkhan *et al.*, 2016).

The intercontinental migration of *D. septosporum* happened as a consequence of anthropogenic movement of pines, their seeds or fungal spores (Barnes *et al.*, 2014). Shorter distances, such as Estonia to Finland and spreading across East Africa, were likely covered by wind-borne ascospores, and even the Tasman Sea (at least 2000 km) may have been crossed by spores in moist air currents (Bulman *et al.*, 2016).

DNB first received attention when it caused massive damage to exotic pine plantations in the Southern Hemisphere in the 1960s, such as in Kenya, Chile and New Zealand (Watt *et al.*, 2009). In Western Canada, outbreaks have been common in recent years, while records of the blight go back to the 1830s (Welsh *et al.*, 2009). More dramatic epidemics of DNB, at least in Canada and the United Kingdom, are probably due to climate changes, with increased minimum temperatures and more rainfall in spring and summer favouring the disease (Welsh *et al.*, 2014; Brown & Webber, 2008). The increasing threat of DNB to conifer forests is reflected by the Pan-European DIAROD COST action, aiming to address disease management with combined efforts from all participating countries, notably also including South Africa and New Zealand (http://www.forestry.gov.uk/fr/diarod). Awareness of the disease was increased and it is not clear if recent DNB recordings in Eastern and Northern Europe are due to more rigorous inspection, including molecular identification, or actual recent spread which could be promoted by climatic conditions. It is established that DNB can be found virtually everywhere in the presence of a susceptible host (Bulman *et al.*, 2016).

Woods *et al.* (2016) noted that the long and global record history of DNB, even though records are not standardised, make it well-suited for correlations to changing climate. The El Niño-Southern Oscillation is a major global climate variability driver. The authors found that DNB outbreaks could be linked to strong El Niño events over the last 60 years, as these caused temperature increases and rainfall patterns conducive to *D. septosporum* spore dispersal, earlier pre-sporulation, spore release, conidia germination, and the infection process in the respective regions. Together, this culminated in both increased disease incidence and severity (Woods *et al.*, 2016). Whether this particular correlation holds true may be seen in future events. At the same time, there is little doubt that war-

ming climate promotes both the spread and impact of many fungal pathogens globally, and drastic measures may have to be taken to counter them (Bebber *et al.*, 2013; Fisher *et al.*, 2016).

1.1.4. Infection biology

Dothistroma spp. use conidiospores for local dispersal via rain splash (Ivory, 1967). Long-distance dispersal is suggested to occur via several means, particularly when ascospores are involved: clouds, fog or mist, and anthropogenic sources, i.e., transport of infected seedlings. Conidiospores produce germ tubes which grow over the needle surface until they reach stomatal pores, where they enter the host tissue (Kabir *et al.*, 2015). It is ambiguous whether stomata attract germ tubes, at least in part because this might be host-dependent and observations from the field and laboratory did not give the same result (Peterson *et al.*, 1978; Muir & Cobb, 2005).

The plant has preformed physical defences that hinder penetration. Stomatal wax occlusions could be linked to increased resistance in some hosts including *P. radiata* (Fraser *et al.*, 2015). Also, the wettability of needles could play an important, overlooked role regarding the infection. Wettability is affected by epicuticular waxes as well as surface morphology, and is required by *D. septosporum* to adhere to a needle and to have a sufficiently moist environment to develop an infection (Fraser *et al.*, 2015). Investigating molecules such as fungal adhesins, which might support the pathogen in this pre-penetration phase, would be an interesting area of study.

On average, *D. septosporum* hyphae grow on the needle surface for ten days and might produce secondary conidia (Bulman *et al.*, 2013) before entering plant tissue via stomata (Fig. 1.3). Hyphae could also directly penetrate the epidermis, however, this was only observed in one *P. radiata* study (Gadgil, 1967). Hyphae proceed to grow in the mesophyll (apoplastic) space (Gadgil, 1967). The endodermis and transfusion and vascular tissues can also be colonised (Peterson *et al.*, 1978). In a light and electron microscopy-based study on *P. radiata* seedlings inoculated with *D. septosporum* spores, Kabir *et al.* (2015) reported that the epiphytic phase lasted two weeks or longer, with apoplast colonisation only starting three to five weeks after inoculation. Based mainly on these observations,

the authors also suggested that *D. septosporum* has a biotrophic-like intercellular growth phase enabling asymptomatic proliferation before killing tissue and feeding on it. Some pathogens form haustoria or similar structures for nutrient acquisition and virulence factor delivery during biotrophic growth. However, while intracellular hyphae were observed (Peterson *et al.*, 1978), there is no evidence for the production of such structures by *D. septosporum* (also see section 1.2.4). At the time of early lesions on the needle, dothistromin biosynthesis genes were strongly upregulated, which was followed by massive dothistromin accumulation, mesophyll collapse, and fungal biomass increase up to the sporulation stage (Kabir *et al.*, 2015). Endodermal cells have been reported to collapse without hyphae reaching them, supporting the concept that host cell death occurs in advance to branched mycelial growth and massive colonisation might be limited to necrotic tissue (Gadgil, 1967; Kabir *et al.*, 2015).

Approximately four to ten weeks after needle penetration (6-12 weeks after inoculation), mature sporulating lesions appear in the centre of the red band on the needle, signifying the late infection stage of DNB (Kabir *et al.*, 2015). Brown-black conidiomata of 300-600 μm that developed beneath the epidermis now erupt through this layer and release masses of conidiospores (Bradshaw, 2004; Kabir *et al.*, 2015). When dispersed via rain splash, conidiospores on fresh or detached needles suspended in the tree serve as new inoculum, but generally not from needles on the forest floor, as they are degraded by saprophytes (Gadgil, 1970). Conidiospores produced on attached needles infected during the previous year may be released starting from early spring. Conidiospore production can continue for up to seven months of the year and there can be multiple reinfection waves in one season (Bradshaw, 2004). The life cycle depends on external conditions in favour of physiological optima, i.e., temperature and humidity, as well as further dispersal by water droplets. Most infections occur in a period from late spring to late summer (Bradshaw, 2004).

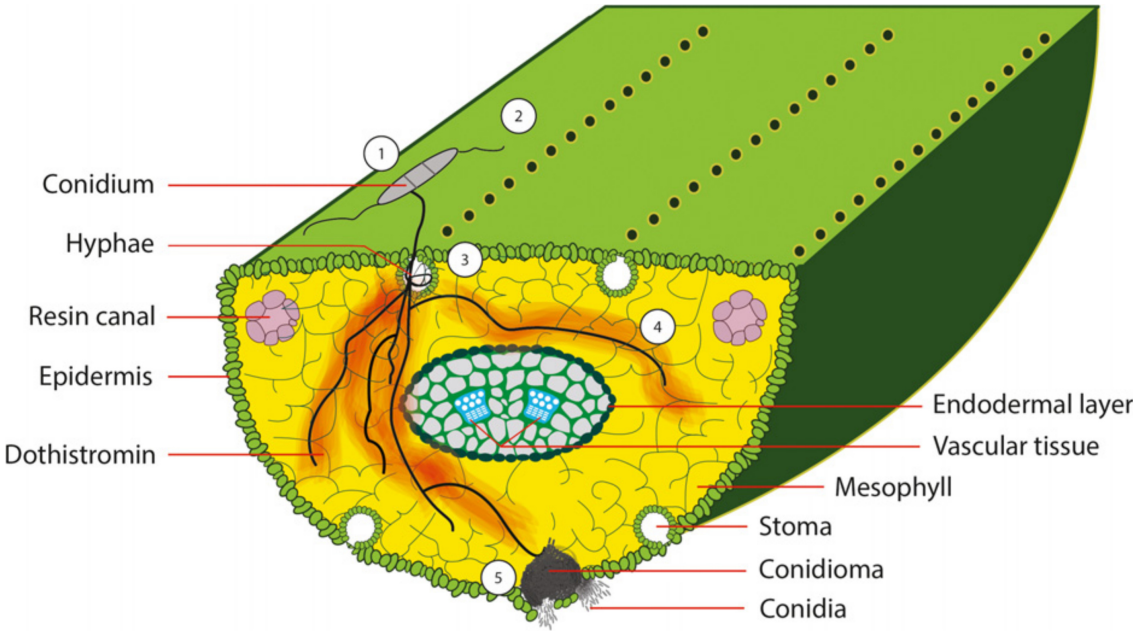

Figure 1.3.: Infection and disease development of *Dothistroma* on susceptible *Pinaceae* species. 1, Conidium germinates on the needle surface; 2, hyphae grow across the needle surface and into stomata; 3, a hypha colonises an epistomatal chamber; 4, intercellular hypha branches out to colonise the mesophyll (=apoplast), producing dothistromin in increasing quantities; 5, conidioma forms and new conidiospores are produced. Structures not to scale. Figure reproduced from Fraser *et al.* (2015) with permission.

1.1.5. *D. septosporum* secondary metabolites are potential virulence factors

In the necrotrophic stage of *P. radiata* infection, *D. septosporum* produces high levels of the non-specific toxin dothistromin, which accumulates in needles (Kabir *et al.*, 2015) and generates oxygen radicals by reductive oxygen activation (Youngman & Elstner, 1984). Thereby it is also toxic to other fungal inhabitants of pine needles (Schwelm *et al.*, 2009). Dothistromin is a polyketide-derived secondary metabolite (SM) structurally similar to versicolorin B (Chettri *et al.*, 2013), the precursor of the well-known 'food poison' aflatoxin (named after its first discovery in *Aspergillus flavus*). Secondary metabolites are by definition not involved in primary metabolism and thus not essential for growth and development of an organism. At least in fungi, they do have multifarious roles that can affect fitness, and often niche adaptation (Ozturk, 2016).

Dothistromin is a *D. septosporum* virulence factor, as mutant *D. septosporum* strains unable to produce the toxin showed restricted needle colonisation and tissue damage, smaller lesions and drastically reduced conidiospore production (Kabir *et al.*, 2015). Ho-

wever, despite dothistromin deficiency, mutant strains were still able to complete their life cycle on *P. radiata*, hence dothistromin is unlikely to be a pathogenicity factor (Schwelm *et al.*, 2009). Direct injection of dothistromin into *P. radiata* needles can trigger a strong defence response (Franich *et al.*, 1986), which would be detrimental to the pathogen during early colonisation. *Cladosporium fulvum*, a close relative of *D. septosporum* that lacks a necrotrophic phase, shares a complete set of dothistromin biosynthesis genes (de Wit *et al.*, 2012). The regulatory gene *AflR* is not completely functional in *C. fulvum*, and two biosynthesis genes are pseudogenised. This suggests a recent loss of the capacity to produce the destructive toxin as part of the shift to a biotrophic lifestyle (Chettri *et al.*, 2013).

Following the discovery that a *D. septosporum* SM is an important factor for the interaction with the host, Ozturk (2016) investigated other SMs. Of 11 'core' SM genes, three were highly induced during a *P. radiata* infection. Of these, *DsPks1* was highly induced at the late stage of infection, it is predicted to produce melanin, and shown to be under purifying selection. This SM could be important for UV protection. *DsNps3* was induced during the asymptomatic colonisation phase and produces an unknown SM. A Δ*DsNps3* mutant strain produced less total biomass in mature lesions compared to the wild type, so *DsNps3* could be a virulence factor (Ozturk, 2016). These findings promoted the continued search for molecules playing a role in the interaction process, including effectors (subsection 1.2.4).

1.1.6. Management of DNB, and breeding perspectives

Disease management strategies have been in use in countries where DNB impact has been considered large enough to require countermeasures, such as New Zealand. Measures include silvicultural methods, such as thinning and pruning of lower branches (Bulman *et al.*, 2013), and spraying of copper-based fungicides, which is not allowed in all affected countries. Copper sprays are relatively inexpensive, but like other synthetic pesticides can be harmful to the environment (Ivkovic *et al.*, 2010). Strategies were comprehensively reviewed by Bulman *et al.* (2016). In summary, there are several measures capable of reducing disease severity, but they have limitations and there is "no single silver bullet"

to DNB. Much rather, integrated long-term approaches need to be developed specific to each country and possibly types of individual plantation sites, taking into account legislation and public acceptance of measures such as copper spraying, and local soil and climatic conditions, respectively.

For *P. radiata* plantation owners in New Zealand, relying on breeding for resistance is one option. DNB resistance appears to be quantitative (additive), with significant genetic variation found in several studies, and estimates of narrow-sense heritability which suggest that selection on this additive genetic variance can lead to genetic gain (Li *et al.*, 2018). DNB resistance is an important selection trait in breeding of *P. radiata* and this has contributed to reduced yield losses (Ivkovic *et al.*, 2010). Kennedy *et al.* (2014) reported that DNB resistance was favourably correlated with the key trait diameter at breast height and thus selection for growth alone would increase resistance. A recent unpublished study, however, suggests that overall yield gain might be as low as 6-7% with inbreeding constraints (mentioned in Bulman *et al.*, 2016). Exploiting genotype by environment (G×E) interactions for gain is a common strategy for breeding, but Li *et al.* (2018) concluded that data from an extensive study did not support an important G×E interaction level with DNB resistance. For regions prone to DNB outbreaks in particular, trade-offs need to be made, further diminishing the gain of time-consuming and costly resistance breeding (Bulman *et al.*, 2016). This is where the current study could provide a major benefit. As explained in the next section, breaking down a host–pathogen interaction to the interactions of a few intruder and defence proteins, which can be essential to the overall outcome, can lead to the development of molecular markers. Host germplasm can be screened with these markers without the need to wait for an adult phenotype.

1.2. Plant–microbe interactions

Symbiosis—"the living together in more or less intimate association or close union of two dissimilar organisms" (Merriam-Webster)—is often mistaken for a mutually beneficial interaction only, but it also includes commensalism and parasitism. The evolution of parasitism has given rise to myriads of pathogens, from those with the genetic resources

to have a versatile, opportunistic lifestyle, to those completely dependent on hosts to complete their life cycle. Various microbial pathogens are regularly quoted as some of the biggest threats we face at present, including diseases of crops and forests. To understand not just genetics (inheritance), but the molecular details of the crucial factors governing plant symbioses, provides a means of containing these threats.

1.2.1. The plant defence system

Plant individuals do not have the option to escape threats by moving away. On top of the exposure to abiotic factors, they are virtually in constant battle against herbivores, pests and pathogens. Plants are equipped with an elaborate defence system of several layers, enabling them to keep thriving during this battle (Spoel & Dong, 2012). Here an overview of interactions with microbes is given, fungal pathogens in particular.

Firstly, plants possess formidable preformed physical barriers to infection. Their outermost tissue layer, the cuticle, is hard or impossible for non-specialised microbes to penetrate. In many species, this barrier is further supported by epicuticular waxes (subsection 1.2.2). Each plant cell is enclosed by a rigid cell wall, providing structural stability, but also protection against intruders. The extracellular space around plant cells, termed the apoplast, is generally hostile to intruders due to toxic SM. Antimicrobial SM compounds are widely shared among plants. They can be classified as constitutively produced phytoanticipins and invasion-induced phytoalexins, however, which class they fall into may vary from species to species (Dixon, 2001). Antimicrobial metabolites comprise terpenoids, such as the saponins tomatine and avenacin, phenolics and phenylpropanoids, including benzoic acid, and nitrogen- and/or sulfur-containing compounds, featuring indole derivatives (Dixon, 2001). To colonise plant tissue, microbes must thus protect themselves or detoxify this environment. Development of such protection usually constitutes host-specific adaptation.

Secondly, plants have an immune system that is not adaptive, but innate to every cell. There are no dedicated, mobile defence cells involved, as we know and understand well from animals, but a diverse array of conserved receptors on each cell. When such receptors are activated, signal transduction via a network ensues, inducing defence responses.

The responses are of varying makeup and severity, such as cell wall reinforcements and local release of phytoalexins, reactive oxygen species (ROS, Torres *et al.*, 2005), hydrolytic enzymes, or inhibitors of plant-damaging enzymes secreted by pathogens (Giraldo & Valent, 2013; Ökmen & Doehlemann, 2014). The most severe countermeasures are the hypersensitive response (HR), which includes callose deposition and programmed cell death in local tissue (Nimchuk *et al.*, 2003), and systemic acquired resistance (SAR, Ryals *et al.*, 1996) which primes the entire plant against further invasion. Therefore, if a microbe succeeds in overcoming the abovementioned primary barriers, it can be detected and the response at least prevents it from spreading further. The molecular understanding of this interaction is subject of subsection 1.2.3.

1.2.2. *Pinus radiata* defences

This subsection is a summary of the pine defence and resistance mechanisms review by Fraser *et al.* (2015). Evidence points towards pathogen-specific roles of these mechanisms, i.e., not all measures confer or support resistance against all diseases, including DNB.

Top layer *Pinus* spp. defences include rough surface topography reducing wettability (compare subsection 1.1.4), epicuticular waxes and diterpenes, stomata morphology, and wax occlusion of the epistomatal chamber.

Defences coming into play after a pathogen penetrates needles appear to be most important against *D. septosporum* infection. These comprise constitutive barriers, such as lignified tissues, and induced responses (see also subsection 1.2.3), such as production of phytoalexins and pathogenesis-related (PR) proteins, and HR induction. Benzoic acid was proposed to be a phytoalexin in *P. radiata*; however, it is not entirely resolved whether it was released to halt fungal growth or as a result of cell death. Induced fortification of cell walls by lignin and other cell wall-bound phenolics as a response to fungal cell wall components was found in *P. radiata* and several other pine species. Terpenoid compounds found in plant resin, such as pinenes and limonene, likely play a role in the interaction with pathogens. Specific monoterpenes inhibited *in vitro* spore germination and mycelial growth of two *Diplodia* species (Blodgett & Stanosz, 1997). However, in a different study a (volatile) monoterpene mix stimulated *D. septosporum* germination (Franich *et al.*, 1982).

Thus, monoterpenes could be an attractive cue for adapted pathogens. Meanwhile, terpenoids could also be involved in SAR in pines, based on one *P. nigra–Diplodia sapinea* study (Wallis *et al.*, 2008). Finally, functional PR proteins including β-1,3-glucanases and chitinases (β-1,4) were found to be important for defence in a range of conifers and other forest tree species (reviewed by Veluthakkal & Dasgupta, 2010). In a study of *P. radiata* and the necrotrophic pine pitch canker pathogen *Fusarium circinatum*, five of seven tested PR or SM-related proteins were associated with resistance based on their induced expression (Donoso *et al.*, 2015).

In brief, terpenoids, phenolics, and antimicrobial protein classes may well constitute a part of *P. radiata* defences against *D. septosporum*, but specific conclusions for this interaction are not available yet.

1.2.3. Plant immunity: Recognition of non-self

Pathogens as well as mutualistic symbionts give away their presence when they intrude plant tissue. This happens by means of certain molecules diffusing towards host cells through the apoplast, which may be structural elements or small proteins the intruders release. These molecules are termed microbe- or pathogen-associated molecular patterns (MAMPs or PAMPs) because they are broadly conserved, for example, chitin (β-1,4-linked N-acetyl-D-glucosamine) and other glycans from fungal cell walls and bacterial flagellin, but also proteins, various types of lipids, or dsRNA from viruses (reviewed by Boutrot & Zipfel, 2017). MAMP and PAMP are often used interchangeably; however, there are also damage-associated molecular patterns (DAMPs), and it is important to distinguish them. DAMPs stem from the host's own tissue, damaged or modified through the action of the microbe, for example, plant cell wall fragments released upon intrusion, or extracellular ATP. In the apoplast, all these pattern types are detected as 'non-self' and 'modified self' by pattern recognition receptors (PRRs) located at the plant plasma membrane. Notably, DAMPs are the least specific indicator of intrusion and thus broaden the recognition range (Boutrot & Zipfel, 2017). Intruders may secrete small molecules called effectors to disable defences (see subsection 1.2.4), which can also be recognised by PRRs.

Plant PRRs are receptor-like kinases (RLKs) or receptor-like proteins (RLPs), both containing a ligand-binding, often leucine-rich repeat (LRR) domain and a transmembrane (TM) domain. RLKs also have an intracellular kinase domain that initiates signal transduction (Liebrand *et al.*, 2014); eventually, both PRR types can recruit receptor-like cytoplasmic kinases (RLCKs). The ligand-binding domains in all immune receptor types are highly diversified. Figure 1.4 shows an overview of ligands and PRRs that have been intensely studied in model angiosperms, such as *Arabidopsis thaliana* (thale cress), *Solanum* spp. (tomato, potato), *Triticum aestivum* (wheat), and *Nicotiana* spp. (tobacco). The RLK 'somatic embryogenesis receptor kinase 3' (SERK3, also called 'brassino-steroid-associated kinase 1', BAK1), plays a part in developmental processes as well as immunity (Couto & Zipfel, 2016). When an LRR domain binds a ligand, the PRR is 'activated' and undergoes a conformational change, upon which SERK3, related SERKs, or for example 'chitin elicitor receptor kinase 1' (CERK1), associate with it. Another important RLK, 'suppressor of BIR1-1' (SOBIR1), recruits SERKs when a ligand-bound RLP forms a complex with it. Either way, this causes transphosphorylation of an RLCK, which in turn phosphorylates a mitogen-activated protein kinase kinase kinase (MAPKKK) or similar, which passes the signal on to a MAPKK, MAPK, and finally transcription factors of defence-related genes (Couto & Zipfel, 2016). By means of the cascade, the signal can be amplified or fine-tuned.

There are also intracellular immune receptors, called nucleotide-binding (NB) LRR receptors (NLRs). NLRs only come into play at a later stage in certain interactions (see subsection 1.2.4). The ligand-binding domains of NLRs are also highly diverse. A recent review highlighted complex interactions that occur in plant immunity and indicated that a new field of plant immune networks is emerging (Wu *et al.*, 2018). The authors promoted a systems biology view of such complex networks to better understand the implications of plant–microbe coevolution.

The invasion pattern (IP) concept

A step towards such an integrated understanding was proposed earlier: Because MAMPs, DAMPs and effectors are essentially perceived in the same manner, unifying them under

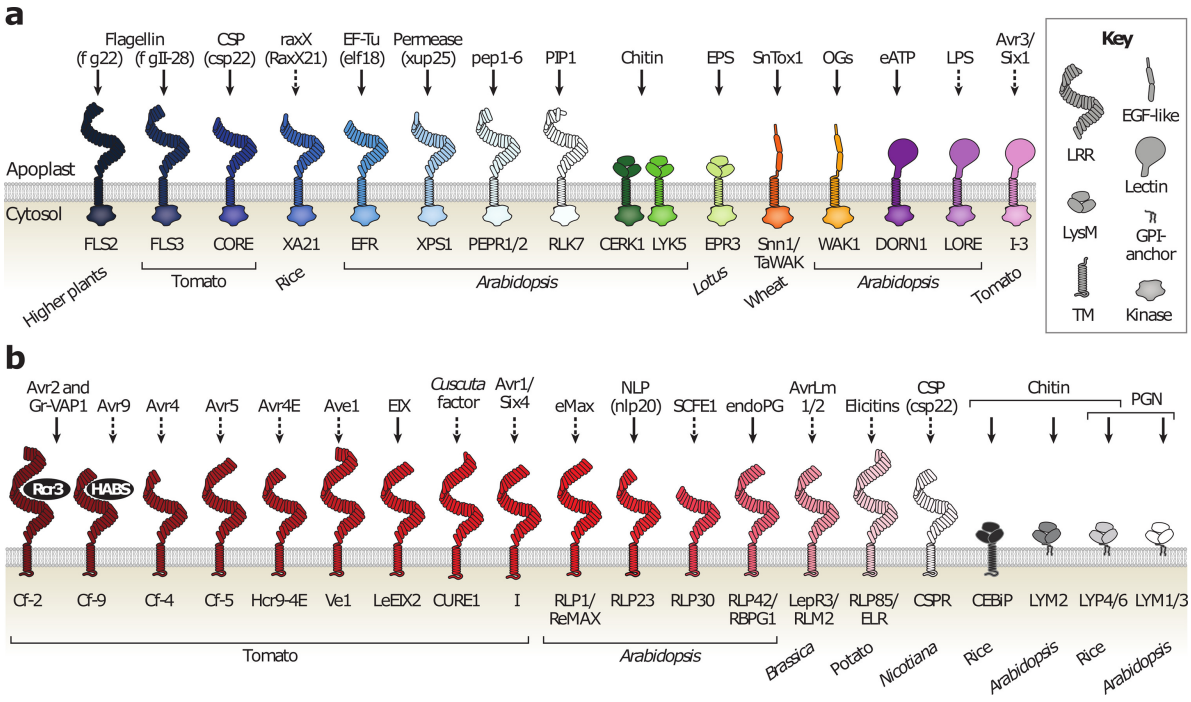

Figure 1.4.: Proven and potential plant pattern recognition receptors (PRRs) with known ligands (Boutrot & Zipfel, 2017). (a) Receptor kinases (RLKs), (b) Receptor-like proteins (RLPs). Ligands, shown at the top of each panel, and PRRs are represented in the text by specific examples. Solid arrows indicate demonstrated direct binding; dashed arrows indicate a current lack of evidence for direct binding. EGF, epidermal growth factor; EIX, ethylene-inducing xylanase; EPS, extracellular polysaccharides; GPI, glycophosphatidylinositol; LPS, lipopolysaccharide; LRR, leucine-rich repat; OGs, oligogalacturonides; PGN, peptidoglycan; TM, transmembrane. Figure reproduced from Boutrot & Zipfel (2017); ©2017 by Annual Reviews.

the term invasion pattern (IP) (Cook *et al.*, 2015) seems sensible. With this perspective, it may be easier to understand overlaps of interactions in a wide range of host–microbe relationships. The primary function of IPs from the view of the pathogen may vary, but the perception of IPs always leads to an immune response. Since the IP model was proposed relatively recently, the original terms are used for referencing here. However, for new findings and discussions in this thesis, IP is the standard term and the more specific categories are only used with respective supporting evidence.

1.2.4. Effectors: The modulators of symbiosis

General

Effectors are small secreted molecules that have evolved to promote host colonisation (Giraldo & Valent, 2013). They are seemingly omnipresent in both pathogenic and non-pathogenic microbes, nematodes, and insects, infecting plants, animals or other microbes

(Lozano-Torres *et al.*, 2012; Plett *et al.*, 2014; Guiguet *et al.*, 2016; Cen *et al.*, 2017). Effectors can detoxify the extracellular space (Ökmen & Doehlemann, 2014), or prevent the detection of MAMPs in various direct and indirect ways (de Jonge *et al.*, 2011). The vast majority of effectors are proteins, but some are small RNAs or SMs (Wang *et al.*, 2015; Weiberg *et al.*, 2015; Wang *et al.*, 2017a).

Effectors are diverse and often unique to species. In a few cases, however, effectors across kingdoms as diverse as fungi, chromista (oomycetes) and bacteria share conserved domains or even high overall sequence similarity and thus have common functions. With growing knowledge about effectors, it becomes increasingly apparent that certain targets in plant hosts are far less diverse than the effectors themselves. Plants encode hundreds of receptors as part of their defence arsenal; however, they are generally linked to the same type of downstream MAPK signalling pathways that lead to defence responses (see subsection 1.2.3). A number of host proteins involved in defence appear to be the shared targets ('hubs') for many pathogens (Ökmen & Doehlemann, 2014; Mukhtar *et al.*, 2011). Host proteases, for example, are targeted by at least one apoplastic effector from four distantly-related species; another well-documented target hub is the salicylic acid (SA) pathway (Lo Presti *et al.*, 2015).

Considering that plants relied on interactions with microbes as soon as they came onto land (Plett & Martin, 2018), it is likely that coevolution supporting mutualistic symbiosis dates back at least as far as that period. The occurrence of (fungal) plant pathogens, which could have happened later, may have given rise to the respective parts of the plant immune system, i.e., recognition of particular IPs. In any case, mutualistic microbes must have been (among) the first to adapt to a plant/apoplast environment increasingly hostile towards any invaders, and some of the well-established mechanisms first described as host–*pathogen* interactions may have rather emerged from such mutualism.

Since the presence of effectors can disadvantage plants, the ability to recognise effectors among IPs, resulting in an immune response, will be selected for. Recognised effectors are called avirulence (Avr) factors. The compromised invader must modify its effector arsenal to avoid recognition, shifting pressure to adapt back on the host, and so forth. This is referred to as the zig-zag model (Jones & Dangl, 2006; also see section 1.2.4,

Ma *et al.*, 2017). In the zig-zag model, any response not involving effectors was called PAMP-triggered immunity (PTI), a pathogen's 'response' resulted in effector-triggered susceptibility (ETS), and the host response specific to the respective (Avr) effector via one cognate 'resistance (R) protein' was labelled as effector-triggered immunity (ETI). It was broadly accepted that only ETI encompasses strong responses, namely the HR and SAR, providing molecular confirmation of the 'gene-for-gene' resistance hypothesis (Flor, 1955). This strict division is simplistic—it was shown that PTI can also involve strong responses (Thomma *et al.*, 2011).

Generally speaking, it was long believed that IPs with different degrees of specificity a) strictly cause different immune responses, which b) is due to separate underlying molecular pathways. This was reinforced by applying the PTI-ETI dichotomy to new discoveries in the field for many years with little reflection. It is now increasingly understood that IP receptors and the coupled signalling network are universally responsible for any immune response (Wu *et al.*, 2018) and that the idea of a binary perception, categorically separating PAMPs from effectors, is flawed. With regard to (a), it holds true that most effectors, if recognised, cause more severe and sometimes additional responses, compared to those attributed to PAMPs, such as rapid programmed cell death and increased ROS accumulation. With regard to (b), however, it is evident that such an outcome is the result of intricate interplay within the network (Plett & Martin, 2018) (rather than "activation of receptor A leads to response B"). In the network, monitoring of nutrient fluxes, signal thresholds and balance of signals likely provides important additional information to the host regarding the state of the symbiosis it is engaged in (Plett & Martin, 2018). Ultimately, the host must be able to distinguish friend from foe based on the summary of these inputs. For example, under the assumption that mutualists do not cause sustained DAMP signals, a low DAMP to MAMP ratio may be sufficient to prevent induction of a defence response (Plett & Martin, 2018).

Keeping this bigger picture in mind, it is clear that effectors can be extremely powerful in the sense that a single highly expressed effector can indeed change the outcome of an interaction, however, in some cases, this is likely the result of a balance being disturbed just enough.

Adaptation at its best: When hosts kill themselves for pathogens

The suppression of immune responses and thus continuation of symbiosis is in the interest of biotrophic pathogens and mutualists, both depending on living host tissue for their survival. For necrotrophs (and hemibiotrophs in necrotrophic phase), the situation is different. They destroy host tissue and feed on lysed, dead cells. While the 'brute' mode of using turgor pressure and sending out masses of plant cell wall-degrading enzymes (PCWDEs) seems like an effective way to achieve this, adaptation has brought forward a more subtle way for necrotrophs. The recognition of specific fungal proteins, which will trigger a programmed cell death response to protect the plant, can be exploited by such pathogens (Friesen *et al.*, 2008). For example, specific wheat and maize pathogens secrete 'host-selective toxins' (now under the broader term necrotrophic effectors) that target plant receptors, or their guards (see section 1.2.4), for their own benefit (Oliver & Solomon, 2010; Yang *et al.*, 2018). A successful infection depends on the presence of the host target, i.e., a pathogen strain with the necrotrophic effector is only pathogenic on host cultivars that carry the corresponding target. This led to the establishment of the term 'inverse gene-for-gene interaction', and can be highly useful for breeding (see subsection 1.2.5).

Specific functions of effectors

One way to broadly categorise effectors is by their location. Effectors that function in the apoplast generally 1) mask or sequester IPs, 2) damage the host, or 3) inhibit, detoxify or provide protection from anti-invader proteins or secondary metabolites, whilst intracellular (cytoplasmic) effectors may achieve the same but through alteration of host gene expression or metabolic reprogramming (Lo Presti *et al.*, 2015). There are a few documented exceptions to these two 'attack point' options, such as the *Pseudomonas syringae* effectors COR, HopF1 and HopM1, which facilitate stomatal opening (Asai & Shirasu, 2015).

After penetrating the cuticle, hyphae exploring the apoplast will usually tightly associate with mesophyll and other host cells and initiate effector secretion. In pathogens thought to be strictly apoplastic, such as *C. fulvum*, *D. septosporum*, and *B. cinerea*,

effectors are released into the narrow apoplastic space in between the fungal and plant cell wall, but other effectors need to be delivered into host cells, a process which is still poorly understood in fungi and oomycetes (Petre & Kamoun, 2014). Bacteria use needle-like structures to directly penetrate host cells and inject effectors, whereas eukaryotic symbionts seem to rely on membrane transport. Commonly known feeding structures called haustoria (pathogens and endophytes) and arbuscules (mycorrhiza) breach the cell wall but not the plasma membrane. Tips of *Magnaporthe oryzae* invasive hyphae apparently form a similarly dedicated structure, encased by the plant membrane (biotrophic interfacial complex, BIC). At either interface, a specialised membrane with particular transmembrane transport proteins is found (Giraldo & Valent, 2013). Still, the actual monitoring of effector traffic in this situation is methodically challenging (Petre & Kamoun, 2014; Lo Presti *et al.*, 2015).

A brief summary of intracellular effectors is given to showcase their diversity, but since there is no evidence that *D. septosporum* enters host cells or delivers effectors into them, the main focus will be on apoplastic effectors. Table 1.1 gives a representation of fungal effectors roughly grouped by function, and Fig. 1.5 provides an illustrated overview.

Table 1.1: Selected fungal effectors with described functions.

Mode of action	Name	Species	Phylum[a]	Ls[b]	Host	Loc[c]	Reference
Invasion pattern-related							
Chitin masking (protection)	Avr4	*Cladosporium fulvum*	Doth	B	Tomato	A	van den Burg *et al*., 2006
Chitin sequestering (detection prevention)	Ecp6	*Cladosporium fulvum*	Doth	B	Tomato	A	de Jonge *et al*., 2010
Chitin sequestering (detection prevention)	Slp1	*Magnaporthe oryzae*	Sord	H	Rice	A	Mentlak *et al*., 2012
Chitin masking (protection)	Mg1LysM	*Zymoseptoria tritici*	Doth	H	Wheat	A	Marshall *et al*., 2011
Chitin masking and sequestering	Mg3LysM	*Zymoseptoria tritici*	Doth	H	Wheat	A	Marshall *et al*., 2011
Glucanase inhibition	Fumonisin B1	*Fusarium verticillioides*	Sord	N	Maize	A	Sánchez-Rangel, Sánchez-Nieto, and Plasencia, 2012
Apoplast detoxification or similar							
Peroxidase inhibition and ROS scavenging	Pep1	*Ustilago maydis*	Usti	B	Maize	A	Hemetsberger *et al*., 2012
Inhibition of cysteine proteases	Avr2	*Cladosporium fulvum*	Doth	B	Tomato	A	Song *et al*., 2009
Inhibition of cysteine proteases	Pit2	*Ustilago maydis*	Usti	B	Maize	A	Mueller *et al*., 2013
Inhibition of serine protease	AvrP123	*Melampsora lini*	Ured	B	Flax	A	Ravensdale *et al*., 2011
Degradation of tomatine (toxic SM)	Tom1	*Cladosporium fulvum*	Doth	B	Tomato	A	Ökmen & Doehlemann, 2014
Degradation of avenacin (toxic SM)	Avenacinase	*Gaeumannomyces graminis var. avenae*	Sord	B	Oat	A	Ökmen & Doehlemann, 2014
Defense / cell death suppression							
Inhibition of lignification	Tin2	*Ustilago maydis*	Usti	B	Maize	C	Tanaka *et al*., 2014
Chorismate mutase (SA synthesis inhibition)	Cmu1	*Ustilago maydis*	Usti	B	Maize	C	Djamei *et al*., 2011
Chorismate mutase (SA synthesis inhibition)	Vdlsc1	*Verticillium dahliae*	Sord	H	Multiple	C	Liu *et al*., 2014
Inhibition of SA and ET signalling	AvrLm4-7	*Leptosphaeria maculans*	Doth	H	Canola	C	Nováková *et al*., 2015
Inhibition of JA signalling	MiSSP7	*Laccaria bicolor*	Agar	M	Poplar	C	Plett *et al*., 2014
Inhibition via E3 ubiquitin ligase	AvrPiz-t	*Magnaporthe oryzae*	Sord	H	Rice	C	Park *et al*., 2006
Suppression of I-2/Avr2-mediated signal	Six6	*Fusarium oxysporum f. sp. lycopersici*	Sord	H	Tomato	X	Gawehns *et al*., 2014
Suppression of PR1 and PR17	CSEP0055	*Blumeria graminis f. sp. hordei*	Leot	B	Barley	A	Zhang *et al*., 2012
Cell death induction							
Photosynthesis disruption	PtrToxA	*Pyrenophora tritici-repentis*	Doth	N	Wheat	C	Manning *et al*., 2009
Photosynthesis disruption	ToxA	*Parastagonosporum nodorum*	Doth	N	Wheat	C	Oliver *et al*., 2012
Perforation of mitochondrial membrane	T-toxin	*Cochliobolus heterostrophus*	Doth	N	Maize	C	Baker *et al*., 2006
Perforation of plasma membrane	ACT	*Alternaria alternata*	Doth	N	Citrus	C	Tsuge *et al*., 2012
Other / multiple							
Plant and fungal cell wall remodelling	SsCVNH	*Sclerotinia sclerotiorum*	Leot	N	Multiple	A	Lyu *et al*., 2015
Sucrose import (plant transporters outcompeted)	Srt1	*Ustilago maydis*	Usti	B	Maize	A	Wahl *et al*., 2010
Derepression of cell wall-degrading enzymes	Snf1	*Leptosphaeria maculans*	Doth	H	Canola	C	Feng *et al*., 2014

[a] Ascomycetes: Dothideomycetes, Sordariomycetes, Leotiomycetes; Basidiomycetes: Ustilaginomycetes, Urediniomycetes, Agaricomycetes.

[b] Lifestyle: Biotrophic, Hemibiotrophic, Necrotrophic, Mutualistic.

[c] Localisation: Apoplastic, Cytoplasmic, Xylem.

Intracellular effectors. Intracellular effector molecules are translocated into host cells, where they carry out their biological functions. They often suppress immune response pathways, allowing for colonisation. Cmu1 from *Ustilago maydis*, a biotroph of maize, is one of many effectors that interfere with the salicylic acid (SA) pathway which broadly controls cell death (Djamei *et al.*, 2011). Both Cmu1 and Vdlsc1 from *Verticillium dahliae*, a broad host range necrotroph, inhibit metabolism of chorismate to SA (Liu *et al.*, 2014). Likewise the bacteria *Ralstonia solanacearum* and *Pseudomonas syringae*, broad host range necrotrophs, deploy a range of effectors to manipulate defence responses associated with the SA pathway. Functions of the 'Hop' effectors include suppression of SA accumulation, inhibition of vesicle trafficking and degradation of jasmonic acid (JA) pathway repressors, resulting in SA signalling suppression (Asai & Shirasu, 2015). The oomycete *Hyaloperenospora arabidopsidis*, an obligate biotroph of *Arabidopsis* spp., uses at least four different effectors to each achieve SA signalling disruption. HaRxL44, best studied among these four, degrades a JA/SA pathway balance mediator subunit in the nucleus (Caillaud *et al.*, 2013; Asai *et al.*, 2014; Anderson *et al.*, 2012). Further, the ectomycorrhizal fungus *Laccaria bicolor* deploys MiSSP7 to the nucleus to protect a negative regulator of JA (JAZ6) from degradation by JA. Thus, MiSSP7 effectively represses JA action on downstream defence-related genes and enables symbiosis (Plett *et al.*, 2014). Similarly, *Rhizophagus irregularis* (ex *Glomus intraradices*), an arbuscular mycorrhizal fungus, uses SP7 to interact with a transcription factor of several defence-related genes. These target genes were apparently down-regulated, as root colonisation progressed (Kloppholz *et al.*, 2011).

These examples illustrate how different strategies with a similar outcome have evolved in distantly or unrelated symbionts. Another example of this is the ubiquitin-proteasome system which is crucial for the regulation of plant defence responses, including the oxidative burst, hormone signalling, induction of defence genes and programmed cell death (Lo Presti *et al.*, 2015; Ökmen & Doehlemann, 2014). AvrPiz-t from *Magnaporthe oryzae*, a hemibiotrophic rice pathogen, suppresses an E3 ubiquitin ligase (APIP6; Park *et al.*, 2012); GALA from *R. solanacearum* and Avr3a from the oomycete *Phytophthora infestans*, a hemibiotrophic Solanaceae pathogen, have a similar target. Avr3a notably

stabilises the E3 ligase in the biotrophic phase to suppress cell death triggered by one of *P. infestans*' PAMPs (González-Lamothe *et al.*, 2006; Bos *et al.*, 2010; Park *et al.*, 2012; Petre & Kamoun, 2014).

Another effector of *U. maydis* demonstrates the potential for diverse approaches, rather than focusing on one type of target, to lead to successful infection. Tin2 interferes with an SM pathway of maize. It seems to bind and stabilise a protein kinase (ZmTTK1), promoting anthocyanin biosynthesis. This happens at the expense of lignin production, as anthocyanins and lignin have a common precursor. Subsequently, lignification of plant cell walls is reduced, weakening this physical barrier (Tanaka *et al.*, 2014). *P. infestans* AvrBlb2 meanwhile suppresses secretion of host proteases in addition to apoplastic effectors which inhibit their activity (see below). Yet another method to prevent defence responses was found in *B. cinerea*, a broad host range necrotroph, and suggested in *V. dahliae*: Small RNAs 'hijack' the host's own RNA interference (RNAi) system and cause selected defence-related genes to be silenced (Wang *et al.*, 2015).

Intracellular effectors may be recognised as IPs by NLRs, which in most cases, but not all, leads to an HR-like response. As mentioned above (section 1.2.4), NLRs or other host proteins can be exploited by necrotrophs. The effector ToxA, found in the Dothideomycete fungi *Parastagonospora nodorum*, *Pyrenophora tritici-repentis*, *Phaeosphaeria avenaria tritici* and *Bipolaris sorokiniana*, all necrotrophic barley and/or wheat pathogens occurring on different continents (McDonald *et al.*, 2018), targets ToxABP1, a chloroplast protein likely to be important for thylakoid formation. The interaction probably causes dysfunctional photosynthesis and consequently cell death (Manning *et al.*, 2009; Oliver *et al.*, 2012). Finally, victorin from *Cochliobolus victoriae*, a necrotroph of maize, interacts with a mitochondrial glycine decarboxylase, leading to cell death, and T-toxin from the related pathogen *C. heterostrophus* also targets mitochondria (Baker *et al.*, 2006; Oliver & Solomon, 2010).

Extracellular (apoplastic) effectors. Apoplastic effectors generally make the apoplast less hostile for the intruder by targeting antimicrobial agents such as toxins and hydrolytic enzymes, or inhibiting detection or production of IPs (Fig. 1.5). One of the most well-characterised IP-related effectors is Avr4 from *C. fulvum*. Avr4 binds to chitin

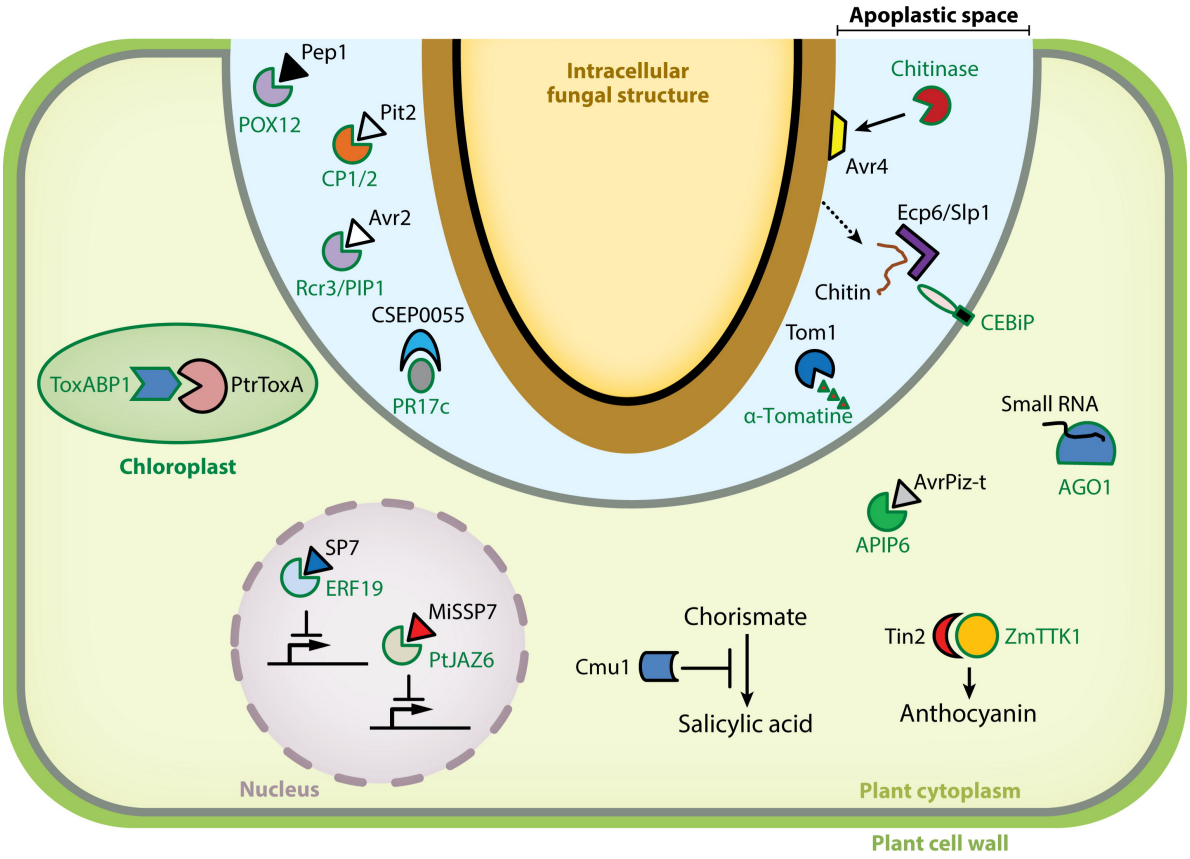

Figure 1.5.: Model overview of effector types in filamentous fungi (Lo Presti *et al.*, 2015). A non-specified fungal structure (biotrophic hypha, part of haustorium or arbuscule) invades the plant cell while the plasma membranes stay intact. The plasma membrane of the fungal structure (black) is surrounded by an extrahaustorial membrane EHM (in case of appressoria) or periarbuscular membrane (in case of arbuscle) (dark brown). Shown effectors are described in the text. Figure reproduced from Lo Presti *et al.* (2015) with permission; ©2015 by Annual Reviews.

at the fungal cell wall, shielding it from chitinases and helping to prevent release of chitin fragments (MAMPs)(van den Burg *et al.*, 2006). *C. fulvum* Ecp6 and its homologues Mg3LysM in *Zymoseptoria tritici* (*ex Mycosphaerella graminicola*), a hemibiotroph of wheat, and Slp1 in *M. oryzae*, have chitin-binding LysM domains (de Jonge *et al.*, 2010; Marshall *et al.*, 2011; Mentlak *et al.*, 2012). The Ecp6-like effector proteins 'scavenge' and also shield loose chitin oligosaccharides to prevent IP-triggered immunity. Furthermore, Slp1 out-competes the rice PRR chitin elicitor binding protein (CEBiP) with the same domain due to a higher binding affinity (Mentlak *et al.*, 2012).

Another way to prevent accumulation of glycan IPs is to stop plant enzymes before they hydrolyse microbial cell walls. *Phytophthora sojae*, a hemibiotroph of soybean, secretes GIP1 to inhibit endo-β-1,3-glucanase activity (Rose *et al.*, 2002); *Fusarium verticillioides*, capable of switching from endophytic to necrotrophic lifestyle on maize, uses the mycotoxin fumonisin B1 (FB1) to directly inhibit a glucanase but probably has other virulence functions as well (Sánchez-Rangel *et al.*, 2012).

Peroxidases are key to generating harmful ROS bursts. Pep1 from *U. maydis* inhibits a peroxidase (POX12) and thus lowers the toxicity of the environment (Hemetsberger *et al.*, 2012). Host proteases are frequently targeted by apoplastic effectors. Pit2 (*U. maydis*), EPI1, EPI10, EPIC1, EPIC2b, PmEPIC1 (*P. infestans*), Avr2 (*C. fulvum*) and Gr-VAP1 (*Globodera rostochiensis*, a nematode) all target cysteine or serine proteases that are involved in defence activation signalling or directly attack fungal structures like hyphal cell walls (Mueller *et al.*, 2013; Tian *et al.*, 2007; Song *et al.*, 2009; Lozano-Torres *et al.*, 2012). The CSEP0055 effector of *Blumeria graminis f. sp. hordei*, an obligate biotrophic pathogen of barley, interacts with members of the host PR1 and PR17 protein families that are secreted under biotic stress, and is thought to suppress their defensive actions (Zhang *et al.*, 2012). The biotrophic tomato pathogens *C. fulvum* and *Septoria lycopersici* as well as *Gaeumannomyces graminis* var. *avenae*, a biotrophic pathogen of oat, secrete enzymatic effectors (tomatinase Tom1, or avenacinase) to detoxify the plant-produced antifungal compounds tomatin and avenacin, respectively (Ökmen & Doehlemann, 2014).

Apoplastic effectors can also damage the host. Necrosis and ethylene inducing protein (NEP1)-like proteins (NLP) are a class of such effectors that generally kill plant

cells by eliciting plasma membrane permeabilisation. They are known in fungi, oomycetes and bacteria (Feng *et al.*, 2014a), and intriguingly used for infection of mono- and dicotyledonous plants (Ottmann *et al.*, 2009). The role of NLPs in virulence towards monocotyledons remains obscure (Motteram *et al.*, 2009). The *Parastagonospora nodorum* virulence factors Tox3 and ToxA can both induce cell death in susceptible wheat leaves, and each was found to interact with PR1 proteins (Liu *et al.*, 2009; Lu *et al.*, 2014; Breen *et al.*, 2016). It could be that this protein interaction constitutes a case of cell death exploitation (Breen *et al.*, 2016).

Fungal PCWDEs are a large and diverse group themselves and they can be viewed as effectors. Investigating PCWDE function with reverse genetic approaches (gene knockouts or silencing) targeting single genes has not been entirely conclusive due to the redundancy of enzymatic functions. Knocking out a protein kinase (SNF1) involved in catabolite repression of a set of CWDEs in *Leptosphaeria maculans* meanwhile caused down-regulation of most of the CWDEs and loss of pathogenicity (Feng *et al.*, 2014b).

Compelling examples of the host–pathogen arms race in the apoplast

There are a few remarkable examples of the zig-zag-like adaptation of host and pathogen.

Additional to the direct interaction of host and pathogen molecules, effectors (and other IPs) can also interact with targets which are not PRRs but 'monitored' by them. In this case, the PRR recognises changes in the target and through this initiates the defence response signalling; this is embodied in the Guard model (Jones & Dangl, 2006). The target or 'guardee' is subject to opposing selective forces: Increasing affinity to the effector(s) will improve effector recognition and lead to a strong response. However, in the absence of the guarding PRR this will be in favour of susceptibility, thus, guardees with lower affinity will be selected. This conflict can be solved by evolution of a host 'decoy' protein which structurally mimics the guardee. The purpose of a decoy is to bind to effectors so that they do not bind to the guardee. The decoy must not have a function that promotes susceptibility, but the PRR, if present, monitors it. In the absence of the PRR, the decoy may still reduce the virulence of the pathogen as it competes with the original target for effector binding (van der Hoorn & Kamoun, 2008). Notably one

example of this model involves *C. fulvum* Avr2 (see above). The Avr2 effector is a virulence factor and recognised as IP in hosts carrying the PRR Cf-2. Avr2 targets and inhibits two proteases thought to act in the basic defence layer, Pip1 and Rcr3, which causes immunity mediated by Cf-2. Additional findings suggested that Rcr3 is not highly expressed and its inhibition does not contribute to virulence, however, the absence of Rcr3 resulted in similar virulence increase as the absence of Cf-2 (Dixon *et al.*, 2000). The hypothesis is that Rcr3 is mainly a decoy to Pip1, trapping Avr2 to activate Cf-2 (Rooney *et al.*, 2005; Shabab *et al.*, 2008).

Apparently, not only plants have evolved decoys dedicated to serve in the interaction battle. In *P. sojae*, a novel mechanism of preventing IP recognition was discovered recently. The glycoside hydrolase 12 PsXEG1 was previously described as virulence factor and PAMP (that is, the protein itself rather than DAMPs resulting from its activity). However, PsXEG1-triggered immunity could be suppressed by intracellular effectors (Ma *et al.*, 2015). In the host soybean (*Glycine max*), PsXEG1 was found to interact with a protease-like glucanase inhibitor protein named GmGIP1 (Ma *et al.*, 2017). This host 'counter-effector' inhibited the enzymatic activity and virulence effect of PsXEG1, giving soybean the upper hand. However, *P. sojae* secretes a paralog of XEG1, XLP1, which was found to be bound by GmGIP1 with five times higher affinity than XEG1. Thus, it was suggested that PsXEG1 can carry out its virulence function almost unhindered in the presence of PsXLP1, and the sole purpose of PsXLP1 is to interfere with GmGIP1 (notably it also does not appear to be an IP). Hence, PsXLP1 was termed pathogen/ effector decoy with reference to the decoy defence concept. Moreover, this entire interplay is mirrored in a compatible *P. parasitica–N. benthamiana* interaction, supporting the suggestion that such an effector decoy strategy could occur in various pathogens (Ma *et al.*, 2017). Indeed, two *Xanthomonas* spp. produce truncated versions of important effectors that modulate host transcription. These could have the same ultimate effect as PsXLP1 (Paulus *et al.*, 2017).

In the terms of the arms race image, these snapshots of coevolution illustrate how two adversaries have developed their armoury for a very particular aspect of the battle in response to new weapons on the other side.

Research of apoplastic effectors in *Cladosporium fulvum* pioneered the field

The Dothideomycetes are the largest and most diverse subphylum of the Ascomycetes and several of its members are highly relevant agricultural crop or forest tree pathogens, including the genera *Cochliobolus, Leptosphaeria, Mycosphaerella and Stagonospora* (note: many *Mycosphaerella* species have been renamed; Videira *et al.*, 2017). As demonstrated in the overview of characterised effectors, many studies have already addressed effector biology in these species, that is, in food-related pathosystems foremost. Relying on the concept of gene homology in related species, some of the findings of these studies served as a foundation of this thesis.

Cladosporium fulvum, the causative agent of tomato leaf mould, is of special interest as a close relative of *D. septosporum* (Fig. 1.2). It has a biotrophic lifestyle and is among the best studied filamentous fungal pathogens. Early identification and cloning of both avirulence (*Avr*) effectors and their cognate resistance (*R*) genes provided compelling evidence for the gene-for-gene hypothesis. The recognition of at least ten *C. fulvum* Avr effectors, including Avr2, Avr4, Avr9, and extracellular protein 2 (Ecp2), is mediated by cognate PRRs (Thomma *et al.*, 2005; de Wit *et al.*, 2009b; see Fig. 1.4). Identifying these receptors in wild tomato races led to successful integration of resistance into cultivation populations via breeding. However, *C. fulvum* strains have adapted to avoid recognition (Stergiopoulos *et al.*, 2007; Iida *et al.*, 2015); one striking report determined a single amino acid change in Avr4 as the reason for lost resistance (Joosten *et al.*, 1994). In a recent study, ten new Ecps caused HR in wild tomato plants, providing a highly promising lead for additional Avr-PRR pairs to be used for breeding (Mesarich *et al.*, 2017). Furthermore, functional studies in this model pathosystem laid some of the basics of host–pathogen interactions, such as the finding that chitin is directly and indirectly prevented from becoming a detectable IP, and that this is achieved by small cysteine-rich proteins secreted into the apoplast (van den Burg *et al.*, 2006; de Jonge *et al.*, 2010).

The genomes of *C. fulvum* and *D. septosporum* were sequenced for a comparison of closely related pathogens that have different lifestyles and hosts. Intriguingly, the analysis of the hemibiotrophic *D. septosporum* genome uncovered the presence of nine predicted proteins that are homologues of *C. fulvum* Avr effectors (de Wit *et al.*, 2012). Of these,

DsAvr4 triggered HR mediated by Cf-4, the cognate tomato PRR, in *Nicotiana benthamiana* leaves, using the *Agrobacterium tumefaciens* transient transformation assay (ATTA). DsAvr4 was later shown to also bind chitin (Mesarich *et al.*, 2016). One of the other effector homologues, DsEcp2-1, triggered an HR in a tomato line with the Cf-Ecp2 resistance trait, using the potato virus X (PVX)-based transient expression system (de Wit *et al.*, 2012). Other Dothideomycete species with publicly available genomes were also analysed (Stergiopoulos *et al.*, 2010). Avr4 homologues were found in *Pseudocercospora* (ex *Mycosphaerella*) *fijiensis*, a devastating banana pathogen, and the economically important wheat pathogen *Z. tritici* (do Amaral *et al.*, 2012). Ecp2 homologues were identified in *P. fijiensis* only. The functions of Cf- and Pf- Avr4 and Ecp2-1 have been assessed and directly compared by using *Agrobacterium*-PVX mediated delivery into tomato as well as ATTAs in *N. benthamiana* (Stergiopoulos *et al.*, 2010). *P. fijiensis* effectors triggered HR, indicating their recognition by the tomato R proteins Cf-4 and Cf-Ecp2, respectively. Based on these findings, the authors concluded that the *C. fulvum* effectors Ecp2 and Avr4 are not species-specific but rather 'core' effectors of closely related Dothideomycetes. These effectors might be preserved for basic virulence function, but also due to conservation of their target molecules in different hosts. As a comparison, this is evidently not the case for *C. fulvum* Avr2, Avr4E and Avr9, which are found much less frequently in other species. This could reflect adaptation to novel or mutated defence proteins in different hosts or cultivars through loss or mutation (Stergiopoulos *et al.*, 2010). Notably PfAvr4 induced an HR-like response in leaves of a resistant banana cultivar, adding rare evidence of an Avr effector (likely) being recognised by PRRs of more than one host (Isaza *et al.*, 2016).

The finding that DsAvr4 and DsEcp2-1 were both recognised by tomato PRRs is highly interesting as the gymnosperm hosts of *D. septosporum* are barely related to tomato (de Wit *et al.*, 2012). For Avr4 proteins of various pathogens, indeed a single residue within a relatively conserved domain was determined to be crucial for the interaction with Cf-4 (Mesarich *et al.*, 2016). DsAvr4 was found not to be expressed during a *D. septosporum* infection of *P. radiata* (Bradshaw *et al.*, 2016). In a pathogenicity assay with a Δ*DsAvr4* strain, no changes in the infection were observed (Guo, 2015). It could be that

DsAvr4 is not important for this interaction and has thus not been subject to selective pressure. To directly determine if DsAvr4 and DsEcp2-1 are recognised in *P. radiata*, preliminary experiments with protein solutions and detached DNB-susceptible *P. radiata* needles were carried out (Guo, 2015). Vacuum-infiltrated solutions with either protein caused small necrotic lesions on these needles, warranting further investigation. The results for DsEcp2-1 were ambiguous, and this is discussed in chapter 5 of this thesis.

Effectors of forest microbes

Studies of effectors from (eukaryotic) microbes associated with forest tree species are rare. Therefore, evidence for similar molecular interaction mechanisms as described above is limited for such symbioses. This especially applies to fungal diseases of gymnosperms.

The rust fungus *Cronartium ribicola* causes white pine blister rust (WPBR) on many five-needle pine species around the world (Liu *et al.*, 2015). Qualitative resistance to WPBR has been assigned to four major *R* genes, *Cr1* to *Cr4*, all found in different hosts. This implied the presence of single corresponding *Avr* effector genes in the fungus. However, sugar pine (*P. lambertina*) *Cr1*- and western white pine (*P. monticola*) *Cr2*-based resistance can each be overcome by *C. ribicola* races carrying the genes *vcr1* or *vcr2*, respectively (Kinloch Jr & Dupper, 2002; Kinloch Jr *et al.*, 2004; Schoettle *et al.*, 2014). Since *vcr1* and *vcr2* restore virulence, their gene products are effectors, but it is still not known what their mode of action is (Sniezko *et al.*, 2014). A *C. ribicola* transcriptome study identifying *in planta* expressed secreted proteins has provided an important step towards a better molecular understanding of WPBR (Liu *et al.*, 2015).

There are a few other examples of Avr effectors recognised in fungal interactions with hosts such as poplar, but their primary functions remain elusive. Poplar is also one of few tree species with an abundance of genomic and growing transcriptomic resources.

Heterobasidion annosum is a saprotroph but also a necrotrophic pathogen of mainly Scots pine (*Pinus sylvestris*), when it encounters live tree tissue on the ground. This basidiomycete fungus is among the most destructive conifer diseases in northern Europe (Raffaello & Asiegbu, 2017). In *H. annosum sensu stricto*, a secreted cerato-platanin protein, HaCPL2, was identified as an inducer of cell death in *P. sylvestris* seedlings

as well as in *N. tabacum* (Chen *et al.*, 2015). For *H. annosum sensu lato*, a list of 58 putative secreted effector proteins without any sequence homologues was presented, and these HaSSPs were tested for induction of cell death and defence gene transcription in the non-host *N. benthamiana*. Eight HaSSPs induced such immune responses (Raffaello & Asiegbu, 2017), and could be taken forward for further functional studies.

Phytophthora plurivora, a root pathogen of European beech (*Fagus sylvatica*), apparently relies on α-plurivorin for colonisation. A-plurivorin is one of many elicitins, proteins highly conserved in *Phytophthora* spp. and elicitors of immune responses in various plants (Kamoun *et al.*, 1998), and may help to suppress host defences (Dalio *et al.*, 2017a). Upon so-called immunodepletion (specific blocking of a protein by antiserum *in vivo*) of α-plurivorin immediately before artificial inoculation of *F. sylvatica* seedling roots with zoospores, an immunity response was successfully mounted and the interaction stopped very early. In contrast, without this treatment the pathogen killed the seedlings within four to eight days.

Mycorrhiza are a tight association of roots and fungal hyphae and a common form of mutualistic symbiosis. Ectomycorrhizae (ECM) in particular are found in the vast majority of trees. Compared to host–pathogen interactions occurring in forests, more molecular work has been done to investigate this type of symbiosis. As noted above, the ECM fungus *L. bicolor* delivers an effector to the host nucleus to repress the JA defence pathway (Plett *et al.*, 2014), and *Rhizophagus irregularis* suppresses immunity genes more directly via a transcription factor (Kloppholz *et al.*, 2011). The root endophyte *Serendipita* (ex *Piriformospora*) *indica* secretes a β-glucan-binding lectin, FGB1, specifically protecting its cell wall (Wawra *et al.*, 2016). Even though β-glucans are far more abundant in the fungal cell wall than chitin, and present in oomycete cell walls, little is known about their role in immunity (Fesel & Zuccaro, 2016). FGB1 prevented β-glucan-triggered ROS production in different hosts, which could represent a 'new' strategy for stealth (Wawra *et al.*, 2016). It would complement the evasion of IP-triggered immunity strategy via chitin binding by LysM effectors, and it would not be surprising to find this mechanism to be conserved.

As a potential primer for molecular pathology of trees in general, Dalio *et al.* (2017b)

provide a comprehensive overview of citrus and its interactions with various pathogens from all kingdoms, addressing a total of ten citrus diseases. It shows that *Citrus* spp. immune systems are modulated in many different ways by different intruders. The pathogens include the fungi *Colletotrichum acutatum* (hemibiotrophic) and *Alternaria alternata* (necrotrophic). Two *C. acutatum* proteins are important for its virulence but their function remains unclear. Meanwhile, *A. alternaria* secretes the ACR- and ACT-toxins which are characterised necrotrophic effectors (Dalio *et al.*, 2017b). As in other hosts of *A. alternaria* (Tsuge *et al.*, 2012), these non-ribosomal peptide-PKS hybrids induce cell death and are essential for the pathogenicity of the fungal strain.

Taken together, little is known about the effectors of fungal symbionts of forest tree species. There is a particular gap in this area concerning ascomycete foliar pathogens of gymnosperms.

1.2.5. Effectoromics: A modern approach to combat plant pathogens

On an evolutionary scale, the vast majority of plant–microbe interactions see plants on the winning side (as they have not all been killed by pathogens, Plett & Martin, 2018). However, if a pathogen species or strain breaks the resistance, the outcome can be disastrous, especially in monoculture crops where every host individual can be infected and become a source of additional inoculum.

As explained by the IP–PRR interplay, such adaptation has occurred via single genes. When these molecular players are identified, their specific interactions can be used for the benefit of the crop. For example, the discovery of a conserved motif (RxLR) in oomycete effectors greatly accelerated Avr effector identification. At least for *P. infestans*, this has resulted in improved understanding of *Avr–R* gene interactions, and potato breeders have recognised the use of such information (Vleeshouwers & Oliver, 2014). In the case of necrotrophic effectors, conferring virulence only if the host carries a target susceptibility gene, the search for resistant host genotypes is theoretically the easiest. Once isolated and cloned, a necrotrophic effector can be directly used to screen host germplasm for an HR, indicating susceptibility based on the single gene, granted that it can be delivered to its target. Susceptible lines can then be removed from the current breeding pool. Using

this approach, hundreds of millions of dollars in yield loss of wheat in Australia due to tan spot disease have been prevented (Vleeshouwers & Oliver, 2014).

Computing power is ever-increasing and sequencing costs decreasing. Thus it is not surprising to find "omics" as part of many current studies addressing plants and their pathogens, where effectoromics is defined as a high-throughput functional genomics approach that uses effectors for probing plant germplasm to detect *PRR* genes. This increased interest results in new and growing databases, and smarter and novel software to work with them. This has allowed the scientific community to rapidly identify effector genes in pathogens such as *Magnaporthe* spp., *Phytophthora* spp. and *C. fulvum* supported by computational work (*in silico*). Still, comparatively little is known about effectors in forest pathogens or *R/PRR* genes of their hosts (Raffaello & Asiegbu, 2017). The genome investigation and comparison of the close relatives *D. septosporum* (representing forest pathogens) and *C. fulvum* was a pioneer study aiming to change that (de Wit *et al.*, 2012), leading up to this study.

Disease resistance can be achieved via a qualitative trait, i.e., a single pathogen-specific *R* gene, or quantitative traits, where several unknown genes contribute to overall reduced disease. To select for a single *R* gene in breeding imposes high selection pressure on the pathogen, which can often adapt quickly through various options (outlined in subsection 1.2.4). This strategy has been shown to only be a transient solution regarding resistance (e.g., potato, Fry, 2008, wheat and rice, Cruz & Valent, 2017, tomato, Luderer *et al.*, 2002b; Joosten *et al.*, 1997). When multiple *R* genes are combined (pyramiding), chances of adapting to all of them greatly decrease and the pathogen population might die out before this is achieved. Despite successes, molecular genetics-driven resistance research is probably only now growing out of infancy. Further, it seems that the threats to global food security have been far from eradicated, with virtually any piece of recent scientific literature naming the pathogen it investigated "devastating" or similar dramatic terms. In many cases, these are no exaggerations, such as the "continued emergence" (Fry *et al.*, 2015) of the historically infamous potato late blight (caused by *P. infestans*, which has risen to the status of model pathogenic organism), or the most recent wheat blast outbreak in Bangladesh (Cruz & Valent, 2017) which resulted in a quickly assembled open

international collaboration to counter it[1].

In the last two decades, there have been staggering advances in the understanding of plant–microbe interactions, from precise monitoring of what exactly happens during contact of hyphae with the infected plant at tissue and cellular level (haustoria formation, BIC etc.), and gene expression patterns on both sides, to localisation and function elucidation of effector molecules. In recent years, it has become a standard that intensive bioinformatics support these efforts or are even at their base. Compared to these invaluable functional insights in crop host–pathogen systems, limited information is available concerning forest plant species and their symbionts. Molecular resources for forest microbes, including identification tools and (meta-)genomics and transcriptomics, have been reviewed by Stewart *et al.* (2018), but they have not been applied in experiments to a great extent. Over-abundance of such information on DNA and RNA highlights a bottleneck. Achieving experimental verification of predictions, such as effector functions, cannot easily be scaled up for any given pathosystem. For the slowly growing gymnosperms it is pivotal to design efficient screening methods for CEs that enable stringent conclusions.

1.3. Focus and aims of the study

The focus of this study was to identify putative effectors of *D. septosporum* by mining its genome and transcriptome, and then to test these effector candidates for their ability to trigger immune system-related cell death in both *P. radiata* and non-host plants. A bioinformatics pipeline was created to identify at least 50 effector candidates for functional analysis. To screen these candidates, a delivery system for pine needed to be developed because effector delivery systems that work for other pathosystems cannot necessarily be applied to pine. For non-host screening, functional analyses of *D. septosporum* effectors in tobacco plants (*N. tabacum* and *N. benthamiana*) was carried out. Ultimately, the goal was to find effectors that a) are both indispensable to the pathogen and can be recognised by host individuals carrying cognate immune receptors or b) require a host susceptibility target crucial for pathogen virulence, possibly allowing for selection of pine lineages that

[1]The Twitter tag #openwheatblast to inspire sharing of resources is still in use today.

lack the target. Either of those could assist durable resistance breeding.

Research aims

1. To identify at least 50 novel candidate effectors of *D. septosporum* using an approach based on bioinformatics and pre-existing transcriptome data.
2. To develop an effector delivery and screening method for pine that enables the identification of *D. septosporum* effectors capable of triggering host cell death responses.
3. To characterise the virulence and/or avirulence functions of *D. septosporum* effector candidates in pine and non-host plants.

Objectives

1. To identify at least 50 novel candidate effectors of *D. septosporum* using an approach based on bioinformatics and pre-existing transcriptome data.

   To acquire a set of candidate genes from *D. septosporum* with high likelihood of encoding effectors, candidates will be selected from amongst gene models using stepwise filtering by the following approaches:

   - *D. septosporum* proteins that are secreted by classical pathways will be predicted using a series of well-established sequence-based prediction tools, generating a robust secretome.
   - A minimum *in planta* expression value based on transcriptome data will be applied to filter out genes that are only expressed at background levels.
   - Expressed secreted proteins will be categorised into groups based on size and cysteine content. Small secreted cysteine-rich proteins (SSCPs) will be prioritised.
   - Further information on each candidate will be gathered to support or weaken its selection for functional analysis. Genome sequences of a global collection of 18 *D. septosporum* isolates will be queried for presence/absence, as well as single nucleotide polymorphisms in the coding sequence regions of the candidate genes.

2. To develop an effector delivery and screening method for pine that enables the identification of *D. septosporum* effectors capable of triggering host immune system-related cell death responses.

   This will be achieved by:

   - Heterologous expression of *D. septosporum* proteins in a *Pichia pastoris* system building on work from previous student from which several *D. septosporum* and *C. fulvum* effectors are available (Guo, 2015). New positive controls for necrosis (proteins from other pathogens) could be trialled.
   - Developing a high-throughput protein expression and collection method using *N. benthamiana* leaves.
   - Confirming protein expression (western blot) in the two above methods.
   - Revisiting and optimising the vacuum infiltration of pine needles tested by Guo (2015): Detached pine needles as well as rootless pine shoots will be used.
   - Trialling a tissue culture method, established with fungal extracts at Scion.

3. To characterise effectors in pine and non-host plants.

   To determine whether candidate effectors identified in objective 1 have virulence or avirulence functions by:

   - Characterisation in non-host plants by cloning candidate effector genes in *Agrobacterium tumefaciens* for infiltration of *N. benthamiana* and *N. tabacum* and non-host cell death assessment.
   - Co-expression of known HR elicitors with selected candidate effectors to detect suppression of HR by the candidate effectors, indicative of a possible virulence function (avoidance of defence response).
   - Characterisation in pine by delivery of candidate effector proteins into *P. radiata* of different genotypes (detached needles or cotyledons; see objective 2) to assess avirulence function or toxicity, as well as testing in a whole pine infection assay with *D. septosporum* mutants by knockout, or over-expression, to identify virulence function.

Chapter 2.

Materials & Methods

2.1. Biological materials used in this study

2.1.1. Microorganisms and plasmids

Microorganisms and plasmids used in this study are listed in Table 2.1. Unless otherwise mentioned, plasmids were kindly provided by Dr. Kee Hoon Sohn (formerly School of Agriculture and Environment, Massey University). The template for HaCPL2 was kindly provided by Dr Tommaso Raffaello (Faculty of Agriculture and Forestry, University of Helsinki). The *Dothistroma septosporum* strains that were used for genome sequencing are listed in Table 2.2.

2.1.2. Plants

Pinus radiata seedlings, derived from open-pollinated crosses (parentage is confidential), were obtained from the Scion nursery. Seedlings from the healthiest DNB-susceptible seed lot, as previously determined by a susceptibility rating in field trials (Scion, Rotorua), were chosen for the pathogenicity assay with *D. septosporum* strains.

P. radiata clonal shoots grown from embryogenic tissue under sterile conditions (Hargreaves *et al.*, 2004) were also provided by Scion. Genotypes encoded as S1-S6 (rated as susceptible based on field data) and R1-R4 (rated as resistant) were used in the study.

Nicotiana tabacum Wisconsin 38 (also named Havana 38) and *N. benthamiana* were used in this study. Seeds were kindly provided by Dr. Kee Hoon Sohn.

Table 2.1: Microorganisms and plasmids used in this thesis.

Strain / name	Relevant characteristics / purpose	RBG[a]	Source / reference
Dothistroma septosporum			
FJT75	NZE10 wild-type	FJT75	B. Doherty
FJT141	NZE10 *ΔEcp2-1*	FJT141	Guo 2015
FJT142	NZE10 *ΔEcp2-1*	FJT142	Guo 2015
FJT143	NZE10 *Ecp2-1* complement	FJT143	Guo 2015
Escherichia coli			
DH5α	*fhuA2 lacΔU169 phoA glnV44 Φ80' lacZΔM15 gyrA96 recA1 relA1 endA1 thi-1 hsdR17;* cloning	n/a	Taylor *et al.* 1993
Agrobacterium tumefaciens			
GV3101	Disarmed strain carrying pMP90 (pTiC58); C58C1; Rif^R, Gm^R; host for transient transformation assay (ATTA)	n/a	Koncz & Schell 1986; Hellens *et al.* 2000
AGL1::p19	Carrying p19 expression vector; counteracts RNA silencing in ATTA	154	K. Sohn; Xiang *et al.* 1999
Pichia pastoris			
GS115	Histidine-auxotrophic strain; enables selection on histidine deficient media	n/a	Invitrogen
Plasmids			
pPic9xHis6	Expression vector for *P. pastoris,* complements histidine auxotrophy, methanol inducible promoter, 6xHis tag for purification	n/a	Invitrogen
pPic9xHis6::CfNLP	*C. fulvum* NEP1-like protein fused to N-FLAG; reference for *P. pastoris* culture filtrate infiltration	n/a	Guo 2015
pPic9xHis6::Ecp2-1	*D. septosporum* Ecp2-1 fused to N-FLAG; testing of avirulence effector in *P. pastoris* culture filtrate infiltration	n/a	Guo 2015
pICH41021	pUC19B, modified shuttle vector with BsaI sites removed, Amp^R; *lacZ* complementation, Golden Gate cloning (entry vector)	5	S. Marillonet
pICH86988	Binary vector, contains 35S CaMV promoter and NosT terminator,	7	S. Marillonet
pBIN-Plus::Avr3a	Expression vector for *P. infestans* effector Avr3a (ATTA)	29	J. Win
pCB302-3::R3a	Expression vector for *S. tuberosum* R3a (ATTA)	28	J. Win
pCB302-3::Inf1	Expression vector for *P. infestans* effector INF-1 (ATTA)	45	J. Win
pK2GW7::DsAvr4	Expression vector for DsAvr4 (ATTA)	33	Y. Guo
pICH41021::N-PR1a-3xFLAG	Entry vector holding fused PR1α and 3xFLAG tag; Amp^R; N-terminal universal secretion signal and tag for immunoblotting	55	Y. Guo
pICH86966::N-3xFLAG-GFP	Expression vector for GFP (ATTA)	46	Y. Guo
pICH86988::N-PR1a-3xFLAG-Ds70155	Expression vector for DsCPL1 (ATTA)	47	Y. Guo
pICH86988::N-PR1a-3xFLAG-HaCPL2	Expression vector for *H. annosum s.s.* CPL2 (ATTA)	48	Y. Guo
pICH86988::N-PR1a-3xFLAG-DsEcp2-1	Expression vector for DsEcp2-1 (ATTA)	54	Y. Guo
pICH86988::N-PR1a-3xFLAG-Ds52422	Expression vector for Ds52422 (ATTA)	17	This study
pICH86988::N-PR1a-3xFLAG-Ds72737	Expression vector for Ds72737 (ATTA)	30	This study
pICH86988::N-PR1a-3xFLAG-Ds70694Slv	Expression vector for Ds70694_Slovakia (ATTA)	31	This study
pICH86988::N-PR1a-3xFLAG-Ds68958	Expression vector for Ds68958 (ATTA)	122	This study
pICH86988::N-PR1a-3xFLAG-Ds69113	Expression vector for Ds69113 (ATTA)	123	This study
pICH86988::N-PR1a-3xFLAG-Ds69335	Expression vector for Ds69335 (ATTA)	124	This study
pICH86988::N-PR1a-3xFLAG-Ds70694	Expression vector for Ds70694 (ATTA)	129	This study
pICH86988::N-PR1a-3xFLAG-Ds73723	Expression vector for Ds73723 (ATTA)	130	This study
pICH86988::N-PR1a-3xFLAG-Ds43416	Expression vector for Ds43416 (ATTA)	131	This study
pICH86988::N-PR1a-3xFLAG-Ds70057	Expression vector for Ds70057 (ATTA)	132	This study
pICH86988::N-PR1a-3xFLAG-Ds71487	Expression vector for Ds71487 (ATTA)	147	This study
pICH86988::N-PR1a-3xFLAG-Ds75130	Expression vector for Ds75130 (ATTA)	148	This study
pICH86988::N-PR1a-3xFLAG-Ds70694Rus	Expression vector for Ds70694_Russia (ATTA)	149	This study
pICH86988::N-PR1a-3xFLAG-Ds72870	Expression vector for Ds72870 (ATTA)	150	This study
pICH86988::N-PR1a-3xFLAG-Ds131290	Expression vector for Ds131290 (ATTA)	151	This study
pICH86988::N-PR1a-3xFLAG-Ds73520	Expression vector for Ds73520 (ATTA)	152	This study
pICH86988::N-PR1a-3xFLAG-Ds131885	Expression vector for Ds131885 (ATTA)	153	This study

[a] Rosie Bradshaw Glycerol stock number: Internal code for glycerol stocks in -80°C freezer.

Table 2.2: Wild-type *Dothistroma septosporum* strains used for genome comparison

CMW[a]	Country	Collection year	*Pinus* host
15843	Austria	2004	*P. sylvestris*
23429	Bhutan	2005	*P. radiata*
14823	Canada	1996	*P. contorta v. latifolia*
10798	Chile	2001	*P. radiata*
37193	Colombia	2011	*P. elliotii x taeda*
37194	Colombia	2011	*P. kesiya*
40004	Denmark	2013	*P. aristata*
10211	Ecuador	2001	*P. radiata*
13121	Germany	1996	*P. mugo*
37965	Greece	2012	*P. burtia / P. nigra*
44207	Guatemala	1983	*P. tecumumanii*
38941	Guatemala	2012	*P. oocarpa*
NZFS4520	New Zealand	1965	*P. ponderosa*
MU_NZE8	New Zealand	2004	*P. radiata*
11707	New Zealand	2005	*P. radiata*
44656	Russia	2013	*P. sylvestris*
13123	Slovakia	1996	*P. sylvestris*
11305	South Africa	2002	*P. radiata*
14822	USA	1983	*P. ponderosa*

[a] Commonwealth Mycological Institute collection number.

2.2. Media used

If not explicitly mentioned, laboratory procedures were carried out under sterile conditions.

2.2.1. Media for bacteria

Bacterial cultures were grown in Low Salt medium (LS): 10 g/l bacto tryptone (Becton, Dickinson and Company, Sparks, MD, USA), 5 g/l yeast extract (Life Technologies, Paisley, Scotland), 5 g/l sodium chloride (Panreac Qumica S.A.U., Barcelona, Spain), 1 g/l D-glucose (Univar, Wellington, New Zealand); 15 g/l bacteriological agar (Neogen, Lansing, MI, USA) for plates.

Unless otherwise specified, antibiotics were added at the following final concentrations where appropriate: Kanamycin (Kan^R) 50 μg/ml, Ampicillin (Amp^R) 100 μg/ml, Rifampicin (Rif^R) 10 μg/ml, Gentamycin (Gm^R) 30 μg/ml.

2.2.2. Media for *Dothistroma septosporum*

D. septosporum was propagated, as described in detail in subsection 2.3.1 and subsection 2.5.1, on the following media.

Dothistroma medium (DM): 50 g/l malt extract (Difco/BD, Franklin Lakes, NJ, USA) and 23 g/l nutrient broth (Scharlau, Mas d'en Cisa, Spain); 15 g/l bacteriological agar for plates.

Dothistroma sporulating medium (DSM): 20 g/l malt extract, 5 g/l yeast extract, 15 g/l bacteriological agar.

Pine minimal (salts) medium with glucose (PMMG; McDougal *et al.*, 2011): Fresh pine needles from Massey Turitea campus were soaked in milli-Q water (MQ; water ultrapurified by an EMD Millipore system or similar) (10% w/v) for 24 h. Needles were then removed and the treated water was supplemented with: 0.2 g/l magnesium sulphate heptahydrate (Merck), 0.9 g/l di-potassium hydrogen orthophosphate (BDH, Poole, England), 0.2 g/l potassium chloride (Sigma-Aldrich, St. Louis, MI, USA), 1.0 g/l ammonium nitrate (Sigma-Aldrich), 0.002 g/l iron sulphate (APS Chem. Ltd., NSW, Australia), 0.002 g/l zinc sulphate heptahydrate (BDH), 0.002 g/l manganese chloride (BDH), 2 g/l asparagine (Sigma-Aldrich), 3 g/l glucose (APS Chem. Ltd.), 15 g/l bacteriological agar. pH was adjusted to 4.0-6.2.

2.2.3. Media for *Pichia pastoris*

Buffered glycerol complex broth (BMGY): 1% yeast extract, 2% mycological peptone (Oxoid, Hampshire, United Kingdom), 100 mM potassium phosphate buffer, pH 6.0, 1.34% yeast nitrogen broth (YNB, Invitrogen, Carlsbad, CA, USA), 0.4 mg/l biotin, 1% glycerol.

Buffered complex methanol medium (BMMY): As BMGY, glycerol substituted for 0.5% methanol. Yeast extract and peptone were dissolved in dH_2O and autoclaved. Filter-sterilised solutions of the remaining ingredients were mixed into the broth at room temperature.

2.2.4. Media for *Pinus radiata* tissue culture

Tissue culture shoots (2.1.4) were maintained on modified Quoirin and Lepoivre medium (Quoirin & Lepoivre, 1977) with charcoal (LPch): 18 g/l KNO_3, 1.2 g/l $Ca(NO_3)_2{\cdot}4H_2O$, 0.4 g/l NH_4NO_3, 0.36 g/l $MgSO_4{\cdot}7H_2O$, 0.27 g/l KH_2PO_4, 8.6 mg/l $ZnSO_4{\cdot}7H_2O$, 3.1 mg/l H_3BO_3, 20 mg/l $MnSO_4{\cdot}4H_2O$, 0.25 mg/l $CuSO_4{\cdot}5H_2O$, 80 μg/l KI, 0.25 mg/l $Na_2MoO_4{\cdot}2H_2O$, 25 μg/l $CoCl_2{\cdot}6H_2O$, 0.4 mg/l Thiamine HCl; 40 mg/l Na_2EDTA, 30 mg/l $FeSO_2{\cdot}7H_2O$; 5 g/l activated charcoal; 12 g/l agar.

2.3. RNA and DNA isolation

2.3.1. RNA extraction from fungal cultures

For RNA extraction, *D. septosporum* NZE10 was grown in liquid DM for 7 d at 22°C and mycelium was harvested by filtration using nappy liners (Woolworths, Bella Vista, Australia) and snap-frozen with liquid nitrogen. Under RNase-free conditions, approx. 0.5 g of mycelium was ground to a powder with mortar and pestle, 5 ml TRI Reagent® (Ambion/Thermo Fisher Scientific Inc., Waltham, MA, USA) was added and the mix incubated at room temperature (RT) for 5 min. For each 5 ml, 1 ml of chloroform was added and shaken for 15 s, then incubated for 5 min at RT. The mix was centrifuged at 3220×g for 10 min (Eppendorf 5810, Hamburg, Germany). The aqueous supernatant was collected and mixed with 70% isopropanol and 1.2 M sodium chloride. The solution was kept at RT for 10 min and then centrifuged at 16100g, 4°C for 10 min (Eppendorf 5415 R). The supernatant was discarded and 70% ethanol added; this was mixed by vortex and centrifuged at 16100×g, 4°C for 5 min. The wash was repeated once. The pellet was air-dried for 10 min and re-suspended in 50 μl MQ pre-treated with 0.1% diethyl carbonate (DEPC, Sigma-Aldrich).

RNA concentration and purity were estimated with a NanoDrop® ND-1000 UV-Vis spectrophotometer and NanoDrop® software version 3.1.0 (Nanodrop Technologies Inc, Wilmington, DE, USA), following the manufacturer's instructions. RNA integrity was checked via a denaturing formaldehyde agarose gel (Sambrook *et al.*, 1989): 1.2% (w/v) agarose (HydraGene, Xiamen, China), 10% (v/v) 10× MOPS buffer (400 mM 3-(N-

morpholino) propanesulfonic acid (MOPS), 100 mM sodium acetate, 10 mM ethylenediaminetetraacetic acid (EDTA; Sigma-Aldrich), 16.6% (v/v) formaldehyde). Gel electrophoresis and glass equipment was treated with 2% hydrogen peroxide for 30 min to inactivate RNases. Approximately 750 ng of RNA were mixed with an equal volume of RNA loading buffer (50% glycerol, 1 mM EDTA, 0.4% bromophenol blue, 0.4% xylene cyanol FF) and incubated at 65°C for 10 min for denaturation. Electrophoresis was carried out at 80 V for 45 min in 1× MOPS buffer in a Mini Sub-cell GT gel box (Bio-Rad, Hercules, CA, USA). The gel was stained in 1 mg/ml ethidium bromide for 10-15 min and subsequently destained in dH_2O for 10-15 min. Nucleotide bands were visualised and photographed with a Gel-Doc™ XR linked to ImageLab™ imaging software (both Bio-Rad). To minimise genomic DNA (gDNA) contamination, samples were treated with TURBO™ DNase (Ambion) according to the manufacturer's instructions. To confirm absence of gDNA, polymerase chain reaction (PCR) was carried out using intron-spanning primers of β-tubulin (Joint Genome Institute (JGI) 'Dotse1' protein ID 68998; Table B.1). The mix contained 1× PCR buffer, 2 mM $MgCl_2$, 0.1 mM dNTPs, 0.25 μM each primer, 0.2 U Taq polymerase (Life Technologies, Carlsbad CA, USA), approx. 10 ng of sample or gDNA control, and MQ. Conditions were: Initial denaturation at 94°C for 2 min, 30 cycles of denaturation at 94°C for 30 s, annealing at 51°C for 30 s and extension at 72°C for 25 s, final extension at 72°C for 5 min. Products were visualised after gel electrophoresis (1.5% agarose in Tris borate buffer (TBE, 10.8 g/l Tris, 0.93 g/l EDTA, 5.5 g/l boric acid; pH 8.2) similar to the previous step.

2.3.2. Complementary DNA (cDNA) synthesis and control

For cDNA synthesis, qScript™ cDNA SuperMix (Quanta BioSciences Inc, Beverly, MA, USA) was used according to the manufacturer's instructions and samples were diluted 4-fold with DEPC-treated MQ for PCR applications. To check the cDNA samples for quality and gDNA presence, several reference genes, including *Ds75009* (*Hdp1*), the most highly expressed gene in culture (Bradshaw *et al.*, 2016), and *β-tubulin*, were amplified using specific intragenic primers (Table B.1). Protocols were adapted according to primer melting temperatures and fragment length.

The gDNA contamination check relies on primer pairs, with at least one 'intron-spanning' primer binding to the immediate flanking regions of an intron, which can only occur in exon-only templates. Primer pairs with at least one intron-binding primer serve as negative control in the PCR with RNA or cDNA, and with gDNA control templates, the outcome is the opposite (intron-binding primers, no amplification with intron-spanning primers).

2.3.3. Genomic DNA (gDNA) extraction for whole-genome sequencing

Eighteen isolates of *D. septosporum* (Table 2.2) were chosen for whole-genome sequencing with the main goal to screen them for presence/absence and single nucleotide polymorphisms across all effector candidates and thereby determine if there is evidence of selection pressure to adapt.

For DNA extraction, New Zealand 1965 and 2008 isolates (Table 2.2) were grown on DM agar plates. Four 4 mm agar plugs with mycelium were taken from an actively growing culture with a cork borer and placed on a new DM agar plate, which was sealed with Parafilm® M (Bemis Company, Inc., WI, USA) and incubated at 22°C for at least 10 d. Approximately 1 cm^2 of mycelium was then cut out with a scalpel, placed in a microcentrifuge tube with up to 400 μl of MQ and macerated with a micropestle. Two hundred μl of this liquid was added to 25 ml DM broth in a flask sealed with cotton wool and tin foil and incubated at 22°C and 250 oscillations per minute (opm; BIO-LINE 4610 Incubator Shaker, Edwards Instruments Company, NSW, Australia) for 7 d. Mycelium was harvested by filtration with a nappy liner, snap-frozen in liquid nitrogen and freeze-dried overnight (DuraDry MP, Kinetics Thermal Systems). DNA was extracted using a modified hexadecyl trimethyl ammonium bromide (CTAB) method (Möller *et al.*, 1992): Samples were macerated and 750 μl 2% CTAB extraction buffer (2% CTAB (Sigma-Aldrich), 1% Polyvinylpyrrolidone (PVP) 40 (Sigma-Aldrich), 1.4 M NaCl (Merck), 20 mM EDTA and 0.1 M Tris-HCl (Invitrogen), pH 8; heated to 60°C to dissolve CTAB and PVP) and 4 μl of RNase (20 mg/ml (MQ) Ribonuclease A (Sigma-Aldrich) boiled for 15 min, stored at -20°C) were added to the sample. The mix was vortexed then incubated at 65°C for 20 min. After cooling, an equal volume of 25:24:1 phenol:chloroform:isoamyl

alcohol was added and gently mixed to prevent DNA shearing. Separation into aqueous and non-polar phases was achieved by centrifugation at 16000×*g* for 10 min (Eppendorf 5415 R). The aqueous supernatant (containing DNA) was transferred to a fresh tube, where an equal volume of 24:1 chloroform:isoamyl alcohol was added. After brief mixing, the centrifugation step was repeated. The supernatant was transferred once more and mixed with twice the volume of chilled 100% ethanol, this was then incubated at -20°C for 20 min. Centrifugation was repeated and the supernatant decanted, then 700 μl 70% ethanol was added. This washing step was repeated once. Finally, after decanting the supernatant, the DNA pellet was dried at 37-40°C and re-suspended in 1× Tris-EDTA buffer (TE, for 10× solution: 100 mM Tris buffer (Pure Science), 10 mM EDTA, adjust pH to 8.0-8.5 with HCl; pH re-adjusted for 1× solution).

For quality assessment of gDNA extracted from New Zealand strains as above, as well as gDNA extracted from other strains by Dr Irene Barnes (University of Pretoria) using a similar method, a number of tests were carried out. For purity of the sample, a NanoDrop® ND-1000 UV-Vis spectrophotometer and NanoDrop® software version 3.1.0 was used, following the manufacturer's instructions. If the A260/A280 ratio was between 1.8 and 2.0, the sample was considered pure (NanoDrop Technical Support Bulletin T009). If it was lower than 1.8, salt/ethanol precipitation was applied (see below). A higher value than 2.0 indicated RNA contamination. To check for integrity and RNA contamination, 2 μl (approx. 40 ng) were run on a 1.5% agarose gel with reference uncut Lambda DNA (20, 30, 100 ng) and visualised. To determine the concentration of DNA, a Qubit™ fluorometer (Invitrogen) was used according to the manufacturer's instructions.

An ethanol precipitation protocol was applied to several gDNA samples shown or expected to be impure (containing residues of extraction solvents or proteins). These included freshly extracted DNA as well as DNA obtained from Dr Barnes. The sample volume was made up to 200 μl with TE. To this, 100 μl 5 M ammonium acetate and 500 μl 100% ethanol were added and mixed by flicking. Tubes were stored at -80°C for at least 1 h, centrifuged at 16000×*g* and 4°C for 30 min (Eppendorf 5415 R). The supernatant was discarded and the pellet washed twice with 300 μl 4°C 70% ethanol. Following centrifugation for 5 min as above, the supernatant was discarded and the pellet resuspended in

TE once air-dried.

2.3.4. Sequencing and mapping of genomic DNA reads

Library preparation and Next-Generation Sequencing of the 18 additional strains shown in Table 2.2 was carried out by the Australian Genome Research Facility Ltd., Westmead, NSW, Australia: Illumina HiSeq2500 HT, version 4 chemistry, generating 125 bp paired-end reads.

Raw sequencing data were processed as follows by Mr A. Sim, based on a pipeline used for re-sequencing of *Z. tritici* (McDonald *et al.*, 2015): Reads were trimmed for adapter, primer and low quality sequences with SolexaQA (Cox *et al.*, 2010). Trimmed reads were aligned to the New Zealand reference genome (http://genome.jgi-psf.org/Dotse1/; de Wit *et al.*, 2012) using Bowtie2 v 2.2.6 with –sensitive and –end-to-end parameters (Langmead & Salzberg, 2012). Then the coverage across all genomes was calculated with BEDtools (Quinlan & Hall, 2010; Quinlan, 2014) genomeCoverageBed requiring $\geq 10\times$ coverage. Single nucleotide polymorphisms (SNPs) in the sequences of functionally investigated proteins (chapter 4) were identified by manually examining the consensus sequences of paired-end reads from the respective gene region in each of the 18 sequenced genomes. Sequences were compared using BioEdit (Hall *et al.*, 2011).

For the genome-wide SNP analysis and estimations selection (Bradshaw *et al.*, submitted), mapped reads were analysed using freebayes v1.1.0-46 (Garrison & Marth, 2012) with ploidy set to 1 (haploid) to detect variants between each of the 18 samples and the NZE10 reference[1]. The resulting VCF files were annotated based on the *D. septosporum* NZE10 gene models using SnpEff v4.3t with default parameters, before quality filtering at Q $\geq$ 30 with SnpSift (Cingolani *et al.*, 2012). To estimate selection pressure acting on individual genes within the strain collection from the SNP data, the ratio of non-synonymous to synonymous nucleotide substitutions (dN/dS) was determined for each gene between each pair of the 19 genomes using codeml from the PAML v4.8 package (Yang, 2007). A phylogeny of concatenated SNPs from all of the genomes was built by

[1]The NZE10 reference genome is considered reliable due to its high-quality chromosome-level assembly. JGI uses a combination of gene prediction programmes as well as BLAST homology searches to create gene models, and expressed sequence tag (EST) support is available for this genome. This also improves the confidence for SNP calling.

aligning nucleotide sequences with MAFFT using the E-INS-I parameters (Katoh *et al.*, 2005). Trees were then built using PhyML with default parameters for the maximum likelihood (ML) method (Guindon *et al.*, 2010) (SH-like approximate likelihood ratio-test (aLRT); WAG substitution model; number of substitution rate categories: 4; Gamma parameter: estimated; proportion of invariable sites: estimated; transition/transversion ratio (DNA/RNA): 4).

2.3.5. DNA extraction from infected *Pinus radiata* needles and quantitative PCR.

Lesions obtained from the pathogenicity assay of *P. radiata* with *D. septosporum* (see subsection 2.5.1) were cut, flash frozen with liquid nitrogen and crushed with a plastic micro pestle. A Genomic DNA Mini Kit (Plant) (Geneaid Biotech Ltd., New Taipei City, Taiwan) was used to extract genomic DNA from this tissue following the manufacturer's instructions.

Fungal biomass estimation was based on qPCR as follows. Standard samples were prepared using a dilution series of gDNA from pine needles (100, 20, 4, 0.8 ng, 160, 32, 6.4 pg) and *D. septosporum* wild-type mycelium (20, 4, 0.8 ng, 160, 32, 6.4, 1.28 pg). Primer pairs for *P. radiata* cinnamyl alcohol dehydrogenase (*CAD*) and *D. septosporum AflJ* or *PksA* (Table B.1), respectively, were used with these qPCR conditions: pre-amplification at 95°C for 10 s, 50 quantification cycles with denaturation at 95°C for 5 s, annealing at 60°C for 10 s and elongation at 72°C for 20 s, melting curve to 97°C and subsequent cooling to 40°C (LightCycler® 480 with software release 1.5.0 SP3, Roche, Mannheim, Germany). Fluorescence was detected at 72°C. The first cycle at which the fluorescence can be distinguished from background is the cycle threshold (Ct) value. Standard curves were prepared for reference (*CAD*) and target (*AflJ*/*PksA*) by plotting the logarithm of the plant and fungal standard samples against the Ct values. The same qPCR was done in technical duplicates for each lesion gDNA sample, and biomass was estimated as target to reference ratio for comparison among the different strains in each tree clone.

2.4. Bacterial cultures and cloning

2.4.1. Electrocompetent bacterial cells

To make *Escherichia coli* DH5α and *Agrobacterium tumefaciens* GV3101 cells competent for electroporation with plasmids, they were prepared as follows: A single colony of each strain was incubated in 25 ml LS at 37°C (*E. coli*) or 30°C (*A. tumefaciens*), for approx. 16 h with shaking at approx. 180 opm. Each culture was diluted 40-60×, achieving an optical density (OD_{600} determined by a Pharmacia Biotech Ultrospec 2000 Spectrophotometer (Scinteck Instruments LLC, Manassas, VA, USA)) of approx. 0.1 for the next step. The cultures were incubated in 500 ml LS at the same conditions as above. After 3 and approx. 5 h, respectively, cultures were collected with an OD_{600} of approx. 0.7. Cultures were chilled on ice for 30 min and then transferred to centrifuge tubes pre-cooled on ice. They were centrifuged at 3836×g for 20 min at 4°C (Sorvall RC6+, Thermo Fisher). The supernatant was discarded and 500 ml of 10% glycerol pre-cooled at -20°C were added. Cells were resuspended by gentle swirling on ice and the centrifugation was repeated. The supernatant was discarded and 250 ml of 10% glycerol were added for resuspension. The solution was centrifuged for 15 min, and this wash was repeated three times, halving the added volume each time. Several ml of supernatant were retained in the tubes, sufficient to acquire a milky final cell suspension. This was aliquoted (40 μl) for storage at -80°C to 0.6 ml tubes pre-cooled at -20°C, and snap-frozen using liquid nitrogen.

Cells of both species were tested for electro-competence by electroporation with pUC19B. The cells were thawed on ice and transferred to electroporation cuvettes (Hybaid, Ashford, UK) on ice with approx. 15 ng of pUC19B and subsequently transformed with a Micro-Pulser™ (Bio-Rad) using 2.50 kV for 5.6 ms. Then they were incubated in 1 ml LS for 1 h at 37°C and 30°C, respectively. Twenty-fiveμl of each culture was spread on LS (with 15 g/l agar) supplemented with Amp. Plates with *E. coli* also contained 2.4 μl/ml 2% X-gal and 2.4 μl/ml 20% isopropyl β-D-1-thiogalactopyranoside (IPTG, lac operon inducer). As controls, non-supplemented LS and non-transformed cultures with the same treatment were used. Cultures were incubated overnight (max. 16 h) at 37°C (*E. coli*)

and 30°C (*A. tumefaciens*).

2.4.2. Effector gene cloning

For any module assembly using adhesive overhangs, it is crucial that each overhang pair is unique. Specifically, sequences of interest must not contain restriction enzyme (*Bsa*I) binding sites creating overhangs that match existing overhangs of any other module used. Thus the CE sequence set was scanned for *Bsa*I sites using a custom Python 2.7.1[2] script[3], indicating the 4 bp overhangs of any *Bsa*I site present.

Polymerase chain reaction (PCR) and purification.

To amplify the candidate effector genes for subsequent cloning, individual primers (Table B.1) adding *Bsa*I recognition sites and 4 bp overhangs specific for Golden Gate modular cloning (Engler *et al.*, 2008, 2009), and excluding the start codon and signal peptide sequence, were designed using Primer3 (Untergasser *et al.*, 2012) implemented in Geneious 8.1.8 (Kearse *et al.*, 2012). Primers were synthesised by Integrated DNA Technologies (IDT, Coralville, IO, USA). For the cloning process it is common to use cDNA for the amplification of genes of interest to ensure the correct coding sequence is amplified. However, sufficient RNA/cDNA was not available for all candidate genes due to low expression. If amplification from cDNA (mycelial culture, or late lesion RNA obtained previously (Bradshaw *et al.*, 2016)) was not possible, gDNA was used, provided that the gene did not have any introns predicted (JGI gene model). For four candidates, for which acquiring the (correct) amplicons was not possible, the coding sequence was custom synthesised by IDT.

The 20 μl PCR mix contained 1× Phusion buffer, 0.2 mM dNTPs, 0.5 μM of each primer, 0.4 U Phusion HF polymerase (New England Biolabs, Ipswich MA, USA), 10 ng of template, and MQ. Conditions were: Initial denaturation at 98°C for 1 min, 30 cycles of denaturation at 98°C for 10 s, annealing at 54-58°C for 25 s and extension at 72°C for 25 s, final extension at 72°C for 5 min. Amplicons were visualised after gel electrophoresis (1% agarose in TBE; DNA loading buffer: 20% w/v sucrose (BDH), 5 mM

[2] www.python.org
[3] https://github.com/hulu1/seqIO_basics

EDTA, $Na{\cdot}2H_2O$ (BDH), 1% w/v SDS (BDH), 0.2% w/v bromophenol blue (J.T. Baker Chemical Co, Center Valley, PA, USA) and 0.2% w/v xylene cyanol (Sigma-Aldrich)) and purified via column (High Pure PCR Purification Kit, Roche). If multiple bands were present, the amplicon with the correct size was excised from the gel and purified with a PureLink™ Quick Gel Extraction Kit (Life Technologies, Paisley, Scotland). To increase yield, cDNA amplicons purified from the gel were used as template for a second PCR. If gDNA contamination was apparent, i.e., if larger amplicon with intron(s) appeared on the gel, the cDNA product was gel-purified again, if not, it was purified via column. Product concentrations were estimated with NanoDrop®.

To obtain the 'entry vector' pUC19B, colonies from an *E. coli* DH5α strain carrying the plasmid were incubated in 4 ml LS containing Amp at 37°C overnight with 225 opm shaking. Three ml of the culture were used for plasmid extraction by kit (High Pure Plasmid Isolation Kit, Roche). Plasmid concentration and purity were determined by NanoDrop®.

To create candidate modules, pUC19B was linearised by digestion with *Sma*I. One μg of vector DNA was mixed with 1 μl (10 U) *Sma*I in a 50 μl reaction with 1× CutSmart® buffer (both New England Biolabs), incubated at 25°C for 1.5 h and inactivated at 65°C for 20 min. Then, amplicon and digested vector were ligated using initially a 3:1 (insert:vector) molar ratio. In the 20 μl reaction, 20 ng of vector was mixed with the equimolar amount of the candidate module (depending on concentration and amplicon size), 1.5 μl (7.5 U) T4 ligase (Thermo Fisher), 1× T4 buffer, and MQ. This was incubated at 14°C for 16 h.

Transformation of bacterial cells and plasmid recovery

For plasmid multiplication, 40 μl of competent *E. coli* DH5α cells (see subsection 2.4.1) were thawed on ice and transformed with 5-10 μl of ligation products by electroporation with a MicroPulser™ using 2.50 kV for 5.6 ms. Then they were incubated in 1 ml LS for 1 h at 37°C and subsequently centrifuged at 5000×g for 8 min. The supernatant was discarded and the pellet resuspended in 100 μl LS, 50 μl of which was each spread onto LS (with 1.5 g/l agar) supplemented with Amp, 2.4 μl/ml 2% X-gal and 2.4 μl/ml

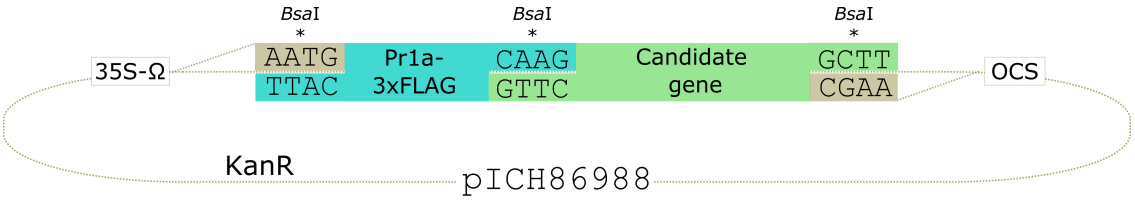

Figure 2.1.: Simplified assembly scheme in the binary expression vector pICH86988. Four-bp overhangs created by *Bsa*I for cohesive ligation are indicated. Insertion of modules also disrupts the *lacZ* gene (not shown). KanR, kanamycin resistance cassette; 35S, cauliflower mosaic virus (CaMV) 35S promoter region, OCS, octopine synthase gene (enhancer of transcription in plant cells).

20% IPTG. Plates were incubated in the dark at 37°C overnight. White colonies were toothpicked into 4 ml LS supplemented with Amp and incubated at 37°C overnight with shaking at 225 opm. Three ml of the culture were used for plasmid extraction by kit (High Pure Plasmid Isolation Kit, Roche). Plasmid concentration and purity were determined by NanoDrop®. To confirm insertion into the vector, 500 ng of plasmid were digested with 0.5 μl (0.5 U) *Bsa*I (New England Biolabs) with 1× CutSmart® buffer in a 20 μl reaction, incubated at 37°C for 1.5 h and inactivated at 65°C for 20 min. Fragments were visualised on a 1% agarose gel.

Candidate modules were sequenced by Massey Genome Service (BigDye® Terminator V3.1 Chemistry) using 300 ng of plasmid and 3.2 pmol M13 primers flanking the insertion site (Table B.1), and stored at -20°C.

Golden Gate assembly

For the one-pot Golden Gate assembly (Engler *et al.*, 2008, 2009), 20 fmol of pUC19B modules, or the purified PCR products directly, were added to 10 fmol of pICH86988, 20 fmol of pUC19B::PR1α-3xFLAG, 3 U T4 ligase with 1× T4 buffer, 1 U *Bsa*I with 0.1% BSA (all New England Biolabs) and MQ in a total reaction volume of 20 μl. The shuffling conditions were: 10 cycles of restriction-ligation at 37°C for 5 min and 16°C for 10 min, digestion at 50°C for 5 min, heat inactivation at 80°C for 5 min. A model of the assembly is shown in Fig. 2.1. For plasmid propagation, 40 μl of electro-competent *E. coli* DH5α cells were transformed with 5 μl of the assembly reaction mix. After recovery (1 h at RT) they were streaked onto LS agar supplemented with Kan, 2.4 μl/ml 2% X-gal and 2.4 μl/ml 20% IPTG, and incubated in the dark at 37°C overnight. White

colonies were transferred (toothpick) into 4 ml LS supplemented with Kan and incubated at 37°C overnight with shaking at 225 opm. Three ml of the culture were used for plasmid extraction (High Pure Plasmid Isolation Kit, Roche). Plasmid concentration and purity were determined by NanoDrop®. To confirm correct assembly, 500 ng of plasmid were digested with 0.5 μl *Mfe*I (New England Biolabs; the vector and PR1α fragment contain one *Mfe*I recognition site each) with 1× CutSmart® buffer in a 20 μl reaction and incubated at 37°C for 1-1.5 h. Fragments were visualised on a 1% agarose gel. Constructs were sequenced as described above using primers flanking the insertion site (pICH86988 For/Rev, Table B.1), and stored at -20°C.

To create stock cultures for the *Agrobacterium* transient transformation assay (ATTA, subsection 2.6.2), 40 μl of electro-competent *A. tumefaciens* GV3101 cells were transformed with approx. 20 ng of construct and incubated in 1 ml LS for 1 h at RT for recovery. Then, 100 μl of these cells were plated on LS agar supplemented with Kan and Rif. Plates were incubated in the dark at 30°C for 2 d (approx. 40 h). Colonies were incubated in 4 ml LS in the dark at 30°C with shaking at 200 opm for at least 16 h. An aliquot of each culture was mixed with 20% glycerol (final concentration) and snap-frozen in liquid nitrogen for storage at -80°C.

2.5. Fungal culturing

2.5.1. *D. septosporum*

To obtain *D. septosporum* spores, all strains were cultured in three stages. DM is a standard maintenance medium and the DSM-PMMG sequence results in the highest sporulation and germination rates (Kabir *et al.*, 2013; Dr Pranav Chettri, pers. comm.). First, mycelium was cultivated on DM agar at 22°C for 7-10 d (from previous culture or glycerol stock). Secondly, mycelium was cut from a growing colony and ground using a plastic pestle in 200 μl of MQ. Fifty μl of this mixture was spread onto DSM agar and incubated at 22°C for 7 d. Thirdly, mycelium was sub-cultured in the same manner onto PMMG agar. After 7 d, the plate was incubated with 1 ml MQ for 10 min, and spore solutions were collected with a pipette after gently scraping the tilted plate with a Drigalski

spatula.

Spore concentrations were assessed by manual counting using a cytometer and phase contrast microscope (Zeiss Axiophot Compound Light Microscope).

2.5.2. *P. pastoris*

Yeast transformants created by Y. Guo and M. Denton-Giles using the 'Pichia Expression Kit' (Invitrogen) were employed in this study: In these, PCR products of the *D. septosporum* homologues of *C. fulvum* effector *Ecp2-1* as well as *Cf-NLP* were each inserted into a pPic9×His6 expression vector, which was then transformed into the *P. pastoris* strain GS115. *B. cinerea* SSP2 and *Sclerotinia sclerotiorum* SSP3 were inserted into pPICZα and strain X-33 was used (Denton-Giles, 2014). Empty vector transformants of the respective strains were also included in the experiments.

Single colony isolates of *P. pastoris* strains were incubated in BMGY in baffled flasks at 30°C and 200 opm shaking for at least 16 h to reach an OD_{600} of at least 2. Cultures were centrifuged at 2880×g for 5 min (Eppendorf 5810). For induction of protein expression, harvested cells were resuspended in BMMY to a starting OD_{600} of 1. This was incubated in baffled flasks at 30°C and 200 opm shaking for 48 h, with methanol (for maintained induction) added to a concentration of 0.5% after 24 h. Cultures were centrifuged at 2880×g (later 4696×g, Hereaus Megafuge 16R, Thermo Fisher) for 10 min and culture filtrates (supernatants) were collected. Culture filtrates were filter-sterilised (ReliaPrep™ syringe filters with cellulose acetate membrane, 0.45 μm, Ahlstrom, Helsinki, Finland) and stored on ice.

2.6. *Nicotiana* spp. growth and assays

2.6.1. *Nicotiana* growth

N. benthamiana and *N. tabacum* seeds were germinated in pots with Dalton's Premium Seed Mix soil (Fruitfed, New Zealand) at 24°C, >70% humidity (not regulated) and 11 h light and 13 h dark photoperiod with 80-85 μ mol $m^{-2}s^{-1}$. After two weeks, seedlings were transferred to individual pots with Dalton's Potting Mix soil supplemented with coarse

grain vermiculite and grown under the same conditions with approx. 60% humidity (not regulated). Infiltration assays were carried out approx. three weeks after transfer; plants were watered in the morning (2-3 h before infiltration) to promote stomata opening.

2.6.2. *Agrobacterium* Transient Transformation Assay (ATTA)

To prepare cultures for infiltration of leaves, *A. tumefaciens* cells from glycerol stocks were streaked on LS plates supplemented with Kan, Rif and Gm (see subsection 2.2.1), and grown in the dark for at least 24 h at 30°C. Colonies were incubated in LS in the dark overnight at 30°C with shaking at 200 opm. Cultures were centrifuged at 3000×*g* for 5 min (Eppendorf 5810), re-suspended in infiltration buffer (10 mM $MgCl_2$, 10 mM MES (Sigma-Aldrich) in KOH, pH 5.6, 0.2 mM acetosyringone (Sigma-Aldrich), MQ) and subsequently diluted in the buffer to the desired optical density. For cell death induction screening, OD_{600} 0.6 and 1.0 were used. For protein collection (see subsection 2.6.6), OD_{600} 0.4-0.5 was used and *A. tumefaciens* AGL1::p19 (inhibiting expression silencing in *N. benthamiana*) was added at a final OD_{600} of 0.1. Infiltration cultures were incubated for 3 h at RT.

One ml needleless syringes (Terumo, Elkton, MD, USA) were used to infiltrate the abaxial side of *N. benthamiana* leaves 2, 3 and 4 (Ma *et al.*, 2012), and the two fully expanded *N. tabacum* leaves, with the diluted cultures. Conditions in this growth room were variable, with plants being exposed to natural light, while 22°C was maintained. Development of necrosis was monitored for up to 7 d, when photographs were taken.

2.6.3. Cell death suppression assays using ATTA

Cell death elicited by *Phytophthora infestans* INF1, the positive control used in my ATTAs, can be suppressed by the intracellular *P. infestans* effector Avr3a in *N. benthamiana*; Avr3a protein can be recognised by *Solanum tuberosum* receptor R3a, which triggers a hypersensitive response (HR) (Armstrong *et al.*, 2005; Bos *et al.*, 2006; section 4.2.4). Constructs (Table 2.1) for the expression of these proteins were used here.

To screen for a) candidate effector (CE)-induced cell death suppression by Avr3a and b) INF1- or CE-induced cell death suppression by other CEs (not inducing cell death),

the following co-infiltration setup was used. Cultures were used with a final OD_{600} of 0.4 each in infiltration buffer. The putative cell death suppressing CEs were infiltrated first (day 0). The cell death eliciting candidates were infiltrated to the same area 24 h later (day 1). Avr3a and INF1 were used as cell death suppression control, and R3a as separate control for Avr3a expression in each leaf (i.e., co-expression of Avr3a and R3a leads to HR). Cell death development was observed for up to 7 d.

2.6.4. Cell death quantification: ion leakage assay

To support the visual assessment of cell death in *Nicotiana* spp., an ion leakage assay was conducted with infiltrated leaves based on Oh *et al.* (2010). The measurement relies on the electrolyte function of ions leaked out of damaged or dead cells, increasing the conductivity of a solution. The measured conductivity is thus a function of total tissue damage.

Effects of ATTA (subsection 2.6.2) were surveyed 90 min ('0 d'), 3 d and 5 d after infiltration. An approx. 0.785 cm^2 leaf disc was taken from each infiltrated zone with a cork borer, including the centre of the infiltration spot, i.e., where the blunt syringe was applied. Two discs from the same leaf were gently agitated in 1.5 ml of dH_2O for 1 h. Three biological replicates were used (discs from three leaves on different plants). After shaking, conductivity was measured by loading 60 μl of liquid onto the sensor cell of a B-173 Twin-Cond device (Horiba, Kyoto, Japan). After each measurement, liquid was removed with a Kimtech Science Kimwipes delicate task wiper (Kimberly-Clark Professional, Roswell, GA, USA).

2.6.5. Cell death quantification: fluorescence imaging

As an additional means of investigating cell death quantitatively, image analysis was conducted. Upon cell death, phenolic compounds accumulate (Heath, 2000a). These compounds are strongly fluorescent under UV excitation, which can be quantified. Total fluorescence intensity was assumed to be a function of cell death in this case.

Infiltrated leaves were assessed 6 dpi. Each leaf was exposed to UV light and photographed using a Gel-Doc™ XR linked to ImageLab™ imaging software (both Bio-Rad).

The standard settings (ethidium bromide preset) were used, except that the exposure was set to 3 s for *N. benthamiana* (not causing pixels to become saturated, i.e., over-exposed in any of the samples). Images were analysed with ImageJ (Abramoff *et al.*, 2004; Schneider *et al.*, 2012). Regions of interest (each infiltration zone) were approximated with the Freehand tool and the Raw Integrated Density (the sum of the grey values of the pixels in the selection) was included in the measurements. Raw Integrated Density was divided by the infiltrated area for normalisation. The resulting value was used for the comparative analysis.

Basic statistics and plotting were carried out in Microsoft Excel.

2.6.6. Collection of apoplastic wash fluid (AWF) from leaves

The *N. benthamiana* ATTA was used to generate proteins of interest (CEs) for applications including immunoblotting and infiltration of protein solutions. The CE proteins are expected to be secreted to the apoplast, thus a method for collection of the apoplastic fluid (O'Leary *et al.*, 2014) was customised. Materials and equipment were pre-cooled at -20°C and kept cold where reasonable.

To overcome likely post-transcriptional gene silencing in the ATTA (Johansen & Carrington, 2001), the viral RNA silencing suppressor p19 is often used (Qu & Morris, 2002; Lombardi *et al.*, 2009; Boivin *et al.*, 2010; Garabagi *et al.*, 2012). An additional strain with the p19 expression vector was thus mixed with each final infiltration culture (see subsection 2.6.2). Fully extended leaves (ideally leaves 2-5 as per Ma *et al.*, 2012) were completely infiltrated using multiple infiltration sites and max. 1 ml of culture per leaf. Empty vector culture (pICH86988), also mixed with p19, served as general AWF negative control.

Leaves were collected 24-48 h after infiltration. Plants were watered approx. 2 h prior to collection. Leaves were set up in a metal cage, separated by string (Fig. 2.2). This was submerged in dH_2O in the vacuum chamber. Full vacuum was applied for at least 1 min, with occasional brief shaking. Then the vacuum was gently released over 10 s. This was repeated once, after which leaves were completely infiltrated by water, as assessed by their transparency. Leaves were cut in half along the main vein with

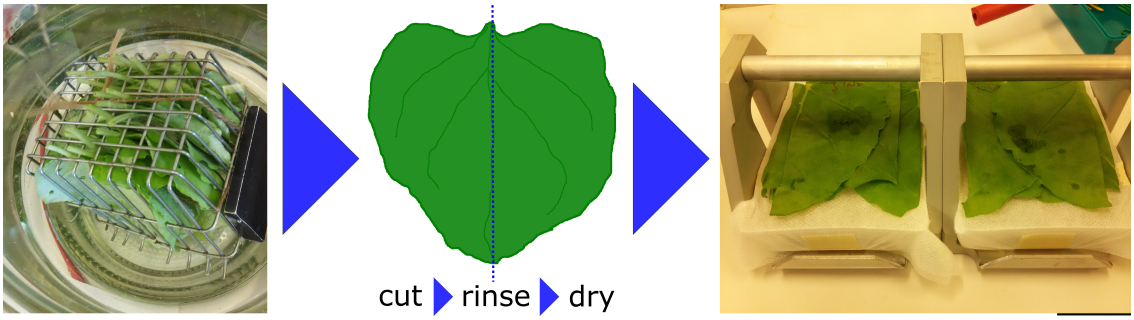

Figure 2.2.: Overview of the vacuum infiltration-centrifugation process for apoplastic wash fluid extraction. Left to right: top view of vacuum chamber, grid setup with string; cutting options (dotted lines); centrifugation assembly example: leaf pieces on top of nappy liner over collection container (shown after centrifugation).

a scalpel blade, and the petiole was removed. All cuts and wounds were rinsed with dH_2O to minimise contamination with intracellular components. Then the leaves were patted dry with blotting paper. For centrifugation, a layer of nappy liner was fitted over the detached plastic lid of a 200 μl tip box with tape stretching the tissue (Fig. 2.2). These fluid collection devices were placed under UV light for 15 min to minimise protease activity, and pre-cooled at -20°C. Up to four surface-dried leaf halves were placed on the liner and fluid extraction was achieved by centrifugation at 1000×g for 9 min (Eppendorf 5810). AWF was collected in one corner of the container and transferred to fresh tubes on ice. The same containers were repeatedly used for the same construct. Protease inhibitor cocktail made up from 1 cOmplete™, Mini, EDTA-free tablet (Sigma-Aldrich) per 10-15 ml was added and dissolved by shaking. For smaller volumes, approx. 10% v/v of concentrated protease inhibitor cocktail made up from one tablet in 1 ml MQ was added to the final volume. Samples were centrifuged at 4696×g at 4°C for 15 min (Hereaus Megafuge 16R, Thermo Fisher) to precipitate plant debris residues. The fluid was filter-sterilised (ReliaPrep™ syringe filters, 0.2 μm) and stored on ice.

2.6.7. Infiltration of AWF into non-hosts

AWF samples were infiltrated into *Nicotiana* spp. with blunt syringes as in the ATTA. Sample aliquots were kept on ice at all times.

2.7. *Pinus radiata* growth and assays

2.7.1. *P. radiata* growth

P. radiata seedlings were provided by Scion in 5×8 plastic trays. At approx. four months age they were transferred to individual pots with Dalton's Potting mix soil in a glasshouse (natural light) at 25°C.

2.7.2. *D. septosporum* pathogenicity assay

To reproduce the observations regarding a potential avirulence effector role of DsEcp2-1 (Guo, 2015), the artificial seedling inoculation assay optimised by Kabir (2014) was repeated.

Approximately seven months old trees of one seed lot, with similar vigour, were selected for the *D. septosporum* infection assay. Each tree was evenly inoculated with an approx. $3.8 \cdot 10^6$ spores/ml solution using a multipurpose hand sprayer (one per *D. septosporum* strain). In order to achieve the highest possible coverage of needles and reduce loss of solution, the spraying took place from four sides (rotating the pot) and in front of the other three replicates. Trees were briefly left to dry and then set up in the assay chamber with two misters, as described originally (Kabir, 2014). Initial double bagging (individual trees covered with a plastic bag within the chamber) was maintained for 4 d. The experiment was carried out in four chambers with 12 seedlings, each chamber representing a replicate.

Two independent *Ecp2-1* knockout strains (A, B) and one *Ecp2-1* complemented knockout (A) strain were used in each replicate. Each chamber also contained two independent wild-type controls, one uninoculated control, and six other seedlings for a secondary metabolite study.

The final assay was terminated in week 11 due to spreading of a contaminating fungus and insect infestation in spite of countermeasures. Collected needles were stored at -20°C. The number of needles with DNB symptoms (i.e. at least one potential developing lesion or clear late lesion) as well as total number of needles per tree were recorded. Lesions were confirmed with a Leica MZ10F binocular microscope (Wetzlar, Germany); needles with doubtful symptoms were discarded.

The fungal biomass in the lesions was determined via DNA extraction and subsequent qPCR as described in subsection 2.3.5.

2.7.3. Vacuum infiltration of tissue culture shoots and detached fascicles

Developing a method for the functional investigation of CEs in pines was one of the main goals of this study. A protocol to infiltrate sterile AWF containing CEs (based on methods outlined in subsection 2.6.6) into clonal rootless pine shoots (subsection 2.1.2) was developed.

The clonal material was kept on LPch agar in glass jars at RT. The callous base of each shoot was washed in sterile water (to remove agar). The shoot was then placed in a 50 ml conical tube (BD Falcon™, Bedford, MA, USA) upside down, avoiding needle or stem damage. The tube had a hole in the lid and contained approx. 30 ml of sample fluid, such that 70-90% of the tissue was submerged. Samples were exposed to vacuum in a glass chamber for at least 3 min. With gas bubbles released from the tissue (aided by shaking), vacuum was gently released, enforcing fluid uptake. The process was repeated once.

Shoots were briefly rinsed in 70% ethanol, followed by sterile dH_2O, and then placed in sterile tap water in a biosafety flow cabinet. Needles were air-dried for max. 5 min. The AWF tubes were returned to ice and reused for subsequent samples (order was recorded). Four shoots were placed in one glass jar with approx. 70 ml LPch agar. The Petri dish lid was sealed with Parafilm® M. Shoots smaller than approx. 4 cm (early trials), or shoots cut in half with a scalpel before the vacuum infiltration, were placed in 1% water agar in a 12-well cell culture plate, and thereafter not kept sterile.

Alternative methods tested prior this protocol are described in Appendix G.

2.8. SDS-PAGE

To assess whether proteins of the predicted sizes were present in the samples, sodium dodecyl sulphate polyacrylamide gel electrophoresis (SDS-PAGE, based on Laemmli (1970)) and western blotting was conducted. To achieve protein separation, 12% separating and

5% stacking gels were used (12% separating gel: 40% v/v 29% bis-/ 1% tris-acrylamide mix (Bio-Rad), 25% v/v 1.5 M Tris (pH 8.8), 1% v/v 10% SDS, 1% v/v 10% fresh ammonium persulfate (APS, Thermo Fisher), 0.04% tetramethylethylenediamine (TEMED, Thermo Fisher); 5% stacking gel: 17% v/v 29% bis-/ 1% tris-acrylamide mix, 13% v/v 1 M Tris (pH 6.8), 1% v/v 10% SDS, 1% v/v 10%, APS, 0.04% TEMED). Both APS (free radical source for polymerisation) and TEMED (stabiliser) were added immediately before casting the gels. For the gel electrophoresis, a Mini-PROTEAN II Electrophoresis Cell system (Bio-Rad) was assembled according to the manufacturer's instructions. Approximately 4 ml of separating gel was pipetted in between the glass plates, then 1 ml of 50% ethanol was used to make the top of the gel horizontal. The gel was left to polymerise for 30 min. The ethanol-water mix was then removed by tilting the casting frame and using suction from Whatman paper (Whatman, Maidstone, UK). Approximately 1 ml of stacking gel was pipetted on top of the set gel and a comb was inserted. This gel was also left to polymerise for 30 min.

Forty-eight μl of each protein sample were mixed with 12 μl 5× SDS sample buffer (25% v/v 1 M Tris-Cl (pH 6.8), 8% w/v SDS, 0.1% w/v bromophenol blue, 40% v/v glycerol, dH_2O) and denatured in a heating block at 96°C for 10 min. In the chamber with SDS running buffer (1× Tris-glycine (TG, 30.3g/l Tris-base, 144 g/l glycine (United States Biochemical Corp./Thermo Fisher), pH 8.3, 10 g/l SDS for 10× stock; diluted to 1× in dH_2O), 18 μl of each sample was loaded onto the gel along with 14 μl of PAGE-RULER™ prestained protein ladder (Thermo Fisher).

Electrophoresis was carried out using a PowerPac 300 (Bio-Rad) at 60 V until the dye uniformly reached the separating gel (roughly 20 min), followed by 150 V until it moved to approx. 1 cm from the bottom of the gel (roughly 60 min).

2.9. Western blot

After electrophoresis, the gel was removed from the glass and its surface washed with dH_2O. It was placed on a piece of Whatman paper pre-wetted in blotting buffer (70% dH_2O, 20% methanol, 10% TG). An Immun-Blot® PVDF membrane (Bio-Rad) pre-wetted in methanol was placed on top of the gel, followed by another piece of Whatman

paper. Any air bubbles were eliminated. The 'sandwich' assembly with foam buffer pieces was then placed in the blotting chamber containing blotting buffer. Transfer was carried out overnight (15-16 h) at 20 V (approx. 145 mA) in a 4°C room. After disassembly, the membrane was blocked in Tris-buffered saline with Tween (TBST, 20 mM Tris, 0.15 M NaCl, MQ, pH ˜7.6, 0.2% Tween® 20 (Sigma-Aldrich)) with 3% skim milk for 1 h with gentle agitation. Then the buffer was exchanged with anti-FLAG® M2 antibody produced in mouse (Sigma-Aldrich) diluted to 80 ng/ml in TBST with 3% milk and the membrane was gently agitated for 1 h. The membrane was washed three times with TBST for a total of 20 min. It was then incubated with the secondary antibody, anti-mouse IgG, conjugated with horseradish peroxidase (HRP; Santa Cruz Biotechnology, Dallas, TX, USA) diluted to 50 ng/ml in TBST with 3% milk, for 2 h with gentle agitation. The blot was washed as before and incubated on 0.5-1 ml of SuperSignal™ West Dura Extended Duration Substrate (HRP substrate mixed 1:1 with buffer; Thermo Fisher) for 5 min. Digital imaging was conducted using chemiluminescence mode of an Azure c600 imager (Azure Biosystems, Dublin, CA, USA). Thereafter, the blot was stained with Ponceau S solution (Sigma-Aldrich) to visualise protein transferred from gel to membrane.

2.10. Computational work to identify and describe candidate effector (CE) proteins

2.10.1. Prediction of CEs

To acquire a shortlist of CEs, the following seven-step pipeline (also shown as Fig. 2.3) was adapted from others (do Amaral *et al.*, 2012; Haddadi *et al.*, 2016):

1. The genome sequence of *D. septosporum* NZE10 (CBS 128990), as well as gene models and predicted protein sequences (de Wit *et al.*, 2012), were downloaded from the Joint Genome Institute (JGI; http://genome.jgi.doe.gov/Dotse1.home.html).

2. Effectors generally have to be secreted and contain an N-terminal secretion signal (signal peptide). Signal peptides that direct proteins through the classical fungal secretory pathway were predicted using the SignalP 3.0 programme (Bendtsen *et al.*, 2004).

3. Some non-secreted molecules, namely integral membrane proteins, membrane-bound proteins and various intracellular organelle proteins are known to also possess a signal peptide sequence (Emanuelsson *et al.*, 2007). To provide increased confidence that the predicted proteins passing (2) are secreted, those sequences were further queried with the following algorithms: TMHMM 2.0 (Krogh *et al.*, 2001) to ensure absence of transmembrane domains (helices outside of the signal peptide domain) which would indicate localisation at the plasma membrane, BIG-PI (Eisenhaber *et al.*, 2004) to check for glycosyl-phosphatidylinositol (GPI) lipid anchoring to the membrane and TargetP 1.1 (Emanuelsson *et al.*, 2000) for a prediction of subcellular localisation based on the N-terminal mitochondrial targeting peptide (mTP) and other intracellular locations. Proteins with any of these features were discarded; the remaining set of proteins was labelled as secretome for future reference.

4. To identify candidates most relevant to the *D. septosporum*–pine interaction (i.e., expressed during infection of pine), expression data from the time-series infection transcriptome study (Bradshaw *et al.*, 2016) were employed. More specifically, these expression data were used to select genes encoding candidate proteins from the predicted secretome with a normalised RNA abundance value (RPMK; Reads Per Million per Kilobase) above an arbitrary threshold. Candidates with more than 50 RPMK in at least one infection stage (Fig. 2.4) were considered potentially important for the interaction.

5. The candidates that passed the threshold in step 4 were divided into four categories: small secreted cysteine-rich proteins (SSCPs), small secreted proteins (SSP), large secreted proteins (LSP) and carbohydrate-active enzymes (CAZys or CAZymes). SSCPs comprised the category of most interest since many effector proteins described so far are SSCPs, including the homologues in *C. fulvum* (Rep, 2005; Kamoun, 2006, 2007; de Wit *et al.*, 2009a; Liu *et al.*, 2012), and the strong disulphide bonds formed by cysteine pairs are thought to confer stability in the plant apoplast (Luderer *et al.*, 2002a). CAZys were treated as a distinct group because they are increasingly shown to be involved in infection (Cantarel *et al.*, 2008; Ökmen *et al.*, 2013; Lombard *et al.*, 2013; Lyu *et al.*, 2015), and are well curated for the *D. septo-*

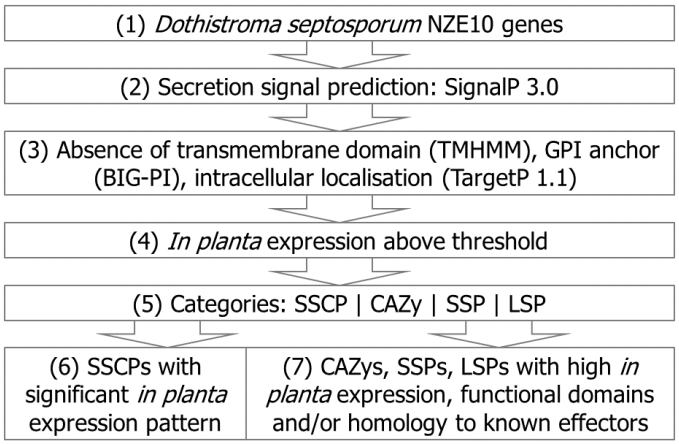

Figure 2.3.: Pipeline for the selection of candidate effectors (CEs). Numbers on the left refer to the steps outlined in the text. SSCP, small secreted cysteine-rich proteins; SSP, small secreted proteins; LSP, large secreted proteins; CAZy, carbohydrate-active enzymes. The two bottom boxes represent the CE shortlist. Figure modified from Hunziker *et al.* (2016) with permission.

sporum genome (de Wit *et al.*, 2012); notably they include some SSC-type proteins. The remaining secreted proteins were labelled as SSP (i.e., max. 300 amino acids with less than four cysteine residues), and LSP (more than 300 amino acids).

6. The SSCP type was further assessed for high or low expression at specific *in planta* stages of infection at 3 weeks ('Early', biotrophic/symptomless stage), 8 weeks ('Mid', early nectrophic lesions), and 12 weeks ('Late', mature sporulating lesions) post-inoculation compared with in culture (Kabir *et al.*, 2015; Bradshaw *et al.*, 2016). Those SSCPs significantly up-regulated at least two-fold ($q<0.05$; Storey *et al.*, 2003) in the Early stage were selected as CEs likely to generally support colonisation (biotrophic), and those in Mid or Late stage as CEs likely to promote the destruction of host tissue (necrotrophic).

7. To add further CEs of interest, the selection was augmented by genes in the three other categories (SSPs, LSPs, CAZys) if they had very high *in planta* expression (at least 500 RPMK) or homology to known effectors or pathogenesis-affiliated domains such as LysM, based on previous annotations from Interpro scans and Gene Ontology terms (de Wit *et al.*, 2012).

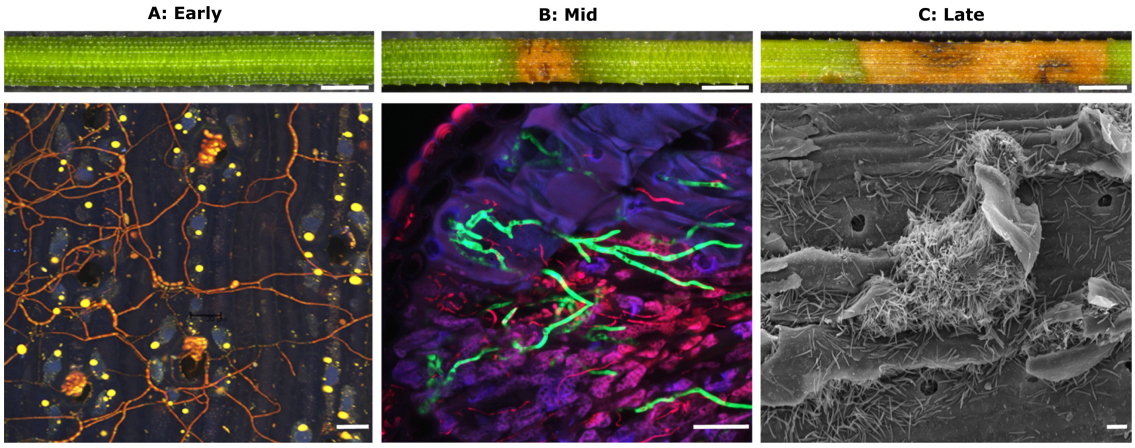

Figure 2.4.: Stages of Dothistroma needle blight on *Pinus radiata* needles used for transcriptome samples. A-C, Early, Mid and Late stages of disease caused by *D. septosporum* NZE10 on *P. radiata*. A) Confocal view of epiphytic fungal growth, stained with trypan blue, over the needle surface at Early stage; hyphae have penetrated the needle through stomatal pores and colonized epistomatal chambers (bottom), but there are no macroscopic needle symptoms (top). B) Confocal needle cross-section showing mesophyll colonization by a green fluorescent protein-labelled strain (Kabir *et al.*, 2015) at Mid stage (bottom) when lesions are first evident on the needle surface (top). C) Scanning electron microscopy image of needle surface at Late stage when masses of spores are released from an erupted mature lesion in the needle (bottom). Extended necrotic bands with black fruiting bodies are evident on the needle surface (top). Macroscopic (top) and microscopic (bottom) size bars are 1 mm and 20 μm, respectively. Figure reproduced from Bradshaw *et al.*, 2016.

2.10.2. Further investigation of CEs

Effectors can be unique to a species, to a group of related species, or widely shared. To determine which is the case for each of the 55 *D. septosporum* CEs, sequence homology searches were conducted.

To identify similarities to proteins of related pathogens and possibly sequences associated with virulence functions, the full protein sequence of each CE was subjected to BLASTp 2.5.1+ (Altschul *et al.*, 1990, 2005) on the NCBI website, querying Dothideomycetes (taxid 147541) only and using an Expect (E) value threshold of 1E-05. Sequences of CEs that induced cell death (chapter 4) were resubmitted more recently (BLASTp 2.8.0+), and they were queried against the 123 Dothideomycetes and 145 Sordariomycetes genomes available at the JGI portal (same threshold).

To find similarities, or paralogues, among candidates, local BLASTp 2.5.0+ was carried out with the set of 55 CE versus itself (local database) with an E value threshold of 0.01. The best hits for each protein were compared and reciprocal matches flagged. The set was

also queried against all *D. septosporum* proteins. Annotations of candidates and top hits, if available, were compared. Paralogues, if predicted to be secreted, were then considered to be included in the functional screening as well.

Given the progress since the genome comparison of *D. septosporum* und *C. fulvum* in 2012, a renewed comparison of the current CEs of these two species was conducted. BLASTp at the JGI server was used to determine orthologues of *D. septosporum* and *C. fulvum* with filtered gene model (proteins) databases (E<1E-05); the best hit was queried reciprocally and direct orthology was assumed if the original gene was the best hit in the species. This information was added to the corresponding candidate for potential follow-up investigation of orthologues.

Since protein structure can be conserved even if the primary sequence is not (de Guillen *et al.*, 2015; chapter 3), homology searches were extended to the secondary structure. Thus, each CE protein sequence was submitted to the structure prediction programme HHpred (Söding, 2004; Zimmermann *et al.*, 2018) using default parameters. The quality of matches was assessed based on the author's suggestions found in the Help section of the HHpred website. Most importantly, homology was only assumed if the probability was over 80% and the alignment was of a biologically meaningful length (e.g., the signal peptide was ignored). The cell death inducing CEs and CEs with high-scoring HHpred hits were further investigated as follows. For comparison of results and investigation of intrinsic disorder, protein sequences were also submitted to PsiPred (Jones, 1999; Buchan *et al.*, 2013) including the optional pGenTHREADER (Lobley *et al.*, 2009). Tertiary structures were predicted and compared to default existing databases with the i-TASSER suite (Yang *et al.*, 2015).

To gain additional confidence in the apoplastic localisation of proteins, the CE sequence set was furthermore submitted to ApoplastP. This machine learning algorithm predicts whether pathogen or plant proteins localise to the apoplast based on classifiers identified from positive and negative training sets (Sperschneider *et al.*, 2017; also see Appendix C).

The heat map for the CE expression data was created with R (RStudio Team, 2016) using the heatmap.2 function of the gplots package for R. The circular genome illustration was created with Circos (Krzywinski *et al.*, 2009).

2.10.3. Protein alignments

Protein sequence alignments using Clustal Omega (Sievers *et al.*, 2011) were carried out in Jalview (www.jalview.org) with default similarities shading (30% conservation). Cysteine residues were highlighted manually.

Using these alignments, phylogenetic trees were calculated via www.phylogeny.fr using PhyML 3.1 with defaults (SH-like approximate likelihood ratio-test (aLRT); WAG substitution model) (Dereeper *et al.*, 2008; Guindon *et al.*, 2010).

Chapter 3.

Identification of new candidate effectors of *Dothistroma septosporum*

3.1. Introduction

Plant pathology research has been revolutionised by computational biology. Cheap genome sequencing, paired with high-quality assembly methods, have made the availability of microbial genomes, and with them the prediction of effectors, a common part of molecular pathology studies. Effectors of plant pathogens are diverse in function and sequence (see section 1.2.4). The sequence diversity makes effector identification challenging, even in the age of genomics, and is exemplified by fungal effectors which lack common sequence identifiers that an initial genome-wide search could be based on (Sperschneider *et al.*, 2017). The first basic step to identify effectors is scanning for signatures of secretion in a given set of predicted protein sequences—this has been done in virtually every effectoromics study to date. Further, information on protein expression during the infection of the host is highly useful to make an 'educated guess' about which proteins are specifically important for successful infection. Lastly, predictions of the protein functions based on similarity to characterised proteins can aid in elucidating the purpose of a specific CE.

In a study by de Wit *et al.* (2012), where the genomes of the close relatives *D. septosporum* and *Cladosporium fulvum* were investigated and compared, it was shown that some fungal effectors are conserved in both sequence and function. Homologues of several functional *C. fulvum* effectors were found in the genome of *D. septosporum*. For two of

these effectors, Avr4 and Ecp2-1, avirulence function was shown to be conserved (de Wit *et al.*, 2012). A subsequent study revealed that, for Avr4, virulence function was also conserved (Mesarich *et al.*, 2016). These findings are particularly interesting, given that the hosts of *D. septosporum* and *C. fulvum* (pine and tomato) are distantly related.

In contrast to the insights of de Wit *et al.* (2012), sequence homology appears to be rather uncommon among fungal effectors. However, apoplastic fungal effectors, including the conserved Avr4, Ecp2-1, and Ecp6 (Stergiopoulos *et al.*, 2010), are small secreted cysteine (Cys)-rich proteins (SSCPs) of less than 300 amino acids in length with four or more Cys residues (Sperschneider *et al.*, 2015), and this gave rise to the concept that small secreted fungal proteins rely on disulphide bridges formed by Cys pairs for increased stability in the hostile environment of the apoplast (Joosten *et al.*, 1997; Luderer *et al.*, 2002b; van den Burg *et al.*, 2003). Supporting this, 23 of 29 experimentally characterised apoplastic effectors in the most recent fungal dataset are SSCPs (Sperschneider *et al.*, 2017). Further, a study by de Guillen *et al.* (2015) showed that sequence-unrelated ascomycete effectors can have very similar structures and thus conserved functions. More specifically, the structure-stabilising disulphide bridges of Cys pairs were found in similar positions in the investigated proteins. The authors argued that during an overall diversifying selection, basic protein architecture may often be conserved while surface properties could rapidly evolve. This would be a reason why sequence homology, unless in closely related species, can no longer be detected. In contrast, "structure-informed and pattern-based searches reveal the hidden relatedness of ascomycete effectors" (de Guillen *et al.*, 2015). Conserved structures of effectors are also found within other taxonomic groups, such as basidiomycete rusts (Franceschetti *et al.*, 2017).

While most extracellular fungal effectors appear to be SSCPs, there are also other secreted molecules reported to have roles as effectors, such as NRPS-PKS hybrid products, and carbohydrate-active enzymes (CAZys) which are often larger than 300 aa and not necessarily Cys-rich, e.g., Tom1 (345 aa, 2 Cys) from *C. fulvum* (Lo Presti *et al.*, 2015). Thus, such proteins or proteinaceous molecules outside the SSCP definition should also be considered when predicting novel effectors (Sperschneider *et al.*, 2015). Given the difficulty in identifying fungal effectors, machine (statistical) learning software has recently

been developed to assist with effector prediction. The tool EffectorP predicts effectors from secretomes (Sperschneider *et al.*, 2016, 2018), while ApoplastP determines which proteins are likely to be apoplastic (Sperschneider *et al.*, 2017). The confidence in these tools, based on how they work, is discussed in Appendix C.

The first aim of the thesis was to determine an unbiased set of candidate effectors (CEs) in *D. septosporum* with a high potential of functioning as virulence or, additionally, avirulence factors in DNB by combining protein characteristics, *in planta* expression data and functional predictions. This work is described in this chapter. As ApoplastP and EffectorP 2.0 were released well after establishing the shortlist of *D. septosporum* CEs, the respective prediction results were added for discussion and future consideration.

3.2. Results

3.2.1. General effector prediction pipeline

The genomes of fungal pathogens are generally small compared to those of their plant hosts. Still, they encode myriads of genes and it is not a trivial task to determine which genes are specifically required for pathogenicity or virulence. Thus, the pool of genes needs to be narrowed down, eventually applying educated guesses about which genes are of interest. Here a bioinformatics pipeline similar to others, published previously and since (do Amaral *et al.*, 2012; Haddadi *et al.*, 2016; Kamel *et al.*, 2017; Sharpee *et al.*, 2017), was assembled to identify CE genes from *D. septosporum*.

The predicted proteome of *D. septosporum* NZE10 was narrowed down as follows (Fig. 3.1): SignalP predicted 1,487 proteins to have a signal peptide (Fig. 3.1, steps 1 and 2; SignalP version 3.0 was used as recommended by Sperschneider *et al.* (2015) due to its overall performance on fungal test data sets). Of these, only 875 were predicted to be secreted based on absence of transmembrane helices, GPI anchors and target peptides for cell compartments (step 3). To find proteins of interest that are relevant to infection, the time-course expression data from Bradshaw *et al.* (2016) was employed. Of the 875 putative secreted proteins, 397 showed expression *in planta* above the arbitrary threshold of 50 Reads Per Million per Kilobase (RPMK) (step 4), suggesting their potential to

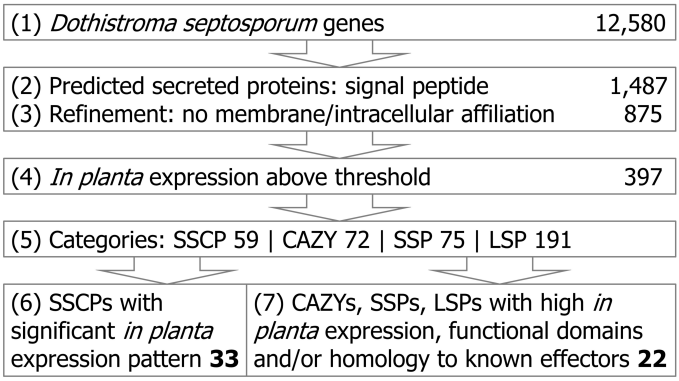

Figure 3.1.: Pipeline results for the selection of candidate effectors (CEs). The number of CEs remaining after each step is shown on the right. SSCP, small secreted cysteine-rich protein; SSP, small secreted protein; LSP, large secreted protein; CAZy, carbohydrate-active enzyme. Proteins selected at steps 6 and 7 constitute the working shortlist of CEs. Figure reproduced from Hunziker *et al.* (2016) with permission.

function in the *D. septosporum-–P. radiata* interaction. Step 5 shows the distribution of 'expressed' candidates in the four categories distinguishing Cys-rich from Cys-poor SSPs, as well as large secreted proteins (LSP) and proteins identified as CAZys. Finally, 33 SSCPs showed significant at least two-fold up-regulation in at least one *in planta* stage compared with in culture growth (step 6). Then, 22 other secreted proteins with at least two-fold up-regulation and very high expression, and/or sequence features of characterised fungal effectors such as LysM domains or glycoside hydrolase activity (O'Connell *et al.*, 2012) were also selected (step 7). The final size of the set was arbitrarily capped at 55 candidates. The protein sequences of these CEs are listed in Table C.1.

The 33 *in planta*-induced SSCPs include homologues of the previously characterised *C. fulvum* effectors CfEcp2-1 and CfEcp6 (de Wit *et al.*, 2012), as well as direct orthologues of *C. fulvum* effector candidates CfEcp19-2, CfEcp20-1, CfEcp20-3, CfEcp45, CfEcp57-1, CfEcp58-1 and CfPhiA-2 (Mesarich *et al.*, 2017; Table 3.1, Table 3.2). They were correspondingly named DsEcps and DsPhiA-2 here. The homologues of CfAvr4, CfEcp13 and CfEcp14-1 were included among the 22 other secreted proteins of interest for the sake of completion, even though they showed very low expression levels during the infection of pine.

3.2.2. Expression profiles

Gene expression data (Bradshaw *et al.*, 2016) corresponding to the three infection stages of pine (Kabir *et al.*, 2015) are shown in Table 3.1 in two formats. Firstly, normalised reads values (Reads Per Million per Kilobase, RPMK) allow for direct comparison of RNA abundance *in planta*. Secondly, the heatmap represents expression profiles during infection as fold changes compared to RPMK in culture, highlighting genes that were highly induced *in planta*, regardless of abundance.

There was a minor trend for strong up-regulation in the Late infection stage, compared to in culture, among all 55 candidates (Fig. 3.2; overall average/median fold changes: Early 7.5/2.4, Mid 14.9/2.4, Late 44.9/5.1). Of 26 genes significantly up-regulated at least 10-fold, this was the case for eight exclusively in the Late stage, but only for two in Mid stage and three in Early stage. This trend may be linked back to the finding that *D. septosporum* has waves of gene expression and the largest proportion of SSCPs is induced at the Late (necrotrophic) stage rather than the earlier stages where defence-manipulating effectors generally act (Bradshaw *et al.*, 2016). Here it does appear that mainly CEs with unknown function, 57% of which are SSCPs, were strongly up-regulated and/or highly expressed in the Late stage (Table 3.1, Table C.1).

3.2.3. Homology search and functional annotations

To predict virulence functions, or plant-pathogen interaction functions in general, the 55 shortlisted CEs were queried for homology in the Dothideomycetes (NCBI database). Additionally, secondary structures were predicted with HHpred. Twenty-eight CEs had hits to hypothetical proteins of unknown function, with a large range of hit numbers (Table 3.1). The remaining 27 CEs showed hits to proteins for which general characteristics had been predicted (e.g., cell wall-associated), superfamilies, or specific domains as expected based on existing annotations (e.g., LysM). It was expected that for members of diverse families, such as the glycoside hydrolases, copious homologues would be found. This was indeed the case, however, high hit numbers were not limited to these classes. Six CEs (DsCE15, DsCE21, DsCE23, DsCE26, DsCE30, DsEcp58-1) showed similarities with over 50 other hypothetical proteins, one among them with over 100 and one over 200 hits. On

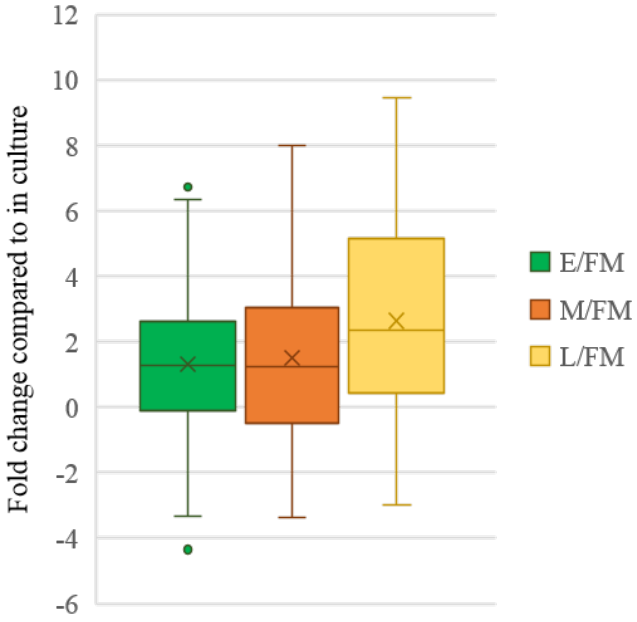

Figure 3.2.: Range of expression ($\log_2$) fold changes of 55 candidate effectors in the *Dothistroma septosporum* NZE10 infection stages Early, Mid and Late (E, M, L) compared to in culture (fungal mycelium, FM). The lower and upper hinges correspond to the first and third quartiles and the upper (lower) whiskers extend from the hinge to the largest (smallest) value that is within 1.5× the interquartile range of the hinge. Data beyond the ends of the whiskers are outliers.

the other side of the spectrum, one CE strikingly only matched with CfEcp19-2. Last, two pairs of paralogous CEs were identified: DsCE2/DsCE4, and DsCE21/DsEcp58-1 (Table C.2).

In summary, CEs selected from the *D. septosporum* secretome show at least some sequence similarities with either known or yet unknown proteins in related species.

Table 3.1.: Features and expression of *Dothistroma septosporum* secreted candidate effector proteins.

ID[a]	Name	Length[b]	Brief description / predictions[c]	Abs. and rel. expression *in planta*[d]					
				Early	Mid	Late	Early	Mid	Late
44908	DsCE1	170 (0)	Similar to hypothetical proteins	134	57	874			
75147	DsCE2	616 (10)	Glycoside hydrolase 13	153	43	680			
71487*	DsCE3	180 (5)	Similar to hypothetical proteins	239	145	982			
70643	DsCE4	493 (8)	Glycoside hydrolase 13	40	19	534			
43416*	DsCE5	125 (4)	Similar to hypothetical proteins	233	193	3732			
72737*	DsCE6	239 (4)	Similar to hypothetical proteins	491	245	8995			
58479	DsCE7	684 (4)	Similar to enzymes	54	24	791			
74875	DsCE8	110 (4)	Similar to hypothetical proteins	10	0	133			
72859	DsCE9	533 (5)	Similar to hypothetical proteins	295	293	774			
21892	DsCE10	256 (16)	Similar to hypothetical proteins	155	69	61			
73520*	DsCE11	114 (0)	Similar to hypothetical protein	819	438	5421			
130443	DsCE12	287 (2)	Ferritin-like superfamily	235	98	1555			
37163	DsCE13	106 (6)	Similar to hypothetical protein	0	46	87			
70694*	DsEcp20-3	135 (4)	Alt a 1- / PevD1-like	4	205	115			
52422*	DsCE14	164 (12)	Expansin/cerato-platanin-like	29	834	532			
131885*	DsCE15	126 (10)	Similar to hypothetical proteins	9	369	203			
158381*	DsEcp2-1	149 (5)	Ecp2-like (Hce2 family)	8	244	18			
51311	DsEcp20-1	145 (4)	Alt a 1- / PevD1-like	62	53	57			
36849†	DsCE16	251 (3)	NAD-binding oxygenase (Rossman)	82	43	76			
69335*	DsEcp57-1	264 (5)	CAP superfamily	1448	1012	554			
71428	DsEcp14	105 (9)	Hydrophobin-like	0	9	6			
71400†	DsCE17	210 (4)	Similar to hypothetical proteins	14	23	62			
73409	DsCE18	280 (11)	Similar to hypothetical proteins	13	19	64			
75848	DsCE19	446 (5)	Glycoside hydrolase 71	166	380	814			
74790	DsCE20	188 (8)	Similar to hypothetical proteins	18	49	159			
72870*†	DsCE21	176 (5)	Putative polyketide cyclase	23	53	130			
75965†	DsCE22	120 (5)	Similar to hypothetical proteins	5	8	64			
73114	DsCE23	159 (8)	Similar to hypothetical proteins	37	26	109			
70053	DsCE24	209 (4)	Similar to hypothetical proteins	125	11	182			
72280†	DsCE25	168 (4)	Putative esterase	21	10	238			
36233	DsEcp19-2	84 (4)	Ecp19-2-like (no other hits)	19	94	68			
69113*	DsPhiA-2	176 (4)	Phialide A-like	83	257	342			
70057*	DsEcp32-3	189 (5)	Similar to hypothetical proteins	467	2569	3312			
73723*	DsCE27	115 (6)	Similar to hypothetical proteins	42	404	556			
36707	DsAvr4	148 (8)	Avr4-like (CBM14 superfamily)	0	14	2			
90760	DsEcp13	82 (4)	Ecp13-like	2	34	59			
70155*	DsCPL1	130 (4)	Cerato-platanin-like	71	507	1303			
46236	DsEcp6	204 (8)	Ecp6-like (3x LysM)	6	606	171			
75692†	DsCE28	481 (4)	VerB (P450 monooxygenase)	17	571	270			
33818	DsCE29	118 (4)	Similar to hypothetical proteins	84	17	37			
75130*	DsCE30	166 (0)	Similar to hypothetical proteins	6349	860	1647			
75932	DsCE31	274 (5)	Expansin-like; endoglucanase	1665	425	491			
132625†	DsCE32	192 (5)	HNHc superfamily	123	7	39			
74062	DsCE33	356 (3)	Similar to hypothetical protein	6386	391	1369			
73248	DsCE34	478 (6)	Similar to enzymes	2888	504	153			
68580	DsCE35	286 (6)	Thaumatin-like	4873	1348	1055			
44875	DsCE36	571 (5)	Similar to hypothetical proteins	2894	675	496			
74289	DsCE37	112 (6)	Similar to hypothetical proteins	165	12	18			
131290*	DsCE38	175 (10)	Chitin binding, LysM	637	89	174			
76918	DsCE39	374 (12)	Similar to hypothetical proteins	48	11	604			
68958*	DsEcp58-1	176 (4)	Putative polyketide cyclase	181	753	3500			
75009	DsHdp1	92 (8)	Hydrophobin	455	6494	4862			
29350	DsCE40	85 (6)	Hydrophobin	133	85	2			
139477†	DsCE41	156 (5)	PhoE family	53	2	2			
62617	DsCE42	434 (7)	Glycoside hydrolase 64	2608	137	16			

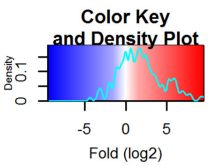

[a] Protein ID in JGI catalogue. Asterisk indicates the gene was cloned for functional analysis in this study. Dagger indicates non-apoplastic localisation prediction (ApoplastP).

[b] Mature protein length (predicted N-terminal signal peptide removed) in amino acids; number of cysteine residues in brackets.

[c] Function predictions based on BLASTp ($E < 10^{-5}$) and HHpred.

[d] Expression during infection stages of *Pinus radiata* (Early, Mid, Late; Bradshaw et al. 2016). Left, Reads Per Million per Kilobase (RPMK); right, heatmap representing fold ($\log_2$) changes relative to in culture expression.

Following the new predicted functions, the CE list is comprised of the following function types: Alt a 1 allergen-like (2), chitin-binding CBM14 (1), chitin-binding/sequestering (LysM) (2), Hce2 superfamily (1), cerato-platanin (1), ferritin-like (1), endonuclease superfamily (1), CAP family (1), PhoE family (1), hydrophobin (3), thaumatin-like (1), phialide A-like (1), NAD-binding monooxygenase (Rossmann fold) (1), structural protein (1), VerB/P450 monooxygenase (1), glycoside hydrolase (4), expansin-like/endoglucanase (2), polyketide cyclase (2), other enzymes (2), unknown (27). These types are discussed in section 3.3.

3.2.4. Protein sizes and cysteine residues of CEs

Foreign proteins secreted into the apoplast of a host must withstand the harsh conditions of this environment. Double bonds between the sulphur atoms of Cys pairs contribute to structural rigidity of proteins, and have been shown to be a feature of most extracellular effectors (see section 3.1). The Cys content of the mature CEs (predicted N-terminal signal peptide removed) in Fig. 3.3 shows that Cys residues often occur in even numbers and that 11 'large' (>300 aa) CEs selected regardless of Cys number still had at least one pair. The 33 DsSSCPs were defined as containing a minimum of four Cys in maximal 300 aa, corresponding to 1.3% Cys abundance. Including the larger CEs, 43 proteins well surpassed this mark (Fig. 3.3). The total average and median was 3.2%, and the peak at 8.7% in one of the smallest CEs (92 aa); the highest absolute number was eight Cys pairs (in 256 aa; 6.3%). In summary, it can be stated that high abundance of Cys pairs, and thus probably conservation of disulphide bridges, is a feature of highly expressed secreted proteins of *D. septosporum*.

3.2.5. Further orthologues to *C. fulvum* extracellular proteins/CEs found

The comparison of the *D. septosporum* and *C. fulvum* (de Wit *et al.*, 2012) genomes had revealed shared avirulence effectors, which provided part of the rationale for this study. Like the *D. septosporum* transcriptome (Bradshaw *et al.*, 2016), new resources have been generated for *C. fulvum* as well since the comparative genome study, including a thorough

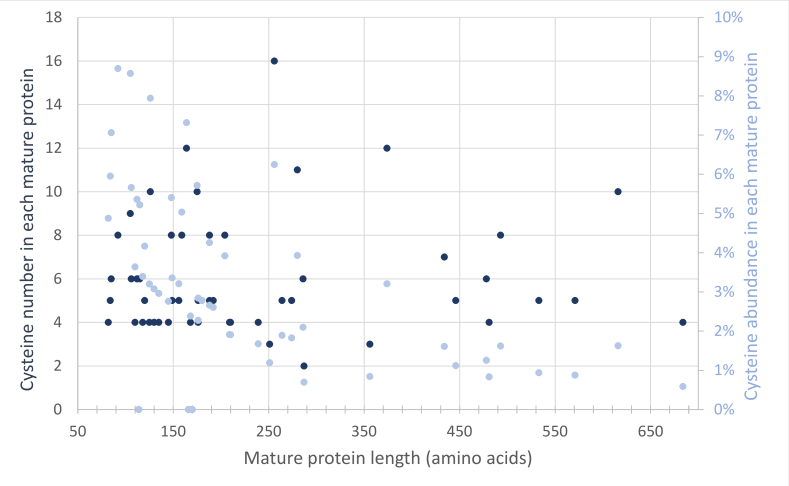

Figure 3.3.: Plot of *Dothistroma septosporum* candidate effector (CE) protein lengths and cysteine counts in their sequences. Each dot represents one CE. Dark blue refers to the absolute cysteine number (left axis) in the mature sequence and light blue to the relative abundance (right axis).

investigation of the *C. fulvum* protein secretome in the tomato apoplast (Mesarich *et al.*, 2017).

Here, the sequences of new DsCEs were compared to newly described *C. fulvum* apoplastic proteins (or extracellular proteins, Ecps) to identify secreted orthologues (top hits in reciprocal BLASTp). The summary with 11 new and 5 known orthologues is given in Table 3.2 (also Mesarich *et al.*, 2017). Seven other proteins had homologues in *C. fulvum* but not direct orthologues (not shown). The individual functional predictions, where available, match well for orthologous genes in the two species. This investigation, amended by HHpred results, uncovered a total of four Ecp20-like orthologue pairs in the two species (see also subsection 3.3.6).

Since *C. fulvum* is biotrophic, and *D. septosporum* has a biotrophic stage, gene expression *in planta* (relative to in culture) was compared between *C. fulvum* and *D. septosporum*. This comparison uncovered contrasting expression of several Ecps in the two fungi (Table 3.2).

Table 3.2: Likely orthologues of small secreted proteins from *Cladosporium fulvum* .

Ds name[a]	Cf name[b]	*C. fulvum* direct orthologue protein description[b]	Fold Cf[c]	Ds E/FM[d]	Ds M/FM[d]
DsAvr4	CfAvr4	Avr effector recognized by the Cf-4 immune receptor, protects cell wall chitin. CBM_14 domain (PF01607)	87.2	-1.1	12.6
DsEcp2-1*	CfEcp2-1	Avr effector recognized by the Cf-Ecp2-1 immune receptor. Hce2 domain (PF14856)	2209.5	5.9	185.8
DsEcp6	CfEcp6	Avr effector recognized by the Cf-Ecp6 immune receptor. Prevents chitin-triggered immunity. 3x LysM (PF01476)	63.3	-8.0	12.9
DsEcp13	CfEcp13	Possible avirulence effector protein. Similar to hypothetical proteins	1039.6	-2.4	6.4
DsEcp14	CfEcp14	Possible avirulence effector protein. Class II hydrophobin	32.2	-3.2	2.9
DsEcp19-2	CfEcp19-2	Similar to hypothetical proteins	12.6	1.7	8.2
DsEcp20-1	CfEcp20-1	Predicted Alt a1 allergen-like fold. Similar to hypothetical proteins	59060.6	3.3	2.8
DsEcp20-2[p]	CfEcp20-2	Predicted Alt a1 allergen-like fold. Similar to hypothetical proteins	16.0	1.7	5.8
DsEcp20-3*	CfEcp20-3	Predicted Alt a1 allergen-like fold. Similar to hypothetical proteins	61.5	-1.1	44.8
DsCE5/Ecp20-4*	CfEcp20-4†	Ecp20-like. Not identified in tomato apoplast	n/a	3.2	2.6
DsCPL1*	CfEcp45	Cerato-platanin protein, single PF07249 Cerato-platanin domain	30.5	-3.6	2.0
DsEcp57-1*	CfEcp57-1	CAP domain (PF00188)	-1.2	3.4	2.4
DsEcp58-1*	CfEcp58-1	Similar to hypothetical proteins. Structure similar to polyketide cyclase, limonene-1,2-epoxide hydrolase	-14.2	-8.8	-2.1
DsPhiA-2	CfPhiA-2	Phialide protein	8.3	1.6	4.8
DsCE42	Cf186242	Glycosyl hydrolase 64 protein, single cd09220 GH64-GluB-like domain	4.3	38.7	2.0
DsCE15*	Cf190095	Similar to hypothetical proteins. Not identified in tomato apoplast	n/a	6.2	255.9

[a] Assigned protein name, or JGI protein ID of the *D. septosporum* Candidate Effector (CE). Asterisk indicates functional analysis in this study. [p] Incorrect protein model in JGI.

[b] Assigned protein name, or JGI protein ID, and function description/prediction of the *C. fulvum* SSP (Mesarich *et al*. 2017; †Battaglia *et al*. unpublished; Avr4 originally identified by Joosten *et al*. (1994), Ecp2-1 by Lauge *et al*. (2000), Ecp6 by Bolton *et al*. (2008)).

[c] Highest recorded fold change of expression of the CfEcp/SSP *in planta* compared to in culture (Mesarich *et al*. 2017). N/A, not available.

[d] Fold change of expression of the DsCE/SP in the early (biotrophic) and 'mid' infection stage compared to in culture (FM).

3.2.6. Distribution of genes encoding secreted proteins in the *D. septosporum* genome

The genomic location of genes can indicate how strongly they are exposed to processes that create drastic changes. Also, in genomes of basidiomycete smut fungi, effector genes were found in clusters (Dutheil *et al.*, 2016). This is thought to facilitate co-regulation of genes with a similar purpose. The genome of *D. septosporum* NZE10 was assembled to chromosome level (de Wit *et al.*, 2012), enabling mapping of genes. In *D. septosporum*, no physical proximity of CE genes to each other was noted (the shortest distance of two CEs was 30 kb, Table C.1). An overview of the genome shows a fairly even distribution of the selected 55 CE genes across all chromosomes (Fig. 3.4). Further, with the positions of all genes encoding predicted secreted proteins and expressed secreted proteins (representing steps 2-4 in the pipeline, Fig. 3.1) plotted, no patterns were found (e.g., specific localisation of a majority of expressed secreted proteins to a certain genomic region; two inner circles in Fig. 3.4).

Proximity to telomeres or repetitive elements (repeats) is sometimes associated with gene loss or mutation in fungi (Chuma *et al.*, 2011; de Wit *et al.*, 2012). The deletion of three (Avr4E, Avr5, Avr9) and inactivation of one (Avr2) *C. fulvum* avirulence effectors was suggested to be linked to repeat proximity and specifically transposon insertions, respectively (Luderer *et al.*, 2002b; de Wit *et al.*, 2012; Mesarich *et al.*, 2014). However, it was already noted that while genes for some *D. septosporum* effector homologues of *C. fulvum* are close to repeat-rich regions (*DsEcp2-1* and *DsEcp13* in particular, Table C.1), the biological significance of that is yet unclear (de Wit *et al.*, 2012). Additional to the effector homologues, the *DsPhiA-2* (69113) gene is fourth-closest to repeats in the genome. It is located 1088 bp away from a long terminal repeat (LTR) retrotransposon, with six further repeats within less than 2,000 bp of its locus. Further, *DsCE6* (72737) and *DsCE19* (75848) were found less than 20 kb from repeats. *DsCE24* (70053), *DsCE28* (75692) and *DsHdp1* (75009) were found within 30 kb of a telomere on their respective chromosomes.

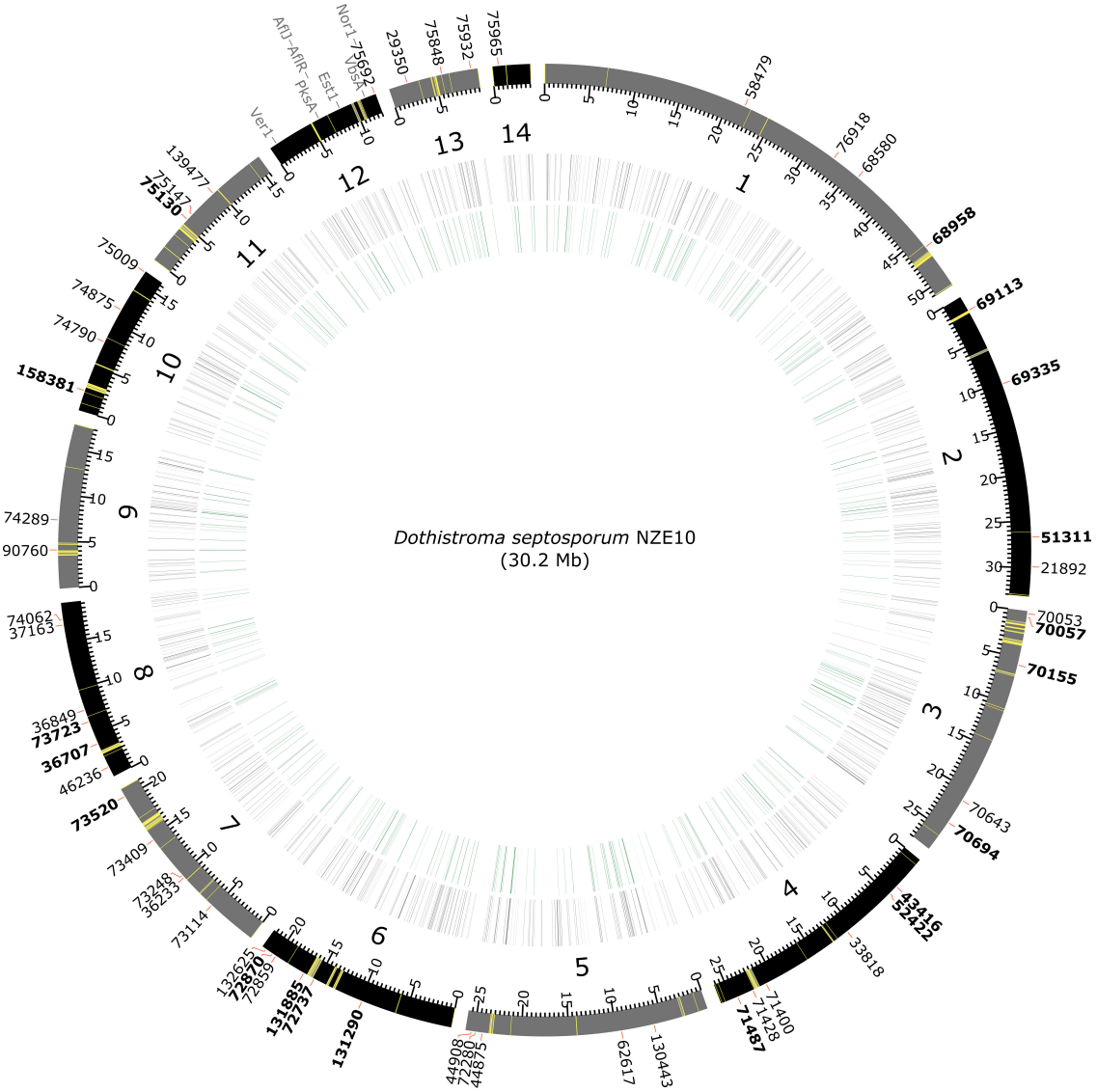

Figure 3.4.: Location of 55 candidate effector (CE) genes in the *Dothistroma septosporum* NZE10 genome. The 14 NZE10 chromosome-level scaffolds are represented by the outer bars. Each minor tick marks 5000 bp from the start of the scaffold; yellow stripes indicate the location of curated repetitive elements >200 bp (Ohm *et al.*, 2012). Outer numbers are protein IDs corresponding to the 55 CE genes, with cloned CEs in bold font. For reference, the positions of the dothistromin biosynthesis gene loci are also shown (chromosome 12, grey labels). Within the inner rings, grey bars represent the 875 genes encoding secreted proteins, and green bars (innermost) represent those for the 397 *in planta* expressed (RPMK >50) secreted proteins.

3.2.7. Sequence variability of CEs in 19 *D. septosporum* genomes

It is established through the arms race concept that effector genes are often subject to rapid evolution. If a crucial effector becomes an IP that is recognised by a host plant, its mutation, down-regulation or loss has to occur in order to escape recognition, unless another effector (or mechanism) interferes with this IP recognition (example given in section 1.2.4). In some cases, mutations may alter the PRR interaction site but not protein function, as shown in *Fusarium oxysporum* Avr2 (Di *et al.*, 2017) and *C. fulvum* Avr4 (Hurlburt *et al.*, 2018). If an IP protein is indeed indispensable for the fitness of the pathogen, such mutations are the only viable option for the IP to escape recognition. The investigation of sequence variability in different strains of a pathogen can thus provide valuable information regarding selection acting on CEs.

The following work represents an extract from a *D. septosporum* genome comparison study. I contributed to the genome sequencing of 18 *D. septosporum* strains selected from diverse geographic locations (some collected up to 50 years ago) and a range of pine host species, mainly with laboratory work preparing the genomic DNA. The main results of this study, which are not presented in this thesis, have been submitted for publication.

Phylogeny based on gene polymorphisms

Most strains showed high overall alignment of reads to the NZE10 reference genome sequence and over 70× coverage. Exceptions were the Guatemala and Colombia strains. Genome coverage and mapping statistics are summarised in Table C.3A. Single nucleotide polymorphisms (SNPs) compared to the NZE10 reference genome were also determined in the 18 genomes. Based on the average number of SNPs per gene, the two New Zealand strains isolated in different years and locations, NZE2 and NZE8, are highly similar to NZE10 (˜0.01 SNPs per gene; Table C.3A), which is in line with the New Zealand population being described as clonal (Barnes *et al.*, 2014). All Colombian and Guatemalan (COLN, COLS, GUA1 and GUA2) strains were found to be the most different from NZE10 (˜29 SNPs per gene; Bradshaw *et al.*, submitted). A whole-genome SNP-based phylogeny performed by Dr P.-Y. Dupont shows that, in general, strains group geographically and while the Colombian and Guatemalan strains are genetically most distant from all others,

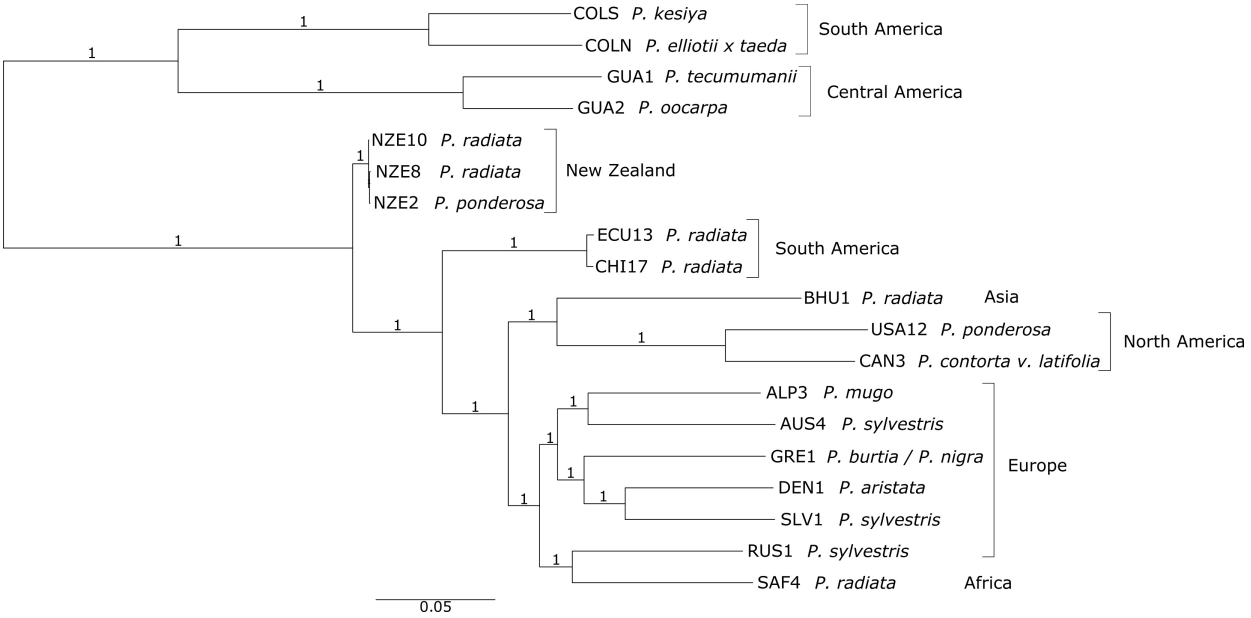

Figure 3.5.: Whole-genome SNP phylogeny of the 19 sequenced strains of *Dothistroma septosporum*. Unrooted maximum likelihood phylogeny based on 5851 concatenated SNPs. The size bar represents the number of mutations per nucleotide. The numbers at the nodes (1) are approximate likelihood ratio test (aLRT) values, indicating high confidence in the branches. (Courtesy of P.-Y. Dupont.) The *Pinus* host each strain was isolated from is indicated.

there is also considerable distance between them (Fig. 3.5). Interestingly, the Russian (RUS1) and South African (SAF4) strains were closest to each other, and the only Asian representative from Bhutan (strain BHU1) was most similar to the two North American strains (USA12 and CAN3).

General investigation of CEs in 19 *D. septosporum* strains

By the 'zig-zag' nature of pathogen-host interactions (Jones & Dangl, 2006), pressure to adapt is often imposed on the repertoire of effectors (subsection 1.2.5). The presence, potential duplication and sequence variability of the CEs in the 18 new sequenced *D. septosporum* genomes was investigated. Gene deletion strongly indicates that the deleted gene is not essential to the fitness of an organism. The following deletions were suggested computationally based on reads mapped to the NZE10 genome: *DsCE40* (29350), South Africa (SAF4), *DsCE11* (73520), Austria, and *DsPhiA-2* (69113), Colombia North. The annotated gene regions were checked manually (Integrative Genomics Viewer) and this showed that *DsCE40* and *DsCE11* are absent from corresponding loci in the mentioned strains. Furthermore, no reads for all but the last 13 to 15 codons of DsCE11 were found

Table 3.3.: Duplications of CE genes were found in six *Dothistroma septosporum* strains.

Name[a]	Protein ID	Scaffold	Germany (ALP3)	Ecuador (ECU13)	South Africa (SAF4)	Slovakia (SLV1)	USA (USA12)
DsCE42	62617	5				x	x
DsCE12	130443	5				x	x
DsCE36	44875	5	x				
DsCE1	44908	5	x				
DsCE25	72280	5	x				
DsEcp13	90760	9			x		x
DsEcp2-1	158381	10		x			
DsCE30	75130	11	x		x		x
DsCE2	75147	11	x		x		x
DsCE41	139477	11	x		x		x
DsCE40	29350	13		x			
DsCE22	75965	14	x		x		x

[a] Gene duplications in each respective strain are indicated (x).

in the Chile (CHI17), Colombia South (COLS), Ecuador (ECU13), and Slovakia (SLV1) strains. *DsPhiA-2* appears to be present in the Colombia North strain, with low read counts.

Gene duplication can lead to the accumulation of mutations, even functional diversification, since the duplicated copy is not under immediate selection pressure, i.e, missense mutations are inconsequential because an unaltered copy of the gene is still there. Twelve CE genes were found to be duplicated in at least one genome (Table 3.3), based on copy number variant calculations from read mapping (CNVnator) and verification by a quantitative PCR.

Furthermore, the ratio of non-synonymous to synonymous nucleotide changes ($dN/dS = \omega$) can be used as an indicator of overall diversifying (positive) selection of a protein. Here, a computation using CodeML (of the PAML package) was carried out for all CE genes in the 19 genomes. An ω value below 1 signifies that a protein overall is probably not under positive selection. This was the case for all 55 CEs (Tables C.3B and C.4). However, single amino acid sites may still be under positive selection. It takes a more elaborate method to find such sites, such as the Sitewise Likelihood Ratio (SLR, Massingham & Goldman, 2005). An SLR calculation was carried out for *DsAvr4*, *DsEcp2-1*, *DsEcp4*, *DsEcp5*, *DsEcp6*, *DsEcp13*, *DsEcp14* and *DsEcp57-1*. A few positively selected loci among many conserved loci were determined in most of these genes; *DsEcp2-1* and *DsEcp57-1* both

contain two positively selected loci. *DsAvr4* does not show any sign of positive selection (Table C.5). However, it was concluded that the SLR method was not well suited for the examination of positive selection because the sequences in the 19 genomes are too similar (SLR work done by Dr P.-Y. Dupont).

In the scope of functional analysis (chapter 4), 17 of the 55 CEs were cloned. Most of these 17 had a small number of non-synonymous SNPs when sequences were compared across the 19 *D. septosporum* strains. These SNPs reflected the phylogeny (Fig. 3.5) in general, i.e., SNPs were shared in closer strains, and the Colombian and Guatemalan sequences had most SNPs (Tables C.3). The SNPs in these CEs were manually analysed to predict likely meaningful changes to each protein. The amino acid changes are indicated in Fig. E.1 and briefly discussed in subsection 4.2.1.

None of the 55 CEs appeared to be under diversifying selection according to the dN/dS calculation, but it should also be noted that in the NZE10 genome only 306 genes with $\omega > 1$ were determined using this approach. Of these, 41 were predicted to localise to the apoplast with the new tool ApoplastP 1.0 (prediction independent of an N-terminal secretion signal peptide, see Appendix C) and seven of these were also among the secretome but had very low expression (Table C.4). Meanwhile, some proteins with a range of sizes and expression profiles, and mostly lacking functional predictions, were predicted to have a GPI anchor, implying that they act extracellularly but are covalently bound to the fungal cell wall.

Ds73352 (135 aa, 7 Cys, $\omega = 5.25$), a predicted apoplastic SSCP without a signal peptide, has the highest computed ω in the genome. There was no predicted function for this protein based on BLASTp and HHpred queries. Ds73352 had low expression through all stages (FM-E-M-L: 7-57-3-38 RPMK), rendering even the increase from FM to Early negligible. Along with others in this '$\omega > 1$' list, it would be interesting to find out why Ds73352 has accumulated so many mutations.

Ds91219 (308 aa, 11 Cys, $\omega = 2.2$) stood out among GPI-anchored apoplastic proteins because it was the fourth-most strongly up-regulated in the Mid infection stage in the transcriptome (FM-E-M-L: 7-114-1592-120 RPMK). Ds91219 had no sequence homology to proteins in Dothideomycetes (JGI) or other organisms (NCBI) except for a direct

orthologue in *C. fulvum*, Cf187601. Both Ds91219 and Cf187601 were predicted to have structural homology to fungal hydrophobins.

3.3. Discussion

3.3.1. General

Within this chapter, existing genomic and transcriptomic data of *D. septosporum* were mined to improve the foundation for functional studies to better understand the molecular aspects of its virulence. A working resource of 55 *D. septosporum* CEs was generated. This CE set includes many of the most highly expressed and highly up-regulated *in planta* genes of *D. septosporum*. Just over half of them have a variety of possible functions to support the infection of *P. radiata*, including indirect functions like defence against other microbes. The other 27 CEs had no predicted function, which is not unexpected considering the ever-increasing elucidation of the functional diversity among fungal effectors. The shortlist includes newly identified orthologues of *in planta*-induced SSPs (CEs) of *C. fulvum*, most of which also lack a function prediction.

To the best of my knowledge, this is the first time this type of genome-wide approach has been used to identify effectors in a foliar fungal gymnosperm pathogen. Recently, similar work on *Heterobasidion annosum sensu lato* was published (Raffaello & Asiegbu, 2017, section 1.2.4). *H. annosum s.l.* is an opportunistic necrotrophic root pathogen of Scots pine and some other conifers. In that study, a similar selection pipeline for secreted proteins was used, with the notable difference that there were no cut-offs for size or Cys content, and proteins with predicted functional domains or homology to other proteins were excluded. A list of 58 *H. annosum* SSPs was presented, and while these ranged from 58 to 476 aa in length, the majority was 100 to 300 aa, with 1 to 8 predicted Cys-Cys bonds. Thus, even without a preference for small size or Cys content, these numbers are barely different from those of the CEs selected here.

Similar selections based on genome-wide transcription information were made for major fungal and oomycete crop pathogens. These include the Dothideomycetes *Pseudocercospora* spp. (Noar & Daub, 2016; Isaza *et al.*, 2016; Chang *et al.*, 2016), *Zymoseptoria*

tritici (Mirzadi Gohari *et al.*, 2015), *Leptosphaeria maculans* (Haddadi *et al.*, 2016), the Sordariomycetes *Colletotrichum* spp. (O'Connell *et al.*, 2012; McDowell, 2013) and *Magnaporthe oryzae* (Chen *et al.*, 2013b), and the oomycete genera *Phytophthora*, *Pythium* and *Hyaloperonospora* (summarised by Kamoun, 2006). Thanks to these studies, new invasion patterns (IPs) were discovered and at least a handful of putative effectors highly likely to contribute to the success of each pathogen was taken forward for functional studies. In some cases, such discoveries may contribute to effector-based breeding (Mesarich *et al.*, 2017; also see chapter 6).

In *D. septosporum*, CEs overall were slightly more up-regulated in the Late stage than in earlier stages of the infection cycle. This might reflect potential roles of CEs in a) the induction of plant cell death (necrotrophic effectors), b) the need for scavenging and processing of released plant components for metabolism, c) adaptation to a probably changing environment upon the merging of apoplast and plant cell compartments (Keon *et al.*, 2007), and d) increased competitiveness against other (opportunistic) necrotrophic microbes trying to profit from the destruction of host tissue and defences.

To identify homology, or lack thereof, to other proteins is an important step in the characterisation of CEs. Using the BLAST algorithm for this, based on vast numbers of genome sequences available, is among the standard techniques in molecular genetics. However, diverse amino acid sequences can fold into similar protein structures (Illergård *et al.*, 2009). Structure is often linked with function which is in turn subject to selection. Hence, structure is much more likely to be conserved than sequence—this has been demonstrated for a number of ascomycete effectors (Franceschetti *et al.*, 2017). Notably we must differentiate between conserved protein core structure (a 'molecular scaffold' providing stability) and surface properties, which may still be variable, as shown for the MAX effectors (de Guillen *et al.*, 2015). Due to growing databases of fully analysed fungal protein structures and improved prediction software, the focus of homology prediction might shift to secondary and tertiary structure. In the scope of this chapter, the use of HHpred added information about possible CE functions. For the majority of CEs, BLASTp-based functional associations were supported by very similar HHpred results, or no (significant) structural hits were found in the case of BLASTp hits to hypothetical proteins. However,

for eight CEs, HHpred uncovered potential functions, namely: esterase/lipase, Alt a 1 allergen/PevD1-like (2x), bacterial effector Tne2, hydrophobin, polyketide cyclase (2x), expansin-like. These function indications could be valuable for future investigation of the CEs.

As outlined above, Raffaello & Asiegbu (2017) retrieved 58 putative *H. annosum*-exclusive SSPs. I made an HHpred query of randomly selected HaSSPs and this showed that some structural similarities to characterised proteins, such as a lectin, were probably overlooked in this study because only sequence-based homology was considered. In conclusion, structural queries should be carried out in effector prediction studies.

A limitation regarding the expression data used to define the *D. septosporum* CEs should be kept in mind. It has been established that *D. septosporum* has an asymptomatic, biotrophic infection phase before starting to destroy and eventually killing pine needles while sporulating (Kabir *et al.*, 2015). The RNAseq data used in this study was collected from three time points over 12 weeks, representing the three stages 'biotrophic' (Early), 'transition to necrotrophic' (Mid) and 'necrotrophic' (Late). However, the data stem from two biological replicates only, and the infections were not truly synchronous (Bradshaw *et al.*, 2016). The time points had been chosen arbitrarily based on average symptom development, making this representation approximate, especially for the second time point. Thus, the gene expression values (RPMK) do not reflect a precisely defined biological situation. In the following subsections, those CEs with functions predicted by the homology searches (BLASTp and HHpred) are briefly discussed. A short overview with RPMK expression values (FM, fungal mycelium/in culture, Early, Mid, Late) of the CEs in each of these groups is given at the top of each subsection. As in Table 3.1, CEs that were cloned for functional studies (chapter 4) are marked with an asterisk.

3.3.2. Expansin-like proteins: cerato-platanins

Name	Length (Cys)	FM	E	M	L
DsCE14*	164 (12)	13	29	834	532
DsCPL1*	130 (4)	257	71	507	1303
DsCE31	264 (5)	465	1665	425	491

DsCE14 (52422) was labelled as an unknown protein based on BLASTp (hits to 15 hypothetical proteins); however, it had high scoring predicted structural matches to plant and bacterial expansins, and expansin-like proteins. Matches to the latter included a mollusk β-endoglucanase (GH45), papaya kiwellin, a fungal papain inhibitor (transglutaminase), plant defence elicitors, and fungal cerato-platanins. This diversity is most probably owed to a similar double-$\Psi\beta$-barrel fold occurring in expansin-like proteins across kingdoms (de Oliveira *et al.*, 2011). DsCE31 (75932) had very similar predictions. A function within the cerato-platanin group seems likely for secreted fungal expansin-like proteins. DsCPL1 (70155) was specifically predicted as a cerato-platanin homologue with high consistency among approaches (1°, 2° and 3° structure prediction).

Cerato-platanin (CP) from the plane tree pathogen *Ceratocystis platani* is a virulence factor. Other genes encoding cerato-platanin proteins (CPPs) have so far been found in over 50 fungal genomes, but not in other Dikarya (Chen *et al.*, 2013a). Thought to act mostly in host-pathogen interactions, CPPs are generally secreted and/or cell wall-associated, and have multifarious roles (Pazzagli *et al.*, 2014). Cerato-platanin itself induces cell death, salicylic acid (SA) signalling and phytoalexin synthesis (Baccelli *et al.*, 2014). A CP orthologue in *C. populicola* (*ex C. populorum*), Pop1, was shown to trigger a set of such responses as well (Lombardi *et al.*, 2013). Phytoalexins are associated with disease resistance (see subsection 1.2.1), and indeed the presence of CP increased the resistance of *Arabidopsis thaliana* against two other pathogens via the phytoalexin camalexin (Baccelli *et al.*, 2014). In turn, the *B. cinerea* CPP BcSpl1 is phytotoxic by causing plant cell shrinkage and chloroplast disorganisation (Frías *et al.*, 2014). BcSpl1 also caused non-specific cell death (Frías *et al.*, 2011). *Magnaporthe grisea* MSP1 was suggested as virulence factor, while *M. oryzae* SM1 is among the CPPs that elicited localised defence responses (Jeong *et al.*, 2007; Yang *et al.*, 2009). Further, Sm1 and Epl1 of the mutualists *Trichoderma virens* and *T. atroviride*, respectively, could contribute to the biocontrol function of these fungi by inducing systemic acquired resistance (SAR). Most recently, *Sclerotinia sclerotiorum* CP1 was characterised as a virulence factor and inducer of cell death and SA signalling (Yang *et al.*, 2018). It was shown to directly interact with a PR1 protein in the apoplast of *A. thaliana*. This is intriguing because the

PR1 family so far has been generally associated with defence against hemi- and biotrophic pathogens, and *S. sclerotiorum* is a necrotroph. Then again, PR1 proteins were also reported to be targeted by SnTox3 and SnToxA (necrotrophic effectors, see section 1.2.4). This could mean that PR1 is a non-conserved target of necrotrophic pathogens, exploited for cell death induction—the expression profile of SsCP1 supports this (Yang *et al.*, 2018).

Cerato-platanin proteins can bind carbohydrates including chitin with high affinity, but not cellulose. Like cellulose-binding expansins, however, they may be involved in cell wall loosening, which leads to turgor-driven cell expansion and rupture (Pazzagli *et al.*, 2014). Since some CPPs localise to the fungal cell walls of hyphae, conidia and ascospores, it was hypothesised that this expansin-like mode of action plays a role in the remodelling of fungal cell walls during growth (de Oliveira *et al.*, 2011). Furthermore, the secreted CPP Epl1 of *T. atroviride* was described as similar to hydrophobins since it self-assembles to protein films enabling hyphae to grow in particular environments. However, Epl1 would rather act as 'hydrophilin' as it increases surface or solution polarity and thus wettability (Frischmann *et al.*, 2013; Pazzagli *et al.*, 2014). It is also possible that a major CPP function is to shield or sequester the MAMP chitin to prevent triggering of defence responses, like *Fusarium graminearum* CPPs and *Verticillium dahliae* VdCP1 (Quarantin *et al.*, 2016; Zhang *et al.*, 2017b), and *Moniliophthora perniciosa* MpCP5 (de O. Barsottini *et al.*, 2013), reminiscent of CfAvr4 and the Ecp6 effectors, respectively.

In summary, few CPPs seem to have exclusive roles. In general they can be considered IPs, priming the plant defence system to various degrees (local response or SAR), and some CPPs appear to have important roles in virulence. Particular CPPs could also be crucial for fungal growth/development during infection.

Expression of DsCE14 was greatly increased in the Mid and Late *in planta* stages. This is in favour of a necrotrophic function, such as cell death induction. It could also be that DsCE14 is active in *D. septosporum* cell wall remodelling during this extensive growth phase throughout the mesophyll/apoplast (Kabir *et al.*, 2015). DsCE31 appeared to be constitutively expressed in culture and *in planta*, with only 3.6-fold up-regulation in Early stage, making it difficult to assign a specific function to this CE. DsCPL1, on the other hand, was down-regulated at the beginning of the infection and then up-

regulated again towards the Late stage (five-fold compared to in culture). I propose the following DsCPL1 functionality based on this expression profile: 1) A housekeeping-like function at the cell wall in the absence of the host—there are no other expressed CPPs annotated in the genome, 2) down-regulation to avoid IP recognition in the biotrophic colonisation phase, 3) gradual up-regulation to promote host cell death, or enable rapid hyphal growth, as the necrotrophic phase unfolds. There is a finding that theoretically supports a cell death induction function of DsCPL1. In the conifer pathogen *H. annosum*, the secreted CPP HaCPL2 caused cell death in both its host *Pinus sylvestris* and the non-host *N. tabacum* (Chen *et al.*, 2015). DsCPL1 has approx. 41% amino acid similarity to HaCPL2. To investigate whether the two pine pathogen proteins share similar roles, they were functionally tested in non-hosts (see chapter 4) and *P. radiata* (see chapter 5).

3.3.3. Lectins

Name	Length (Cys)	FM	E	M	L
DsCE6*	239 (4)	41	491	245	8995
DsCE38*	175 (10)	399	637	89	174
DsEcp6	204 (8)	47	6	606	171
DsCE30*	166 (0)	1338	6349	860	1647

DsCE6 (72737) is encoded by the most highly expressed CE gene *in planta* (highest value in Late stage in transcriptome and second-highest value among secreted proteins across all *in planta* stages). Its up-regulation compared to in culture was also among the top 20. DsCE6 was predicted to have a C-type lectin domain (Cummings & McEver, 2009) by the EuKaryotic Orthologous Groups (KOG) tool. Sequence homology searches resulted in two hits which were hypothetical proteins from the hemibiotrophic banana pathogens *Pseudocercospora fijiensis* (*ex Mycosphaerella fijiensis*) and *P. musae* (*ex M. musicola*). The *P. fijiensis* protein was also predicted to be secreted and had the same KOG annotation (Chang *et al.*, 2016). Interestingly, however, there were no matches of DsCE6 to secondary or tertiary structures in the queried databases (HHpred and i-TASSER tools).

Lectins have high binding affinity for carbohydrates and are known to be important

for plant PRRs and thus immunity (Lannoo & Van Damme, 2014). In pathogens, lectins with LysM domains in particular can be used to bind the MAMP chitin. The *C. fulvum* effector CfEcp6 can sequester loose chitin oligomers in the apoplast via LysM domains to mask the fungus from detection by the plant (Bolton *et al.*, 2008). CfEcp6 in fact contains three LysM domains, two of which dimerise and out-compete the chitin binding affinity of the plant receptor (Sánchez-Vallet *et al.*, 2013). DsEcp6 (46236) was highly up-regulated in Mid stage rather than Early, where 'stealth' factors like Ecp6 would be expected to be most useful. DsCE38 contains one LysM domain and showed high expression in the Early colonisation phase. Two DsCE38 proteins could potentially dimerise to play a role in recognition avoidance via chitin binding in the apoplast. LysM is notably also found in non-pathogenic fungi and may have roles in protection against other microbes while living outside of a host (Kombrink & Thomma, 2013). Apart from this possibility, it remains unclear what the function of DsCE6 is in the Late stage.

DsCE30 (75130) was one of seven CEs with in-culture expression of over 1000 RPMK and clearly the most strongly *in planta*-induced among the seven. In the Early infection stage, it was the second most highly expressed CE. In the genome annotation it had been classified as C-type lectin (KOG) and structural component of the cell wall (GO). The homology search resulted in many hits to hypothetical proteins in over 20 species, plus seven mentions of 'cell wall constituent'; the DsCE30 predicted structure had no matches. Since its sequence passed all the filters for secretion, structural affiliation to the fungal cell wall seems unlikely. PSIPRED/DISOPRED3 predicted that DsCE30 is highly intrinsically disordered. Intrinsically disordered proteins (IDP) in general lack a hydrophobic core and are highly soluble despite not being folded. Most importantly, IDP are extremely conformationally dynamic. This makes their function hard to predict, but grants the proteins properties such as fast and flexible interaction with binding partners, assembly to functional macromolecules, but also instability (Dyson & Wright, 2005; Xue *et al.*, 2012), all of which could be favourable for effectors. With its high expression level throughout and conspicuous up-regulation in the colonisation phase followed by a drop towards Mid (early disease symptoms), it is possible that DsCE30 is not directly involved in virulence (like DsCE31). It might play one of the many effector roles, such

as indirectly inhibiting host defence functions or promoting the mode of action of other virulence factors.

3.3.4. CAZys

Name	Length (Cys)	FM	E	M	L
DsCE2	616 (10)	14	153	43	680
DsCE4	493 (8)	8	40	19	534
DsCE7	684 (4)	6	54	24	791
DsCE19	446 (5)	6	166	380	814
DsCE34	478 (6)	1217	2888	504	153
DsCE42	434 (7)	67	2608	137	16

Several CAZys, including glycoside hydrolase (GH) enzymes, were highly expressed and up-regulated *in planta*. DsCE42 (62617) was strongly up-regulated in the Early stage of infection and annotated as GH64. β-1,3 glucanases of this type are thought to be involved in fungal cell wall remodelling. For example, in the hemibiotroph *Colletotrichum higginsianum*, GH64 and other glucanases are up-regulated in the biotrophic stage. There they could be used for appressorium formation or the degradation of plant-derived glucan deposits that hinder fungal entry (O'Connell *et al.*, 2012). In *D. septosporum*, the latter might apply, or general cell wall remodelling when switching from epi- to endophytic growth (Bradshaw *et al.*, 2016). Oppositely, the paralogous GH13-type CAZys DsCE2 (75147) and DsCE4 (70643) (Table C.2) showed strong up-regulation in the Late stage. GH13 α-amylases were hypothesised to hydrolyse starch which accumulates in 'green islands' that form next to DNB lesions (Bradshaw *et al.*, 2016). DsCE7 (58479) is structurally similar to bacterial GHs (HHpred), however, it could also be a glutaminase, and has three conserved domains of unknown function (DUF). As it was strongly induced in the Late stage, a plant cell wall-degrading function is likely. DsCE19 (75848) was annotated as GH71, and DsCE34 (73248) as GH10 (HHpred) and GH128 (BLASTp). Secreted expressed *Fusarium commune* xylanases (GH10) were identified as efficient decomposing agents of hemi- and cellulosic biomass (Huang *et al.*, 2015); thus, DsCE34 could hypothetically aid *D. septosporum* to penetrate needles by degrading their cell walls at the beginning

of the infection, if stomata are sealed. The other enzyme types have not been associated with pathogenicity so far.

Fungal CAZys in general are suggested to have important roles in both biotrophic and necrotrophic infection (Lyu *et al.*, 2015), such as detoxification of the apoplast and the breakdown of cell wall ultrastructural elements, respectively (see 1.2.4). Interestingly, a GH12 in the hemibiotrophic soy pathogen *Phytophthora sojae* was shown to be crucial for virulence, but also recognised as a PAMP in a very early infection stage (Ma *et al.*, 2015). The hemibiotrophic cotton pathogen *V. dahliae* secretes two GH12 proteins that are crucial for virulence based on their cellulase activity, and as PAMPs induce cell death in the non-host *N. benthamiana*. Curiously, the triggered immunity of *N. benthamiana* was suppressed by the cooperation of a carbohydrate-binding module (CBM1) expressed as part of the GH12, demonstrating effector interaction to overcome host immunity (Gui *et al.*, 2017). Certainly, the functional investigation of CAZys in *D. septosporum* would add further valuable insight to this picture.

3.3.5. Hydrophobins

Name	Length (Cys)	FM	E	M	L
DsHdp1	92 (8)	9234	455	6494	4862
DsCE40	85 (6)	2	133	85	2
DsEcp14	105 (9)	37	0	9	6
Ds91219	308 (11)	7	114	1592	120

The hydrophobin DsHdp1 (75009) was among the most highly expressed SSCPs. It was highly expressed *in planta* (in Mid and Late stage); however, even higher in culture with the highest recorded RPMK in the secretome. As hydrophobins were previously associated with virulence (Kershaw *et al.*, 1998; Lacroix *et al.*, 2008), DsHdp1 was investigated in *D. septosporum*, but deletion of the DsHdp1 gene did not affect spore adhesion or virulence in the fungus (Guo, 2015). It was intriguing to find that, despite being very highly expressed, DsHdp1 had no apparent role in virulence. There are three other DsHdp genes and only DsHdp1 was knocked out, so it could be that functional redundancy masked a true effect (Guo, 2015).

Even though it was not selected as CE, Ds91219 is a putative hydrophobin of interest due to its mutation rate indicating diversifying selection (see subsection 3.2.7). Notably, Cf187601, its orthologue in *C. fulvum*, was found in the experimentally determined *C. fulvum* apoplastome (Battaglia *et al.*, unpublished), and strikingly is encoded by one of the most highly expressed genes during the *C. fulvum*-tomato interaction (Dr C. Mesarich, pers. comm.). Like Ds91219, it was predicted to have a GPI anchor and thus not considered an Ecp (Mesarich *et al.*, 2017; Battaglia *et al.*, unpublished). Both proteins have predicted structural similarity to hydrophobins, among them the *M. grisea* class I hydrophobin Mpg1 which was shown to contribute to *M. grisea* pathogenicity on one of its hosts, wheat (Inoue *et al.*, 2016).

In general, fungal hydrophobins are secreted to the cell surface and self-assemble to an amphipathic monolayer (Sunde *et al.*, 2017) when encountering an interface of water and air or a hydrophobic surface. This monolayer serves filamentous fungi as a tool to break surface tension on a substrate (Wessels, 1994), allowing them to grow aerial hyphae and subsequently a more efficient gas exchange, or to efficiently attach to hydrophobic surfaces (Wösten *et al.*, 1994; Kershaw *et al.*, 2005; Inoue *et al.*, 2016). Such attachment is important to achieve infection of plants ((Wösten *et al.*, 1999; Kim *et al.*, 2005; Talbot *et al.*, 1993). It was also suggested that, on *Aspergillus fumigatus* spores, a hydrophobin layer of RodA rodlets acts as coating of the immunogenic cell wall components to prevent immune responses (prior to germination) of plants and humans (Aimanianda *et al.*, 2009; Dagenais *et al.*, 2010).

While the small, Cys-rich fungal hydrophobins are usually secreted, the full RodA protein contains a GPI anchor (Aimanianda *et al.*, 2009). Thus, it could make sense that Ds91219 and Cf187601 are not released from the fungal cell wall due to their predicted GPI anchor, but still form a layer to achieve the abovementioned coating function, like RodA. It should be noted that Ds91219 has no sequence homology to the described DsHdps. Hydrophobins have four Cys pairs forming disulphide bonds which are important to maintain a structure that is soluble, however, their sequences outside of the Cys-rich region are hardly conserved at least in class I hydrophobins (Wösten & Scholtmeijer, 2015). Therefore hydrophobins cannot necessarily be determined by sequence homology,

which was shown to be the case with Ds91219 and Cf187601. The similarity of both proteins to fungal hydrophobins is based on the part of their structure likely inferred by Cys residues (91219 has four predicted Cys bridges).

In the mutualistic symbiont *Trichoderma longibrachiatum*, the hydrophobin HYTLO1 was shown to be a MAMP, inducing a systemic immunity response providing increased defences against other microbes, if present in a sufficient dose (Ruocco *et al.*, 2015). Concurrent with previously reported roles of hydrophobins, HYTLO1 had direct antifungal abilities, making it even more important for the beneficial *T. longibrachiatum*-plant interaction. Perhaps a pathogen like *D. septosporum* could have evolved hydrophobins to fend off other fungi on the host, and this might explain the the high in culture expression of DsHdp1.

DsCE40 (29350) was strongly up-regulated in Early stage compared to in culture, to the moderate abundance level of 133 RPMK. The protein has weak sequence similarity (43% and 41%, E < 2E-8) to one uncharacterised SSCP each in *P. fijiensis* (Mf204808) and *C. fulvum* (CfEcp49-1). CfEcp49-1, which is more similar to another (non-expressed) DsSSCP, was up-regulated 16-fold early (4 dpi) during the infection of tomato, albeit also to a relatively low total abundance. Mf204808 was reported as not expressed *in planta* (Noar & Daub, 2016). DsCE40 was identified as a likely hydrophobin through an HHpred query. Thus, the *C. fulvum* and *P. fijiensis* proteins were also queried, and their structural prediction had the same match. Perhaps DsCE40 and its homologues have redundant functions to other hydrophobins in each fungus and are thus not highly expressed.

In contrast to DsHdp1 and Ds91219, DsEcp14-1 (71428), a homologue to the hydrophobin-like CfEcp14-1 which is likely an avirulence effector in *C. fulvum* (Mesarich *et al.*, 2017), had negligible RPMK values. This is also the case for the CfAvr4 and CfEcp13 homologues. Since DsAvr4 is suggested to to function as gene-for-gene avirulence effector (subsection 1.2.4), down-regulation as a result of adaptation seems likely. It would be interesting to find out if DsEcp14-1 represents a similar fate in *D. septosporum* pine infection.

3.3.6. Alt a 1 allergen-like

Name	Length (Cys)	FM	E	M	L
DsEcp20-1	145 (4)	19	62	53	57
DsEcp20-3*	135 (4)	5	4	205	115

DsEcp20-1 (51311) was identified as likely orthologue of Alt a 1 allergen-like CfEcp20-1 and accordingly named. The protein Alt a 1 from *Alternaria alternata*, a mould associated with allergic diseases including asthma, elicited IgE-mediated responses in approx. 80% of *Alternaria*-sensitive patients and it was shown that it contains several peptides similar to IgE binding sites. The structure of Alt a 1 is only found in fungi (Chruszcz *et al.*, 2012).

Structural queries of DsEcp20-1 furthermore uncovered likely similarity to PevD1, a recently described protein with an Alt a 1 fold. The structural homology result was almost the exact same result as for DsEcp20-3, which is discussed in subsection 4.3.4 (also see sequence alignment, Fig. 4.8). The DsEcp20-1 sequence only showed weak matches (E>1E-5) to two unnamed *Z. tritici* proteins and a hypothetical secreted protein of *Zasmidium cellare*, one of few saprobic Dothideomycetes. The poor similarity of the DsEcp20-1 and DsEcp20-3 sequences to each other was not picked up by BLASTp with E<1E-2. DsEcp20-1 is one of the most lowly expressed CEs in all conditions and, while induction *in planta* was the main reason for the inclusion of this candidate, a maximum change of 3.3-fold at this low expression level seems barely meaningful in light of other, much higher values. It might well be strategically kept at low expression levels as a result of adaptation. Redundancy of paralogues is briefly discussed in subsection 4.3.4.

3.3.7. CAP family

Name	Length (Cys)	FM	E	M	L
DsEcp57-1*	264 (5)	426	1448	1013	554

DsEcp57-1 (69335) is likely a direct orthologue of the apoplastic CfEcp57-1. Both proteins contain a conserved domain of the 'cysteine-rich secretory proteins, antigen 5, and pathogenesis-related 1 proteins' (CAP) superfamily, also known as sperm-coating protein (SCP) superfamily. Moreover, DsEcp57-1 has strong predicted structural homology to

Pathogen-related in yeast (Pry)-1, a lipid-binding CAP protein of *Saccharomyces cerevisiae* (Darwiche *et al.*, 2017), as well as 21 other CAP proteins. Pry-1 was shown to bind sterols and fatty acids independently. It was suggested that Pry-1 acts like the tobacco defense protein PR-1a and its close relative in tomato, P14c. These two small secreted plant proteins exhibited antimicrobial function by a) scavenging extracellular sterols to make them unavailable to other microbes, and/or b) sequestering sterols in plasma membranes (Gamir *et al.*, 2017). Sterol binding as a defense mechanism is effective against oomycetes, as they are sterol auxotrophs (Gamir *et al.*, 2017). Various *Phytophthora* spp. are foliar pathogens of *P. radiata* (Scott & Williams, 2014; Brar *et al.*, 2018) and can be found on the same needles as *D. septosporum*. Thus, it might be that the fungus, itself unaffected by the sterol scavenging of DsEcp57-1, directly fights its oomycete competitors with this tactic during pine needle colonisation. This could be determined with *in vitro* co-cultivation assays.

DsEcp57-1 is also a likely orthologue of *Venturia inaequalis* candidate effector 14 (ViCE14). In a recent study, ViCE14 attenuated cell death responses induced by *Pseudomonas syringae* HopAS1 in *N. benthamiana* ATTAs (Prokchorchik, 2017). Since DsEcp57-1 was highly expressed in the Early (biotrophic) stage of *D. septosporum* infection, it would be interesting to determine a potential cell death pathway suppression function of this CE.

3.3.8. Proteins with other functional predictions

Name	Length (Cys)	FM	E	M	L
DsCE41	156 (5)	2	53	2	2
DsPhiA-2*	176 (4)	53	83	257	342
DsCE16	251 (3)	30	82	43	76
DsCE24	209 (4)	30	125	11	182
DsEcp58-1*	176 (4)	1595	187	53	3500
DsCE21	176 (5)	14	21	10	239
DsCE12	287 (2)	3	235	98	1555
DsCE32	192 (5)	29	123	7	39
DsCE35	286 (6)	2020	4873	1348	1055

DsCE41 (139477) was predicted to be non-apoplastic, and has a predicted histidine phosphatase (PhoE) domain (BLASTp and HHpred). Since this is a very broad function and DsCE41 expression throughout was the third-lowest among CEs, any functional suggestions would be highly speculative. This could be a redundant protein.

DsPhiA-2 (69113) is likely a direct orthologue of CfPhiA-2 which in turn has homology to CfPhiA-1 and phialide A of *Aspergillus nidulans*. Phialide A is a cell wall-associated protein necessary for the development of conidia as well as phialides, sporogenous cells that produce and release conidia (Melin *et al.*, 2003). CfPhiA-2 was moderately induced during *C. fulvum* infection of tomato, corresponding well with the expression pattern of DsPhiA-2 (see also Table 3.2). However, the *in planta* induction of CfPhiA-1 (over 3600-fold) was one of the highest recorded and dwarfs that of CfPhiA-2. Assuming that these two proteins share their main function, it is evident that CfPhiA-2 is redundant. DsPhiA-2 may contribute to conidia formation when *D. septosporum* shifts to forming sporulating lesions.

DsCE16 was predicted to be non-apoplastic, and appears to have a Rossmann fold, an "ancient" repeat fold mainly found in oxidoreductases (Burton, 2018). Since there are many oxidoreductases in the genome which were also highly expressed, DsCE16 with low expression could be considered redundant.

DsCE24 (70053) has a domain of unknown function (DUF4237) that is found in bacteria

and fungi. Recent structural prediction revealed distant homology to an NAD-binding protein (also containing DUF4237) as well as Tne2, a *Pseudomonas syringae* type 6 secretion effector. Even though DsCE24 had comparatively low expression, functional relatedness to Tne2 could be investigated.

DsEcp58-1 (68958) and DsCE21 (72870) are paralogues (Table C.2); however, DsCE21 was predicted not to be apoplastic (Table C.1). They were annotated as unknown proteins but the latest HHpred query indicated that part of their structure is similar to polyketide cyclases. Thus, DsEcp58-1 and DsCE21 might be involved in the processing of polyketide secondary metabolites (SM). In addition to the toxic SM dothistromin (subsection 1.1.5), such SMs could be used either against other microbes, or for plant destruction. Small secreted microbial polyketide cyclases are scarcely mentioned in the literature. The much higher expression of the apoplastic DsEcp58-1 is striking. Interestingly, no amino acid changes were found in DsEcp58-1 sequences in the 19 *D. septosporum* strains, whereas DsCE21 had a small number of mutations, like most other CEs. In combination with relatively low expression, this indicates that DsCE21 could be a duplicate that was allowed to accumulate mutations without being counter-selected. Finally, even though DsEcp58-1 is the fourth-most highly expressed CE in the Late stage, high expression in culture makes an exclusively infection-related function unlikely.

DsCE12 (130443) is a putative oxidoreductase with a domain of the 'ferritin superfamily'. Ferritin is an iron complex used by plants, animals and bacteria for the storage of iron, an essential nutrient for nearly all organisms (Haas *et al.*, 2008). Siderophores are microbial proteins that mediate the uptake of iron and can be particularly important in competitive situations. 'Ferritin-like proteins' are among siderophores, however, there are few described examples of such proteins in fungi (Haas *et al.*, 2008). In *Cronartium ribicola*, a protein with the ferritin domain was induced during infection of white pine (Liu *et al.*, 2015). DsCE12 was among the top 20 up-regulated genes in the Early stage compared to in culture, and the third-most highly up-regulated in Late stage (of the CEs, only DsCE11 had higher values in both cases). It could be that DsCE12 is important for iron acquisition especially during the Late stage, when host tissue is already heavily damaged and opportunistic microbial competitors may appear.

Among SSCPs, DsCE32 (132625) was one of the least expressed CEs that was included in the list. It showed similarity to various hypothetical proteins and has a predicted domain of unknown function (DUF1524). This domain is similar to an endonuclease domain and widely shared in proteins across kingdoms. It seems elusive whether this CE has a role during the infection of pine.

Finally, the highly expressed DsCE35 (68580) had sequence similarities to some thaumatin-like proteins. This seems odd, as thaumatins are defence proteins of plants (PR5). However, HHpred later showed that the predicted DsCE35 structure is similar to MoHrip2, a secreted *M. oryzae* protein which induced cell death in *N. tabacum* and increased rice resistance against *M. oryzae* (Liu *et al.*, 2016; Wang *et al.*, 2017b). Crystal structure analysis unveiled that MoHrip2 has a β-barrel fold with high similarity to the thaumatin superfamily protein 'thaumatin-like xylanase inhibitor'. This could explain why DsCE35 has sequence similarity to thaumatin-like proteins. As hypothesised for MoHrip2 (Liu *et al.*, 2016), DsCE35 could be an inhibitor of defensive plant enzymes in the apoplast. The third-highest expression value of secreted proteins in the Early stage supports this, even though it does not represent a strong up-regulation from in culture growth.

3.3.9. Uncharacterised proteins

For the remaining 27 CEs, no functional prediction was available. Six of these were cloned and functionally investigated (chapter 4). While the expression patterns of these CEs without homology to effectors or IPs say little about their potential roles, the following should be noted: Compared to in culture growth, *DsCE11* was among the top 20 up-regulated genes in the Early stage and the most up-regulated gene in the Late stage, where *DsCE6* (which may or may not be a lectin) was also among the top 20; *DsCE15* was the third-most up-regulated gene in Mid stage. DsCE11 further stood from these as its only similarity was to one hypothetical *P. eumusae* protein (E≈4E-10).

3.3.10. *D. septosporum*–*C. fulvum* CE orthologues

The close phylogenetic relationship of *D. septosporum* and *C. fulvum* provides an opportunity for comparative analyses of effector repertoire and function. New transcriptome

data and functional assay data for *C. fulvum* (Mesarich *et al.*, 2014, 2017), enabled comparison of extended lists of extracellular CEs of *D. septosporum* and *C. fulvum*. Likely orthologues were examined for commonalities and differences.

While the lifestyles of these two fungi are similar (see section 1.2.4), they are different in many aspects of their ability to cause disease, such as host and environment. Differences in *in planta* expression between orthologous genes in the two fungi might be due to numerous reasons. The initial assumption was that orthologous proteins have similar roles in infection and would thus have similar expression profiles. The advantage of deploying any such protein can be reversed if the plant defence system recognises it as an IP. For example, it makes sense that the chitin-binding effector Avr4 is highly induced during biotrophic colonisation as it protects cell wall chitin from degradation and recognition, however, presence of Avr4 enables its specific recognition and causes a Cf-4-mediated HR (section 1.2.4). In such cases, selection pressure may lead to mutation or other means to evade recognition. If the protein is not essential for the pathogen to complete its life cycle, non-expression would be effective. This might be the situation for DsAvr4, which was not expressed in the early stage of *D. septosporum* infection. In fact, all apoplastic orthologues except DsEcp57-1, DsEcp58-1 and DsCE42 were more clearly highly induced in *C. fulvum* compared to *D. septosporum* during the Early stage. These 11 DsCEs, except for DsEcp20-1, were all much more induced in the Mid stage, with six of them turning from down- to up-regulation compared to in culture. This could indicate that secreted proteins with likely biotrophy functions in *C. fulvum* have been subject to adaptation through gene regulation in *D. septosporum* because they are recognised as IPs in *P. radiata*, and are likely not as important for *D. septosporum* as for *C. fulvum*. Consequently, it would indicate that at Mid stage, recognition and its consequences is either irrelevant, or exploited as necrotrophy begins.

DsEcp20-3 is one of the proteins with the higher Mid stage expression pattern. Together with CfEcp20-3 and the pairs Ds/CfEcp20-1, Ds/CfEcp20-2 and Ds/CfEcp20-4, where notably 'CfEcp20-4' may not be secreted, it is predicted to have structural homology to the Alt a 1 allergen of *A. alternata*. This is discussed in chapter 4. Based on their similarity, these eight proteins were putatively grouped as Ecp20s. Differences in their

expression profile within each pathogen could be due to functional redundancy. It was suggested that CfEcp20-1/2/3 are not recognised in wild tomato (Mesarich *et al.*, 2017). Direct functional comparison of all eight Ecp20 proteins in various plants, importantly the hosts of both pathogens, would most probably shed light on this finding.

The role of DsEcp2-1 has been investigated in the *P. radiata* infection via gene deletion, and might help us better understand the transition from biotrophic to necrotrophic mode of *D. septosporum* infection. DsEcp2-1 is discussed in chapter 5. DsAvr4 and DsEcp6 have a similar expression pattern (down- followed by up-regulation) and chitin binding function, but the expression of DsAvr4 through all stages can be disregarded as negligible—it is lower than the median (and average) of the entire secretome. The roles of these conserved alleged avirulence effectors could most easily be elucidated if the presence of their cognate *R* genes were determined in the genome of pine hosts.

3.3.11. CEs in genomic and pan-isolate context

In general, *D. septosporum* NZE10 has an excellent chromosome-level assembly of 14 scaffolds and a remarkably low overall repeat content (3.2%, de Wit *et al.*, 2012), with the second-lowest transposable elements content (0.67%) among 14 Dothideomycetes genomes (Ohm *et al.*, 2012). This makes the observation that CEs are not clustered in the genome reliable. McDowell (2013) noted that in the hemibiotroph *Colletotrichum* species, effector candidates are randomly distributed in the genome and—in contrast to oomycete effectors—not associated with repeats. In addition to 'waves' of gene expression during infection (O'Connell *et al.*, 2012), this seems to be another similarity of *D. septosporum* and *Colletotrichum* of the Dothideomycetes sister group Sordariomycetes. Furthermore, *D. septosporum* 'pathogenesis-associated gene classes' (original annotations) were not enriched in the proximity of repetitive elements, unlike several other Dothideomycetes (Ohm *et al.*, 2012), and few (17%) gene loci outside the repeat regions were affected by repeat-induced point mutation (RIP) (de Wit *et al.*, 2012). DsPhiA-2 could be the sole exception as the gene fourth-closest to repetitive elements in the genome. It has the most non-synonymous SNPs (16, 9.1%) found in 19 *D. septosporum* genomes (subsection 3.2.6) among the 55 CEs, which could be due to RIP.

To generate a phylogenetic tree of these 19 strains, genome-wide SNP data were used. This offered the advantage of a more comprehensive comparison over using core eukaryotic genes only. The analysis showed interesting differentiation of the strains, in particular those from Guatemala and Colombia. However, each of these four strains was isolated from a different *Pinus* species compared to all other strains and this alone may account for the differences found. Host specificity studies are required to elucidate this.

The 12 CE genes found to be duplicated in at least one genome fall into regions of scaffolds that were apparently duplicated in the respective strains. If some of these CEs are indeed important for infection, they would be prime candidates to further investigate regarding diversification in the various strains (Bradshaw *et al.*, submitted).

The deletion of *DsCE40* in one strain and of *DsCE11* in five strains could mean that the presence of these genes was detrimental to the pathogen in the respective strains by means of recognition by the host. The deletions were not host species-specific, which generally would not support this hypothesis, however, *Pinus* spp. are intraspecifically diverse. Using *DsCE11* presence in particular as a genetic marker in a large range of field samples from each of the original regions could provide clarity. A more simple explanation is that the genes (despite the high *in planta* expression in the case of *DsCE11*) were functionally dispensable, and thus their deletion did not affect the fungus' fitness.

The finding that transcript reads of *DsPhiA-2* were found among mapped read data (of the Colombia North strain), even though it was listed as deleted, demonstrates that with automated bioinformatics methods, certain parameters represent a trade-off between false positives and negatives. In this case, the cut-off value for calling gene deletions might have been too high. Oppositely, it was intriguing to find that even though no reads were mapped to almost the entire DsCE11 gene locus in four strains, it was not reported as deleted by the software. A true verification of presence or absence could be carried out by PCR with combinations of primers for gene-flanking and intragenic sequences. To put the CE deletions into whole-genome perspective, a total of almost 600 genes appeared to be deleted in at least one strain. Of these, 77% had very low expression levels *in planta* (<20 RPMK) in NZE10, which may suggest that they are not important to the *D. septosporum–P. radiata* interaction (Bradshaw *et al.*, submitted). Some genes deleted

in the Colombian and/or Guatemalan genomes, however, were more highly expressed, such as *DsCE11*. Given that most of these genes had no predicted function or a redundant function (such as oxidoreductase), meaningful implications of the gene absences would be speculative.

3.3.12. Summary

I created and presented a set of 55 candidate effectors for the forest pathogen *Dothistroma septosporum*. It is not to be viewed as fixed, as knowledge about effectors steadily increases, and *in silico* prediction methods improve accordingly.

The description of the 55 CEs fulfils the first research aim of this thesis. I then cloned selected genes from the list for functional testing in non-hosts, primarily to test for non-specific IP recognition. This work is shown in the next chapter.

Chapter 4.

Functional analysis of *Dothistroma septosporum* candidate effectors in non-host plants

4.1. Introduction

Effectors of microbial pathogens can have multifarious roles in interactions with plants, most generally assisting infection by interfering with the plant immune system (see subsection 1.2.1). Due to an ongoing evolutionary arms race, some effectors are recognised as invasion patterns (IPs) by extracellular plant IP receptors, termed pattern recognition receptors (PRRs), while others are recognised as IPs by intracellular IP receptors (NLRs) termed R proteins. In both cases, recognition activates one of a few intracellular signaling cascades, leading to immune responses that are typically sufficient to prevent further local pathogen growth (subsection 1.2.1).

Given powerful genomic and transcriptomic background information as well as a rapid and efficient screening process, effectors, and subsequently their receptors, can be identified using host infection experiments. This approach, however, is severely limited in terms of throughput in systems with slow growth on either the host or pathogen side, or both. For example, the pathogenicity assay for *D. septosporum* on *Pinus radiata* developed in this laboratory (Kabir *et al.*, 2013) takes up to three months to reach a conclusion about infection, not including preparation of fungal spores (two to three weeks) and acquiring

pine seedlings at an age of at least six months. In comparison, tomato plants are usually infected with the biotroph *Cladosporium fulvum* at the age of four to five weeks and assessed two weeks later (Mesarich *et al.*, 2014); wheat leaves can be infected with the hemibiotroph *Zymoseptoria tritici* at ten days of age and assessed within three weeks (Kema *et al.*, 1996; Keon *et al.*, 2007; Friesen *et al.*, 2008).

When such slow and laborious artificial infection of host plants cannot be accelerated, functional analysis of genes in fast-growing non-hosts provides a good alternative. Studies employing the model plants *Nicotiana benthamiana* and *N. tabacum* have furthered basic understanding of many pathogens. Both species carry a wide array of characterised and uncharacterised IP receptors, making them ideal for broad screenings of pathogen IPs (Ma *et al.*, 2012; Wang & Bennetzen, 2015). Transient transformation assays with 'disarmed' (non-pathogenic) *Agrobacterium tumefaciens* strains to express genes of interest locally in leaves of *Nicotiana* species are relatively quick, easy and well-established. Using this type of assay, it has been shown for the highly host- and tissue-specific and strictly apoplastic *Z. tritici* that 13 of 63 tested [small apoplastic] candidate effectors (CEs) induce cell death in *N. benthamiana* leaves. Of these, 12 only induced cell death when directed to the apoplast using an amino (N)-terminal secretion signal (signal peptide) (Kettles *et al.*, 2017). This suggests that a considerable proportion (˜20%) of small *Z. tritici* proteins secreted to the apoplast are recognised as IPs by extracellular IP receptors in *N. benthamiana*, triggering non-host resistance (Heath, 2000b) in the form of a cell death response (Kettles *et al.*, 2017). This represents a response that keeps the fungus from colonising most plants further. However in wheat, which *Z. tritici* has adapted to, there are two options for a successful infection. *Z. tritici* could circumvent the recognition via various biotrophic strategies, or exploit cell death if it shifts to necrotrophy.

The model plants could also be useful for the same type of assays with *D. septosporum*. The tree foliage pathogen is family- rather than species-specific in terms of its host specificity; however, the lack of reported host jumps to other than Pinaceae on a global scale, including other species planted for timber, suggests it is indeed unable to infect other plants under natural conditions. *D. septosporum* is also hemibiotrophic and highly likely apoplastic once inside the host needles (Kabir *et al.*, 2015; subsection 1.1.4). Furthermore,

it shares important avirulence effectors with the closely related, strictly apoplastic and intensely studied *C. fulvum* (de Wit *et al.*, 2012). Along with many other Dothideomycetes, none of these three fungi, *C. fulvum*, *Z. tritici* and *D. septosporum*, are known to possess dedicated mechanisms to deliver effectors into host cells. Thus it seems likely that their effectors function in the apoplast (as shown for CfAvr2, CfAvr4, CfAvr9, CfEcp2 and CfEcp6).

All of this was in favour of choosing a non-host approach for investigating putative secreted (apoplastic) effectors of *D. septosporum*. Seeking a uniform method, the predicted native signal peptides of all CEs were replaced by the broadly used *N. tabacum* PR1α signal peptide in the cloning process to direct secretion of the proteins into the apoplast. The main goal of the screen was to find CEs that induce non-host resistance following recognition by cognate PRRs. However, CEs that trigger cell death independently of a cognate PRR through toxicity effects (i.e., not involving the immune system) could also be discovered in these assays.

4.2. Results

4.2.1. DsEcp2-1 and four additional CEs induced cell death in *N. tabacum*

Candidate effectors (CEs) were cloned for *Agrobacterium* transient transformation assays (ATTAs) using the Golden Gate approach. Genes with small size, no introns and no internal *Bsa*I sites were prioritised in this process. The 17 successfully cloned CEs (Table 3.1) were screened for cell death induction in the non-host *N. tabacum*. The *Phytophthora infestans* elicitin infestin 1 (INF1), which has been previously shown to trigger cell death in *Nicotiana* species (Kamoun *et al.*, 1998), was used as positive control, and an empty expression vector as negative control. Four CEs consistently triggered cell death in *N. tabacum* (Fig. 4.1) with no notable difference between the optical densities (OD_{600}, hereafter OD) of the infiltration cultures used (0.4, 0.6 and 1.0), i.e., the lowest OD was sufficient to trigger the response. DsEcp2-1 (158381) induced strong cell death indistinguishable from INF1 in every replicate. DsEcp32-3 (70057), DsEcp20-3 (70694) and DsCE15 (131885)

also induced strong cell death. However, in most of these cases a large patch of cell death rather than cell death across the full infiltration zone was observed. Ninety-seven percent of all DsEcp32-3 infiltration zones were counted as cell death responses, 92% of DsCE15, 66% of DsEcp20-3, and 58% of DsCE3.

The other 12 cloned and tested CEs, (Table 3.1), did not cause cell death in *N. tabacum* when tested in at least three independent experiments.

For some of the DsCEs, alternative alleles were discovered in a global population study (see subsection 3.2.7). Mutations leading to amino acid changes in IP proteins can lead to loss of interaction with PRRs. For example, this was shown for the dothideomycete 'core' avirulence effector Avr4 (Joosten *et al.*, 1994; Mesarich *et al.*, 2016). For DsEcp20-3, alleles of the Slovakian (SLV1) and Russian (RUS1) *D. septosporum* isolates, that contained non-synonymous SNPs compared to the NZE10 reference strain (Fig. E.1), were tested for their ability to trigger cell death in *N. tabacum*. In the SLV1 allele, a substitution of proline to leucine at position 63 (full-length protein) was considered particularly interesting, as proline residues can alter protein folds and are often highly conserved (Betts & Russell, 2003). In RUS1, a tyrosine to histidine substitution at position 131 stood out, as histidine is unlikely to be substituted in general because it has a unique chemistry giving it versatility (Betts & Russell, 2003), and the substitution was only present in this isolate. However, alignment of the predicted structures of the two variant DsEcp20-3 proteins to the NZE10 did not support notable differences (Fig. E.2) Cell death screening with the SLV1 and RUS1 proteins showed the same results as the NZE10 protein (Fig. E.2). This strongly indicates that these amino acid changes did not affect their ability to be recognised as IPs.

4.2.2. Four CEs induced cell death in *Nicotiana benthamiana* via agroinfection

The 17 cloned CEs were also screened for cell death induction in the alternative non-host plant *N. benthamiana* using ATTAs. Alongside the results observed for *N. tabacum* (Fig. 4.1; see above), DsEcp32-3 (70057), DsEcp20-3 (70694), DsCE15 (131885) and DsCE3 (71487) also induced cell death in *N. benthamiana*. This supports that these four

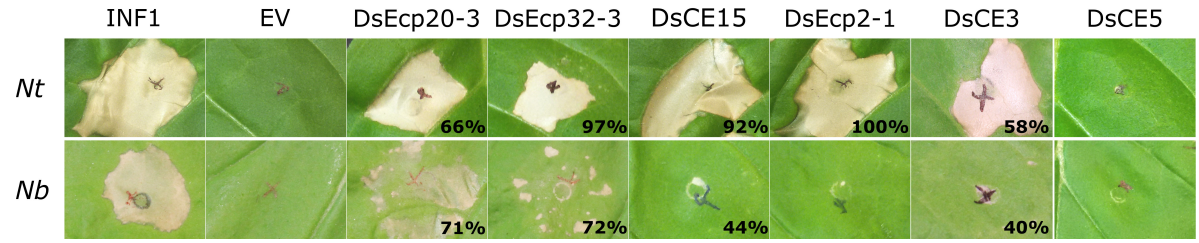

Figure 4.1.: *Dothistroma septosporum* NZE10 candidate effectors induced cell death responses in non-hosts. *Agrobacterium* transient transformation assay of *Nicotiana tabacum* (top) and *N. benthamiana* (bottom). INF1, elicitin positive control; EV, empty vector negative control. Representative images and percentages of cell death occurrences (7 days post-inoculation [dpi]; $n \leq 24$ infiltration zones, from at least 3 independent experiments) are shown. DsCE5 was included as an illustration of a secreted CE protein not inducing cell death in either non-host.

CEs are recognised as IPs in *Nicotiana* non-hosts, or toxic.

For DsEcp32-3, the cell death response was fairly consistent across replicates (>70% of zones counted as cell death), but not as strong and clear as the necrotic area triggered by the positive control. Most infiltration zones scored as positive (cell death) showed separate small necrotic areas, with the largest necrotic patches along the perimeter (Fig. E.3). There was also variability in the response severity for DsEcp20-3 (all three alleles), however it was overall very similar to INF1 (Fig. E.3).

DsCE15 and DsCE3 induced weak cell death along the perimeter of infiltration zones (Fig. 4.1) in 44% and and 40% of all cases, respectively. This was best illustrated by exposing leaves to UV transillumination (backlight) to highlight dead cells based on leaked fluorescent phenolic compounds (Fig. 4.2). It was demonstrated that the apoplastic effector DsEcp2-1 does not trigger a cell death response in *N. benthamiana*. Specifically, infiltration zones with DsEcp2-1 (a secreted effector inducing strong cell death in *N. tabacum*) were indistinguishable from the negative control. This also suggested that the weak effect seen with DsCE15 and DsCE3 was a specific response to the presence of each respective CE (Fig. 4.2).

4.2.3. Minimum infiltration culture densities to induce cell death were found for two CEs

After identification of the five cell death inducing CEs, the OD range was expanded to determine a response threshold at lower cell concentrations. The cell death-inducing

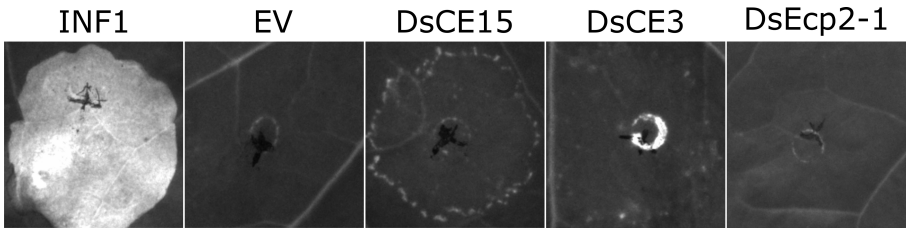

Figure 4.2.: UV imaging showed that DsCE15 and DsCE3, but not DsEcp2-1, induced a weak cell death response in *Nicotiana benthamiana*. Representative images for INF1, elicitin positive control, and EV, empty vector negative control, are shown; numbers on the left indicate the OD_{600} for the CEs. Leaves were imaged 6 dpi; $n \leq 8$ infiltration points from two independent experiments.

CEs were tested at ODs 0.05, 0.1, 0.2, 0.4 and 0.8. It was found that OD 0.4 was sufficient to induce cell death of at least equal intensity to previous results obtained at ODs 0.6 and 1.0 for all five CEs (Fig. E.4). The positive control (INF1), DsEcp32-3, and DsCE15 consistently still induced strong cell death down to the lowest OD (0.05) in *N. tabacum* (*N. benthamiana* not tested). DsCE3 and DsEcp2-1 showed a trend of lower OD correlating with less cell death (Fig. E.4). Due to unexpected very weak responses, results for DsEcp20-3 were ambiguous in this experiment.

In a separate *N. benthamiana* experiment testing ODs 0.4, 0.6, 0.8 and 1.0 of DsEcp20-3, DsEcp32-3, and DsCE15 only, DsEcp20-3 induced cell death more quickly at 0.4 and 0.6 than at 0.8 and 1.0, and subsequently led to a stronger response at 6 dpi. Cell death responses to DsEcp32-3 and DsCE15 (not shown) were consistent across the four ODs (Fig. E.5).

In summary, I found that two of five CEs induced less frequent and less severe cell death correlating with lower infiltrated cell densities, while another one displayed the opposite.

4.2.4. Cell death in *N. benthamiana* could be quantified

DsEcp32-3 and DsEcp20-3 induced the strongest cell death responses in *N. benthamiana*. To investigate the effect of these two CEs further, two approaches to quantify the extent of damage caused by the CE infiltration were taken. First, the leakage of ions from dead cells was measured. This method allowed a more precise differentiation of responses to the two CEs. Higher conductivity from DsEcp20-3 samples, compared to DsEcp32-3 (Fig. 4.3), indicated a 1.35-fold-stronger cell death induction, although this difference was not statis-

tically significant. INF1 treatment showed higher ion leakage than all other treatments. Second, leaves were exposed to UV transillumination to increase visibility of dead cells (compare Fig. 4.2). Fluorescence intensity was subsequently analysed with ImageJ. Specifically, a quantitative comparison of cell death in the infiltrated zones was carried out using pixel grey values representing fluorescence intensity (of phenolic compounds released on cell death), with the assumption that these are proportional to the number of dead plant cells. In this assay, DsEcp20-3 cell death was significantly greater than that of DsEcp32-3 by a factor of 1.46 ($p = 0.002$). Interestingly, the DsEcp20-3 values were also greater than the positive control, INF1, in this experiment ($p = 0.048$). Previously in this work, INF1 was observed to clearly and most quickly induce the strongest cell death response compared to other single elicitors.

In summary, additional evidence was collected that DsEcp20-3 is the more potent cell death elicitor in *N. benthamiana* than DsEcp32-3.

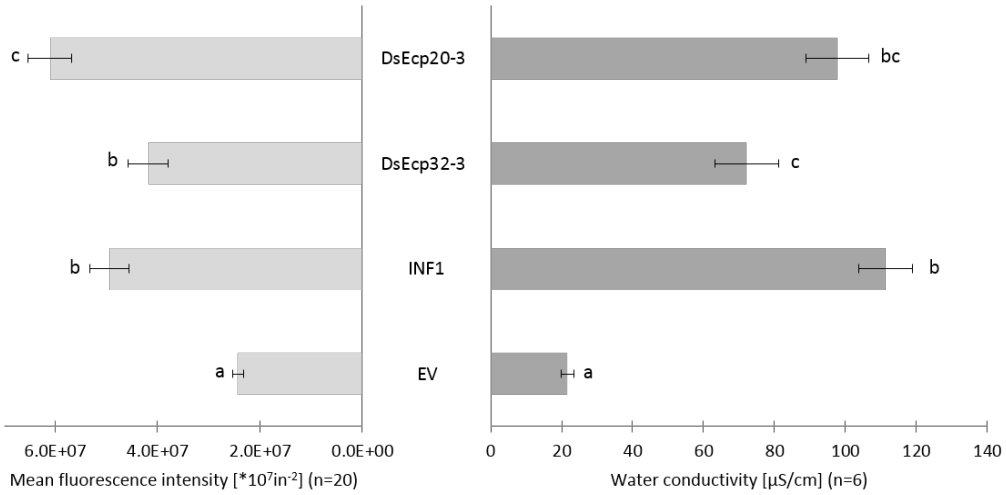

Figure 4.3.: Cell death quantification in *Nicotiana benthamiana* based on two different methods. For fluorescence intensity (left), digital image analysis was carried out with ImageJ. Intensity for each infiltration zone was calculated as Raw Integrated Density (sum of pixel grey values corresponding to fluorescent area) divided by the total infiltrated area. Conductivity in dH_2O (right) was measured from two leaf discs each for each of 6 replicates and the conductivity value for dH_2O was subtracted. Error bars show standard errors (SEM). Different letters indicate significant differences between samples (Student's t-test, $p < 0.05$). EV, empty vector negative control; INF1, elicitin positive control; DsEcp20-3 and DsEcp32-3, *D. septosporum* candidate effectors. Assays were carried out 6 dpi.

4.2.5. Confirmation of CE protein expression by western blot

To confirm that the CEs were expressed in leaves of *N. benthamiana*, immunoblotting using anti-FLAG primary antibody was carried out. Making the assumption that the secreted proteins accumulate in the apoplast, a method was developed to efficiently collect apoplastic wash fluid from *N. benthamiana*. Fluid samples were collected from whole-leaf infiltrations of *N. benthamiana* using a customised vacuum infiltration-centrifugation method described in chapter 5.

DsEcp2-1 (expected size 19 kDa with 3xFLAG tag), DsEcp20-3 (17.5 kDa), DsEcp32-3 (23 kDa), and DsCE3 (22.5 kDa) were each detected in these samples (subsection 4.2.5), but not DsCE15 (16 kDa) or INF1 (14 kDa; data not shown). Furthermore, DsCPL1, DsCE5, DsCE38 and DsPhiA-2 were detected from among the CEs that did not induce cell death (Fig. 4.4; Fig. E.6).

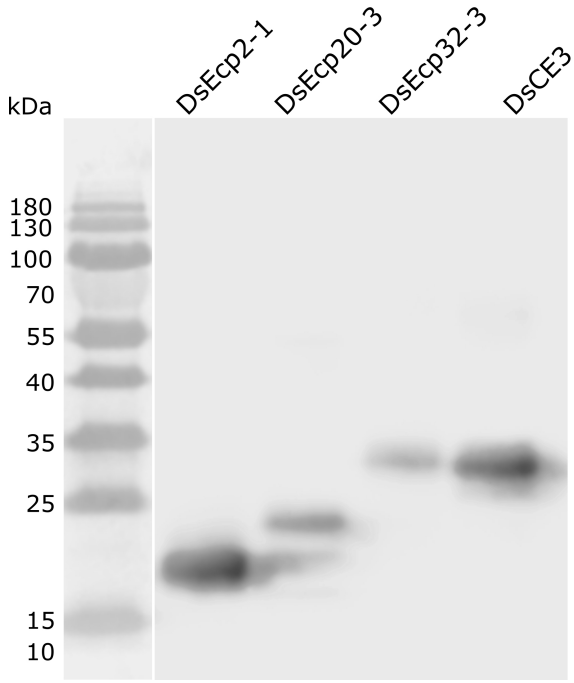

Figure 4.4.: Four of five cell death-inducing candidate effectors (CEs) were detected by western blot. Frozen apoplastic wash fluid samples (2 dpi) were used for the protein assays. Immuno-detection was based on primary anti-FLAG antibody. Expected sizes with 3×FLAG tag: DsEcp2-1, 19 kDa, DsEcp20-3, 17.5 kDa, DsEcp32-3, 23 kDa, DsCE3, 22.5 kDa.

4.2.6. Cell death induced by DsEcp32-3 and DsEcp20-3 in *N. benthamiana* was not suppressed by *P. infestans* effector Avr3a

To get a better understanding of how the putative *D. septosporum* CEs induce cell death in a plant, a suppression assay was carried out. The *P. infestans* elicitin INF1 causes strong cell death in *N. benthamiana* via a CMPG1-dependent pathway, and co-expression of the *P. infestans* effector Avr3a inhibits this pathway, resulting in the suppression of cell death (Bos *et al.*, 2010; Gilroy *et al.*, 2011). To test whether DsEcp20-3 and DsEcp32-3 trigger the same cell death pathway as INF1, each was co-infiltrated with Avr3a to determine if it also inhibits the cell death response induced by these *D. septosporum* effectors.

Fig. 4.5 shows representative results (6 dpi) with both bright light and UV exposure. As expected, INF1 induced a cell death response that was strongly inhibited when it was co-infiltrated with Avr3a. Expression of Avr3a was furthermore indirectly confirmed in every leaf by co-infiltration with its cognate potato receptor R3a, causing HR as expected. Meanwhile, Avr3a and R3a did not induce cell death when infiltrated alone. Both DsEcp20-3 and DsEcp32-3 caused moderate cell death across the infiltrated area, with small patches of stronger cell death. When co-infiltrated with Avr3a, cell death was not reduced, indicating no involvement of the CMPG1-dependent pathway. In fact, cell death appeared to be enhanced. The fluorescence cell death quantification method (subsection 4.2.4) was used for this experiment as well. These data showed that variability was large, yet they confirmed that (unexpected) differences between certain samples were significant (Fig. 4.6). Specifically, both CEs induced a stronger response in combination with Avr3a than when infiltrated alone. The response of INF1 was stronger compared to DsEcp32-3 but not DsEcp20-3. It was also clearly weaker compared to the Avr3a-R3a pair, which induced the strongest response throughout. The INF1-Avr3a 'suppression control' was in between INF1 and 'no cell death' results of separate R3a and Avr3a zones.

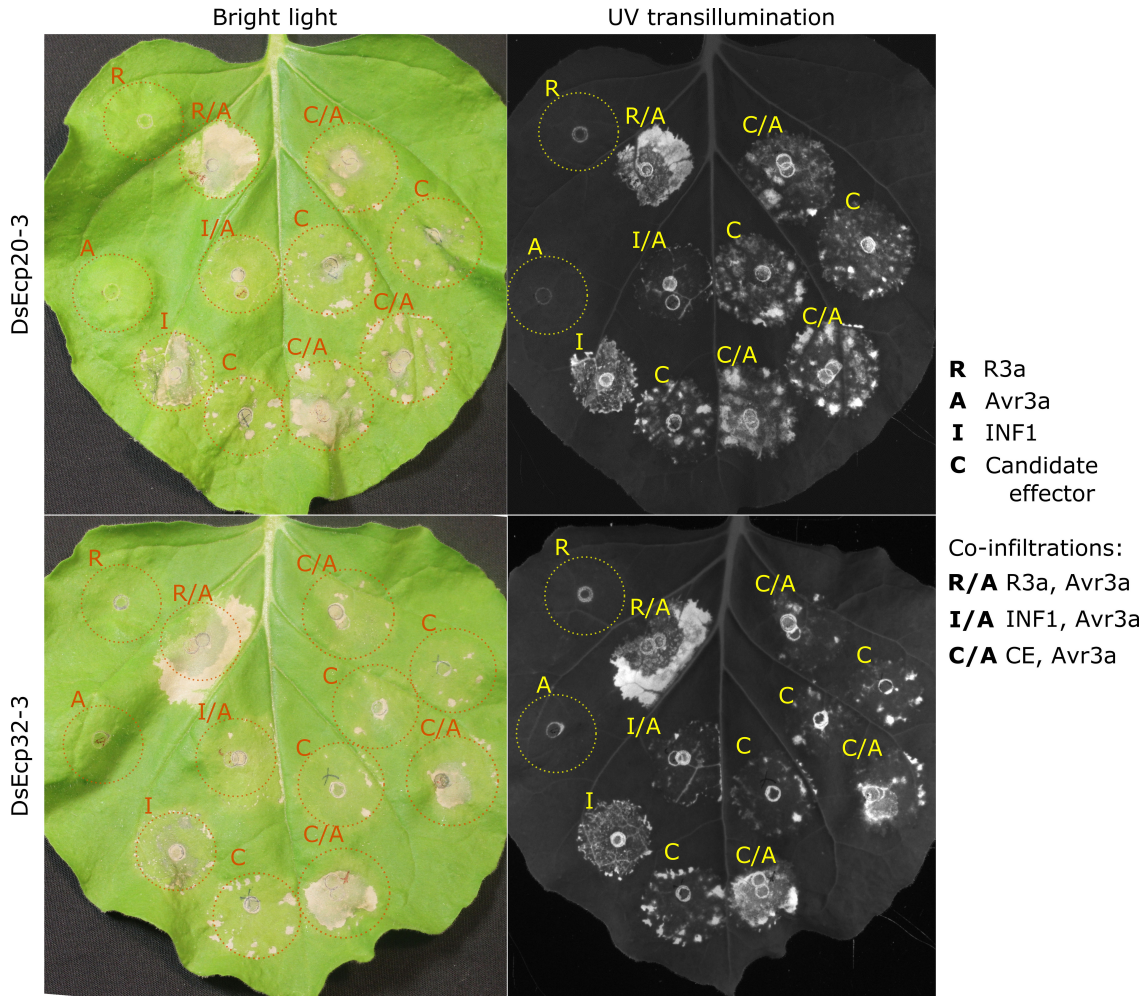

Figure 4.5.: Cell death suppression assay using co-infiltration in *Nicotiana benthamiana* demonstrated that DsEcp20-3- and DsEcp32-3-induced cell death was not suppressed by Avr3a. The left and right panels show the same leaf. Circles approximately indicate the infiltrated areas. Avr3a was infiltrated 24 h prior to all effectors/elicitors. Representative images shown (6 dpi; $n = 13$ leaves for each CE).

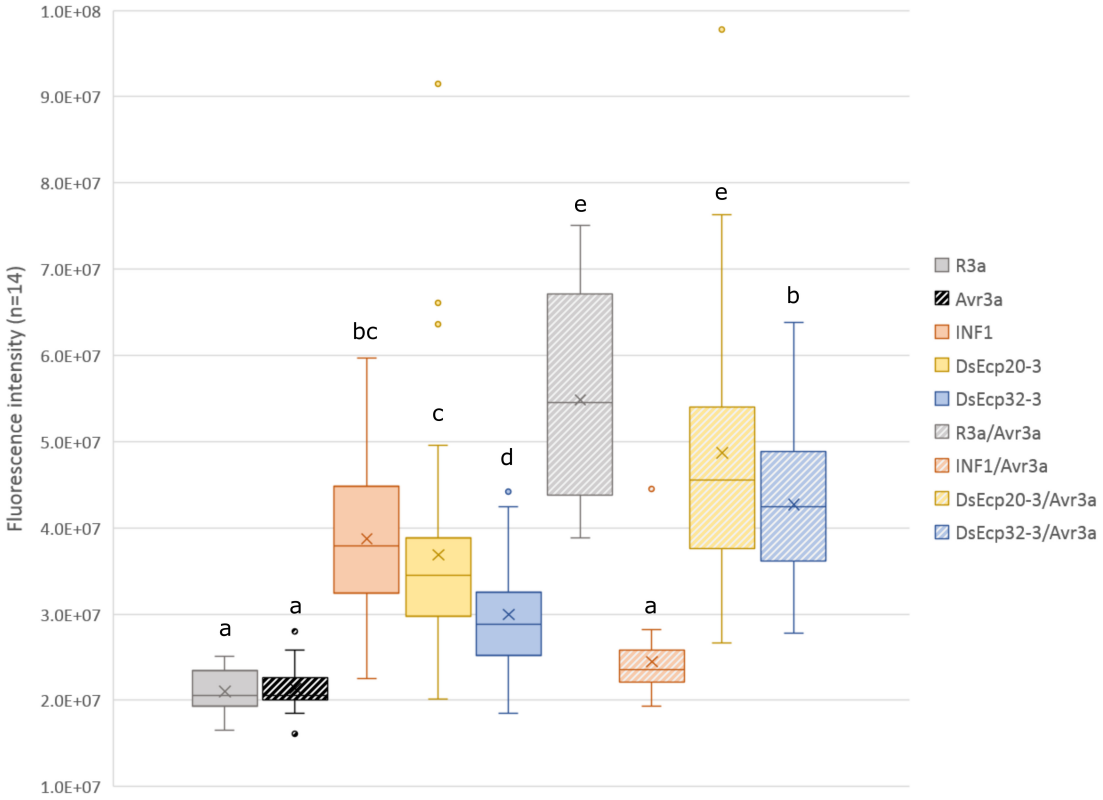

Figure 4.6.: Cell death in *Nicotiana benthamiana* suppression assay represented by tissue fluorescence after UV exposure. For fluorescence intensity, digital image analysis was carried out with ImageJ. Fluorescence intensity for each infiltration zone was calculated as Raw Integrated Density (sum of pixel grey values corresponding to fluorescent area) divided by the total infiltrated area. For each of the two CEs and CE/Avr3a co-infiltration, data collected from three individual infiltration areas per leaf were pooled ($n = 14$ leaves per CE). Different letters indicate significance of differences between samples and was assessed using t-tests ($p < 0.05$; most comparisons had $p < 0.001$). The lower and upper hinges correspond to the first and third quartiles and the upper (lower) whiskers extend from the hinge to the largest (smallest) value that is within 1.5× the interquartile range of the hinge. Data beyond the ends of the whiskers are outliers.

4.2.7. Cell death elicitors from *D. septosporum* are homologous to small secreted proteins from other pathogens

Invasion patterns (IPs) include proteinaceous molecules that are widespread among plant-associated microbes. Based on the finding that several DsCEs induced cell death in non-host plants, it is suggested that these DsCE could be recognised as IPs, and could thus be found in other pathogens (or non-pathogens). JGI BLAST searches showed that protein sequences homologous to those of candidates DsEcp20-3, DsEcp32-3, DsCE15 and DsCE3 are present at least in the Dothideomycetes family, based on a search of 123 genomes. The Sordariomycetes (145 genomes), which contain a large proportion of plant-pathogenic taxa such as the mostly hemibiotrophic *Colletotrichum* spp. (de Silva *et al.*, 2017), were also separately queried and homologues were found for DsEcp32-3, DsCE15 and DsCE3 (hit tables of all queries in Table D.1). Furthermore, to allow a wider scan of all other taxa, the NCBI database was used for BLAST queries, excluding Dothideomycetes and Sordariomycetes.

Ds70057 was named DsEcp32-3 as it appears to be a direct orthologue of *C. fulvum* hypothetical protein 189688 (JGI), and both proteins are similar to *C. fulvum* Ecp32-1 and -2 (Fig. 4.7); Cf189688 is not officially annotated as 'CfEcp32-3' because it was not detected in apoplastic fluid samples harvested from a compatible *C. fulvum*–tomato interaction (Mesarich *et al.*, 2017). The group of homologues in *C. fulvum* and *D. septosporum* form part of the 'Ecp32 family', although it should be noted that this family likely extends to many other species as indicated by the following results. DsEcp32-3 also has homologues in the majority of dothideomycete species (142 hits including several hits in many genomes; up to ˜65% aa identity) and some sordariomycete species (27 hits; up to ˜19% aa identity). Sequences from the top nine species of each group are aligned in Fig. E.8; some of these species had multiple hits of similar quality. Furthermore some conservation was found in a broad spectrum of the remaining Ascomycetes (144 hits), as well as *Punctularia strigosozonata* (Basidiomycete, E ≈8E-12), and curiously *Quercus suber* (cork oak, Eudicots, E≈9E-16). The structural queries of DsEcp32-3 yielded no meaningful results.

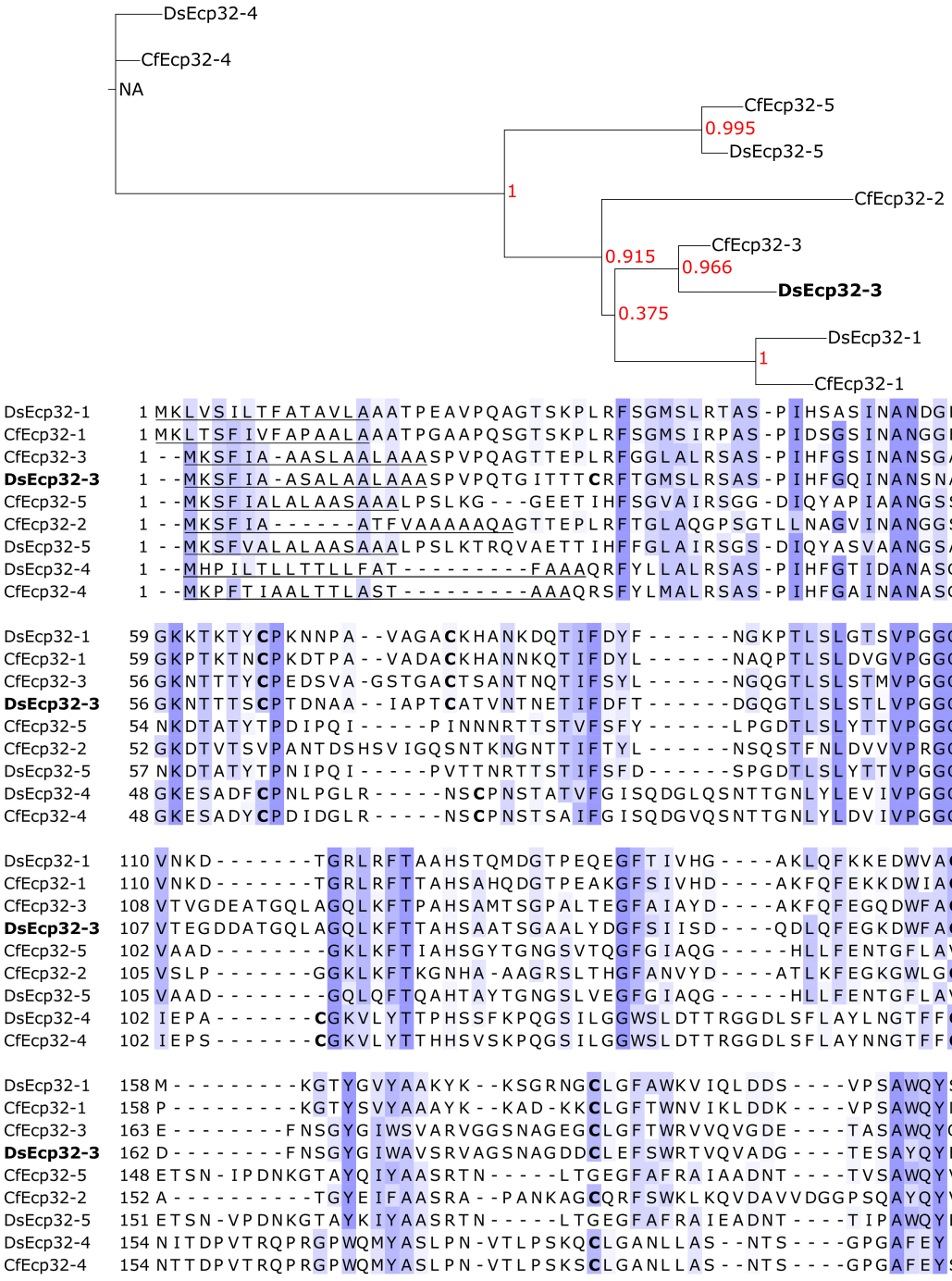

Figure 4.7.: Maximum likelihood protein phylogeny and Clustal Ω protein alignment of Ecp32 homologues in *D. septosporum* and *C. fulvum*. In the tree, supporting values are shown in red. In the alignment, the predicted signal peptides are underlined. Blue shading indicates conservation starting at 30%; Cys residues are in bold font. DsEcp32-4 (95543) and DsEcp32-5 (174276) had incorrect gene models, which was corrected here. CfEcp32-3, -4, and -5 were not confirmed as apoplastic proteins in apoplastic wash fluid samples from a compatible *C. fulvum*–tomato interaction.

DsEcp20-3 sequence homologues were found in a limited number of dothideomycete genomes only (Fig. 4.8; 20 hits in 14 species, with up to ˜65% aa identity). DsEcp20-3 was named after CfEcp20-3 that was identified as a likely direct orthologue (E<1.8E-63) and also shares a structural prediction (Mesarich *et al.*, 2017). Both proteins are predicted to be similar to characterised proteins containing an Alt a 1-like fold. Other members of the Ecp20 family, CfEcp20-1 and CfEcp20-2, also appear to be apoplastic proteins (Mesarich *et al.*, 2017), and DsEcp20-1 (Ds51311, a shortlisted CE) and DsEcp20-2 (Ds51158, a potential paralogue of DsEcp20-3, which lacked a signal peptide sequence in the original JGI gene model) are their likely orthologues (Fig. 4.9; Table 3.2). Other possible additions to the family are DsCE5 and the almost identical Cf191139, which also share the same structural predictions and could be accordingly renamed DsEcp20-4 and CfEcp20-4.

DsEcp20-3 was queried via HHpred again after establishing its cell death elicitor function. This revealed the structural similarity of DsEcp20-3 to the characterised effector protein PevD1 (98.5% probability score; Fig. E.9). Consequently, CfEcp20-3, as well as the potentially very similar DsEcp20-1 and DsCE5, were resubmitted to HHpred, with the updated RCSB PDB[1] containing the PevD1 model. As for DsEcp20-3, all these three sequences produced PevD1 as the best hit with similar scores.

DsCE3 sequence homologues were found in the Dothideomycetes (131 hits), Sordariomycetes (98), other Ascomycetes (58), as well as *Acinetobacter baumanii* (Gamma-Proteobacteria; E≈1E-15). It was noted that a newly identified fungal PAMP named RcCDI1 (Franco-Orozco *et al.*, 2017) is homologous to DsCE3 (E≈5E-39). The alignment of RcCDI1 homologues, including DsCE3, which all induced cell death in non-hosts, is shown in Fig. 4.10. A summary and phylogenetic tree showing the high degree of conservation of the 'PAMP' is available in Franco-Orozco *et al.* (2017).

There are three positions with single amino acid changes only found in DsCE3. Upstream of the first conserved cysteine, S34C is followed by L38Y (positions corresponding to DsCE3 full sequence). Both these changes are slightly less likely than a random change (BLOSUM62 score of -1), along with Y171T (-2) between the fourth and fifth Cys, and could be investigated regarding their relevance for recognition. The G55S change in be-

[1]Research Collaboratory for Structural Bioinformatics Protein Database

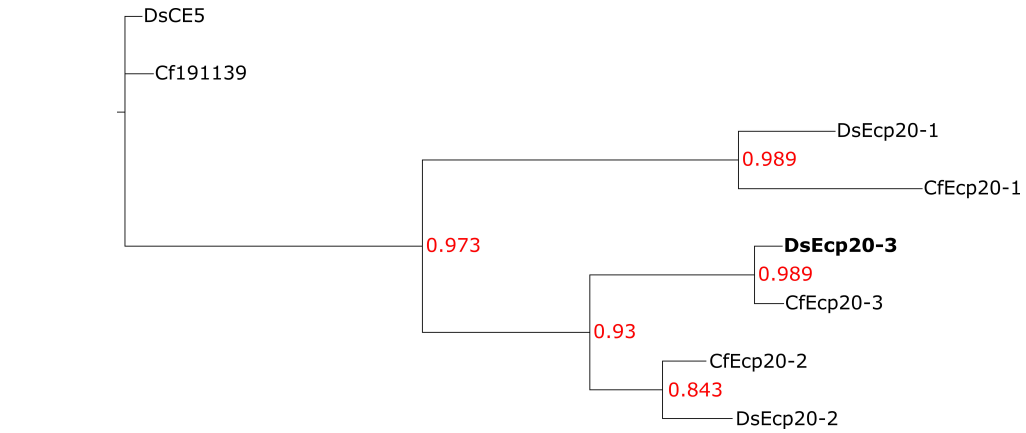


```
DsEcp20-3      1 ------MLASSLLTVAAATLATALPAGVT------PAAAPGQFDITNFIFGCTAGC-FW  46
CfEcp20-3      1 ------MLASSLLTLAAATLATALPAGVE------PAAAPGQFEVTNFVFGCTVGC-DW  46
CfEcp20-2      1 ------MLFTNYLILAGAALAAAVPSELAG-------PKPNQFTITNFVFGCTVGC-DW  45
DsEcp20-2      1 ------MLFTRYLVLAGAALGAAAPSELAN-----KASKPKQFAVTEFVFGCTDGC-YW  47
Cf191139       1 ------MQFTTVLALLSAVAAPALAAPAADPATTSMMAAGPPWTIQNFKRTCGGGVCCTY  53
DsCE5          1 ------MQFTSVLALLSAVAVPALAAPAADPATTNMMASGPQWTVQNFKRTCGGGVCCTY  53
DsEcp20-1      1 MFLNLASTFVLSLGLLSTASAAAIEARQG--------NKPDAWHITTFDASCKNGLCQY  51
CfEcp20-1      1 MFSNVASTLAFSLGLASMASAAAVAAPQSD-------SGDNLWHISGFDARCANARCQY  52

DsEcp20-3     47 YLDIAVHPAV---------A-NHPSVPSSVHC---------QGNLDDNKSFKECDHV--  84
CfEcp20-3     47 YLDIAVHPDI---------AGTHPSVPNGVHC---------EGNLDDNKSFKECAHV--  85
CfEcp20-2     46 SFNVAVQGSG---------PDHPPVKKPVKC---------SGNVNDAKDYVDCGKI--  83
DsEcp20-2     48 NFKVAVQGEG---------PNHPPVQKPVEC---------SGSLDDNKDYVDCGEI--  85
Cf191139      54 DYAINQNNKATKCTYQVKGNPATRASYSNVKCGPYVISSNWSGQFGEGNGFQTLAVV--110
DsCE5         54 DYSVLQNGQATKCNYQVKGSPATRASYNNVQCGPYVISSSWSGQFGDGNGFQTLAVV--110
DsEcp20-1     52 YFQADSNGNDGRPGF--------RAV-----CQG-------QGLQRNDMTLRDCTFPGP  90
CfEcp20-1     53 SFQITSYGDDDIPGF--------SAS-----CQT-------TGISRNDQTWRPCTVTYG  91

DsEcp20-3     85 --TNESKLYAFI------GKDDNLLQLKYEVTNSSTSTVYNYYGEKEVYAATSAYADLQ 135
CfEcp20-3     86 --SNGSKLYAFI------SKDDNLLQLRYEVTDVATSTVYNYYGEKAVYAATSDYADLQ 136
CfEcp20-2     84 --SDTQRIKAYI------VKATNQLKLEYEVQKPNHGAVYRYTGEKKVYAATGEHAKLQ 134
DsEcp20-2     86 --SKTQTIRAYI------VKATNELMLKYEVQKPKQGAMYQYTGEKKVYAATNDPKKLQ 136
Cf191139     111 --NGKQIIYPAY------T--DKQLV-NGQVVKPDQ----------SYAPQ------N 141
DsCE5        111 --NGKQIIYPAY------T--DKQLV-SGQVVTPDQ----------SYTPQ------N 141
DsEcp20-1     91 SPSGIQNVQAYVQLTPLRPGYQSEFKLQVGFTSGRQGIVYYSGTQKNTYREWRDYSASG 149
CfEcp20-1     92 SSDGVQSVKVYLPLTPLRPNSPTQFRIRAAFSDS-DRVTYYTASLNGSYNGWRDTSRRG 149

DsEcp20-3    136 --TPNFNVTEISGTKSKSS                                        152
CfEcp20-3    137 --TPEFNVTEISGTKSKSA                                        153
CfEcp20-2    135 --KPNFVVKETGSTGVA--                                       149
DsEcp20-2    137 --KSSFIVKETSPTRVV--                                       151
Cf191139     142 --LP----------------                                      143
DsCE5        142 --LPS---------------                                      144
DsEcp20-1    150 IYGGVFDVEPKLSSAVL--                                       166
CfEcp20-1    150 SDAGKFDMYPAASAAVA--                                       166
```

Figure 4.8.: Maximum likelihood protein phylogeny and Clustal Ω protein alignment of *D. septosporum* and *C. fulvum* candidate effectors predicted to have structural similarities to PevD1 and Alt a 1. In the tree, supporting values are shown in red. In the alignment, the predicted signal peptides are underlined. Blue shading indicates conservation starting at 30%; Cys residues are in bold font, 100% conserved Cys residues are coloured ochre. In DsEcp20-3, Cys residues 1 and 2 are predicted to form a disulphide bond, as well as Cys residues 3 and 4.

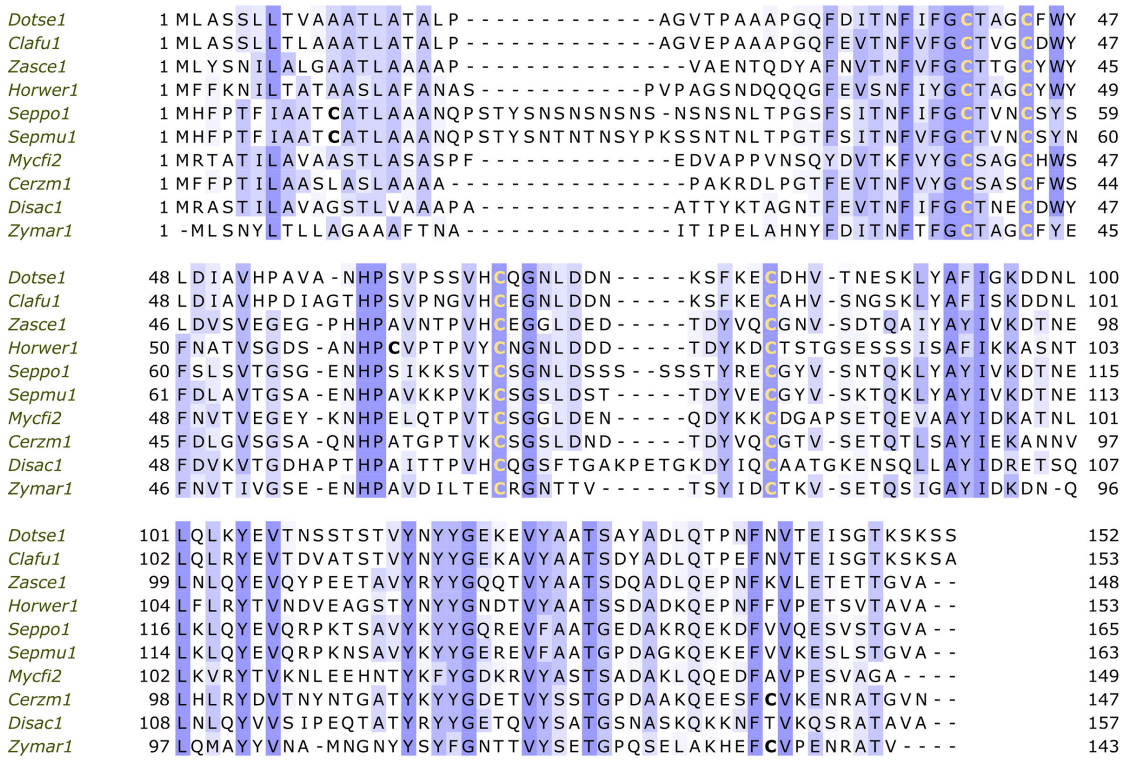

Figure 4.9.: Clustal Ω protein alignment of DsEcp20-3 with top nine homologues in dothideomycete taxa. Cys residues are in bold font, 100% conserved Cys residues are coloured ochre. BLASTp was conducted on the JGI servers in April 2018. Species names and protein IDs are as follows: *Dothistroma septosporum* NZE10 70694 (DsEcp20-3) *Cladosporium fulvum* 192674, *Zasmidium cellare* ATCC 36951 71191, *Hortaea werneckii* EXF-2000 M0 7779, *Septoria populicola* 47895, *S. musiva* SO2202 151343, *Pseudocercospora* (*Mycosphaerella*) *fijiensis* 209811, *Cercospora zeae-maydis* 89740, *Dissoconium aciculare* 380732, *Zymoseptoria ardabiliae* STIR04 1.1.1 774978.

tween the second and third Cys of RcCDI1, could theoretically reduce hydrophobicity and flexibility. However, this change is also found in the *Neurospora crassa* homologue, additional to two other substitutions, and the corresponding *M. oryzae* sequence is almost completely different. Thus, it is unlikely that this domain is crucial for recognition.

The predicted secondary structures of DsCE3 and RcCDI1 were also aligned. This suggested high similarity of the two proteins (Fig. E.10).

Of the cell death inducers, DsCE15 appears to be the most highly conserved in Dothideomycetes (up to ˜84% aa identity) and Sordariomycetes (up to ˜72% aa identity) with 94 and 49 hits, respectively, but also in other Ascomycetes, and oomycetes (up to ˜68% aa identity, *Phytophthora sojae*). A protein alignment of the top DsCE15 homologues in nine different dothideomycete and sordariomycete species each is shown in Fig. 4.11; in many of these species there were multiple hits. In NCBI, comparatively low-scoring hits (<26% aa identity) to the Basidiomycetes *Puccinia* and *Melampsora* spp. were recorded. The structural queries of DsCE15 yielded no meaningful results.

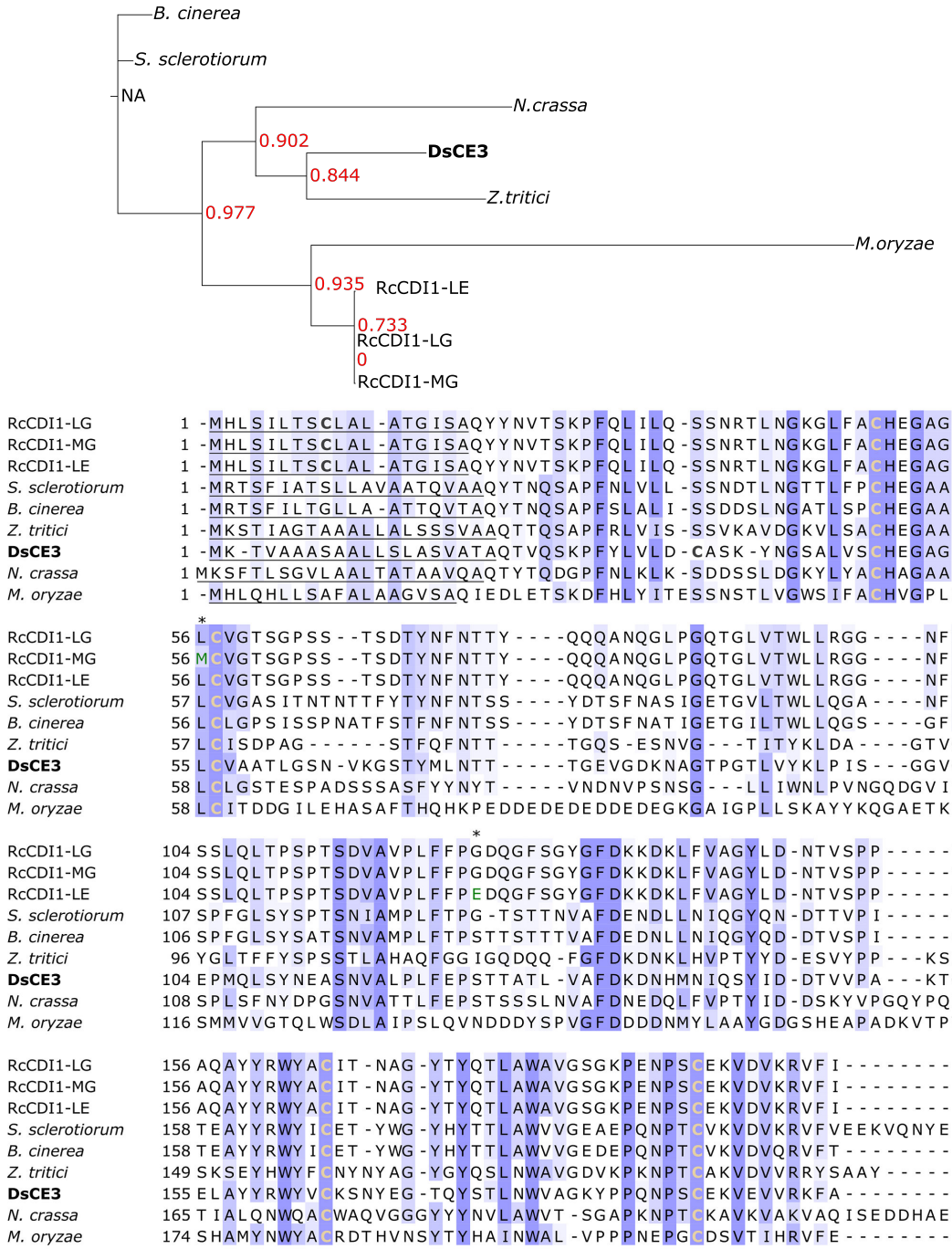

Figure 4.10.: Maximum likelihood protein phylogeny and Clustal Ω protein alignment of three *Rhynchosporium commune* Cell Death Inducing 1 (RcCDI1) alleles and cell death-inducing homologues including DsCE3. In the tree, supporting values are shown in red. In the alignment, the predicted signal peptides are underlined. Blue shading indicates conservation starting at 30%. Cys residues are in bold font, 100% conserved Cys residues are coloured ochre. The asterisks indicate the polymorphic positions in the RcCDI1 sequences. Species names: *Sclerotinia sclerotiorum*, *Botryis cinerea*, *Zymoseptoria tritici*, *Neurospora crassa*, *Magnaporthe oryzae*. The last 113 residues of the *N. crassa* sequence are not shown.

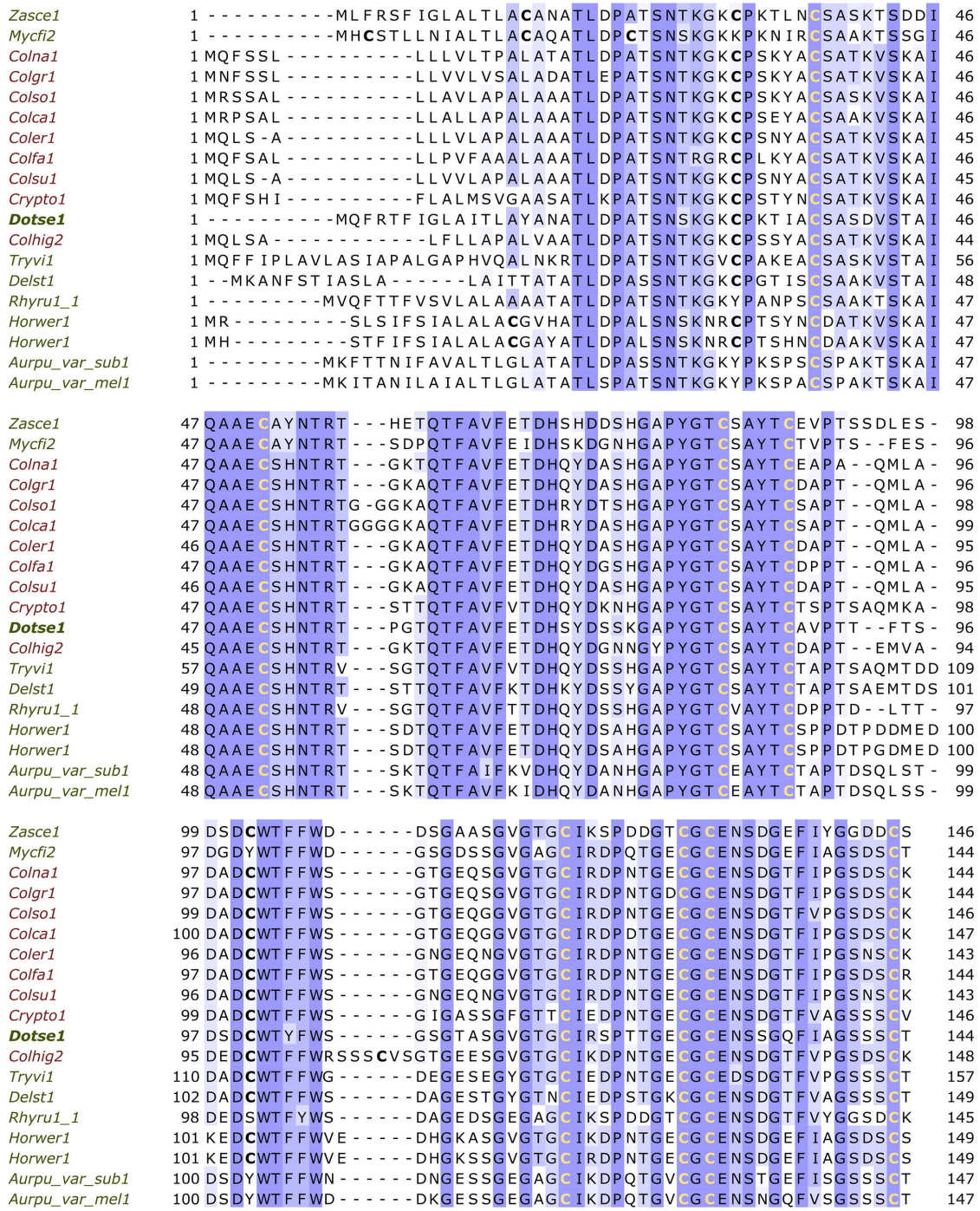

Figure 4.11.: Clustal Ω protein alignment of DsCE15 with top nine homologues in dothideomycete and sordariomycete taxa shows broad conservation. Dothideomycete species are coloured green, sordariomycete species in red; Cys residues are in bold font, 100% conserved Cys residues are coloured ochre. BLASTp was conducted on the JGI servers in April 2018. Species names and protein IDs are as follows: *Colletotrichum navitas* CBS125086 688026, *C. caudatum* CBS131602 622596, *C. somersetensis* CBS 131599 451643, *C. graminicola* M1.001 10636, *C. eremochloae* CBS129661 627608, *C. higginsianum* IMI 349063 1348, *C. sublineola* CBS 131301 676018, *C. falcatum* MAFF306170 24795, *Cryptodiaporthe* sp. AZ0812 527881; *Zasmidium cellare* ATCC 36951 18758, *Delphinella strobiligena* CBS 735.71 376977, *Pseudocercospora* (*Mycosphaerella*) *fijiensis* v2.0 83583, *Trypethelium eluteriae* 508428, *Hortaea werneckii* EXF-2000 M0 11540, *Aureobasidium pullulans var. melanogenum* CBS 110374 87757, *Cladosporium fulvum* 35846, *A. pullulans var. subglaciale* EXF-2481 323739, *A. pullulans var. pullulans* EXF-150 110853, *Dothistroma septosporum* NZE10 131885.

4.3. Discussion

In this chapter, a subset of *D. septosporum* CEs identified in chapter 3 was investigated using a forward genetics approach. This partially addressed thesis aim 3, to determine whether CEs have virulence or avirulence functions, and thus a fundamental aspect of molecular forest pathology. Seventeen CE genes were cloned for *Agrobacterium*-mediated expression in non-host plants to determine whether they induce cell death. Four new cell death inducers were found, and their genes appear to be common among fungi.

4.3.1. Validation of CE protein expression in non-host plants

Using the apoplastic wash fluid (AWF) collection method (see 5.2.1), expression of each CE in *N. benthamiana* was checked by western blot. For eight of 19 tested proteins and the positive control (INF1), a signal based on anti-FLAG antibody was detected. The presence of four out of six cell death inducers expressed in the apoplast (DsEcp20-3, DsEcp32-3, DsCE3, and DsEcp2-1) was indicated by this method. The positive control INF1, and DsCE15 were not detected by western blot in AWF samples. This could mean that expression levels for both these proteins were too low to be detected, although infiltration of the same AWF samples into the plants confirmed that they contained a sufficient concentration of an active compound to induce cell death (subsection 5.2.2). In fact, INF1 samples still triggered strong cell death at a 16-fold dilution in *N. tabacum* (Fig. 5.1). A very similar result was seen in Bos *et al.* (2010), where FLAG-tagged INF1 was not detected via western blot, and dilutions of the same protein solution up to 15-fold still triggered a cell death response in *N. tabacum*. Consequently, absence of a tagged protein in a blot is not to be taken as absence of the same protein in the apoplast. For the other non-cell death-eliciting CEs that were not detectable by western blot, it remains to be determined whether they too were expressed at a level not sufficient for detection or, for example, they were unstable in this non-host environment.

The DsEcp2-1 band matched its expected size and, as a previously characterised protein, DsEcp2-1 serves as an alternative positive control for the new extraction method. The DsEcp32-3 and DsCE3 bands indicated a higher molecular weight than expected. Both proteins have one predicted asparagine glycosylation site, thus, the post-

translational addition of a glycan may have affected the migration of both proteins on the gel. The DsEcp20-3 sample produced a larger band in addition to the expected one, and no glycosylation sites were predicted. It could be that DsEcp20-3 undergoes additional post-translational modifications, or dimerises.

A more direct method to track proteins is to link them to a fluorescent protein. It is possible that this interferes with protein localisation or function (Lo Presti *et al.*, 2015). Visualisation of the CE via fluorescence microscopy could be used separately from the cell death screening to validate not only CE protein expression but also localisation.

4.3.2. Variability in agroinfection assays and analyses

Agrobacterium-mediated screening for cell death, indicating activation of a non-host resistance response, was initially carried out with infiltration culture ODs of 0.6 and 1.0 with all cloned CEs. This represents a compromise on common practice seen in studies using similar agroinfection assays, with final ODs ranging from 0.2 to 2.0 (van der Hoorn *et al.*, 2000; Wei *et al.*, 2007; Clarke *et al.*, 2015; Brendolise *et al.*, 2017; Kettles *et al.*, 2017; Jayaraman *et al.*, 2017; Raffaello & Asiegbu, 2017). Importantly, cell death responses were not observed in empty vector controls or with the majority of apoplastic CEs at ODs 0.6 and 1.0 at their latest observed time point (7 dpi). Thus, non-specific responses of the plant to this treatment can be ruled out.

Variability of cell death intensity was observed throughout the project. Cell death phenotypes in *N. benthamiana* have been shown to be light-dependent, i.e., cell death responses did not or barely develop in the dark (Keon *et al.*, 2007; Kettles *et al.*, 2017). The GMO-approved plant chamber used in my assays was subject to fluctuation of natural light due to a) variation in cloud cover and b) seasonal differences in exposure based on the path of the sun. Light intensity was not monitored. It is likely that differential light intensity correlated with varying severity of cell death. This factor, along with other subtle differences affecting the biology of each plant, probably led to differences in overall stress, affecting how strongly a resistance response could be launched.

Was variability in ATTA results correlated with CE expression efficacy? The OD range for infiltrations was expanded to determine a response threshold at lower cell concentra-

tions. The hypothesis was that infiltrating less dense *Agrobacterium* cultures culminates in less cell death in the infiltration zone. This in turn was based on the assumption that a lower density of infectious cells leads to less CE protein expression. Thus, the the cell death-inducing CEs were tested at ODs serially diluted down to 0.05.

The observations, while not replicated in three experiments with all CEs, strongly suggest that low infiltration culture densities ($\leq$0.4) are at least as effective as high ones ($\leq$0.6). Considering the broad range of infiltration densities reported in the literature (see above), this is not surprising. Doses of purified proteins that are sufficient to cause cell death are usually determined, but reports of results from an OD series similar to this one are scarce. The most obvious explanation for lower ODs being as effective as higher ODs is that the concentration of cell death elicitor protein produced by the lowest density of infectious cells is enough to trigger a cell death pathway, and any surplus in cells will result in an excess of elicitor and no change in the visible response. Of all cell death inducers, only DsEcp2-1 and DsCE3 results supported the hypothesis stated above that lower densities of the respective cultures resulted in less cell death.

Intriguingly, in *N. benthamiana*, DsEcp20-3 showed a trend to induce a quicker and more severe cell death response at the lower two ODs than the higher two ODs used in this experiment. This could be due to a number of reasons. In other studies, it was observed but often not discussed that higher bacterial cell density can be detrimental to infection efficiency (Opabode, 2006). *Agrobacterium* cells cause PTI, which prevents further responses; however, PTI is suppressed shortly after the T-DNA is transferred (Veena *et al.*, 2003). It could be that a defence response ultimately resulting in less CE protein present in the apoplast is caused by the detection of a density of *A. tumefaciens* cells, including dead ones, which is not entirely suppressed. More data is needed, however, if such speculations should be pursued.

Conclusively, lower ODs than 0.4 should be rigorously tested for all cell death inducers to detect a dose threshold. Regarding the differential responses to lower (DsEcp2-1) or higher (DsEcp20-3) ODs, applying a concentration range of CE protein only could yield valuable insight. Specifically, an effect of excess of apoplastic protein on cell death responses could be supported or ruled out. In addition, these results did not contribute

to explaining the variability in ATTAs.

Did Avr3a promote cell death in N. benthamiana, rather than suppress it? In the cell death suppression assay, the question was whether the combination of cell death inducers DsEcp20-3 or DsEcp32-3 with the Avr3a effector would result in reduced cell death due to inhibition of the induction pathway by Avr3a. If this was not the case, an unaltered cell death response was expected. Contrary to this expectation, the co-infiltration with Avr3a resulted in stronger cell death. This could be due to an immunity priming event caused by the Avr3a culture which was infiltrated 24 h prior to each CE culture. It could be tested if the stronger response was purely due to sequential *A. tumefaciens* infiltration in this case, or if either of the transiently expressed proteins (Avr3a, DsCEs) played a specific role.

To elucidate the role of Avr3a in this, the following should be done: a) Invert sequence of infiltrations, b) mix Avr3a with CE culture for co-infiltration, c) substitute Avr3a with empty vector control or a CE that does not trigger cell death, d) infiltrate protein samples rather than cultures. Together, such experiments could at least eliminate the possibility that Avr3a has an unknown function promoting cell death induction.

4.3.3. Assessment of cell death quantification methods

Cell death occurrences in ATTAs are usually reported as percentages of all infiltration sites, or scores for different grades of cell death per site (judged by eye). Visual results may be supported by measurements of effects that accompany IP-triggered cell death, such as electrolyte (ion) leakage from cells, ROS accumulation, or defence gene induction (Frías *et al.*, 2011). Here, ion leakage and UV light emission methods were used to quantify cell death intensity in each infiltration zone. Each method had advantages and disadvantages.

The ion leakage assay is well established, even though the variability in protocol details in the literature reflects some required adaptation to the conditions of each experiment (Bailey *et al.*, 1990; Oh *et al.*, 2010; Frías *et al.*, 2011; Jayaraman *et al.*, 2017). It is particularly well suited for analysis prior to development of visible symptoms (collapse and browning/darkening of tissue, indicating cell death) because these usually indicate the final phase of the response when other representative signals are saturated. Howe-

ver, the leaf discs used for this assay are likely not always representative of the entire response occurring in each zone, which demands a high replicate number. In a small-scale experiment for DsEcp20-3, the standard deviation was higher at 3 dpi than 5 dpi on *N. benthamiana*, but vice versa on *N. tabacum* (with clearly visible cell death at 5 dpi but not 3 dpi in both cases; Fig. E.7).

Applying UV exposure to the leaves facilitated detection of weak cell death responses in subsequent image analysis. The imaging and image data acquisition steps were less time-consuming than the ion leakage method. However, the reliability of this imaging method for cell death quantification was dubious due to high variation between results. While it is possible that natural variation among samples is most accurately reported by this method, variability in data may have been partly introduced by manually capturing each infiltration zone in the digital images ('freehand tool'). Despite this reservation, some differences between treatments were clarified. For example, the data supported the visual observation that INF1-induced cell death is on average not completely suppressed by Avr3a (Fig. 4.6), which corroborates similar reports (Bos *et al.*, 2006). The numbers also showed that DsEcp20-3 induced more severe cell death in *N. benthamiana* than DsEcp32-3. Using percentage of sites with cell death (approx. 70% in both cases), the small difference between these two CE would have remained descriptive. Thus, conducting this quantification added value which may be of interest in the future. To summarise, the UV imaging can provide a useful and quick mode of data collection. If numerical support with digital measurements is deemed unnecessary, UV images still constitute a strong support for observations based on regular photography.

In both approaches it has to be taken into account that natural variation may occur between each plant and leaf (or even area of leaf, pers. comm. J. Jayaraman), and thus a high number of replicates is required. For time-series analyses, further increased replication is needed, as both procedures are destructive to the samples, i.e., each detached leaf can only be analysed once, and detaching may affect the rest of the plant, thus its other leaves have to be sampled at the same time.

4.3.4. Cell death inducer DsEcp20-3 is predicted to be structurally similar to the characterised effector protein PevD1

DsEcp20-3 (70694; 135 aa, four Cys) showed strong up-regulation in the Mid and Late *in planta* stages (45- and 25-fold, respectively) compared to the Early stage and in culture (Table 3.1). In functional assays, DsEcp20-3 induced cell death in 66% of infiltration zones in *N. tabacum*, and in 71% of zones in *N. benthamiana* (Fig. 4.1). In both plants, there was sometimes only a partial cell death response in the infiltrated zone. Regardless, induction of cell death may indicate that DsEcp20-3 is recognised as an IP by a corresponding PRR in these plants.

Predicted structural homology to a protein family with a growing number of characterised members.

DsEcp20-3 is likely a direct orthologue of *C. fulvum* effector candidate CfEcp20-3 and was named accordingly. CfEcp20-3 was up-regulated 62-fold *in planta* and not recognised in wild tomato (Mesarich *et al.*, 2017). It was consistently predicted to have structural homology to the major allergen Alt a 1 from the Dothideomycete *Alternaria alternata* (Mesarich *et al.*, 2017). *A. alternata* is a saprophyte and a broad-range plant pathogen, although it is also known to be an opportunistic pathogen of humans. There is a large protein family (PF16541) named after Alt a 1, and these proteins are specific to Dothideomycetes and Sordariomycetes. Protein functions within this family remain largely unknown, although Alt a 1 itself was found to be an effector protein fulfilling two different functions for promoting plant colonisation of *A. alternata*. In the apoplast, it is capable of mediating detoxification of ROS and inhibiting plant defense proteins belonging to the pathogenesis-related 5-thaumatin-like family (summarised in Mesarich *et al.*, 2017). Structural homology to Alt a 1 was also predicted for DsEcp20-3 by HHpred, with a similar score to that for CfEcp20-3. However, *Verticillium dahliae* effector protein PevD1 (Han *et al.*, 2012) was by far the best hit for DsEcp20-3. PevD1 features a C2-like domain which can be involved in targeting proteins to membranes, and its β-barrel core resembles that in ethylene-inducing peptide (Nep1)-like proteins (NLPs) (Zhou *et al.*, 2017)—a family of elicitor proteins classified as MAMPs as they are found in various fungal, oom-

ycete and bacterial pathogens (Ottmann *et al.*, 2009; Oome *et al.*, 2014). PevD1 notably also shares structural similarity with Alt a 1. The interaction of PevD1 with host proteins was shown to induce early flowering (Zhou *et al.*, 2017), and PevD1 induced cell death in *N. tabacum* (Wang *et al.*, 2012) and *N. benthamiana* (Zhou *et al.*, 2017). The Alt a 1 fold was also found in *Magnaporthe oryzae* HR-inducing protein 1 (MoHrip1). MoHrip1 was highly induced during the infection of *Oryza sativa* (rice), shown to localise to the plant cell membrane, caused cell shrinkage and chloroplast disorganisation in rice and *N. tabacum*, and induced cell death and other typical PTI responses in *N. tabacum* (Zhang *et al.*, 2017a). Also, as with MoHrip2 (see subsection 3.3.8), the presence of MoHrip1 in *O. sativa* increased the plant's resistance against pathogen infection (Wang *et al.*, 2017b).

The structurally related DsEcp20-3, PevD1 and MoHrip1 induced cell death in tobacco species. To my knowledge there is no evidence that tobacco species are hosts to *V. dahliae* or *M. oryzae*. It has already been suggested by Zhang *et al.* (2017a) that apoplastic Alt a 1-like proteins could generally be MAMPs. PevD1 manipulates intracellular proteins and the protein was located in plant cells, but mostly localised to the membrane, thus, a plant transmembrane protein might be involved in the function of PevD1 while it remains in the apoplast (Zhou *et al.*, 2017). Tagged DsEcp20-3 protein was recovered from *N. benthamiana* apoplastic fluid (Fig. 4.4). Conclusively, this supports that Alt a 1-like proteins act as extracellular IPs, recognised by PRRs in non-hosts.

Potential to further elucidate the modular parts of a conserved protein structure.

CfEcp20-3, as well as its homologues CfEcp20-1 and DsEcp20-1, have not been functionally tested in non-hosts. However, DsCE5, one of the most highly expressed (and induced) SSCPs during pine infection, which was later predicted to have structural similarity to PevD1 as well, and thus putatively added to the Ecp20 family, was tested using ATTA and it did not induce cell death in *N. benthamiana* or *N. tabacum* (Fig. 4.1). DsCE5 protein presence in the apoplast was indicated by a western blot in *N. benthamiana* (Fig. E.6). This provides an intriguing lead for further investigation of domains that are involved in IP recognition.

It is remarkable that proteins in the Ecp20 family, PevD1 and MoHrip1 have no or little sequence identity despite their structural similarity. This might represent conservation of particular folds (and function) regardless of the primary sequence (see also section 3.1). Such functional conservation is evident in other fungal protein families such as the 'MAX' effectors (*M. oryzae* Avrs and ToxB of *Pyrenophora tritici-repentis*), in which the characteristic fold is stabilised by at least one disulphide bond. Similarly in *Blumeria graminis*, the 'RALPH' (RNase-like proteins expressed in haustoria) candidate effector group was defined based on striking fold commonalities, however, these folds were computationally predicted and await experimental verification (Franceschetti *et al.*, 2017).

Acquiring a crystal structure of more of the PevD1-like CEs, foremost the cell death inducer DsEcp20-3, could greatly further the understanding of this 'structural family'. Likewise, uncovering the function and actual structure of DsCE5 should be pursued, since this candidate did not induce cell death in my assays. It is assumed that the apoplastic proteins DsEcp20-3 and DsCE5 share a structural scaffold. As briefly discussed by Mesarich *et al.* (2017), a conserved fold may provide core features to IPs, such as stability in the hostile apoplast environment. Meanwhile, diverging regions of the structure could be more likely found on the protein surface, resulting in certain CEs (DsEcp20-3, PevD1, MoHrip1) interacting with PRRs, but not others (DsCE5). Directly comparing the structures of DsEcp20-3 and DsCE5 might yield the key to identifying the domain responsible for PRR recognition.

Alternatively, identification of such a domain could be achieved by the generation of mutants, designed based on the sequence alignment. Groups of diverging amino acids could be substituted, and subsequently single substitutions, with differences in cell death responses to modified proteins being monitored, as was done for Avr4 (Mesarich *et al.*, 2016). To facilitate this, the other members of the Ecp20 family should first be screened for cell death induction. In the case that not all of them trigger cell death, it might prove relatively easy to narrow down the sequences/amino acids relevant for the cell death induction function.

Cell death induced by DsEcp20-3 was not suppressed by the effector Avr3a, suggesting that DsEcp20-3 does not use a CMPG1-dependent cell death pathway. This represents a

first step to further understanding the fate of DsEcp20-3 in the interactions with plant cells.

4.3.5. Cell death inducer DsCE3 has sequence homology to RcCDI1, a recently identified PAMP

DsCE3 (71487, 180 aa, 5 Cys) was most highly induced in the Late stage (36-fold compared to in culture). It has no paralogues in *D. septosporum*, but it does have hits to at least 287 hypothetical/unnamed proteins in other ascomycete species. Secondary and tertiary structure predictions yielded negligible result scores. Interest in DsCE3 greatly increased with the finding that it is homologous (40% aa identity) to a newly identified PAMP of *Rhynchosporium commune* (Franco-Orozco *et al.*, 2017). *R. commune* is an economically relevant pathogen of barley and also a hemibiotroph, from the ascomycete class Leotiomycetes. The PAMP, a small secreted protein termed *R. commune* Cell Death Inducing 1, RcCDI1, was found to be highly induced during the early barley infection stage. RcCDI1 triggered cell death in *N. benthamiana* and *N. sylvestris*, *S. lycopersicum* (tomato) and *S. tuberosum* (potato), but not in several other dicotyledons (incl. *A. thaliana*) or monocotyledons, notably including 65 different genotypes of the host barley. Sequence homologues of RcCDI1 found in five out of 141 ascomycete species were subsequently tested in *N. benthamiana* using the same method. All five proteins, as well as two RcCDI1 alleles each with one amino acid substitution (Fig. 4.10), induced cell death in the non-host, with similar mean percentages of cell death recorded. Furthermore, RcCDI1 did not induce cell death when expressed without a signal peptide (Franco-Orozco *et al.*, 2017). Consequently, it was labelled as an apoplastic ascomycete PAMP.

Does DsCE3 also constitute a PAMP? The DsCE3 and RcCDI1 structures appear to be very similar. Assuming the proteins are recognised by the same PRR, this would constitute the first identification of a described PAMP in a forest pathogen. It supports the notion that conserved ascomycete SSPs are recognized as IPs in non-hosts. It is intriguing that the *D. septosporum* homologue only caused a weak cell death response in *N. benthamiana*. RcCDI1 (heterologous expression in *P. pastoris* followed by purification, as well as ATTA) induced local cell death in *N. sylvestris*, while DsCE3 (ATTA) did on

N. tabacum—unfortunately the direct comparison of both (or all) proteins on both these *Nicotiana* hosts is lacking. From the available literature it is not entirely clear how the three plant species relate to each other phylogenetically (Olmstead *et al.*, 2008; Clarkson *et al.*, 2010; Marks *et al.*, 2011). *N. sylvestris* seems to be established as progenitor of the other two (Kelly *et al.*, 2013). Rich genomic resources (Wang & Bennetzen, 2015) may be able to shed more light on which *Nicotiana* species are more similar to each other regarding their immune receptor repertoire. Until further functional investigation, specifically the testing of RcCDI1 and its close homologues in *N. tabacum* and DsCE3 in *N. sylvestris*, the discussion of the differential responses in these different host species remains speculative. Since DsCE3 was detected by western blot, insufficient expression levels can almost certainly be ruled out, meanwhile, a direct comparison to a sample from *N. tabacum* AWF is also missing. Detection from AWF is solid evidence that DsCE3 actually localises to the apoplast in the assay, and thus is likely to interact with a PRR in *N. benthamiana*.

Even though the hypothesis is that IP receptors are shared among hosts (particularly in the same genus), the recognition of this molecular pattern could occur differently in *N. benthamiana* than in *N. tabacum*. It might be that DsCE3 is recognised by the same *Nicotiana* PRR as RcCDI1 but there are subtle structural differences in the corresponding domains of both effector and receptor, resulting in lower binding specificity. The mechanism underlying recognition could also involve more than one plant protein interacting with the IP. On the IP side, the relevance of amino acid differences could theoretically be inferred from the SSP alignment (Fig. 4.10). However, conclusions were not possible from the available data. Thus, it would be beneficial to identify other proteins with high sequence homology and cell death induction data. Again, diverging domains could then be swapped in the proteins to determine if they affect the IP-IPR interaction outcome.

In conclusion, DsCE3 may be added to the list of RcCDI1-like proteins, together representing a PAMP of diverse ascomycete pathogens. This follows the logic of Franco-Orozco *et al.* (2017), taking the cell death induction of homologues in five other species as 'PAMP activity', while a thorough investigation including testing in other plants was only carried out for RcCDI1 itself. The *D. septosporum* protein would be the first PAMP found in a

conifer pathogen but I would exercise caution to declare it a PAMP. To verify that it is or contains an IP, DsCE3 needs to be functionally tested in a broader range of non-hosts.

4.3.6. Cell death inducers DsCE15 and DsEcp32-3 represent CEs of unknown function

DsCE15 (131885; 126 aa, ten Cys) displayed two positive extremes in the data. First, with ten cysteines it was among the proteins with the highest absolute and relative number of potential disulphide bonds (five bonds predicted by Disulfind). Second, the data showed its expression was up-regulated by 255-fold in Mid stage *in planta*, compared to in culture, which was the highest in the secretome. DsCE15 was found to be highly conserved in a broad range of fungi and some oomycetes. Despite this, predicted structural similarities were limited to very weak hits. Further investigation (pGenTHREADer) even suggested that none of the DsCE15 predicted structure possibilities matched with any known structure. If this is the case, it most likely indicates that the protein contains a novel structural fold (pers. comm. Dr Geoff Jameson). DsCE15 expression elicited cell death in *N. tabacum* leaves in 78% of cases, and a weak response in 44% of *N. benthamiana* leaves. It could be revealing to determine if homologues of DsCE15 also induce cell death in plants.

DsEcp32-3 (70057; 189 aa, five Cys) was one of very few SSCPs both highly expressed and *in planta*-induced. It showed homology to a vast number of small proteins, which were almost exclusively annotated as hypothetical proteins. No, or negligible, hits were found for secondary and tertiary structure. DsEcp32-3 caused HR-like cell death on *N. tabacum* in 97% of infiltrations, and patches of necrotic lesions on *N. benthamiana* in 72% of all cases. Thus it is another representative of uncharacterised fungal SSCPs that are either recognised as IPs, or toxic to plant cells. The cell death suppression assay with Avr3a indicated that DsEcp32-3 most likely did not induce cell death via a CMPG1-dependent pathway. So far, a putative Ecp32 family was named in *C. fulvum* and *D. septosporum*, and additional Ecp32 family members may well be found in the genomes of other relatives and even distant taxa with more than one homologue in their genome as seen in the search. Since Ecp32-like genes were found in some non-pathogenic

species, it would be highly interesting to find out if these genes are functional in these non-pathogenic species. In line with the other cell death-inducing DsCEs, determining whether/which homologues of DsEcp32-3 also trigger cell death and thus support the indication that part of the conserved protein structure constitutes an IP, would be an important next step in this direction.

4.3.7. *D. septosporum* could employ necrotrophic effectors

DsCE3, DsCE15, DsEcp20-3, DsEcp32-3 all caused cell death in non-hosts and were highly induced in the Mid and Late pine infection stages. Triggering cell death in the plant through effector recognition and exploiting it is a strategy used by necrotrophic pathogens (inverse gene-for-gene model; also see section 1.2.4), including the Dothideomycetes *Cochliobolus victoriae* (host-selective toxin: Victorin), *C. heterostrophus* (T-toxin), *C. carbonum* (Tox1), *Parastagonospora nodorum* (ToxA, Tox1, Tox3) and *Pyrenophora tritici-repentis* (ToxA, ToxB), and *B. cinerea* (Nep1-like protein; activation of HR-inducing plant genes *EDS1* and *SGT1* via unknown mechanism) (reviewed by Vleeshouwers & Oliver, 2014). It has previously been proposed that hemibiotrophs such as *D. septosporum* could also promote host cell death (Fraser *et al.*, 2015) when they are ready to enter the necrotrophic phase. It could be investigated if these elicitors have a cell death promotion function, by directly applying protein to pine needles, and creating *D. septosporum* mutants (e.g., via Crispr-Cas9) to determine whether absence of a functional CE gene has a negative impact on pine infection.

4.3.8. Summary and comparison to other pathogens

Seventeen candidate effectors of *D. septosporum* were cloned and tested for their ability to induce cell death in the non-host plants *N. tabacum* and *N. benthamiana* using *Agrobacterium* infiltration. Five of these CEs induced cell death in *N. tabacum* with overall high consistency. Four of those five also induced cell death in *N. benthamiana*, with less consistency and often less severity in individual infiltration zones. Further characterisation of the two strongest elicitors in both non-hosts, DsEcp32-3 (unknown function) and DsEcp20-3 (homology to a characterised, cell death inducing effector protein), was

carried out using cell death quantification methods, and a cell death suppression assay which indicated that neither protein triggered the CMPG1-dependent defence induction pathway.

Similar CE selection pipelines (also see chapter 3) and non-host functional screening via ATTA in *N. benthamiana* were used for the following hemibiotrophic ascomycete pathogens, among others: *Z. tritici* had 63 transcriptionally up-regulated CEs, 14 (22%) of which induced cell death or chlorosis. Thirteen of these had unknown functions, with two protein sequences unique to *Z. tritici*, and one GH53 (Kettles *et al.*, 2017). In a study of the hemibiotrophic *Brassica* spp. pathogen *Leptosphaeria maculans* with a focus on the biotrophic phase, CEs were tested for their potential to suppress rather than induce cell death (Haddadi *et al.*, 2016). Four of 16 (25%) tested highly expressed CEs fully or partially suppressed cell death in *N. benthamiana*. Furthermore, a conserved necrosis and ethylene-inducing peptide-1 (Nep-1)-like protein, NLP, previously found in the *L. maculans* genome was confirmed to be expressed during infection and shown to trigger strong cell death in *N. benthamiana*. Silencing of Lm-NLP also drastically reduced virulence on *Brassica napus* (Haddadi *et al.*, 2016). These findings underpinned the hemibiotrophic lifestyle of the pathogen. From *M. oryzae*, 42 secreted *in planta*-induced CEs were tested in rice protoplasts, where five caused cell death (Chen *et al.*, 2013b). Four of these five also induced cell death when tested in *N. benthamiana*; the other 37 CEs were not assayed in the non-host.

In the banana (*Musa* spp.) pathogen *P. fijiensis*, similar investigations are ongoing. Following genome sequencing of *P. fijiensis*, 172 SSCPs were predicted, and 107 of these had no BLASTp hits (Isaza *et al.*, 2016). Since Pf-Avr4 was previously shown to interact with Cf-4 to trigger an HR (Stergiopoulos *et al.*, 2010), banana leaves were infiltrated with purified Pf-Avr4 protein. This induced severe local cell death in a resistant cultivar but not a susceptible cultivar (Cavendish). Independently, Noar & Daub (2016) discovered 483 of 802 *P. fijiensis* genes that were more highly expressed during infection of *M. acuminata* seedlings than in culture. Thirty of these were SSCPs, six of which contained conserved domains; the two most highly (and differentially) expressed SSCPs had no functional annotations (Noar & Daub, 2016). Also, Pf-Avr4, Pf-Ecp2 and Pf-Ecp6 were

not found to be induced in this dataset. A set of CEs has not been tested in non-hosts, but the Avr4 finding alone could constitute a huge step forward in breeding for resistance against Black Sigotaka disease.

The proportion of DsCEs inducing cell death in at least one non-host was high in comparison to other fungi, with approx. 29% (5 of 17 tested CEs). Based on the data from other pathosystems, identifying *D. septosporum* secreted proteins that act as IPs in non-hosts and thus induce an immune response was not surprising, despite phylogenetic distances between its hosts and the non-hosts used. Effectors from different pathogens were shown to have the same or similar targets. An outstanding example is the inhibition of the tomato cysteine protease Rcr3 by the *C. fulvum* effector Avr2, *P. infestans* EpiC1 and EpiC2B, and nematode *Globoderia rostochiensis* Gr-VAP1 (Rooney *et al.*, 2005; Song *et al.*, 2009; Lozano-Torres *et al.*, 2012). This demonstrates independent evolution of effectors from a fungus, an oomycete, and an animal, interacting with the same apoplastic host protein. As noted in subsection 3.3.2, the defence protein PR1 is exploited for cell death induction by three different necrotrophic fungi, and there are numerous examples of intracellular host targets that are shared by fungal, oomycete and bacterial pathogens hampering the immune system (subsection 1.2.1).

Conclusively, *D. septosporum* was found to secrete small proteins that cause cell death in two closely related non-host plants, which means that these proteins likely constitute invasion patterns (IPs) and are recognised by IP receptors, or are toxic to plant tissue. This is the second study uncovering such molecular factors in a pathogen of forest trees and provides important evidence supporting the non-host resistance of plants.

Chapter 5.

Protein delivery trials for functional analyses of candidate effectors in *Pinus radiata*

5.1. Introduction

Within the broad and deep research body for pine forests, including long-standing breeding, recent advances in remote-sensing technologies (Dash *et al.*, 2017), and exploration of genomic selection (Isik, 2014) and genotyping-by-sequencing (Li *et al.*, 2017), so far there has been little specific research addressing pine-pathogen molecular interactions.

This gap is at least partially due to methodology issues with conifers. For example, transformation of plant tissue with *Agrobacterium tumefaciens* is an established way of expressing genes of interest, such as effectors, *in planta* to study their function (van der Hoorn *et al.*, 2000; Opabode, 2006; Ziemienowicz, 2014). Even though applying this to gymnosperms is difficult (Tang *et al.*, 2014; Maleki *et al.*, 2018), attempts at transforming pine embryos have had some success. Replicable stable transformation was achieved in *P. radiata* (Cerda *et al.*, 2002; Charity *et al.*, 2005) and several other *Pinus* and *Picea* species (Tang & Newton, 2003); however, few of the studies represented more than first steps. Grace *et al.* (2005) reported regeneration of *P. radiata* tissue transformed with a *Bacillus thuringiensis* endotoxin gene, conferring resistance to insect larvae. Most recently, parameters of *P. massoniana* embryo tissue treatment with *A. tumefaciens* for transfor-

mation were thoroughly investigated using a selection marker (Maleki *et al.*, 2018). The resulting 'improved transformation efficiency protocol' for *P. massoniana* was suggested to be applicable to other conifers too.

A different approach to study molecular interactions between pine and its pathogens is the direct application of pathogen structural components or proteins. Earlier, *D. septosporum* 'cell wall elicitors' were added to *P. radiata* cell suspension cultures and were reported to trigger hypersensitive response (HR) symptoms (Hotter, 1997). Extracts from various pathogenic fungi elicited necrosis when injected into the phloem of *P. sylvestris*, among three other conifer species (Polyakova *et al.*, 2008). More recently, a study similar to parts of this thesis was done on the root pathogen *Heterobasidion annosum s.s.* interaction with *P. sylvestris* (Chen *et al.*, 2015). Those authors identified and characterised a potential virulence factor from the cerato-platanin family, HaCPL2. To determine whether the protein induced cell death in the host they applied purified protein to roots of *P. sylvestris* seedlings on agar via filter paper strips. HaCPL2 induced root cell death and defence gene expression in this assay, demonstrating a successful straight-forward method, even in the absence of a known positive control.

Here, the aim was to design a cell death elicitor screening method that is also fast, simple, and reflective of the biology of the *D. septosporum* infection as far as possible. Thus, this aim involved two main tasks: protein generation and protein delivery to *P. radiata* needles. While the two previously proposed *D. septosporum* effectors DsAvr4 and DsEcp2-1 were already available for protein generation (first task) using heterologous expression in the yeast *Pichia pastoris*, the overall purpose of this study was to create a pipeline for efficient screening of new CEs in *Pinus* spp. Transforming *P. pastoris* and selecting transformants with the highest expression levels is a lengthy process for each CE. Thus, other solutions enabling quick production of a broad range of CE proteins were sought. One solution was found in the use of *A. tumefaciens* binary expression vectors used for transient transformation (ATTA). *Nicotiana benthamiana*, employed to express each protein for screening of cell death induction in non-hosts, was also used for protein expression in whole leaves. A protocol had to be devised to efficiently collect apoplastic wash fluid, assumed to harbour secreted CE protein, from a large number of leaves. The

development of this method is presented in this chapter.

The challenge of the second aim, to deliver proteins to *P. radiata* needles, was two-fold. First, pine needles are narrow and often twisted and tough, but surprisingly brittle when detached from the branch, making them recalcitrant towards manipulation, compared to the broad and soft but resilient leaves of *Nicotiana* spp. This had to be addressed in a new protein infiltration method. Second, a positive control had to be established to verify delivery to the needle apoplast. Needle injection and vacuum infiltration were considered as possible delivery methods. These have been used with preliminary success (Guo, 2015) and were considered realistic options for high-throughput screening for genetic resistance in host material.

If any of these methods could be established, they may provide a powerful screening method even without further knowledge of resistance genes.

5.2. Results

5.2.1. Production of CE proteins using a custom apoplastic wash fluid (AWF) collection method

Method establishment for AWF collection

To obtain a source of many different secreted CE proteins for subsequent functional studies was the first goal and foundation of this part of the study. Based on the predicted apoplastic nature of the selected *D. septosporum* CEs, a protein collection method from the leaf apoplast (de Wit & Spikman, 1982) was used. The approach included systems already in place in this project: the comparatively high throughput approach of Golden Gate cloning and ATTA in non-hosts, and the efficient and reliable expression system of *N. benthamiana* (Boivin *et al.*, 2010). The final method is described in subsection 2.6.6. In brief, protein was produced in fully infiltrated leaves, these leaves were vacuum-infiltrated with water, surface-dried, and then stacked on a flat nappy liner fitted over a square container to extract the liquid by centrifugation. Development of the method and limitations of certain aspects of the procedure are described here, and in extended detail in section F.1.

1. Leaf infiltration efficacy with *Agrobacterium* cultures containing binary CE expres-

sion vectors was not at 100%. Some leaves were considerably harder to infiltrate than others. To avoid excessive stress caused by repeated infiltration, such leaves were not used for AWF collection.

2. The time leaves were not actively cooled was reduced to a minimum.

3. For the fluid extraction itself, methods from the literature based on the use of centrifuge tubes (de Wit & Spikman, 1982; O'Leary *et al.*, 2014) were trialled. This resulted in heavily damaged leaves, turbid green collection fluid indicating contamination with intracellular components from damaged cells, and incomplete fluid extraction. In contrast, the flat collection container design using a soft horizontal surface (nappy liner) was efficient for harvesting clear AWF. The leaves remained intact and the recovered fluid was almost colourless. However, fluid was not extracted from the centre of the leaf surface (Fig. F.1). The measures taken minimised this issue and resulted in an improved yield of approx. 750 μl per average-sized leaf compared to less than 500 μl using the initial horizontal setup.

4. Changing centrifugation speed and time had little effect on the recovered volume, or integrity of the leaves. Two to three layers of cut leaves, depending on their size, were determined as the maximum 'loading mass' above which extraction efficacy dropped considerably. Collected AWF samples were centrifuged at $4696\times g$ for 10 min to remove residual plant cell debris, and indeed a thin layer of green matter was separated, indicating presence of chloroplasts from damaged cells. This served as a crude filtering step. To check if there were any further unwanted cellular components, aliquots of random samples were then centrifuged again at $16000\times g$ for 10 min. No pellets were formed, indicating sufficient purity regarding potential contamination with plant cell debris.

5.2.2. AWF samples caused cell death in *Nicotiana* spp. leaves

To determine whether the AWF contained functional protein of interest, it was infiltrated into non-host leaves in the same way as *A. tumefaciens* infiltration cultures. First, a series of negative controls were shown not to induce cell death (or other visible symptoms

Figure 5.1.: Infiltration of *Nicotiana tabacum* and *N. benthamiana* with apoplastic wash fluid samples induced cell death. Infiltrations were carried out with a needleless syringe as with *A. tumefaciens* cultures. A) Screening of INF1 and *Dothistroma septosporum* candidate effectors that previously triggered cell death via ATTA (subsection 4.2.1); EV, negative empty vector control. Images represent similar results from at least 7 different plants. B) Dilution of INF1 up to 16-fold did not affect induction of strong cell death in *N. tabacum*. INF1 AWF samples were serially diluted to indicated dilution factors (2×-16×) with sterile water. Empty vector AWF (EV) was diluted 2-fold. The image represents 17 of 19 leaves (from 10 different plants) that showed the same results.

such as chlorosis) in both *N. benthamiana* and *N. tabacum*. These controls were AWF from untreated leaves, leaves infiltrated with buffer, empty vector culture, and empty vector and p19 (viral protein to increase expression) culture mix. The last one was established as standard negative control after initial tests. INF1 was used as positive control. As in the ATTAs, INF1 consistently induced cell death in both non-hosts. Cell death induction was independent of sample age and even achieved with a 16-fold dilution of INF1 AWF, indicating that the cell death-inducing component was present in excess with this construct.

Successful recovery of the respective CE proteins in AWF was indicated by strong cell death induction for DsCE15 and DsEcp32-3 in *N. tabacum* (Fig. 5.1), DsEcp20-3 and DsEcp2-1 samples caused weak cell death inconsistently (Fig. F.2); DsCE3 was not tested due to weak ATTA results and time limitations. Differences in severity of cell death response were observed, except for INF1 which consistently induced HR-like cell death.

Despite these differences, it was shown that the customised method produced CE proteins that could be used for functional testing in the host, which is addressed in the next section.

5.2.3. Development of CE protein solution infiltration methods with *Pinus radiata* tissue

With the AWF collection established, a method was required to apply the proteins to pine tissues. The physical structure of a pine needle (long and thin, firm at an early age, twisted when mature) is not amenable to manipulation. In an attempt to minimise this challenge, a source of new, softer pine tissue was used, that is, sterile clonal shoots raised on agar medium, without roots. These shoots are the latest available clonal tissue available from Scion, and seemed ideal for my task.

Injection into both stems and needles of these shoots was attempted using a syringe and hypodermic needle. This was unsuccessful as the stem tissue was too dense to take up liquid even in the microliter range, and the needles were too small or too soft to be manipulated for this cause. Those needles that appeared to be successfully infiltrated suffered heavy mechanical damage, which was seen in all negative controls. Thus, this was no improvement to the previously used older needles. Instead, vacuum infiltration was pursued as an alternative option for delivering effector proteins into the pine needles.

Method establishment for pine shoot infiltration

A series of aspects had to be considered for the treatment of the shoots to create a consistent and reliable screening protocol. Development of the method and limitations of the procedure are described here, and in extended detail in section F.2.

1. There was a risk of contamination of the limited pine material. As this could not be eliminated, I used all the shoots in a jar (i.e., same genotype) at a time rather than opening several or all jars.

2. Needles did not take up fluid when pressed against the tube wall or too close together. Thus, even though AWF volumes were limited, having as much pine sample as possible in a given fluid volume was not the best option.

3. There was a risk of damaging tissue by manipulation. Experience showed that shoots of most genotypes were soft and easily damaged. Handling shoots individually and carefully meant considerable time consumption, and together with the observation

that the tissue collapsed within 15-20 min when removed from medium or water, this limited the number of replicates that could be done at one time. Also, collecting needles or fascicles from shoots was considered unnecessarily laborious due to the fragile nature of the young tissue. Thus, whole shoots were preferable to detached needles.

4. It had to be experimentally determined how the shoots would fare after the relatively harsh vacuum infiltration treatment and additional manipulation steps following transient removal from the nutrient medium. It was shown that the shoots stayed healthy on LPch agar and water agar, but not wet foam. There was a risk of tall shoots (over approx. 4 cm) falling over without support, which is why they were kept in glass jars.

5. Variation among pine genotypes was unknown. Initially it was assumed that all shoots would be affected equally by each procedure and negative control. This was shown to be false: Some genotypes demonstrated drastically lower resilience to treatments than others, and could not be used for conclusions.

Description and illustration of trial results

Observations made during the development of the novel methods are described below. The pine shoots provided by for this study (by Scion) are referred to as S1 to S6 and R1 to R4, each representing a different genotype (susceptible or resistant to DNB; subsection 2.1.2). Neutral red (NR) dye in sterile water, constituted both a negative control for the vacuum infiltration treatment and an infiltration efficiency reference. AWF from *N. benthamiana* leaves infiltrated with a mix of empty vector and p19 cultures (EV) was used as a second negative control. The first important steps were to determine whether the tiny pine shoots would survive the infiltration treatment long enough to be assessed for any symptoms, and how efficient the liquid uptake was.

In the first trial (genotypes S1 and S2), near 100% uptake of NR by vacuum infiltration was demonstrated (Fig. 5.2). In contrast, just dipping the shoots in NR solution for the same amount of time did not result in uptake. There were no notable health differences between the dyed shoots and those infiltrated with water. Some containers got contami-

Figure 5.2.: Neutral red solution was successfully infiltrated into whole clonal pine shoots by vacuum. Left, water infiltration; mid and right, 0.01% NR in water, side and top view.

nated, with fungal growth originating from the base of shoots. Generally, here as well as in all other experiments, the shoots coped well with water or neutral red infiltration. Out of nine genotypes, S4 was clearly harmed by the infiltration process, with flat and dry curled needles and severe discolouration. Genotypes R1 and R2 displayed accelerated tip death and more flat needles than others when treated with the AWF negative control.

In parallel, the *D. septosporum* toxic secondary metabolite and virulence factor dothistromin was tested to provide a general verification for the delivery of a compound that could be macroscopically assessed. Dothistromin is insoluble in water but readily soluble in the organic solvent DMSO. A DMSO negative control was included for the dothistromin trial. The small shoots used for this early assay quickly browned and died, including the DMSO controls (Fig. 5.3B). The neutral red samples survived. While dothistromin might have had a stronger effect than DMSO alone, the toxicity of the solvent was considered too strong and this trial was not continued.

The next important step was to establish a positive control for protein delivery. This is the topic of the next subsection.

Figure 5.3.: (Facing page.) Methods tried for protein delivery into *Pinus radiata* using vacuum infiltration. Examples were picked for illustration of methods summarised in Table 5.1. Images B-D are roughly the same scale. A) Needles of ≥18 months old seedlings showed incomplete and inconsistent uptake of neutral red and *Pichia pastoris* culture filtrates; DsEcp2-1 samples were associated with lesion-like symptoms as shown here in 5 of 21 needles. B) Exposure to dothistromin (infiltration or dip only) caused quick death of shoots. The dothistromin solvent DMSO had a similar but weaker effect. C) Shoots vacuum-infiltrated with apoplastic wash fluid (AWF) survived in small wells of water agar for at least 7 d. Two genotypes (1 per row) reacted differently to the infiltration treatment. D) Incubation of infiltrated shoots on LPch agar in glass jars (left) and detached fascicles on oasis (right). The bottom panels show an example of a shoot (genotype R2 in this case) reacting with cell death to empty vector AWF, but not water infiltration.

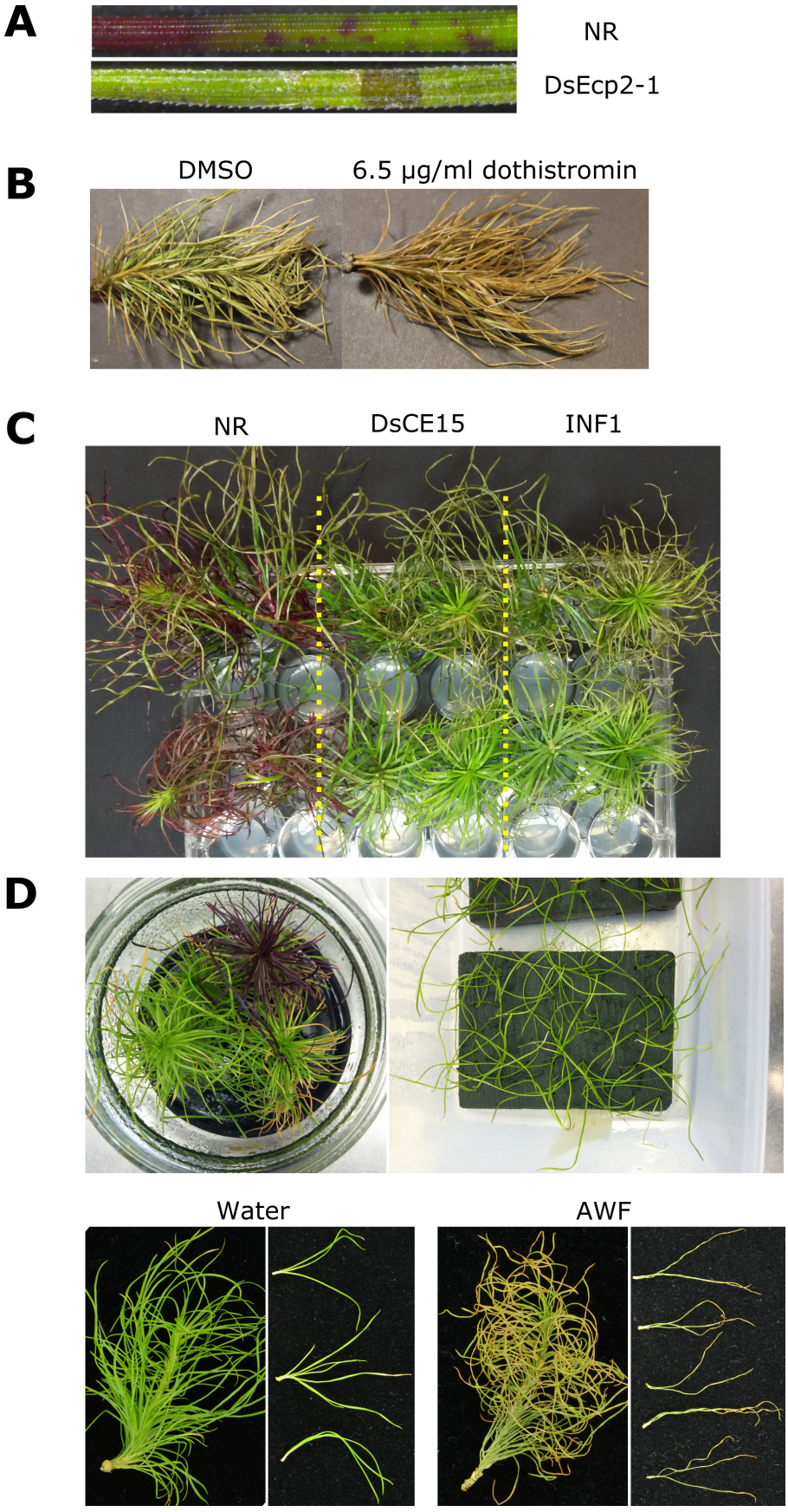

Figure 5.3 (cont.): Methods tried for protein delivery into *Pinus radiata* using vacuum infiltration. Legend on facing page.

5.2.4. AWF samples elicited responses in pine tissue

A positive control for protein delivery and cell death induction had to be found. DsAvr4 and DsEcp2-1 protein previously caused lesions on mature *P. radiata* needles in a small trial (Guo, 2015). I repeated this assay with DsEcp2-1. Cell death-like lesions were seen on approx. 25% of needles (Fig. 5.3.A) Interestingly, neither DsAvr4 nor DsEcp2-1 AWF induced a specific cell death response in the assay with shoots. Other options were the strong *Phytophthora infestans* non-host elicitor INF1, and *Heterobasidion annosum* CPL2 (HaCPL2), as this protein induced cell death in *P. sylvestris* seedlings through roots (Chen *et al.*, 2015).

In a series of trial experiments, no clear responses to any AWF samples were observed in pine. In a trial with INF1, needles of genotype S4 died after infiltration with INF1 as well as DsCE15, but they were also heavily damaged with EV and neutral red (Fig. 5.4). This made it clear that not all pine genotypes tolerate the vacuum infiltration. INF1 and DsCE15 elicited weak necrosis in S2 where the negative controls did not (Fig. 5.4, bottom rows), and R3 represented an intermediate response, showing a minor browning and tip death with all treatments.

In another trial, infiltration of HaCPL2 AWF achieved cell death induction distinguishable from the response to a buffer control with genotype S2 shoots (Fig. 5.5, Fig. 5.6), but not R1. In another assay including DsEcp2-1 and HaCPL2 with genotypes R2, R3 and S3, the S3 shoot treated with HaCPL2 had approx. 50% brown/dead needles two days post infiltration, while all other needles were mostly healthy (Fig. 5.3.D). Unfortunately, this trial had to be terminated prematurely due to contamination.

An overview of the pine-related methods and results is given in Table 5.1.

Table 5.1: Methods tried for protein delivery into *Pinus radiata* .

Figure ref.	Delivery method[a]	Pine tissue	Protein/toxin source[b]	Maintenance method[c]	Proteins tested	Host genotype[d]	Response	Comments
5.3.A; G.2	Complete submersion in 15 ml, vacuum infiltration	Detached needles of >18 months old seedlings	Yeast culture filtrate	Fascicles in wet foam (ns) in plastic box	DsEcp2-1	n/a	Necrotic and chlorotic patches; some needles up to 50% collapsed (from tip)	**Protein potentially delivered and recognised. High replicate number required**
	Syringe injection (~10-100 µl)	Detached needles (>18 months old seedlings and tissue culture shoots)	Yeast culture filtrate	Fascicles in wet foam (ns) in plastic box	DsEcp2-1	n/a; S2	Death of needle parts due to mechanical damage.	**Not suitable**
G.3, G.4	Uptake via LP5+BA agar medium	Tissue culture cotyledons	Yeast culture filtrate	LP5+BA agar medium	DsEcp2-1	54 types (from seedlot)	Both +ve and –ve treatment led to growth impairment or death	**Invalid (unspecific response to negative control)**
5.2	Complete submersion, vacuum infiltration	Tissue culture shoots (short)	n/a	Water agar in tip box	NR and water only	S1	Close to 100% red-purple coloration due to 0.1% and 0.01%, but not 0.001% NR	**First demonstration of infiltration efficiency of the shoot method, NR reference, and survival**
5.3.B	Complete submersion in 15 ml, vacuum infiltration	Tissue culture shoots (short)	*D. septosporum* culture filtrate	Fascicles in wet foam (ns) in plastic box	Dothistromin (6.5 µg/ml in DMSO)	S2, S4	Strong necrotic effect with -ve control (DMSO).	**NR infiltration confirmed; dothistromin invalid (unspecific response to negative control)**
5.3.C, 5.4	Complete submersion, vacuum infiltration	Tissue culture shoots (short)	AWF	Water agar in 12/24- well plate (ns)	DsCE15, (INF1)	S2 S4 R3	Minor damage by INF1, DsCE15 Severe damage by all samples Minor damage by all samples	**Some unspecific responses to negative control. Differences in pine genotypes apparent**
5.3.D, 5.5	Complete or partial submersion in 20-50 ml, vacuum infiltration	Tissue culture shoots; detached needles	AWF	Wet foam (needles); LPch agar in glass jar	HaCPL2 HaCPL2 DsAvr4 DsEcp2-1	S2 S5, R1, R2, R3 R3 S5, R2, R3	Medium damage Minor damage by all samples Minor damage by all samples No or minor damage	**Inconclusive due to lack of working positive control**
5.3.D	Complete submersion in 15 ml, vacuum infiltration	Detached needles of tissue culture shoots	AWF	Wet foam (treated with ethanol) in plastic box	HaCPL2, DsAvr4	S4, R2	Minor to medium damage by all samples (tip death)	**Inconclusive due to lack of working positive control**
(5.3.D)	Complete or partial submersion in 20-50 ml, vacuum infiltration	Tissue culture shoots	AWF	Wet foam (treated with ethanol) in plastic box	DsAvr4	R3	Random death due to treatment	**Wet foam not suited for shoots. High contamination rate**
5.6	Partial submersion in 100 ml, vacuum infiltration	Tissue culture shoots	Yeast culture filtrate	LPch agar in glass jar	BcSSP2, SsSSP3	S2 R4 S6, R2	Needle death specific to SSPs Medium damage by all samples Severe damage by all samples	**Differences in pine genotypes observed. Protein likely delivered and recognised in S2.**

[a] At least partial uptake of respective liquid was confirmed by eye (darkening of tissue) for each method.

[b] Yeast culture filtrate, filter-sterilised filtrate of *Pichia pastoris* culture heterologously expressing proteins of interest (or empty vector, EV); AWF, apoplastic wash fluid from *Nicotiana benthamiana* heterologously expressing proteins of interest (or empty vector) post agroinfection

[c] Indicates where samples were transferred to after treatment, if applicable. Environments were at room temperature and sterile unless mentioned otherwise (ns, non-sterile). LPch, Quoirin-Lepoivre medium with activated charcoal.

[d] Refers to Dothistroma needle blight susceptible (S) and resistant (R) clonal plants.

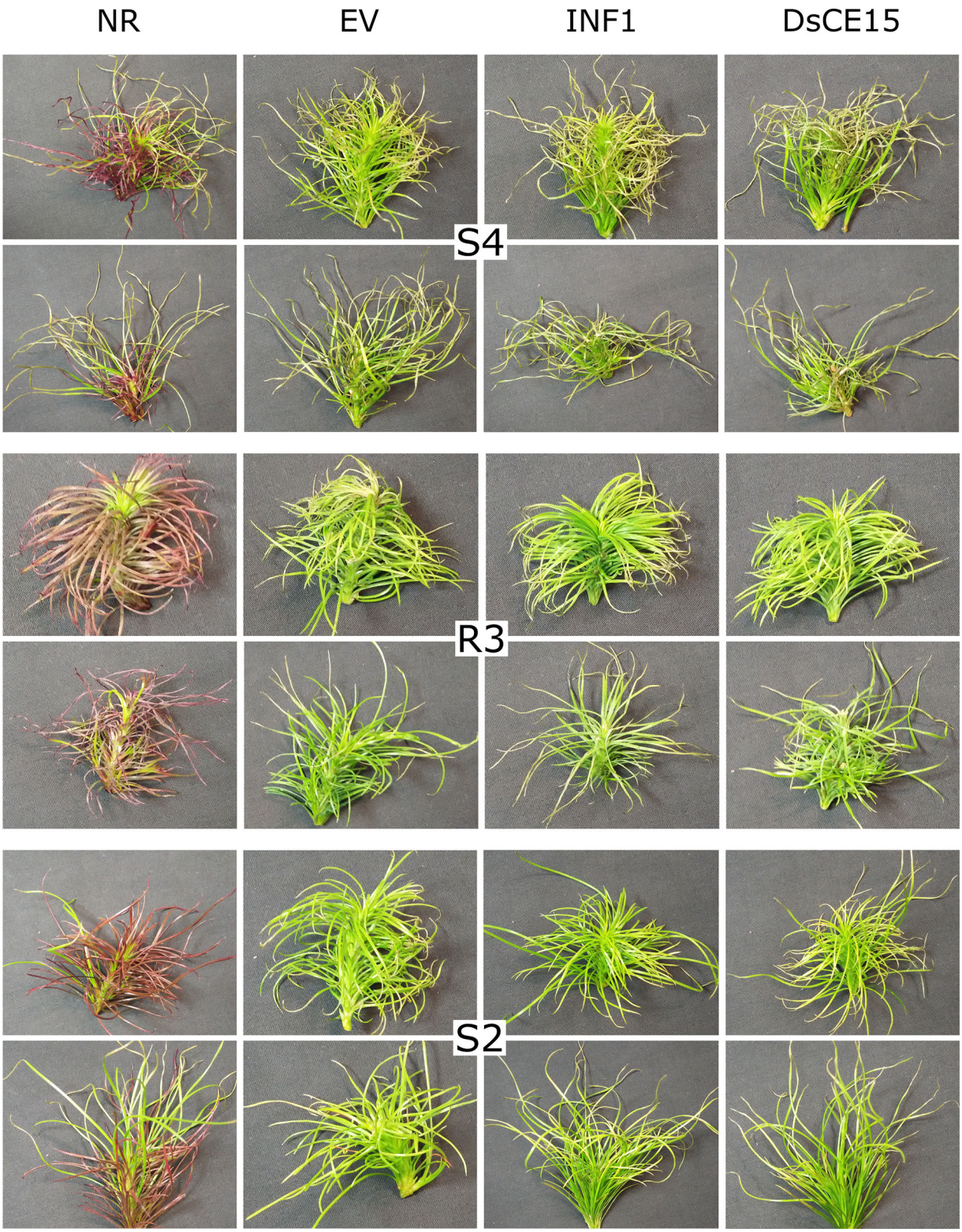

Figure 5.4.: Different pine genotypes reacted differently to the vacuum infiltration procedure. Genotype codes are indicated in the centre of the 8 corresponding images, and samples used on the top. NR, 0.01% neutral red in water (negative control and infiltration reference); apoplastic wash fluid samples from EV (empty vector, negative control), INF1, DsCE15. Shoots were cut in half horizontally, infiltrated, and placed in wells with 1% water agar. Photos were taken 8 dpi.

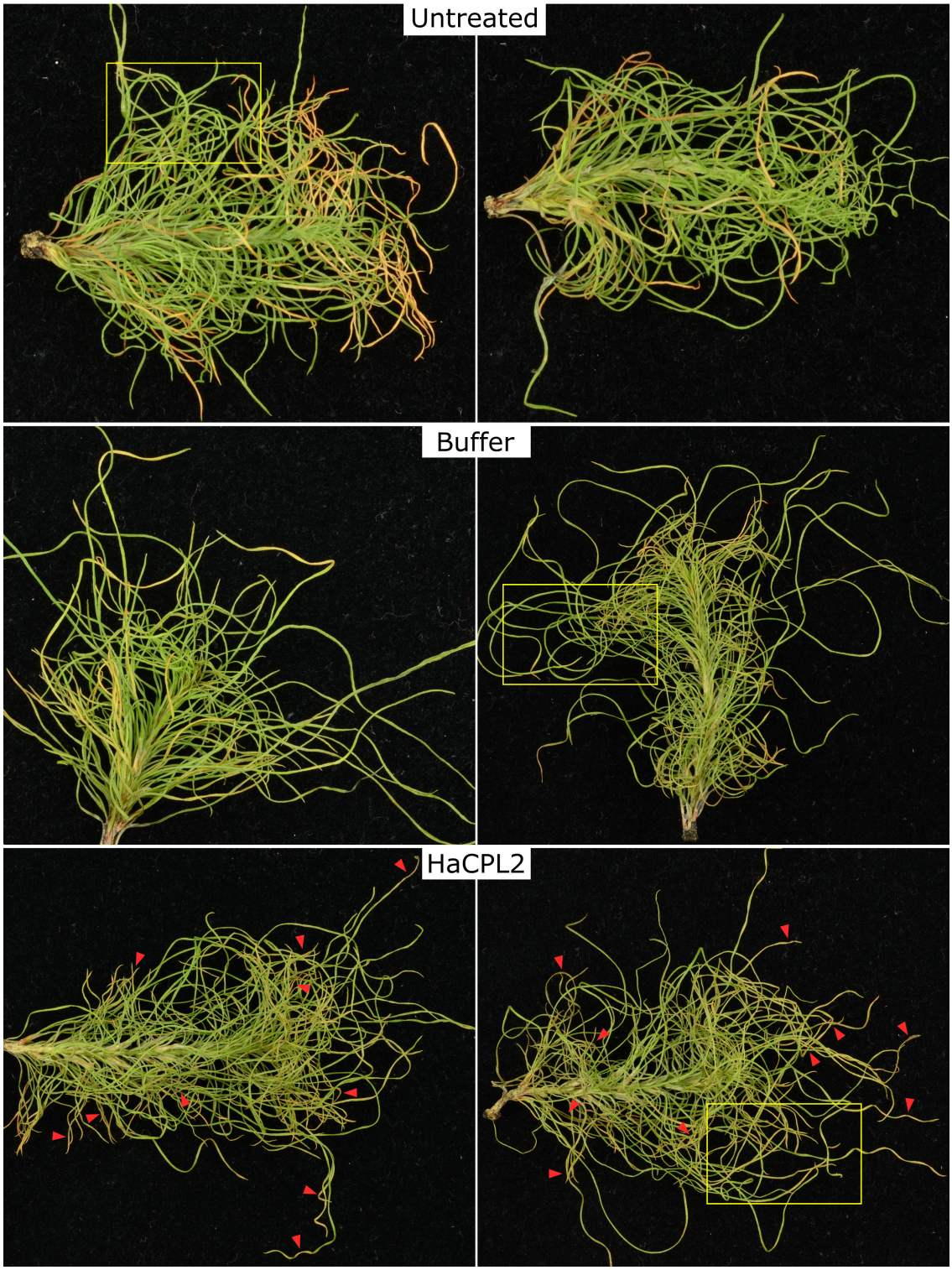

Figure 5.5.: Vacuum infiltration of S2 shoots with HaCPL2 apoplastic wash fluid (AWF) induced weak needle cell death. Two whole shoots of *Pinus radiata* genotype S2 were exposed to AWF from leaves infiltrated with HaCPL2 or buffer. The top panel shows untreated S2 shoots from the same jar. Yellow rectangles indicate areas magnified in Fig. 5.6. Red arrows indicate examples of damaged or dead tissue. As seen in the untreated samples, there were dried and dying needles on some shoots, and these were easily distinguishable from needles damaged by a treatment. Photos were taken 8 dpi.

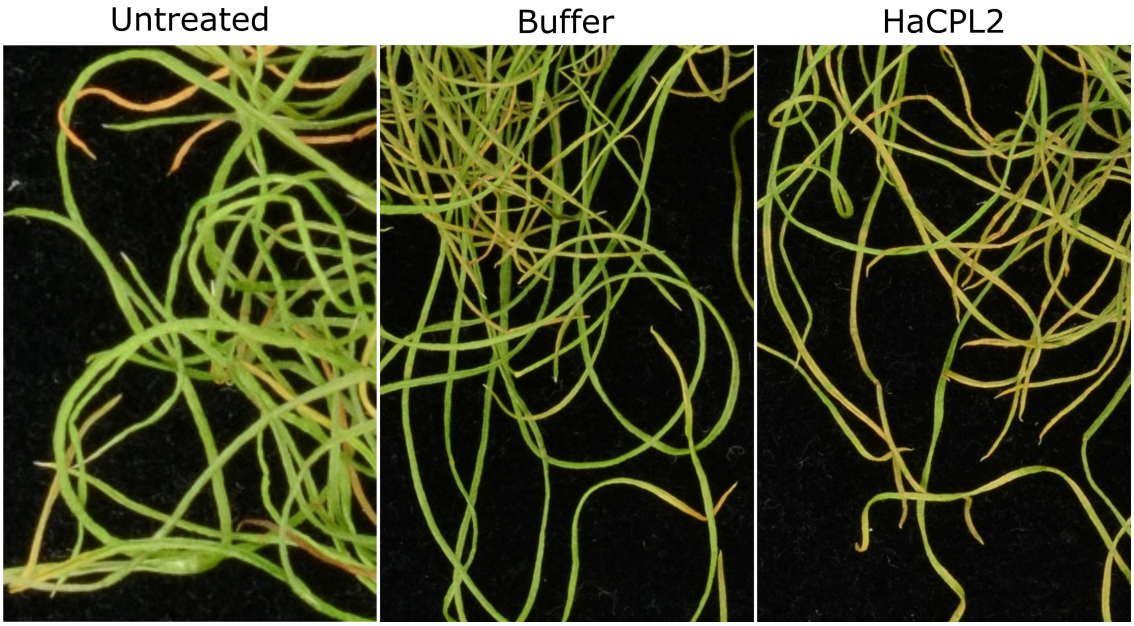

Figure 5.6.: Vacuum infiltration of S2 shoots with HaCPL2 may have induced needle cell death. Areas indicated in Fig. 5.5 are magnified here. Discolouration and curling were interpreted as (cell death) response to the infiltration.

5.2.5. Yeast culture filtrates with SSPs from *Botrytis cinerea* and *Sclerotinia sclerotiorum* induced cell death in pine tissue

At a late stage of this project, proteins unrelated to the investigated pathosystem were included as potential positive controls. *B. cinerea* SSP2 and *S. sclerotiorum* SSP3, both previously identified as strong cell death inducers in *N. benthamiana* and *Camellia lutchuensis* (Denton-Giles, 2014), were readily available as expression constructs in *P. pastoris*, enabling easy generation of sufficient volumes for pine infiltration. Sterile culture filtrates from both proteins, as well as an EV (negative) control, were infiltrated into *Nicotiana* spp. to check their functionality. Cell death was induced by both proteins, but not EV (Fig. 5.7).

Subsequently, since a large volume of yeast culture filtrate was easy to generate using liquid yeast culture, four different pine genotypes were tested at once: R2, R4, S2, and S6. For this, vacuum infiltration of partially submerged shoots was carried out. The neutral red controls demonstrated a good infiltration efficacy in the submerged part. In the genotypes R2, R4 and S6, shoots appeared to respond non-specifically to the culture filtrate with dying needles, i.e., EV had a notable detrimental effect, and could not be used for a conclusion regarding the SSPs. In contrast, in S2, both control treatments were without effect, but BcSSP2, and SsSSP3 with less severity, appeared to cause death in the majority of submerged needles (Fig. 5.7).

5.2.6. *DsEcp2-1* knockout affected *D. septosporum* infection of *P. radiata*

A powerful method to assay for function of CEs is to use gene knockouts in host infection experiments. It was attempted several times to obtain meaningful results from the *D. septosporum–P. radiata* pathogenicity assay (Kabir *et al.*, 2013) using strains with deleted effector genes. Preliminary results were collected before this study, asserting the Δ*DsEcp2-1* strain to cause larger lesions on needles (Guo, 2015), however this result was not supported by a complemented control strain (CO-*DsEcp2-1*). Another assay, including CO-*DsEcp2-1* was carried out during this project, but the overall infection rate was too low to allow conclusions.

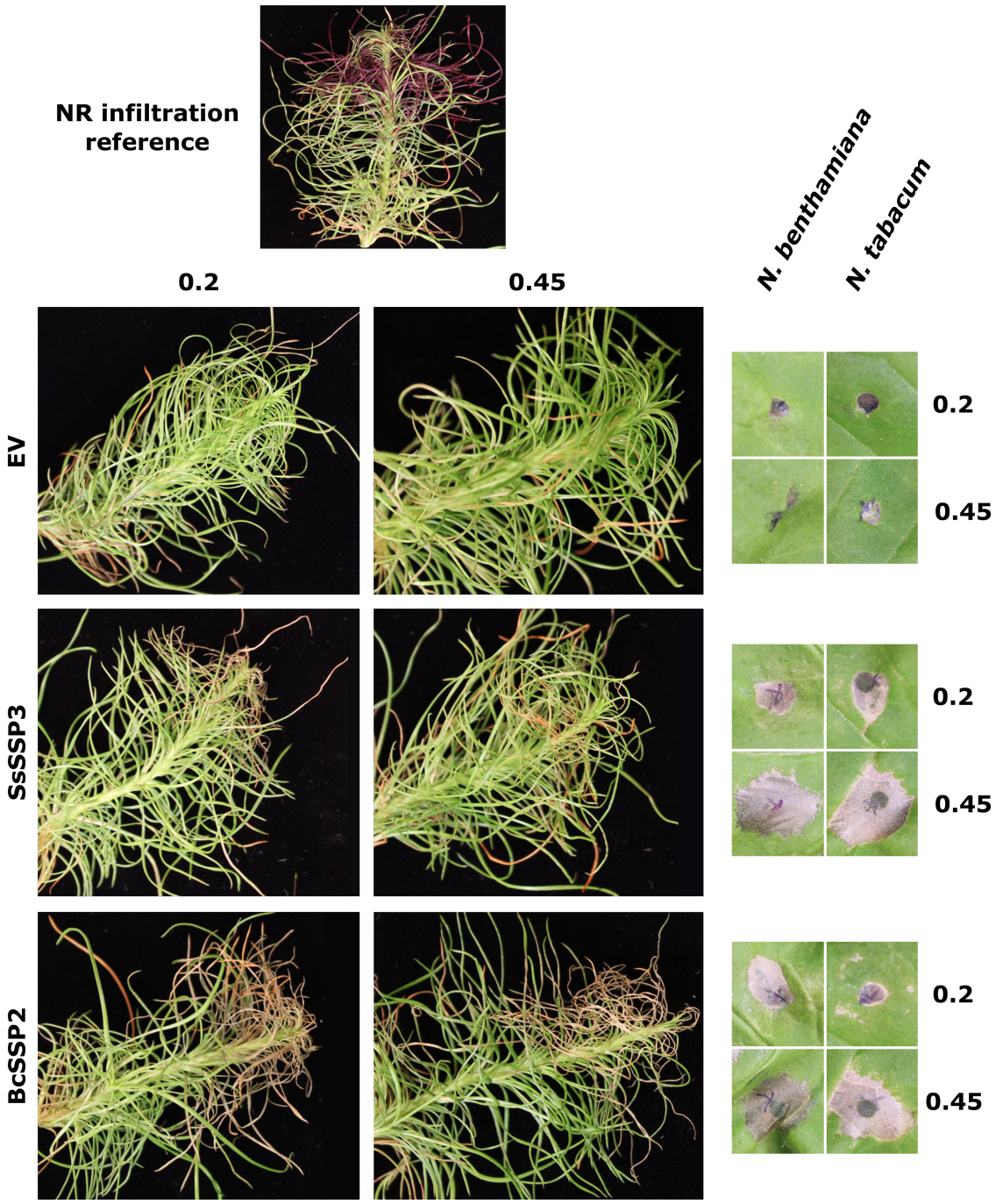

Figure 5.7.: Needles of *Pinus radiata* S2 shoots specifically responded to vacuum infiltration of *Botrytis cinerea* SSP2 with cell death. The genotypes R2, R4, S2, and S6 were used in this experiment, the results for S2 are shown. Approximately the top third of each shoot was submerged in liquid during vacuum infiltration. The top panel shows the infiltration efficacy represented by 0.01% neutral red (NR, 1 of 2 similar shoots). Two shoots each were infiltrated with filter-sterilised culture filtrate of *Pichia pastoris* strains carrying an empty vector (EV), or heterologously expressed *S. sclerotiorum* SSP3 (SsSSP3) or *B. cinerea* SSP2 (BcSSP2). The numbers 0.45 and 0.2 indicate sample filtering with 0.45 μm membrane, or 0.45 μm and subsequently 0.2 μm membrane. Photographs were taken 3 dpi. The culture filtrate samples were also tested in *Nicotiana benthamiana* and *N. tabacum* via blunt end syringe infiltration to confirm presence of each active (cell death inducing) secreted protein, and inertness of the EV sample.

A further assay was carried out with more rigorous internal replication, and achieved higher infection efficiency overall. This provided validity to the following results. The number of infected needles was recorded, and the fungal biomass per lesion was determined via qPCR. The infection rate (lesions per total number of needles) was 1.58% on average for wild-type, 1.95% for Δ*DsEcp2-1*A, 6.77% for Δ*DsEcp2-1*B and 12.72% for CO-*DsEcp2-1* (complemented Δ*DsEcp2-1*A). The two independent Δ*DsEcp2-1* strains were associated with significantly more *D. septosporum* biomass in their lesions compared to the wild-type and CO-*DsEcp2-1* (Fig. 5.8). Data from the qPCR are shown in Table E.1 (p. 190).

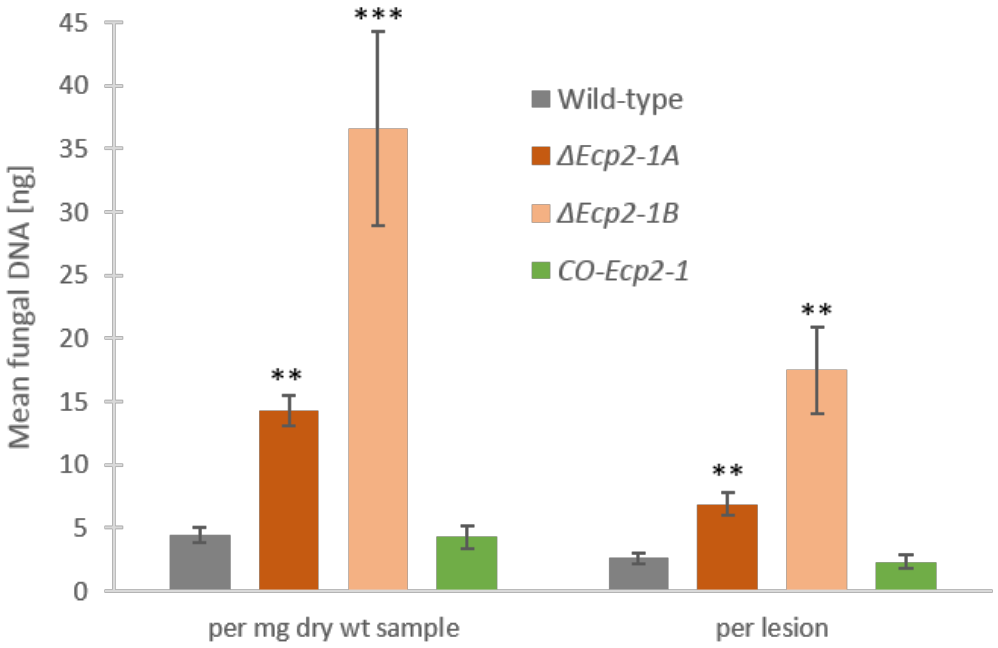

Figure 5.8.: Biomass of *Dothistroma septosporum* in *Pinus radiata* lesions increased in the absence of DsEcp2-1. The biomass is represented by the DNA amount as calculated via quantitative PCR. DNA was extracted from mature lesions 11 weeks post inoculation from $n = 4$ seedlings for wild-type and $n = 3$ seedlings for all other strains. The mass is expressed relative to the total dry weight (wt) of the infected needle sections (sampled lesions; left), and relative to the total number of lesions on the respective seedlings (right). Error bars show standard deviation; asterisks indicate significant differences to the wild-type (Student's t-test, **, $p < 0.01$; ***, $p < 0.001$).

5.3. Discussion

5.3.1. Successful recovery and application of functional CE protein in apoplastic wash fluid from *Nicotiana benthamiana*

It was important for this study to find a method that enabled functional assays for many different proteins that did not involve transformation of the host, but rather direct delivery of proteins. For this, choosing a source of secreted CE proteins was the first step.

Developing the AWF method was time-saving, since no additional expression constructs and strains had to be created for each CE used in the ATTA work in chapter 4. At the same time, collecting AWF using the ATTA setup and then re-applying samples to *Nicotiana* spp. in the same fashion (syringe infiltration) under the same conditions as for the CE screening was a succinct way to show that functional protein was present in the AWF. This was demonstrated for the positive control INF1, DsCE15, and DsEcp32-3; DsEcp2-1 and DsEcp20-3 AWF also induced weak cell death. As shown in subsection 4.2.5, presence of these proteins was also indicated by western blot, except for DsCE15. It could be that DsEcp2-1 and DsEcp20-3 protein solutions were less stable than the others.

The *P. infestans* elicitin INF1 was used as positive control for cell death induction in the non-host assays, with pre-existing evidence that is a reliable control (Du *et al.*, 2017). This was confirmed in the ATTAs (section 4.3). Even though the INF1 strain, when infiltrated into whole leaves and especially when combined with the RNAi suppressor p19, caused rapid HR-like cell death, AWF from these leaves was successfully collected. It was then shown that the AWF samples were highly potent in their ability to induce cell death when re-applied to *N. benthamiana* and *N. tabacum*. Serial dilutions of INF1 AWF up to 16-fold were tested in the non-hosts, and all of these diluted samples consistently triggered strong cell death. It is noteworthy that even with the undiluted INF1 samples, the protein was not detected via immunoblot. This suggests that expression of a potent elicitor does not necessarily need to be confirmed by this standard method.

It is not surprising that the ATTA and AWF assay yielded the same consistent results with dilutions of INF1 samples. Since AWF was collected from leaves infiltrated with *Agrobacterium* cultures at an optical density (OD) of 0.5, theoretically the diluted INF1

samples represented ODs of 0.25, 0.125, 0.0625 and 0.03125. These are comparable to the ATTA ODs 0.4, 0.2, 0.1 and 0.05. For a direct comparison, AWF could be extracted from leaves infiltrated with lower ODs as listed and then tested.

The combined results of ATTA and AWF infiltration suggest that a concentration of INF1 roughly similar to that effective in the ATTA was obtained. This is important to note regarding other proteins. It supports the finding that with CEs, inconsistencies in cell death induction via ATTA were more or less mirrored in the AWF assays, as the non-hosts were perhaps less sensitive to some of the CE proteins. For example, in the ATTA, DsEcp32-3 elicited cell death in *N. benthamiana* in a less consistent fashion than in *N. tabacum*, and when using AWF, cell death responses were also less clear and frequent in *N. tabacum*, and rarely occured in *N. benthamiana*. To determine whether cell death induction by AWF samples is due to proteins as assumed, each sample can be treated with heat and a proteinase and then compared to the untreated sample. Further, protein quantification assays could provide an estimate of secreted CE protein concentrations. If contamination with large intracellular proteins is evident, filtration with size exclusion filter membranes (such as used in Mesarich *et al.*, 2017) should be applied.

In conclusion, my modified AWF method worked well and constitutes a relatively quick and easy method to generate apoplastic CE protein solutions. Stability and high concentration of each protein of interest may not be guaranteed and requires validation via at least one of several assays, such as western blot, cell death induction activity, and tracking via fluorescent tags.

The application of AWF samples to the host is discussed in the next section.

5.3.2. Novel development of functional assays for pine

One of two major goals of this study was to develop a delivery method for CE proteins into pine tissue, preferably with young pine tissue of known genotypes, as *P. radiata* is genetically diverse and DNB resistance is variable even within breeding populations in New Zealand (see subsection 1.1.6). This variability may be due to differences in immune receptor arrays, resulting in different responses of individual trees to the CEs of the pathogen. Using vacuum infiltration of detached needles with *Pichia pastoris* culture

filtrate containing effector proteins was shown to be a promising approach in the preceding study (Guo, 2015).

In the present study, similar results could be replicated. However, infiltration success of neutral red dye was highly variable and thus not reliable (Fig. 5.3.A). It was concluded that older needles were unsuitable for these experiments. This approach was set aside until younger pine tissue was available.

Exploratory attempts were also made using needle/syringe injection. This was discontinued because the mechanical damage from the injection usually killed the needles. In another trial, meristematic pine tissue was exposed to the *P. pastoris* culture filtrates by mixing the filtrates into the growth medium. In that assay, most of the tissue either quickly died or was heavily growth-impaired (no shoot formation) regardless of the the used sample. This effect was stronger with a higher dose of either sample applied. It was concluded that cell death in the meristematic tissue was due to a non-specific response to the fungal culture filtrate (Appendix G).

The successful development of the AWF recovery method (previous section) was a crucial step towards mid- to high-throughput screening assays of CEs in various hosts. Regarding work with the *D. septosporum* host *P. radiata*, promising steps forward have been made with the support of Scion tissue culture resources.

Due to the small size of the clonal shoots and the absence of roots, it was decided that either whole or crudely sectioned shoots would be practical as experimental subjects. This was the main driver to scale up the AWF extraction method, processing several dozen plants per CE to obtain 30 ml of AWF or more.

With the limitations in place, compromises were inevitable. Importantly, glass jars with LPch agar (sterile) were deemed suitable for the incubation of whole shoots, and 12-well plates with water agar (non-sterile) for smaller shoot pieces. Fascicles that detached during the procedure could be saved and kept on wet foam; however, it is impractical to keep this sterile. Pine genotypes R1 and R2 suffered some damage from the treatment using negative controls, and S4 suffered heavy damage, which suggests that these genotypes may not be suitable for screenings, unless the method is further developed to avoid such damage. With minimised unspecific damage, responses to infiltrated proteins could

be distinguished.

5.3.3. Vacuum infiltration of clonal pine shoots with protein solutions could be an effector screening method

The central question in the process of creating a reliable cell death screening method is: If there is no apparent effect, were the tested CE proteins not delivered, or did they not induce a response? After establishing a non-destructive procedure for pine tissue infiltration (demonstrated with neutral red), the main quest was to find a positive control showing that cell death induction by a proteinaceous molecule could be achieved using that procedure.

Theoretically any CE could be recognised as an IP and thus serve as novel positive control in a *P. radiata* setup. At the same time, recognition might depend on the pine genotype, which is included in the very premise of the ultimate thesis goal.

With suggestions by Guo (2015), the logical choice was to test DsAvr4 and DsEcp2-1, conserved avirulence effectors of *C. fulvum* and other Dothideomycetes. DsAvr4 and DsEcp2-1 AWF samples were not rigorously tested on all genotypes, but there was no indication that they induced cell death responses in any of the trialled shoots. This could mean that *P. radiata* requires a specific PRR for each protein that were not present in the used genotypes. DsEcp2-1 AWF induced weak cell death in *N. tabacum* compared to its ATTA, which would support that DsEcp2-1 protein yield was low and potentially insufficient to trigger a response in pine.

Infiltration of *P. infestans* INF1 and DsCE15 AWFs appeared to damage the needles of S2 shoots—not as clearly as those of S4, but arguably different from the empty vector controls. Meanwhile, all R3 shoots appeared mostly healthy (Fig. 5.4). One conclusion from this was that INF1 and DsCE15 AWFs potentially demonstrated successful cell death induction following protein delivery. It would be curious, though, that a non-host-specific IP, INF1, induced cell death only on some genotypes within a non-host species, as this would infer absence of a common IP receptor. A more likely explanation is that the protein(s) were not, or far less efficiently, delivered in R3 compared to S2.

For DsCE15, it does make sense that necrosis occured in a DNB-susceptible host but

not in a resistant host. DsCE15 expression was highly induced in the Mid and Late stage, where *D. septosporum* is thought to engage in a necrotrophic lifestyle. Like necrotrophic effectors, DsCE15 may contribute to plant cell death induction by interacting with a specific target protein, which is recognised (ultimately to the disadvantage of the host, compare section 1.2.4); in a resistant host, this target would be absent. It may also be that DsCE15 is a non-specific toxin and S2 was the only genotype with sufficient protein uptake to develop any response. Since DsCE15 also induced cell death in non-hosts, like INF1, the question is how likely it is for barely related hosts to share an IP receptor, but this receptor is then lost or mutated in some genotypes of the pathogen's host. To support either suggestion (recognition or toxicity), the result needs to be thoroughly replicated with resistant and susceptible host types, and more concentrated DsCE15 samples if possible.

Another promising option as positive control was a cerato-platanin protein (CPP) from *Heterobasidion annosum*, HaCPL2, which was shown to induce cell death in *P. sylvestris* upon application via the root system (Chen *et al.*, 2015). It is not unlikely that a CPP is recognised as an IP (see subsection 3.3.2), and thus a cognate PRR may be shared among related hosts, such as *P. sylvestris* and *P. radiata*. HaCPL2 AWF infiltration into *P. radiata* shoots achieved moderate cell death induction in genotype S2 (Fig. 5.6) and likely S5, both with few replicates. This may be interpreted as more evidence for successful protein uptake and cell death causation. In three other genotypes, responses were observed but could not be specifically ascribed to HaCPL2.

However, there are conflicting results concerning HaCPL2. In *Nicotiana* spp., the ATTA with HaCPL2 did not lead to cell death. *N. tabacum* was one of the proxies used in the HaCPL2 study (Chen *et al.*, 2015) to demonstrate its recognition as IP in a non-host plant species. It was mentioned that HaCPL2 was produced by *P. pastoris* in different isoforms and only one of them exhibited the function. Dimerisation could be the reason for differential activity (Chen *et al.*, 2015), as the CPPs Sm1 and Epl1 (subsection 3.3.2) only induced defence response as monomers, and their dimerisation was prevented by glycosylation (Vargas *et al.*, 2008). This highlights a source of uncertainty in protein work. Given that even a different expression system (*N. benthamiana* instead of yeast) was

used for the functional assays with HaCPL2 in this study, it could well be that HaCPL2 collected within AWF did not undergo correct post-translational modification and that this was the reason for not being able to reproduce its cell death induction function in *Nicotiana* spp. I speculate that a small epitope, regardless of a correct protein fold, could be recognised by a PRR of one host (pine) but not another, but I could not find any precedent in the literature for this. Importantly, the positive result from the pine shoots must be reproduced to discuss this further. The next step is to produce HaCPL2 in *P. pastoris* and directly compare this with the ATTA/AWF product for cell death effects.

Application of yeast culture filtrates could support successful protein delivery

In the final phase of development, additional promising positive control candidates were acquired: *P. pastoris* strains producing small secreted proteins of the necrotrophic pathogens *B. cinerea* and *S. sclerotiorum*, BcSSP3 and SsSSP2. Culture filtrates of these strains induced cell death in *Camellia lutchuensis* and *N. benthamiana* (Denton-Giles, 2014). More explicitly, this was a source of stable protein in high enough concentrations to be taken up by *P. radiata* needles to sometimes cause necrotic lesions, while the empty vector negative control did not affect the tissue (see earlier *P. pastoris* experiments).

Cell death induction upon BcSSP2 and SsSSP3 infiltration of *N. benthamiana* as well as *N. tabacum*, in contrast to symptomless empty vector infiltration, strongly indicated presence of active SSPs in the acquired culture filtrate batch.

The infiltrated parts of all *P. radiata* shoots but genotype S2 were negatively affected by the treatment, or the empty vector control. S2 needles appeared to die specifically due to SsSSP3 and particularly BcSSP2. This suggests the proteins were delivered and induced a specific response. If these results can be replicated, successful uptake of small proteins by *P. radiata* for screening of cell death responses would be demonstrated. CEs of particular interest from *D. septosporum*, but importantly also CEs from other pine pathogens, could be investigated with this method. Since the *P. pastoris* culturing can be scaled up relatively easily, a range of genotypes can be tested. The vacuum infiltration protocol may have to be adapted to ensure the shoots are not harmed by the treatment

itself.

The question remains whether the clear BcSSP2 cell death result in S2, compared to any AWF sample, was specifically due to a highly potent elicitor or the method with which it was produced. The most stringent control to address this would be to express BcSSP2 and SsSSP3 using ATTA and carry out a direct comparison of AWF and *P. pastoris* culture filtrate in both non-hosts and pine. As suggested above, a protocol with minimal unspecific damage to shoots, regardless of genotype and protein solution type, would greatly facilitate the establishment of a positive control for protein delivery such as BcSSP2. This would in turn pave the way for DsCE screenings on a wider range of pine genotypes, potentially uncovering specific (receptor-mediated) responses among the diversity of *P. radiata*.

Other positive controls?

In the HaCPL2 study, *H. annosum* infection was used as a positive control for root necrosis. The fungus caused necrosis and significant growth retardation within 48 h. This was used as a direct reference for the effect of pure HaCPL2 protein, which was similar, and this allowed the conclusion that HaCPL2 is an important necrotrophic effector, supporting colonisation of dead tissue (Chen *et al.*, 2015). It is unlikely that the same could be achieved with *D. septosporum* (i.e., inoculation of shoots with spores), most of all due to its symptomless phase. Cerato-platanin may be a good control, as its direct application to host (plane) and non-host (*N. tabacum*) leaves in nanomolar amounts induced cell death as well as phytoalexin production (Pazzagli *et al.*, 1999; Lombardi *et al.*, 2013). In other studies involving host tissue, effectors unrelated to the pathosystem were used as positive controls, for example, a bacterial cell death inducer in hosts and non-hosts (Chen *et al.*, 2013b). The *P. infestans* elicitin INF1, tried as control here, is another such example. The PAMP RcCDI1, in contrast, induced cell death in dicot non-hosts including *N. benthamiana*, but not the host barley, or other monocots (Franco-Orozco *et al.*, 2017). Homologues of RcCDI1 also induced cell death in *N. benthamiana*, suggesting that a putative PRR of this PAMP confers non-host resistance to a range of pathogens.

Lastly, MfEcp2 is potentially a necrotrophic effector exploiting cell death induction in

several plants (see below), which could be an excellent control considering that *D. septosporum* carries a homologue.

5.3.4. Revisiting the role of Dothideomycete core effector DsEcp2-1 in *D. septosporum*

Ecp2 is established as avirulence effector of several dothideomycete pathogens (see p. 28). DsEcp2-1 was recognised by the Cf-Ecp2 receptor when expressed in MM-Cf-Ecp2 tomato (de Wit *et al.*, 2012). Cloning of various alleles of DsEcp2-1 with different non-synonymous mutations from different *D. septosporum* strains also showed that DsEcp2-1 induced cell death in the non-host *N. tabacum* (Guo *et al.*, unpublished), further supporting its non-specific recognition as an IP. In contrast, DsEcp2-1 did not induce cell death in our assays with *N. benthamiana* (Fig. 4.2). Further, Guo (2015) found that deletion of *DsEcp2-1* does not affect the physiology of the fungus *in vitro*. Previous attempts to provide a clear conclusion about whether DsEcp2-1 plays a role in the *D. septosporum–P. radiata* interaction had failed. It was shown that DsEcp2-1 protein caused necrotic lesions on detached pine needles at a similar, low rate as the positive control, but these experiments were of preliminary nature (Guo, 2015, this study). Here, new results are presented that support an avirulence function in *P. radiata*.

In a pathogenicity assay of *P. radiata* seedlings of 'relatively DNB-susceptible' (Toby Stovoid, Scion) parentage with *D. septosporum* NZE10 wild-type and several mutant strains, an overall satisfactory infection rate was achieved. One *DsEcp2-1* knockout strain caused a similar percentage of lesions as the wild-type. The other DsEcp2-1 knockout strain achieved over four times more lesions than the wild-type; however, the DsEcp2-1-complement strain had eight times more than the wild-type. Thus, this comparison was inconclusive. It could be that the strains have different vigour regarding infection, even though they had all been cultured *in vitro* for spore generation for several weeks at least.

Importantly, the *D. septosporum* biomass per collected lesion was also investigated. Fungal biomass was also used as a parameter for gain or loss of virulence in similar experiments (CfEcp2 knockout (not measured via qPCR), Laugé *et al.* (1997); CfAvr4 knockdown, van Esse *et al.* (2007); CfAvr5 complementation, Mesarich *et al.* (2014);

Mg3LysM knockout, Marshall *et al.* (2011); UmTin2 knockout, Tanaka *et al.* (2014); CfEcp6 knockdown, Bolton *et al.* (2008)). Compared to the wild-type strain, biomass was found to be significantly higher in both knockout strains, but not the complement strain. Hence, the absence of DsEcp2-1 can be linked to increased colonisation of the host (and vice versa).

The existing hypothesis is that a) DsEcp2-1 inhibits activation of a host target that triggers immunity responses in the biotrophic phase, allowing further colonisation (same virulence function as CfEcp2-1), but b) the DsEcp2-1 target is monitored by a guard protein in some pine genotypes, and this activation leads to a strong immunity response, limiting *D. septosporum* growth (Guo, 2015). This hypothesis is not supported by the available expression data for DsEcp2-1: There was only negligible expression of DsEcp2-1 during the biotrophic growth phase. It cannot be excluded that DsEcp2-1 is highly induced at an earlier point in the infection, as in *C. fulvum*, or in between Early and Mid stage. It may also be that *D. septosporum* NZE10 and the used pine seedlings represent the situation in the evolutionary arms race where the pathogen is at a disadvantage by expressing an effector. Thus, whatever its primary function is, DsEcp2-1 could induce a response in the host that reduces the extent of colonisation even at the imminent shift to necrotrophy. It should be kept in mind that the expression data are based on an asynchronous infection and it is feasible that especially the Mid time point contains RNA reads from fungal hyphae in their biotrophic phase.

To confirm the DsEcp2-1 expression profile, it could be reassessed via qPCR, correlating expression with biomass over more than three time points. Ideally, expression of pine defence (PR) genes could also be measured in the same samples. The accumulation of other defence-related compounds, such as ROS, could also be monitored in an experiment with sufficient replication.

The protein MfEcp2 of *P. fijiensis*, a close relative of *D. septosporum*, can be recognised by the tomato R protein Cf-Ecp2 (Stergiopoulos *et al.*, 2010). It is not known whether the host, banana, carries this receptor as well. MfEcp2 surprisingly caused cell death in tomato plants independent of Cf-Ecp2, indicating that this may be its main function in the host, where cell death serves the pathogen during necrotrophy (Stergiopoulos *et al.*,

2010). MfEcp2 was apparently duplicated and its paralogues (MfEcp2-2 and MfEcp2-3) diversified, which was suggested to play a role in adaptive responses, including adaptation to changing hosts (Stergiopoulos *et al.*, 2014). MfEcp2 and MfEcp2-2 were shown to be under positive directional selection, with almost all variants escaping Cf-Ecp2-mediated recognition (Stergiopoulos *et al.*, 2014). The MfEcp2 isoforms also failed to elicit cell death in tomato. Evasion of recognition is in line with repeated findings of *C. fulvum* overcoming qualitative host resistance by mutation of Avr effectors (see p. 28), but it appears that this comes at the cost of also losing the R protein-independent necrotrophic function. As noted, we recently investigated DsEcp2-1 variants from different *D. septosporum* strains and they all induced cell death in *N. tabacum* in the absence of Cf-Ecp2 (Y. Guo, unpublished). It would be intriguing to test these different proteins for recognition by Cf-Ecp2 in order to find out if *D. septosporum*, like its relatives *C. fulvum* and *P. fijiensis*, has also undergone adaptation regarding Ecp2. If so, this would either strongly suggest the presence of a Cf-Ecp2 homologue in *P. radiata*, or that DsEcp2-1 does not play an important role in the interaction and is under no selective pressure. Finally, testing MfEcp2 isoforms for necrosis induction in pine could add evidence to the hypothesis that MfEcp2 has a conserved virulence target in a range of hosts (Stergiopoulos *et al.*, 2014), and would thus improve the fundamental understanding of a dothideomycete core effector.

5.3.5. Summary and outlook

I attempted to develop a methodology to study the potential effectors of pine pathogens. This was successful, although further optimisation is required. The vacuum infiltration protocol may have to be adapted to be less damaging for sensitive shoots, so that a large genotype range can be screened. To establish a positive control, favourably a reference protein of *D. septosporum*, the experiments need to be extensively replicated.

For more stringency regarding the functions of each protein, my approach could be combined with an *A. tumefaciens*-mediated transformation method as presented by Maleki *et al.* (2018). In such studies in the host, I would favour the use of an inducible promoter for the respective gene of interest over a constitutive one (CaMV 35S in Maleki

et al., 2018) to investigate effectors that are expected to cause cell death in the host. This would allow precise monitoring of any effects at different stages of tissue development.

Chapter 6.

Synthesis and future directions

For this thesis, a variety of computational and experimental methods were combined to gain a better molecular understanding of the fungal conifer pathogen *Dothistroma septosporum*, and how it interacts with its host *Pinus radiata*. In particular, effectors were investigated, which are small secreted proteins that modulate host defences or physiology. The wealth of research of fungal crop pathogens, by which major advances in the effector field have been achieved, stands in stark contrast to the sparse knowledge of the molecular cross-talk of forest pathogens and their hosts. This is somewhat concerning, given that forests a) provide important ecosystem functions and could mitigate global climate change (Liebhold *et al.*, 2017), and b) are, like crops, prone to devastation by pathogens or pests under certain conditions.

The case of *Pinus* spp. plantations, which have been under threat by disease or even eradicated in some countries, is a textbook example of a scenario where a pathogen thrives in an unnatural environment due to human activity. Countermeasures have been effective to varying degrees.

The aims of this study were to identify *D. septosporum* candidate effectors (CEs) with computational tools, to functionally screen CEs in non-hosts, and to develop a delivery method to screen CEs in *P. radiata*. This would ultimately enable rapid effector-based resistance screening of *P. radiata* genotypes in laboratory setups prior to field trials, and thus bridge fundamental research and practical applications.

The first two aims were fulfilled, even though further questions were raised. For the third aim, promising progress was made towards the development of a host response

screening method. In the following sections, I briefly address key points related to the main aims of this thesis, I put forward a model to describe the infection of *P. radiata* by *D. septosporum* based on the results of chapters 3-5, and I make suggestions to address remaining and new questions.

6.1. *D. septosporum* in the age of omics: CEs chosen

New CEs of a fungal forest pathogen were defined, which is a novelty at least among foliar pathogens of conifers. The secretome of *D. septosporum* NZE10 was refined, resulting in the prediction of 875 secreted proteins. The focus was placed on small secreted cysteine-rich proteins (SSCPs), as proteins of this category constitute the majority of extracellular fungal effectors. However, this was complemented by CEs without these restrictions, taking discoveries of larger or non-cysteine-rich effectors into account. Based on my selection pipeline, which also took into account the time course expression data from a previous *P. radiata* infection experiment (Bradshaw *et al.*, 2016), a total of 55 *D. septosporum* CEs (DsCEs) were shortlisted for functional analysis. Similar CE numbers are found for many other pathogens.

Twenty-six of the 55 DsCEs had putative functions assigned on the basis of bioinformatic comparisons, including a variety of enzymatic functions. The other 27 DsCEs were similar to predicted proteins of unknown function found in a wide range of the Dothideomycetes or Sordariomycetes, the majority of which are plant pathogens. While one DsCE appears to be exclusive to *D. septosporum* and *C. fulvum*, none were found in *D. septosporum* only. This indicates that the needle pathogen employs, at least in part, similar molecular strategies to establish infection as related microbes. Hence, the finding provides a better understanding of forest pathology. Lastly, it also shows that large proportions of pathogen secretomes are still unexplored.

6.2. Testing of CEs for non-host cell death induction

The induction of plant cell death by secreted fungal molecules can indicate that these are recognised by the plant immune system, i.e., as invasion patterns (IPs) that herald danger

for the plant (subsection 1.2.3). Recognition in a non-host plant suggests the presence of a conserved pattern recognition receptor (PRR) for this IP, contributing to the broad-range immunity of plants against microbes. It is common to test CEs for such recognition as part of their characterisation, which also contributes to the current understanding of molecular plant-pathogen interactions in general.

Seventeen prioritised DsCEs were successfully taken forward for initial functional analysis in model plants, *Nicotiana tabacum* and *N. benthamiana*, which are thought to be non-hosts to *D. septosporum*. Five of the 17 DsCEs that were transiently expressed in plant leaves induced local cell death in either or both hosts. Thus, *D. septosporum* can be added to the list of microbes that secrete proteins which induce cell death in a non-host. While the sample size of functionally tested secreted CEs was comparatively small, the positive rate was rather high. To date, the only other study with a similar aim involving a forest pathogen has been done with *Heterobasidion annosum sensu lato*, an important necrotrophic basidiomycete root pathogen of conifers (Raffaello & Asiegbu, 2017). Eight of 58 putative SSPs likely exclusive to *H. annosum* induced cell death or chlorosis in *N. benthamiana*. Together with the *D. septosporum* study described in this thesis, there is growing evidence to suggest that secreted proteins in gymnosperm pathosystems are recognised as IPs by angiosperm hosts. This in turn indicates development of a common immune receptor array before the divergence of these two major plant groups, or convergent evolution.

6.3. Testing of a new method for CEs screening in pine

A new delivery method for proteins into pine foliage was developed to fulfil a general need in pine and gymnosperm research. Rootless *P. radiata* shoots grown from clonal meristematic tissue were found to be suitable test subjects. Two sources for DsCE protein production were considered. Heterologous protein expression in *Pichia pastoris* is an established way to generate large volumes of culture filtrate containing CEs (Guo, 2015). However, transformation of yeast and selection of transformants with high expression levels is not a high-throughput procedure when working with many CEs. Thus, another heterologous expression system using *N. benthamiana* leaves infiltrated with DsCE

expression constructs created in this study was employed. A novel adaptation of the protocol to collect large volumes of apoplastic wash fluid (AWF), and thereby apoplastic DsCE, from *N. benthamiana* leaves was devised.

Apoplastic wash fluid containing DsCEs was vacuum-infiltrated into *P. radiata* shoots of different genotypes. Some promising results emerged. HaCPL2, a cell death-inducing CE from a necrotrophic pine pathogen, caused tissue damage distinguishable from an empty vector control. However, due to material and time limitations, there was no replication of this result, and no comparison to a positive (cell death) control could be established at the time. Two small secreted proteins from *Botrytis cinerea* and *Sclerotinia sclerotiorum* that are highly similar to each other and induced cell death in *N. benthamiana* and *Camellia lutchuensis* (Denton-Giles, 2014) were tested on pines as well, using existing *P. pastoris* constructs. Infiltration of culture filtrates with the *B. cinerea* protein caused needle death in one of four tested *P. radiata* genotypes. Thus, this protein could serve as a proof of concept for protein delivery.

6.4. *D. septosporum* virulence analysis with DsEcp2-1 mutants

The role of the conserved dothideomycete CE Ecp2-1 in *D. septosporum* is still unclear despite previous functional investigation (Guo, 2015). In the current study, artificial infection of *P. radiata* seedlings with Δ*DsEcp2-1* mutants of *D. septosporum* was repeated. Results showed that *D. septosporum* biomass per lesion significantly increased in the absence of DsEcp2-1. This infers that DsEcp2-1 expression reduces the virulence of *D. septosporum*, possibly through direct or indirect (guarded target protein) recognition. Results supporting the presence of a DsEcp2-1-specific receptor in pine (Guo, 2015) have not yet been conclusively reproduced, and clonal genotypes were not available for the different types of assays (seedling inoculation with the fungus and protein-only infiltration). The standing hypothesis is that DsEcp2-1 very likely has an avirulence function in the *D. septosporum* NZE10–*P. radiata* interaction. Bringing MfEcp2 into the effector delivery trials could provide a big step forward for both the understanding of Ecp2 in three

closely related pathogens (*D. septosporum*, *P. fijiensis*, and *C. fulvum*) and the screening method.

6.5. Illustrated overview of the current *D. septosporum* understanding

Based on the predicted functions of the investigated DsCEs, including antagonism against other microbes, inhibition of the host immune system, and targeted induction of cell death, I propose an updated molecular understanding of the measures *D. septosporum* uses to successfully complete its life cycle on *P. radiata* needles (Fig. 6.1). Dothistromin and other potentially important secondary metabolites (Ozturk, 2016) are also incorporated. To confirm most of the putative DsCE functions, further experiments in future studies are required. This is discussed in the last section.

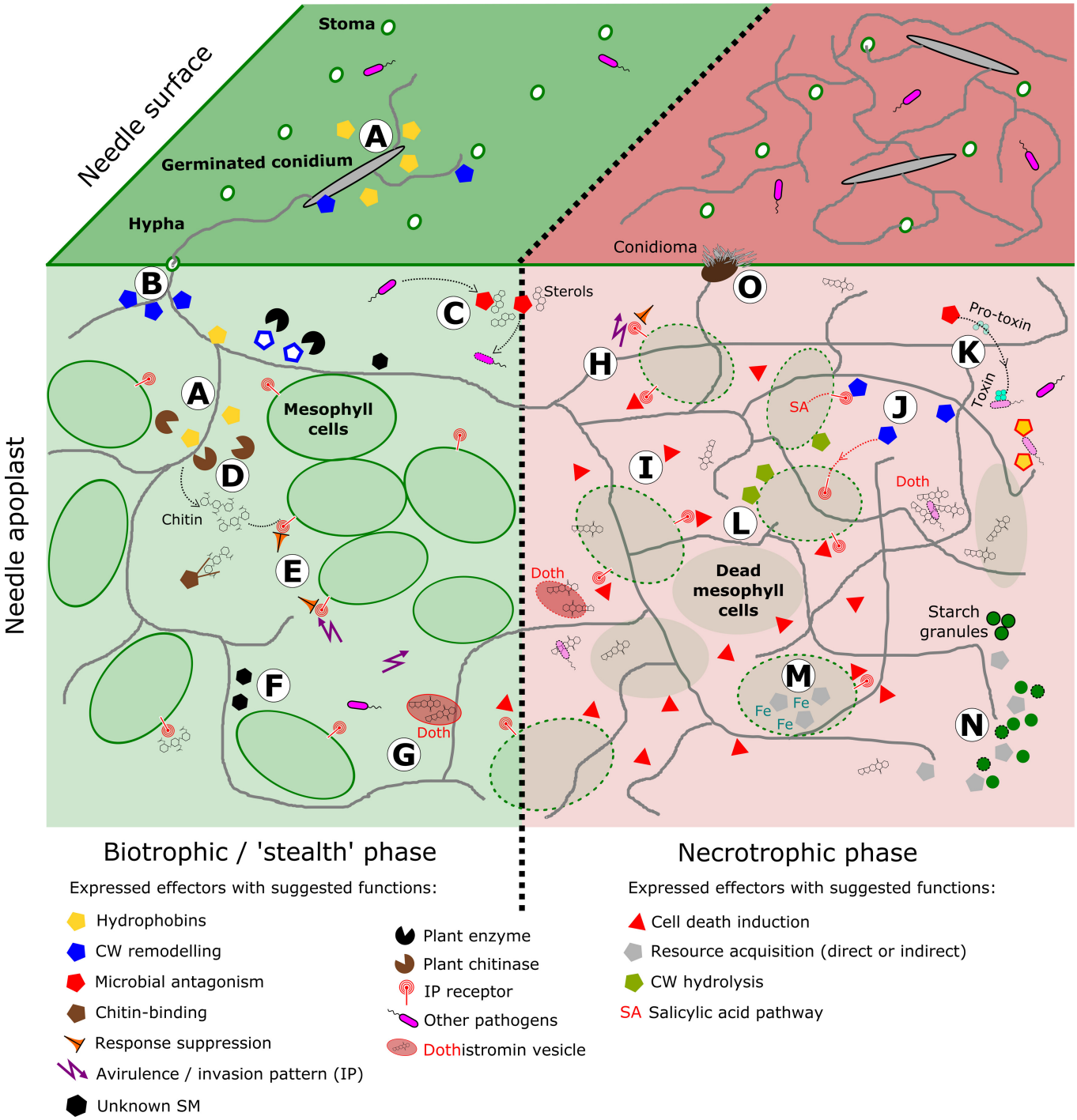

Figure 6.1.: Model integrating current hypotheses of the *Dothistroma septosporum* infection of *Pinus radiata* using secreted candidate effectors (CEs) and secondary metabolites (SMs). Structures and objects are not to scale. Inclusion of gene products is based on the timing of expression. Two major phases of the interaction are shown: Left, *D. septosporum* establishes colonisation of needles without being detected by the plant immune system; right, CEs promote plant cell death and enable *D. septosporum* to sequester nutrients. Dashed lines show degraded structures (cells etc.). A battle against other microbes potentially needs to be carried out at all times. Plant countermeasures are not shown. The events A to O, representing potential functions of secreted molecules, are described on the facing page.

Figure 6.1 (cont.): Model integrating current hypotheses of the*Dothistroma septosporum* infection of *Pinus radiata* using secreted candidate effectors (CEs) and secondary metabolites (SMs).

(A) Hydrophobins allow for attachment to a hydrophobic host surface, formation of aerial hyphae for gas exchange, and they coat immunogenic cell wall (CW) components to prevent recognition (DsCE40, Ds91219; section 3.3.5).

(B) Multiple CW remodelling proteins (blue) are required during rapid hyphal growth on the surface and in the apoplast (expansin and cerato-platanin proteins DsCE14, DsCE31 and DsCPL1; GH64 DsCE42; 3.3.2). DsCE35 (blue with white core) provides apoplast detoxification by inhibiting plant enzymes attacking hyphal CWs (3.3.8).

(C) A 'cysteine-rich secretory protein, antigen 5, and pathogenesis-related 1 protein' (CAP) scavenges sterol compounds from the environment or directly sequesters sterols in the membranes of oomycete competitors (DsEcp57-1; 3.3.7).

(D) Fungal CW degradation through plant chitinases may occur since DsAvr4 is not expressed. Hydrophobins could mitigate this. Chitin oligomers released into the apoplast are scavenged by CEs to prevent invasion pattern (IP) recognition (LysM lectins DsEcp6, DsCE38; 3.3.3).

(E) Host immune response due to recognition of any IPs by host immune receptors is suppressed by action of DsEcp57-1, like its homologue in *Venturia inaequalis*.

(F) An uncharacterised SM contributes to virulence in this phase (DsNps3; Ozturk, 2016).

(G) Biosynthesis of the toxic SM dothistromin is increased as infection proceeds, prior to release it is possibly kept in vacuoles to prevent damage to *D. septosporum*(Bradshaw *et al.*, 2009). Dothistromin kills plant and competitor cells and overall enhances virulence (Doth; Bradshaw, 2004; Kabir *et al.*, 2015).

(H) Expression of DsEcp2-1 leads to a strong immune response that is still able to limit *D. septosporum* growth at this point (5.3.4). Suppression of this effect via DsEcp57-1 may occur (3.3.7).

(I) Plant cell death is caused by several effectors which either exploit the immune system machinery or are toxic (DsCE3, DsCE15, DsEcp20-3, DsEcp20-4, DsEcp32-3; subsection 4.3.7).

(J) Cerato-platanins induce cell death by promoting the salicylic acid pathway or a host-specific target (DsCPL1, DsCE14; 3.3.2).

(K) An unknown compound is cyclised to a steroidal toxin which acts against competing microbes and supports the competitiveness of *D. septosporum* as the needle tissue becomes vulnerable to consumption (polyketide cyclase DsEcp58-1; 3.3.8). This is further underpinned by the hydrophobin DsHdp1 which has a direct antifungal function (yellow with red border).

(L) Enzymes hydrolyse plant CW polysaccharides to support lysis (potential β-xylosidase DsCE7, GH71 DsCE19; 3.3.4).

(M) A ferritin-like CE binds iron molecules for *D. septosporum* metabolism (DsCE12; 3.3.8).

(N) α-amylases hydrolyse starch accumulated in 'green islands' found adjacent to lesions (GH13 DsCE2, DsCE4: 3.3.4).

(O) The sporulation phase begins. Conidia formation is supported by DsPhiA-2 (3.3.8).

6.6. Future directions

While some research questions were addressed in this thesis, new ones emerged. Some may be straightforward to answer in little additional time, but others will require experiments inclusive of various homologous proteins and different hosts for direct functional comparisons, or other microbes sharing the ecological niche of gymnosperm foliage.

Which CEs are truly relevant to a compatible *D. septosporum*–*P. radiata* interaction?

Regardless of specific function, the importance of any CE protein for *D. septosporum* pathogenicity or virulence can ultimately only be determined by removing the protein from the (*in vivo*) interaction (with prior testing of any effects on fungal physiology in absence of the host). The CE genes could be silenced, or deleted. Protoplast-mediated gene deletions in have been accomplished in *D. septosporum*. Deletions could nowadays also be achieved using the type II clustered regularly interspaced short palindromic repeats (CRISPR)/Cas9 system. The efficiency of the CRISPR system for filamentous fungi is constantly being improved (Deng *et al.*, 2017; Foster *et al.*, 2018). Single or multiple mutant *D. septosporum* strains should then be screened on several resistant and susceptible *P. radiata* genotypes.

Ideally, this would complement findings from continued cell death induction screenings of CE proteins on *P. radiata* shoots (and potentially other *Pinus* spp. tissue). The combined pieces of information should allow for a conclusion about if CEs are virulence factors, if their function depends on a specific target (necrotrophic effector), and if some hosts have resistance genes to neutralise them (avirulence effector).

Were the five CEs that induced localised cell death in non-hosts recognised by the immune system, or were they directly toxic (e.g., cell wall perforation)?

Currently, the five DsCEs that induced cell death are being screened in *Nicotiana* spp. plants in which sets of PRRs are being silenced by virus-induced gene silencing (Wang *et al.*, 2018). The PRR genes are silenced in overlapping pools, then single genes are

silenced to determine which, if any, encode a PRR that interacts with each DsCE. This could lead to the discovery of specific PRRs for each of the cell death inducers and enable further studies, such as the validation of the interaction (via co-immunoprecipitation) in non-hosts and potentially also in the host. Additionally, the involvement of known cell death induction pathways could be investigated, such as the cell death suppression assays done with Avr3a for DsEcp20-3 and DsEcp32-3. This may include a) co-infiltration with suppressors of other pathways, such as PexRD2 (King *et al.*, 2014) or *Colletotrichum* spp. effectors (Robin *et al.*, 2018), and b) silencing of host proteins, such as receptor-like kinases (RLKs) BAK1 and SOBIR1 which are both required for Cf4-Avr4 interaction-triggered immunity (Liebrand *et al.*, 2014; Postma *et al.*, 2016). Based on the lack of similar findings for intracellular pathogens, it was speculated that the pathways involving these two RLKs are specific to apoplastic effectors (Kettles *et al.*, 2017). Furthermore, screening for cell death responses in other hosts with receptor repertoires different from *Nicotiana* spp., but also organisms from other kingdoms, could shed more light on this.

Dose-dependent responses may also be indicative of toxicity rather than recognition. This could be tested with dilution series of protein solutions, such as AWF samples.

Are the cell death-eliciting candidate effectors PAMPs?

Even though the five DsCEs constitute IPs by means of inducing cell death in at least one non-host plant, screening in a wider range of plants would be highly interesting to determine how conserved PRR-mediated recognition of these proteins is. Apoplastic wash fluid samples might be useful sources of these proteins in hosts that are not amenable to *Agrobacterium* transformation with protein-encoding constructs.

Could amino acid differences predicted in CE alleles of other *D. septosporum* isolates affect IP function?

Polymorphisms could indicate specific adaptation to hosts. These alleles of the DsCEs could be cloned from the genomic DNA of the overseas isolates of *D. septosporum*. Alternatively, the mutated sequences could be used as templates for *in vitro* targeted mutagenesis in NZE10 genes, or for custom gene synthesis. It should be kept in mind that

all variants of DsEcp2-1 and RcCDI1 still induced cell death. Thus, even if the mutations represent adaptations, that might not affect recognition in the non-host system. In contrast, Avr4 orthologues in different species, while sharing the chitin binding function, were not all recognised by Cf-4. Specifically, the recognition site of Avr4 for Cf-4 was found by swaps of intra-cysteine pair domains and *in vitro* mutagenesis experiments based on the sequences of the interacting Cf-, Ds- and Mf-Avr4 proteins and the non-interacting Ca- and Cb-Avr4 proteins (Mesarich *et al.*, 2016), which this idea is based on.

Could CEs expressed at the same time work together?

It is likely that *D. septosporum* uses a detection prevention or suppression strategy to maintain a compatible biotrophic interaction at the early stage of infection, as mentioned in the model. Regarding specific effector action, DsEcp57-1, a homolog of a *N. benthamiana* cell death-attenuating *V. inaequalis* CE, should be co-infiltrated with cell death elicitors. If a CE is found to consistently induce cell death in the host, AWF of this CE and DsEcp57-1 should be mixed and infiltrated for a closer to *in situ* evaluation.

To accelerate screening for cell death induction in the host (and overcome the limited volume issue), AWF samples of several CEs could be pooled in different combinations.

In *Colletotrichum higginsianum*, an NLP is expressed during the switch from biotrophic to necrotrophic lifestyle. This protein can induce cell death in *N. benthamiana*. *C. higginsianum* CEs that are expressed during the biotrophic stage were shown to suppress this cell death (Robin *et al.*, 2018). Similar observations were made in *C. orbiculare* (Yoshino *et al.*, 2012). Deletion of these CE genes did not affect the virulence of the pathogens; however, "these reports suggest that the balance between effector proteins that induce cell death and those that suppress it may control the switch from biotrophy to necrotrophic development in hemibiotrophic fungi" (Lo Presti *et al.*, 2015). Characterising DsEcp57-1 and potentially other cell death-suppressing DsCEs may add intriguing evidence to this suggestion.

Is the *P. pastoris* culture filtrate infiltration result reliable?

While the cell death result was clear in one pine genotype, it is only based on two individual shoots per treatment. The experiment will be repeated thoroughly to confirm its validity. Furthermore, to strengthen the AWF extraction method, whole *N. benthamiana* leaves could be infiltrated with culture filtrate and immediately extracted again. This fluid could then be applied to the pine shoots to test if the effect is still the same.

How similar in function are the cerato-platanin proteins? Are they essential for virulence of *D. septosporum* and other pine pathogens?

Many known CPPs induce cell death and other immune responses in hosts and non-hosts (subsection 3.3.2). As one of them, and a potential necrotrophic effector of a pine pathogen, HaCPL2 is of special interest. The three DsCPPs, including DsCPL1 with 41% sequence similarity to HaCPL2, may well have different functions. This could be investigated by thorough direct comparisons of the proteins using the same methods and hosts, i.e., *P. radiata* and *P. sylvestris*, for all three DsCPPs as well as HaCPL2. It would also be interesting to determine whether any of these CPPs are IPs to a range of non-hosts and thus likely PAMPs. Foremost, the issue that HaCPL2 expressed in *N. benthamiana* did not induce non-host cell death must be addressed.

Was secretion of the cell death-inducing CEs crucial? What is their exact localisation?

The five DsCEs should be cloned without a signal peptide to demonstrate that they are in fact recognised extracellularly (Yoshino *et al.*, 2012; Prokchorchik, 2017; Kettles *et al.*, 2017; Franco-Orozco *et al.*, 2017). Such an assay may be complicated if a DsCE is indeed toxic independent of its localisation, as this would yield a 'false' result. Furthermore, DsCEs could be tagged with a fluorescent protein to pinpoint their localisation in the plant (Yoshino *et al.*, 2012; Robin *et al.*, 2018; localisation techniques reviewed in Lo Presti *et al.*, 2015).

To further investigate if the AWF collection method resulted in the inclusion of intracellular proteins, the protocol should be applied to leaves transformed with non-secreted

protein constructs, and subsequent re-infiltration as well as western blotting compared to total protein extraction samples from leaf tissue for reference.

Are there substrate-binding functions relevant for the infection?

To better understand the biology of *D. septosporum*, it would be useful to identify key aspects of its metabolism during the infection. General functions such as binding of iron, or starch hydrolysis, could be tested with biochemical and *in vitro* assays.

There are also assays available for virulence-associated functions, such as chitin binding (Stergiopoulos *et al.*, 2010). Hydrophobins can be tested *in vitro* with mutant strains, as it was done for DsHdp1 (Guo, 2015).

Are there other sources to inform selection of proteins for functional assays?

It is evident that functional studies, as initiated here, are urgently required to determine which secreted molecules are actually virulence or avirulence effectors, for a great number of pathosystems. Meanwhile, more information relevant to molecular interactions of microbes with tree hosts could be mined from existing big data sources without experimental effort. For example, in pine pathosystems, meta-level studies of secretomes could indicate which defence traits in pines, or potentially gymnosperms in general, are broadly important. Specifically, all available genomic and *in planta* expression data from all pathogen and pest species of *Pinus* hosts (genus or species, depending on the specificity of each antagonist) could be gathered and analysed for commonalities. A selection pipeline for CEs could be simplified to a) predicting secreted invader molecules, b) separating apoplastic and intracellular patterns using algorithms such as ApoplastP (Sperschneider *et al.*, 2017), and c) finding similar predicted structures rather than sequences. With experimental validation, it is becoming increasingly clear that the stunning sequence diversity of effectors may not accurately reflect their actual, structural diversity (de Guillen *et al.*, 2015).

Another similar source is the information about evolutionary diversification of CEs. Such information on DsCEs was considered for this study as it became available (after the processing of the 18 new genomes data). None of the 55 DsCEs appear to be under

positive selection. However, some examples show that *D. septosporum* proteins filtered out by the DsCE selection pipeline are predicted to be apoplastic despite the lack of a predicted secretion signal peptide and had mutation signatures indicative of positive selection. This small set of proteins should be considered as an additional resource of interesting DsCEs in future studies.

What is the microbial competition situation on pine needles? Could there be synergies?

While *D. septosporum* is clearly a causative agent of DNB, environmental interactions are rarely one-on-one meetings of two organisms. Various *Phytophthora* species may be found on *P. radiata* needles (Scott & Williams, 2014). Some of these species are described as pine pathogens and others are unknown; however, it is unclear what the relationship between all these microbes (including *D. septosporum*) is. In samples collected from an open field infection trial of *P. radiata* seedlings, the presence of *Ph. pluvialis*, *Ph. kernoviae* and *Cyclaneusma* spp. alongside *D. septosporum* was strongly suggested based on transcriptomics (Brar, 2018; pers. comm. R. McDougal). Due to the similarity of the symptoms these pathogens cause, and because such dissection was not the focus of data collection, it was unclear whether the fungi and oomycetes occurred on the same needle in spite of competitors, or if this situation represented succession, or even synergy.

A first step to investigate this important aspect would be minute indexing of all organisms isolated from symptomatic and asymptomatic needles from different environments (such as different local climates). This would be followed by controlled co-cultivation of (foremost) the known pathogens *D. septosporum*, *Phytophthora* spp., and *Cyclaneusma* spp., again under a range of conditions that may favour growth of one organism over others. Ideally this would be carried out using the natural substrate (pine needles), and with different growth rates not all species would be inoculated at the same time. Antagonistic action, as well as factors conducive to the optimal growth of each pathogen could thus be determined. Dothistromin-deficient *D. septosporum* strains (which are available) could be used to remove the broad range toxin dothistromin from the equation.

If growth inhibition of other species through *D. septosporum* is indeed observed, genetic

modification of the putative genes responsible (e.g., DsEcp57-1, DsHdp1) could then provide another step forward to understand these interactions.

Furthermore, the hypothesis that a *Paenibacillus* species is a beneficial symbiont of the fungus arose from the *D. septosporum* genome re-sequencing project. Considerable proportions of *Paenibacillus* spp. reads were found in Guatemalan *D. septosporum* genomes (Bradshaw *et al.*, submitted), same as in new genome assemblies of the plant pathogen *Phytophthora cinnamomi* (Longmuir *et al.*, 2017), and these bacteria have been associated with improved growth of several mycorrhizal fungi (Li *et al.*, 2008). Thus, it could be that these endophyte-like bacteria promote the fitness of *D. septosporum*. Given the likely close association of the two organisms, it might, however, prove difficult to suppress the growth of *Paenibacillus* to investigate this.

Can this research be applied to natural forests?

The study holds the potential for translation to natural forests of *P. radiata* and other gymnosperms. If resistance genes to *D. septosporum* can be identified, the presence of these could be diagnosed in forests, and individuals without the genes may be removed to reduce the chances of fungal inoculum build-up. If it is indeed the case that *D. septosporum* uses necrotrophic effectors and thus exploits susceptibility genes, tree individuals carrying the genes may likewise be removed as a preventative measure.

Understanding better what molecules *D. septosporum* relies on to establish and complete its infection may also lead to the development of highly specific compounds neutralising these molecules (applied like a fungicide).

6.7. Final remarks

Taking a big step back, I would highly recommend the inspiring plant-microbe discussion piece by Plett & Martin (2018) to anyone seeking an understanding of plant well-being in nature—which can only be a holistic understanding.

The complexity of any host-microbe interaction is the product of long co-evolution and hard to picture even with the aid of powerful computational tools. It likely involves hundreds of different signals, processing of which has been fine-tuned on both sides. Thus,

what we are looking at is a delicate balance. A small set of particular protein-protein interactions may just skew the overall outcome in favour of one symbiont, or unveil a mutualist as an opportunistic pathogen (Eaton *et al.*, 2015; Scott *et al.*, 2018) and that is why we investigate effectors and their interaction partners. It is amazing how such fundamental research has contributed to successful breeding programmes, at least for selected crops (Vleeshouwers & Oliver, 2014). Still, this represents but a fraction of the biology of a plant in the environment. The soil microbiome—in reciprocal action with abiotic factors such as the pH of the soil—is hugely important to plants, and most tree species would not survive without mycorrhizal fungi. We are merely starting to comprehend and dissect how the different types of symbionts (mutualistic, commensal, parasitic) affect each other, and, crucially, what potential might be (or has already been) lost when plant hosts are selected for single desirable traits. "What kind of collateral damage might we cause?" Plett & Martin (2018) ask, "How will beneficial or other endophytic microbes be affected? Thus our concept of disease-resistance breeding, and how we approach it, must evolve. Similarly, those working to identify plant proteins that foster mutualism, such that these plants can source nutrients more sustainably through plant-microbe interactions, need to increasingly step outside of their research silos to work with pathologists to ensure that they are not also making new plant varieties that are more susceptible to disease."

This thesis addresses a fungal disease of forests. The important function of forests as ecosystems and natural resources is, in comparison to food crops, often undervalued (Wingfield *et al.*, 2015). Natural and planted forests not only provide wood, food, oxygen, and a carbon sink, but also climate regulation, specialised wood products, biodiversity, and factors improving human health. Forest health is in more grave danger today than ever before (Wingfield *et al.*, 2015). Planted forests, with pine, poplar and eucalypt species that are most often exotic to the plantation region, generally thrive when they are separated from their natural pests and pathogen enemies. However, when these tree species are faced with such enemies, be that of native or imported origin, the forests with little genetic diversity can be severely threatened (Wingfield *et al.*, 2015). Introduction of pathogens, which may also lead to host jumps, has happened countless times across the

globe, and preventive measures such as quarantine were evidently not rigorous enough in various cases (e.g., myrtle rust in Australia, Morin *et al.*, 2012). Also, forests reflect changes in climate rather than weather as they are long-lived (Desprez-Loustau *et al.*, 2016), and indeed warmer climate and extreme events pose a risk to some forests (Allen *et al.*, 2010). Furthermore, climate changes are increasingly shown to be in favour of pathogen life cycles and geographic distributions (Burgess & Wingfield, 2016; Fisher *et al.*, 2012; Bebber *et al.*, 2013; see last paragraph of subsection 1.1.3). It is all the more important to aim for an international strategy to deal with pathogens and pests of planted forests, since epidemics do not stop at country borders. Wingfield *et al.* (2015) urge for a global collaboration governed by a single "clearly identified body" raising funds and monitoring compliance, to share information, identify measures with global impact concerning diseases, promote best practices in biological control, and protect genetic resources of planted hosts.

While this is certainly immensely ambitious, integrated, collaborative thinking (comparable to the aim of mitigating climate change by not just focusing on, for example, forestry) is required to obtain a comprehensive understanding of the interactions of a given species, and even cultivar, with its complete microbiome. As methods are constantly advancing, perhaps in the future genomes and time-course transcriptomes of such an entire system can be analysed to monitor effects of minute disruptions such as absence of single effector gene products.

At least until then, identifying a handful of molecular determinants that can drastically influence the outcome of a specific host-pathogen interaction will remain highly useful for the fundamental as well as the applied aspect. With few similar advances made, my research could contribute to efficiently identify conifer genotypes with increased resistance to *D. septosporum* and other foliar pathogens based on interactions with effectors. This could likely be achieved by exclusion of genotypes with specific susceptibility targets, and promotion of those with PRRs supporting resistance, in forestry breeding programmes. Conclusively, I am hopeful to support the future of forest health with this and future work.

Appendix A.

Statement of contribution to doctoral thesis containing publications.

MASSEY UNIVERSITY
GRADUATE RESEARCH SCHOOL

STATEMENT OF CONTRIBUTION TO DOCTORAL THESIS CONTAINING PUBLICATIONS

(To appear at the end of each thesis chapter/section/appendix submitted as an article/paper or collected as an appendix at the end of the thesis)

We, the candidate and the candidate's Principal Supervisor, certify that all co-authors have consented to their work being included in the thesis and they have accepted the candidate's contribution as indicated below in the *Statement of Originality*.

Name of Candidate: Lukas Hunziker

Name/Title of Principal Supervisor: Prof Rosie Bradshaw

Name of Published Research Output and full reference:

Hunziker, L., Mesarich, C. H., McDougal, R. L., & Bradshaw, R. E. (2016). Effector identification in the pine pathogen Dothistroma septosporum. New Zealand Plant Protection, 69, 94-98.

In which Chapter is the Published Work: 3

Please indicate either:

- The percentage of the Published Work that was contributed by the candidate:

  and / or

- Describe the contribution that the candidate has made to the Published Work:

  The Published Work is an heavily simplified version of a large part of Chapter 3, including the methodology (bioinformatics pipeline). The candidate drafted the manuscript and the supervisors edited it.

Lukas Hunziker — Digitally signed by Lukas Hunziker DN: cn=Lukas Hunziker, c=NZ, email=l.hunziker@massey.ac.nz Date: 2018.09.10 15:40:18 +12'00'

Candidate's Signature — 10/09/2018 — Date

Rosie Bradshaw — Digitally signed by Rosie Bradshaw Date: 2018.09.10 16:31:40 +12'00'

Principal Supervisor's signature — 10/09/2018 — Date

Appendix B.

Primers used in this study

Table B.1.: List of primers used in this study.

Primer name	**Lab #**	**Sequence 5' to 3'**
beta-tub gDNA	1312	GAAATGGCACCTATCACAAG
rt TUB fw II	728	CGGTATGGGTACGCTCT
rt TUB fw I	709	CCGGCGTGTACAATGG
rt TUB rev I	710	CATGCGGTCTGGGAAC
AflR exF	1013	GGAAGAGTAGTGTTACCATTGT
AflR exR	1022	CATCTATTCAACGACCTCACA
rt pksA rev 1	695	CGAACAGAACTACCGACC
rt pksA fw 1	696	CATTATGTCGTCCGAGCAC
Hyd75009F_P	1327	TTGCAACACTCCATCTGTCTCC
Hyd75009R_P	1328	AGCAACTGGAAGGACACAGC
Hdp1-rt-1F	1466	TGACAATACTTCCTAGCATCT
Hyd75009-4R	1460	CCTGGGACAAATCAGCTATG
rt TUB rev II	729	GAAATGGCACCTATCACAAG
Hdp1-rt-1F	1466	TGACAATACTTCCTAGCATCT
Hdp1-rt-2R	1467	TTAGAGGTCGTAGCAGAGAA
AflJ exF	1023	GACCATTGCGGCATTCTG
AflJ exF	1024	GCTGTAGTGTACGGAATCCA
CAD918	935	CAGCAAGAGGATTTGGACCTA

Table B.1 (continued)

Primer name	Lab #	Sequence 5' to 3'
CAD1019	936	TTCAATACCCACATCTGATCAAC
PksA WT fwd	1843	CGCAGTCGAGATGGAGTCTGTT
PksA WT rev	1844	TCTGAGTCGTGCGAGGATCTTG
43416pr1F	1757	GGTCTCCCAAGGCACCGGCCGCGGA
43416pr1R	1758	GGTCTCCAAGCTATGATGGGAGGTTCTGTGGAGT
68580pr1F	1849	GGTCTCGCAAGGACTCTGTTGGAAGCGCC
68580pr1R	1850	GGTCTCAAAGCTATGCGCGGTGGGCGT
68958pr1F	1815	GGTCTCGCAAGGTCCCAAACACCGCGTG
68958pr1R	1816	GGTCTCAAAGCTAAGCAGTACAATTGGTTGGC
69113pr1F	1828	GGTCTCGCAAGGCACCGGCCCAAGGCA
69113pr1R	1817	GGTCTCAAAGCTAAATGTGCGAGTAGGTGCA
69335pr1F	1759	GGTCTCCCAAGGTCCCGTACAACAAGGAGCAG
69335pr1R	1760	GGTCTCCAAGCTACGATGAGCCGGTGTTCCA
70057pr1F	1811	GGTCTCGCAAGTCTCCAGTCCCCCAAACCG
70057pr1R	1812	GGTCTCAAAGCTACTCATACTGATAAGCACTTTCCG
Ds-CP PR1a For	1746	GGTCTCGCAAGACTACTGTCAGCTACGACGA
Ds-CP PR1a Rev	1747	GGTCTCAAAGCTATGCGTTGAATTCGATCG
70694pr1F	1829	GGTCTCGCAAGCTCCCCGCCGGCGTC
70694pr1R	1830	GGTCTCAAAGCTAAGAGCTCTTGGACTTGGTACC
73723pr1F	1835	GGTCTCGCAAGACTCCTCTCGAACCAACTTATC
73723pr1R	1836	GGTCTCAAAGCTAGGTTGTCGTCGCCTTACA
71487pr1F	1859	GGTCTCGCAAGCAGACTGTGCAGTCCAAGC
71487pr1R	1860	GGTCTCAAAGCTAGGCGAACTTCCTCACAAC
72737prFm	1808	GGTCTCGCAAGCTTCCAGGCTACGGCGAAA
72737pr1R	1762	GGTCTCCAAGCTAGTATCCATATCCCTCAGGACCAC
75130pr1F	1861	GGTCTCGCAAGGCCGTGTCCCAGCTTGG
75130pr1R	1862	GGTCTCAAAGCTACAAAACGAAAGCAGCCATGA
73520pr1F	1833	GGTCTCGCAAGGCACCAGCTGCACTCG

Table B.1 (continued)

Primer name	Lab #	Sequence 5' to 3'
73520pr1R	1834	GGTCTCAAAGCTAGGCAAGGTTTGTACCAGCG
72870pr1F	1813	GGTCTCGCAAGAATCCCGCCAAGAGAGCCT
72870pr1R	1814	GGTCTCAAAGCTAAATCATCCTCCTCGGCTTAA
131290pr1F	1763	GGTCTCCCAAGACACCATTTGCCATGCCCG
131290pr1R	1764	GGTCTCCAAGCTAAGCCTTCACACAGACCCAAT
52422pr1F	1857	GGTCTCGCAAGTCGACGTATACTGGCGTGG
52422pr1R	1858	GGTCTCAAAGCTAACAAGAAGCTGGAGTAATGCTG
131885pr1F	1863	GGTCTCGCAAGACTTTGGACCCTGCGACC
131885pr1R	1834	GGTCTCAAAGCTATGTACAGCTAGAACTTCCCG
DsEcp2-1 PR1a For	1799	GGTCTCGCAAGGCAGTCCTCAGCCCGAGGTT
DsEcp2-1 PR1a Rev	1800	GGTCTCAAAGCTACTCGTCGTTCCTCGGGTT
DsEcp6 PR1a For	1869	GGTCTCGCAAGTTCGTTCTCCCACGTACTGATGA CCCGGATTGTGAA
DsEcp6 PR1a Rev	1870	GGTCTCAAAGCTACGCCACAGCAGTAATGTTCAT
Ha-CPL2 PR1a For	1750	GGTCTCGCAAGACTGACGTCCGCTACGACGA
Ha-CPL2 PR1a Rev	1751	GGTCTCAAAGCTACAATCCACACTGGGACG
pICH86988 For	1841	AGGACACGCTCGAGTATAAG
pICH86988 Rev	1842	CATGCGATCATAGGCTTCTC
M13 For	MGS	GCCAGGGTTTTCCCAGTCACGA
M13 Rev	MGS	GCGGATAACAATTTCACACAGG

Appendix C.

On machine learning prediction software

Both the EffectorP and ApoplastP machine learning tools are 'trained' with positive and negative reference datasets, such as experimentally validated fungal effectors or apoplastic proteins (Sperschneider *et al.*, 2017, 2018). In this training analysis, protein attributes and patterns that are unlikely to be identified by human analysis (e.g., net amino acid charge) are determined computationally. This pool of attributes then serves probabilistic predictions based on combinations of the attributes, resulting in classifiers for the original common theme (in these cases, effector prediction or apoplastic localisation). When a new dataset is submitted to the algorithm, a probability score is returned for each queried protein. Theoretically, an entire 'effectorome' or 'apoplastome' can be predicted from a secretome or proteome using EffectorP or ApoplastP, respectively, but the probabilistic nature of these approaches should be kept in mind; false positives/negatives cannot be ruled out. The power of any machine learning method is dictated by the size and quality of the dataset it was trained with. In the recently released EffectorP 2.0, the limited number of available proteins with validated effector functions had increased and the training method was improved (Sperschneider *et al.*, 2018). For ApoplastP, the positive set was considerably larger than for effectors because it included apoplastic plant proteins, and the negative set was larger still, including non-apoplastic proteins from fungi, plants and animals. Thus, providing a high-confidence prediction of fungal proteins with effector classifiers, EffectorP 2.0 could support decision making on which candidate effectors to prioritise in functional screenings. Independently, ApoplastP can be applied to protein sets to predict (non-)apoplast localisation of candidates for the same purpose.

Appendix D.

Supplementary tables to chapters 3–5

The following tables are on the CD (Appendix C Tables.xlsx; one sheet each; Appendix D Tables.xlsx; Appendix E Table.xlsx).
Chapter 3:

- Appendix Table C.1: Extended details of *Dothistroma septosporum* candidate effectors. This table includes the CE type (SSCP etc.), genomic coordinates, machine learning tools results, and protein sequences.
- Appendix Table C.2: Results of local BLASTp of the 55 candidate effectors vs self.
- Appendix Table C.3A: Genome sequencing data summary of 18 *Dothistroma septosporum* strains and total number of SNPs.
- Appendix Table C.3B: Number of single nucleotide polymorphisms of candidate effector genes in 18 *Dothistroma septosporum* strains.
- Appendix Table C.4: *Dothistroma septosporum* predicted apoplastic proteins with $dN/dS > 1$.
- Appendix Table C.5: Sitewise Likelihood Ratio calculation results of previously discussed (Guo, 2015) *Dothistroma septosporum* candidate effectors (courtesy of P.-Y. Dupont).

Chapter 4:

- Appendix Table D.1: BLASTp hits in JGI database to cell death-inducing candidate effector (CE) proteins. The genome sequences of all available Dothideomycetes (top) and Sordariomycetes were queried (E<1E-5). Each sheet contains the hit list of one CE.

Chapter 5:

- Appendix Table E.1: Data from quantitative polymerase chain reaction used for *Dothistroma septosporum* biomass estimation.

Appendix E.

Supplementary figures to chapter 4

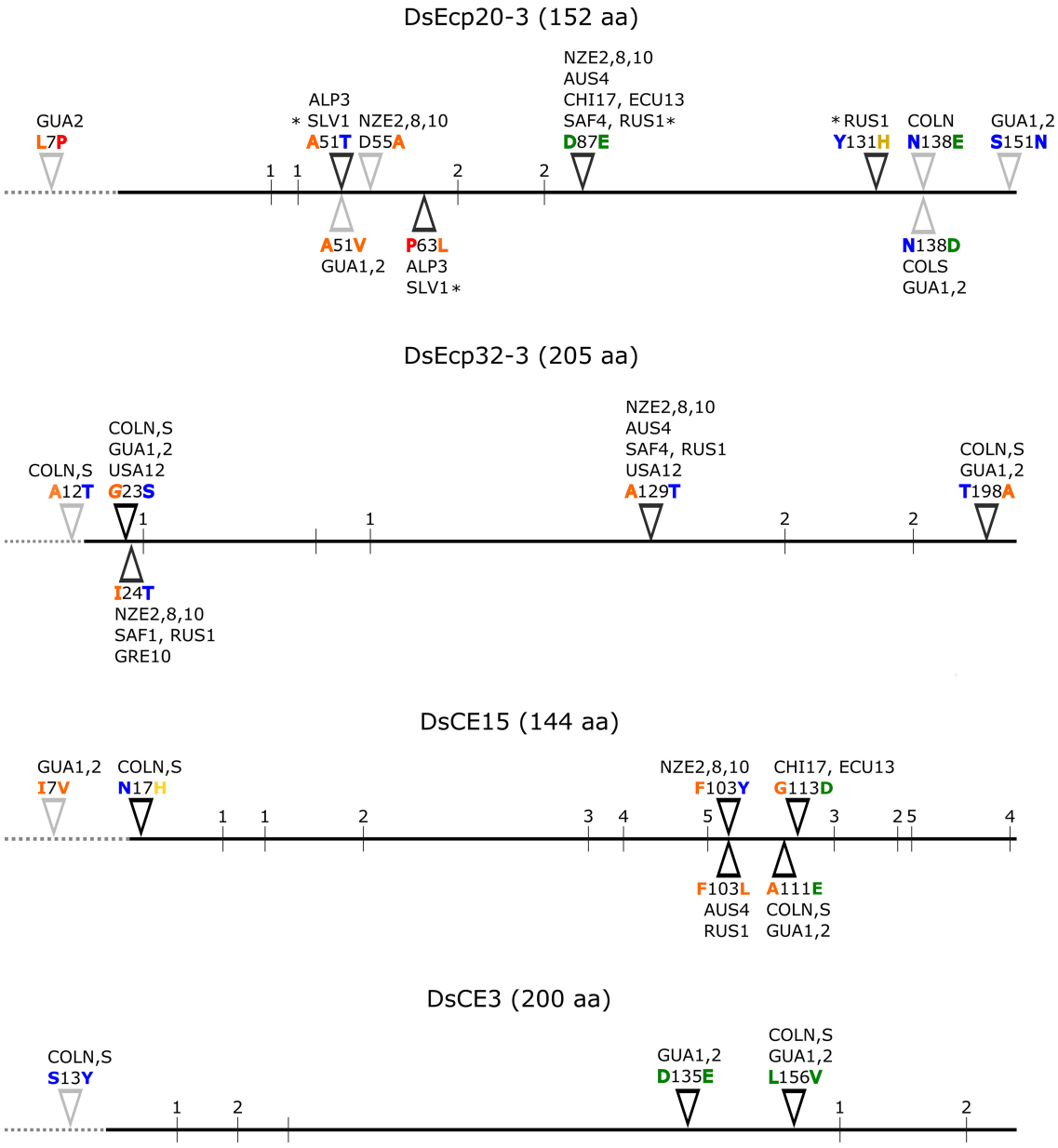

Figure E.1.: Amino acid polymorphisms in cell death-inducing candidate effectors across 19 *Dothistroma septosporum* isolates. Full protein length is shown with amino acid changes from the consensus indicated and the isolates with those polymorphisms listed. The dashed grey line represents the predicted signal peptide. The DsEcp20-3 mutations found in the Slovakian (SLV1) and Russian (SLV1) strains, indicated by asterisks and black markers, were investigated via *Agrobacterium* functional assay. Amino acid colour categories: Orange, hydrophobic; blue, polar/ hydrophilic; green, charged; specific interest as discussed in text: red, proline; yellow, histidine. The vertical lines indicate Cys positions and the numbers show bonding pairs (e.g., Cys 1 forms disulphide bond with other 1) predicted by DiANNA.

```
NZE10 v SLV1    E-value: 1.4E-47   Score: 266.95   Aligned Cols: 152   Identities: 97%   Similarity: 1.408
NZE10 v RUS1    E-value: 1.4E-47   Score: 267.03   Aligned Cols: 152   Identities: 99%   Similarity: 1.414

Q ss_pred       CchHHHHHHHHHHHHHhCCCCCCCCCCCCeEEEEeEEEecCCCcEEEEEEEeCCcccCCCCCCcccceeec
Q DsEcp20-3 1   MLASSLLTVAAATLATALPAGVTPAAAPGQFDITNFIFGCTAGCFWYLDIAVHPAVANHPSVPSSVHCQG  70 (152)
Q Consensus 1   M~f~~~~~~al~~la~aa~~~~~~~~~~~~~w~Vt~f~agC~~gC~Y~FnV~~~~~~~~p~pgf~a~Csg  70 (152)
                |||+++++++|++||+++|+..++.+.++.|+|+|++||+++|+|+|+|+++++++++|+|+|+++|++
T Consensus 1   M~f~~~~~~al~~la~aa~~~~~~~~~~~~~w~Vt~f~agC~~gC~Y~FnV~~~~~~~~p~pgf~a~Csg  70 (152)
T 706_SLV1  1   MLASSLLTVAAATLATALPAGVTPAAAPGQFDITNFIFGCTAGCFWYLDITVHPDVANHPSVLSSVHCQG  70 (152)
T ss_pred       CchHHHHHHHHHHHHHhCCCCCCCCCCCCeEEEEeEEEecCCCcEEEEEEEeCCcccCCCCCCcccceeEeEc

                |||+++++++|++||+++|+..++.+.++.|+|+|++||+++|+|+|+|+++++.+++|+|+|+++|++
T Consensus 1   M~f~~~~~~al~~la~aa~~~~~~~~~~~~~w~Vt~f~agC~~gC~Y~FnV~~~~~~~~p~pgf~a~Csg  70 (152)
T 706_RUS1  1   MLASSLLTVAAATLATALPAGVTPAAAPGQFDITNFIFGCTAGCFWYLDIAVHPDVANHPSVPSSVHCQG  70 (152)
T ss_pred       CchHHHHHHHHHHHHHhCCCCCCCCCCCCeEEEEeEEEeCCCcEEEEEEEeCCcccCCCCCCcccceeec

Q ss_pred       ccCCCCCceecCCCCCCeEEEEEcCCCCEEEEEEEEeCCCCeEEEEEEeeEEeecccCccCCCCCeEE
Q DsEcp20-3 71   NLDDNKSFKECDHVTNESKLYAFIGKDDNLLQLKYEVTNSSTSTVYNYYGEKEVYAATSAYADLQTPNFN  140 (152)
Q Consensus 71  ~~~~~~~y~~C~~~~~~~~V~A~~~~~~~~~Vs~~~~~~~~~~yn~tG~~~v~~~~~~~~~~~~~F~  140 (152)
                ...++++|++|++++..++|.||+.+++++|+|+|+|+.++++.+|||||+++|+++++++++++|+
T Consensus 71  ~~~~~~~y~~C~~~~~~~~V~A~~~~~~~~~Vs~~~~~~~~~~yn~tG~~~v~~~~~~~~~~~~~F~  140 (152)
T 706_SLV1  71   NLDDNKSFKECDHVTNDSKLYAFIGKDDNLLQLKYEVTNSSTSTVYNYYGEKEVYAATSAYADLQTPNFN  140 (152)
T ss_pred       ccCCCCCceecCCCCCCeEEEEEcCCCCEEEEEEEEeCCCCeEEEEEEeeEEeecccCccCCCCCeEE

                ...++++|++|++++.+++|.||+.+++++|+|+|+|+.++++.+|||||+++|+++++++++++|+
T Consensus 71  ~~~~~~~y~~C~~~~~~~~V~A~~~~~~~~~Vs~~~~~~~~~~yn~tG~~~v~~~~~~~~~~~~~F~  140 (152)
T 706_RUS1  71   NLDDNKSFKECDHVTNESKLYAFIGKDDNLLQLKYEVTNSSTSTVYNYYGEKEVYAATSAHADLQTPNFN  140 (152)
T ss_pred       ccCCCCCceecCCCCCCeEEEEEcCCCCEEEEEEEEeCCCCeEEEEEEeeEEeecccCccCCCCCeEE

Q ss_pred       ecccceeeecCC
Q DsEcp20-3 141 VTEISGTKSKSS  152 (152)
Q Consensus 141 i~~~~~~~~~~~  152 (152)
                |||+++++|+||
T Consensus 141 i~~~~~~~~~~~  152 (152)
T 706_SLV1  141 VTEISGTKSKSS  152 (152)
T ss_pred       ecccceeeecCC

                |||+++++|+||
T Consensus 141 i~~~~~~~~~~~  152 (152)
T 706_RUS1  141 VTEISGTKSKSS  152 (152)
T ss_pred       eecceeeeecCC
```

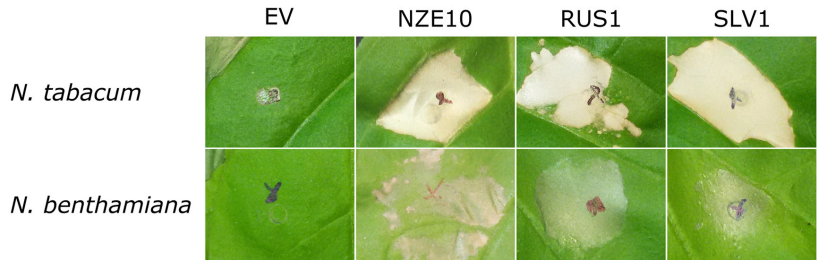

Figure E.2.: *Dothistroma septosporum* candidate effector DsEcp20-3 variants from three different strains have the same predicted secondary structure, and induced cell death responses in non-hosts. Top: The HHpred alignment of the NZE10 and SLV1, and NZE10 and RUS1 protein sequences, respectively, is condensed (NZE10 only shown once). Bottom: EV, empty vector negative control; NZE10, New Zealand, RUS1, Russia, SLV1, Slovakia. Representative images from two independent experiments (total n = 14 leaves) are shown 6 dpi.

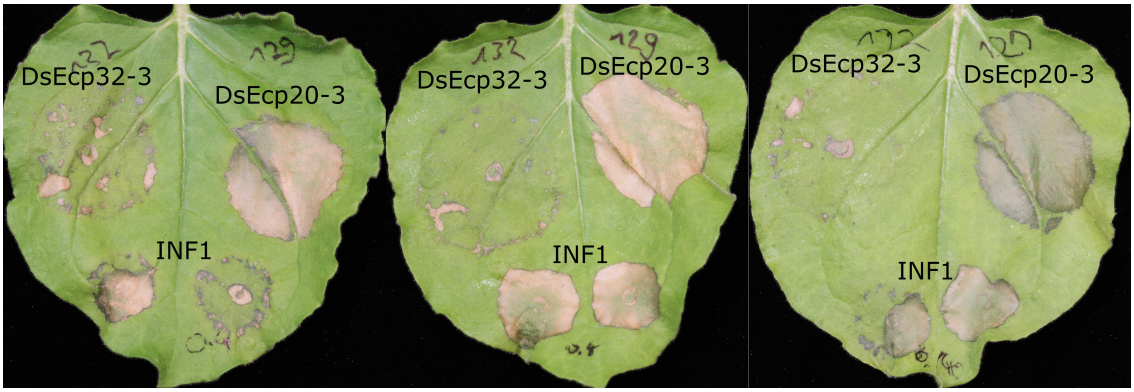

Figure E.3.: Severity of cell death induced by DsEcp32-3 varied in *Nicotiana benthamiana* assays. Leaves were imaged 6 dpi.

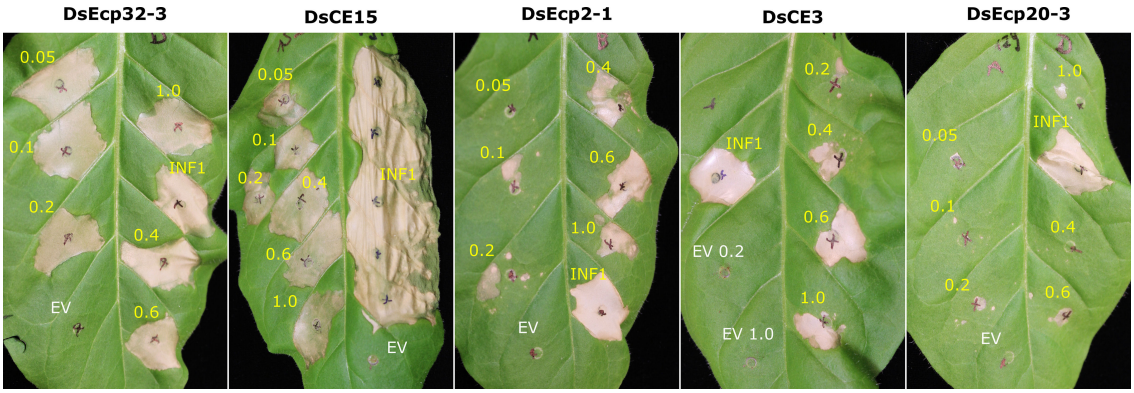

Figure E.4.: Extended optical density range of *Agrobacterium* cultures indicated low concentration thresholds for cell death induction in *Nicotiana tabacum* for some CEs. The yellow numbers indicate the applied OD_{600} of the respective culture. Empty vector negative control (EV) was used at 0.6 except in the DsCE3 panel. The positive control was used at 0.6 except in the DsCE15 panel, where also a range of ODs was tested (from top): 0.05, 0.1, 0.2, 0.6, 1.0. Leaves were imaged 6 dpi; $n \geq 4$ leaves each.

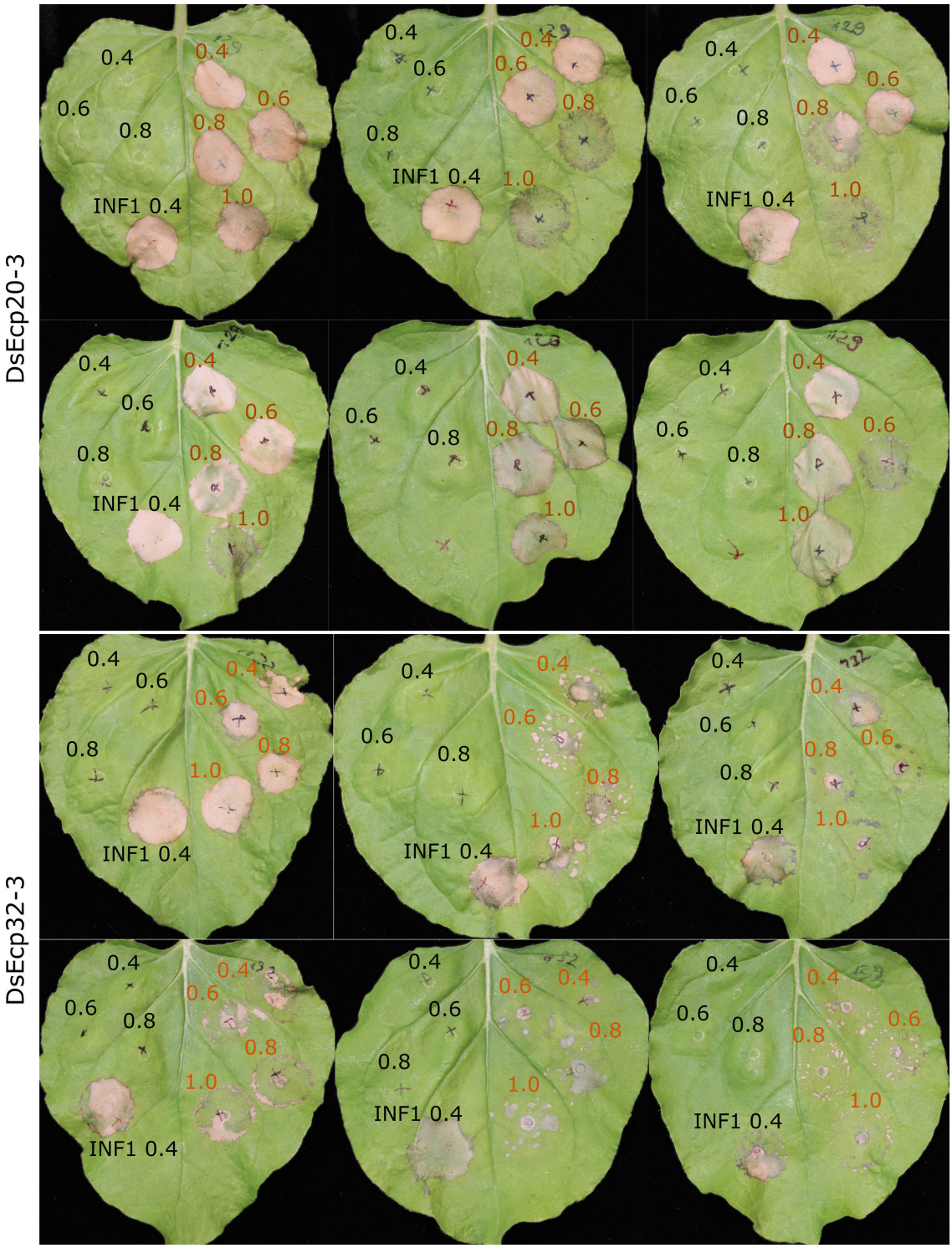

Figure E.5.: Lower optical densities (ODs) of DsEcp20-3 induced cell death more quickly than higher ones in *Nicotiana benthamiana*. The black numbers on the leaves indicate the OD of each empty vector culture, the red numbers the OD of the respective candidate effector DsEcp20-3 or DsEcp32-3. The experiment was replicated with two leaves of three plants each. Leaves were imaged 6 dpi.

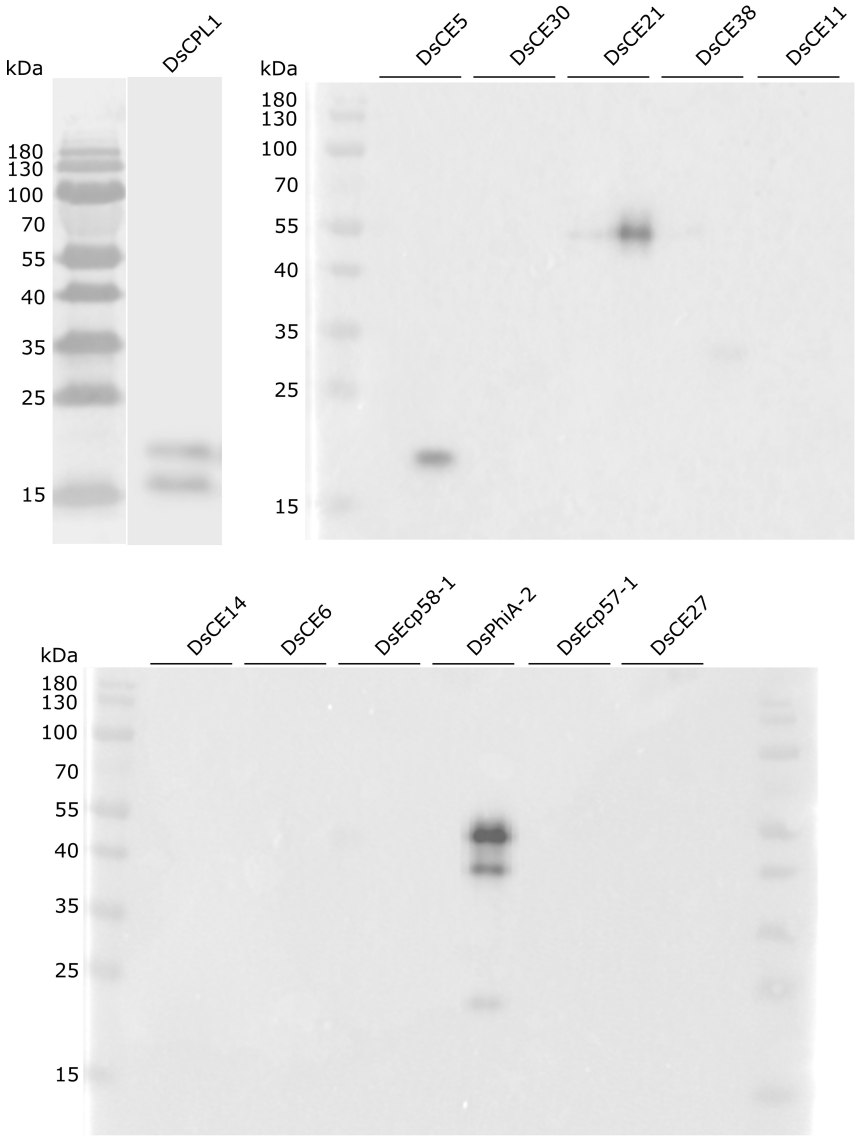

Figure E.6.: Western blot of apoplastic wash fluid (AWF) samples with candidate effectors (CEs) that did not induce cell death in *Nicotiana* spp.. Frozen apoplastic wash fluid samples (collected 1 and 2 dpi for each CE) were used for the protein assays. Immuno-detection was based on primary anti-FLAG antibody. Expected sizes with 3xFLAG tag in kDa: DsCPL1, 16.5; DsCE5, 16.5, DsCE30, 19, DsCE21, 22.5, DsCE38, 22.5, DsCE11, 12; DsCE14, 19.5, DsCE6, 28.5, DsEcp58-1, 22, DsPhiA-2, 22, 31, DsCE27, 15.

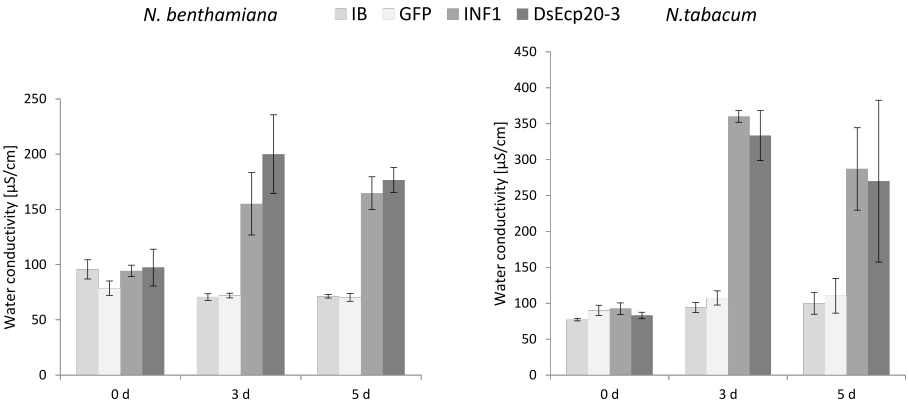

Figure E.7.: Additional ion leakage results for DsEcp20-3. Conductivity in dH_2O was measured from two leaf discs each for each of 3 replicates. Error bars show standard errors (SEM). IB, infiltration buffer negative control, GFP, green fluorescent protein negative control, INF1, positive control.

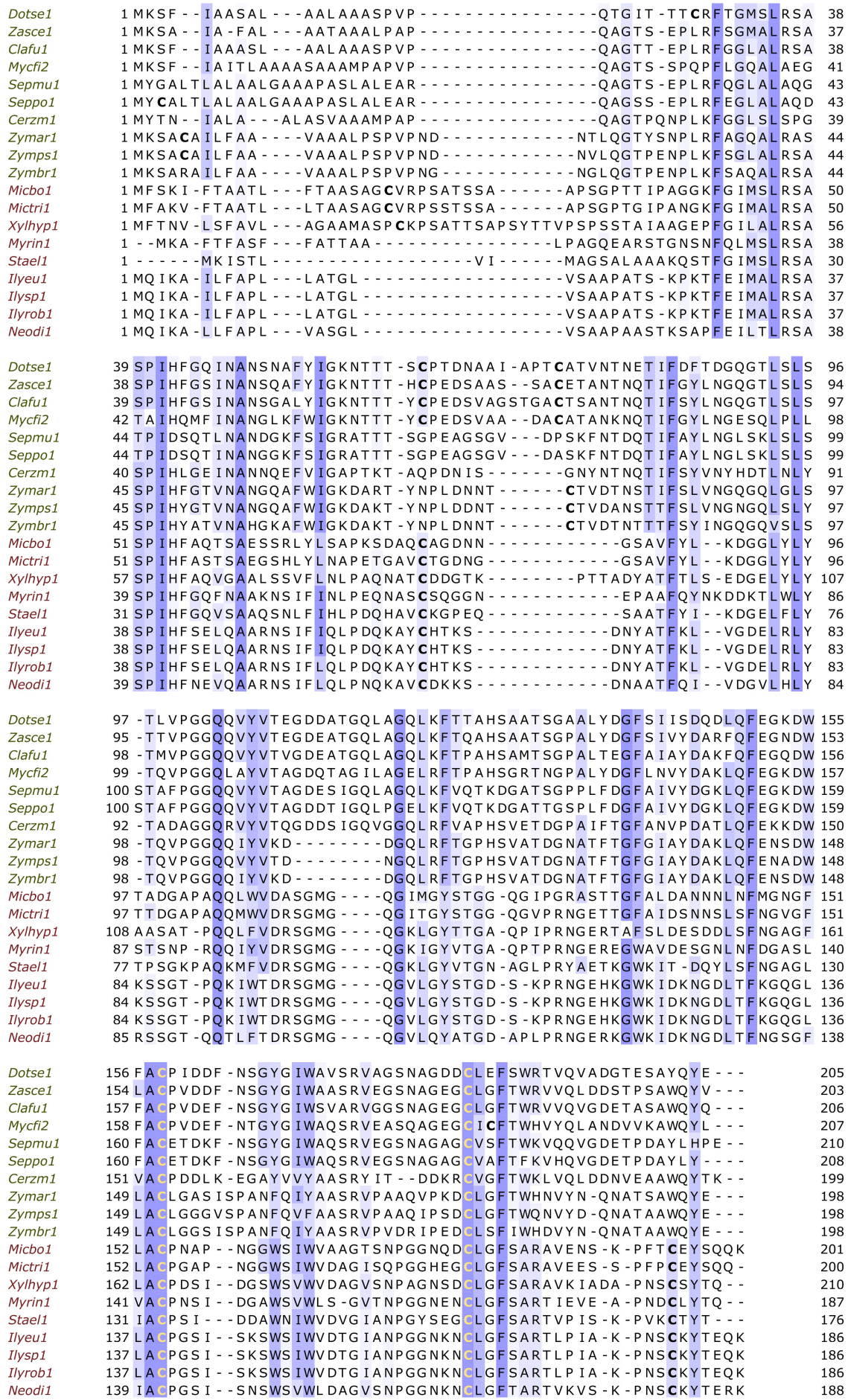

Figure E.8.: Clustal Ω protein alignment of DsEcp32-3 with top nine homologues in dothideomycete and sordariomycete taxa shows broad conservation. Legend on facing page.

Figure E.8 (cont.): Dothideomycete species are coloured green, sordariomycete species in red; blue shading indicates conservation starting at 30%; Cys residues are in bold font, 100% conserved Cys residues are coloured ochre. BLASTp was conducted on the JGI servers in April 2018. Species names and protein IDs are as follows: *Dothistroma septosporum* NZE10 70057 (DsEcp32-3), *Zasmidium cellare* ATCC 36951 30340, *Cladosporium fulvum* 189688 ("CfEcp32-3"), *Pseudocercospora* (*Mycosphaerella*) *fijiensis* v2.0 211999, *Septoria musiva* SO2202 137965, *S. populicola* 74013, *Cercospora zeae-maydis* 86670, *Zymoseptoria ardabiliae* STIR04 1.1.1 773261, *Z. pseudotritici* STIR04 2.2.1 801010, *Z. brevis* Zb18110 5555; *Microdochium bolleyi* J235TASD1 169147, *M. trichocladiopsis* CBS 623.77 332294, *Xylaria hypoxylon* OSC100004 549578, *Myrothecium inundatum* CBS 120646 266514, *Stachybotrys elegans* LAHC-LSPK-M15 415700, *Ilyonectria europaea* CBS 129078 630543, *Ilyonectria* sp. 1686161, *I. robusta* PMI 751 536717, *Neonectria ditissima* R09/05 5471.

Figure E.9.: Alignment of predicted secondary DsEcp20-3 structure to PevD1 (HHpred).

Figure E.10.: Alignments of predicted secondary DsCE3 and RcCDI1 structures (HHpred).

Appendix F.

Details and considerations for new methods

F.1. Apoplastic wash fluid (AWF) extraction method development (subsection 5.2.1)

The details and discussion may contain verbatim repetition of the main text for convenience.

1. Leaf infiltration efficacy with *Agrobacterium* cultures was not at 100%. Some leaves were considerably harder to infiltrate than others. The majority of leaves required eight to ten infiltrations (separate spots) to cover the entire leaf area. While there was no strict cut-off, leaves that clearly required more than 12-14 infiltration attempts were not used for AWF collection. This measure was taken to avoid excessive stress caused by repeated infiltration, and resulted in the use of more backup plants. Differences in the ease of infiltration can probably be attributed to subtle differences in light exposure (less [recently received] light, less stomata opening) and leaf development/age, however, no such information was recorded since the overall infiltration efficacy was satisfactory. No trend supporting a preference for a leaf age (leaves 2, 3, 4 were generally used, and sometimes leaf 5) was observed.

2. The coordination of the AWF collection steps was initially not ideal for upscaled throughput. After detachment from the plants, batches of leaves had to be processed

quickly to avoid possible degradation of protein contained in any non-cooled space. For example, to prevent queueing, the number of leaves detached for each round of vacuum infiltration and subsequent cutting and centrifuging had to be carefully balanced considering the capacity of the following steps. Also, at first leaves in the vacuum chamber were individually attached to the bottom of the metal cage with paper clips, whereas later the metal cage was used as such by turning it upside down, and only this element had to be weighed down as a whole. Cooling the water-filled chamber in the -20° freezer, or directly adding ice prior to the experiment appeared to support the 'refrigeration chain'.

3. For the fluid extraction, method variations adapted from the literature (de Wit & Spikman, 1982; O'Leary *et al.*, 2014) were trialled, using tubes for centrifugation. This resulted in heavily damaged leaves, turbid green collected fluid indicating contamination with intracellular components from damaged cells (chloroplasts), and only partial fluid extraction. In contrast, the flat collection container design using a soft horizontal surface (nappy liner) was efficient for harvesting clear AWF. The leaves remained intact and the recovered fluid was always clear and almost colourless. However, fluid was not extracted from the centre of the surface (Fig. F.1). Improvements to the overall stability of the liner-container assembly proved impractical and time-consuming during manipulation. Specifically, the weak spot of the design is the centre of the tissue area, which would be pushed outwards to touch the bottom of the container during centrifugation. Alterations to the fitting showed that this weak spot was still inevitable as the plastic walls would be bent (under centrifugal force) with a tighter fitting, unless other structural elements were added. Such elements in turn constituted an 'obstacle' for the leaves, thus causing damage. This had to be avoided as it was the point of the design not to introduce any damage to the leaves post cutting and rinsing. Instead, the leaf mass was re-distributed towards the [better supported] borders of the surface, involving changes to how the leaves were cut, and this mitigated the effect. Consequently it was ensured that the box/lid type with the most rigid plastic was selected. These measures together resulted in an improved yield of 90-95% of AWF, making approx. 750 μl per

average-sized leaf compared to less than 500 μl initially. The whole collection device could be easily washed and reused, which was considered a bonus (nappy liners were replaced if they lost their integrity after several experiments).

4. Changing centrifugation variables (force from 500 to 2000$\times g$, time from 5 to 15 min) had little effect on the recovered volume, or integrity of the leaves. A maximum amount of leaf material to be loaded was determined at two to three layers depending on their size, with extraction efficacy dropping considerably if it was exceeded. Deeper containers might have improved this and thus overall throughputs, but were not available. Collected AWF samples were centrifuged at 4,696$\times g$ (maximum available for the large collection tubes) for 10 min to remove residual plant cell debris, and indeed a thin layer (ring at the bottom of tube) of green matter was separated, indicating presence of chloroplasts from damaged cells. This served as a crude filtering step. Aliquots of random samples were then centrifuged again at 16,000$\times g$ for 10 min to separate any further unwanted residues. No pellets were formed, indicating sufficient purity regarding potential contamination with plant cell debris. A systematic assessment of whether leaf centrifugation time or force would affect the purity, or likewise the durability of each nappy liner, was thus considered unnecessary.

F.2. Pine infiltration method development (section 5.2.3)

The details and discussion may contain verbatim repetition of the main text for convenience.

1. There was a risk of contamination. The pine tissue had been growing in a sterile environment. A sudden exposure to environmental microbes might cause overstimulation and false results. Furthermore, it was unknown how long the shoots needed to be maintained post infiltration, and thus a sterile procedure until final assessment was preferable. This was not achieved in all variations of the method, and some results could not be used. While contamination was rarely noticed on the needles, bacterial or fungal contamination of LPch agar and water agar as well

Figure F.1.: Apoplastic wash fluid was not extracted by centrifugation from the centre of the leaf area (transparent areas in circle). The shown leaf represents a cut used early in the method development, which was later changed to vertical.

as wet foam (oasis) occured often. This showed that it was relatively hard to keep shoots sterile during manipulation, which was not in favour of using LPch agar, containing nutrients, for shoot 'incubation'. Importantly, the early observation that even removing shoots from their jar under supposedly sterile conditions could lead to contamination of the jar and yet unused shoots of the genotype, promoted the principle to use the genotypes a jar at a time rather than opening/manipulating all the jars and risking contamination.

The risk concerned manipulation steps and post-treatment maintenance. In one of the two final variations, using water agar in wells, this was ignored for the sake of processing time and to reduce manipulation complications. The contamination rate was low, against expectations.

2. Efficiency of fluid uptake was a trade-off. Maximum exposure of tissue surface had to be provided while minimising the volume of the required liquid to cover the entire (or the desired proportion of) sample, since AWF sample volume was not easily generated. Specifically, if needles were pressed against the tube wall or too close together, fluid uptake was not achieved. Thus, having as much pine sample as possible in a given container was not the best option. This was determined via

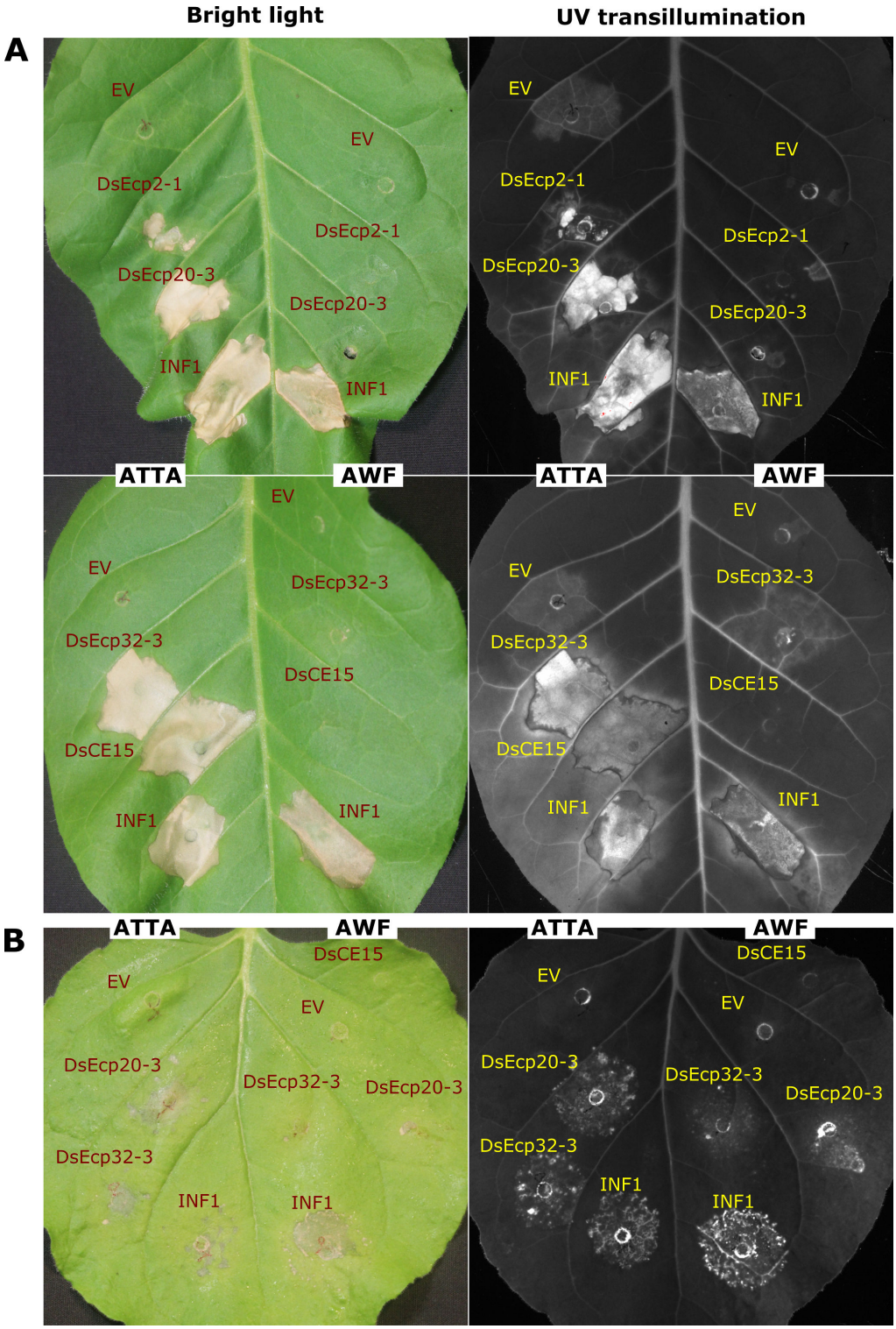

Figure F.2.: Comparison of Agro- and AWF infiltration on same leaf showed varying outcomes. *Agrobacterium* transient transformation assay (ATTA) was carried out as previously with $OD_{600} = 0.6$ on the left side of leaves, and AWF samples were infiltrated on the right side of the same leaf simultaneously. The right hand side panels show UV imaging of each leaf. A) Four CEs inducing consistent cell death in *Nicotiana tabacum*. Images are representative of 9 leaves. B) Two CEs inducing the most consistent cell death in *N. benthamiana*, with DsCE15 for comparison. Image is representative of 20 leaves. Leaves were imaged 6 dpi.

neutral red uptake efficiency and examining random samples.

3. Risk of directly damaging tissue by manipulation. Experience showed that shoots of most genotypes were soft and easily damaged. Also, the tissue collapsed within 15-20 min when removed from medium or water. Due to this finding, the air-dry time after rinsing was reduced to a maximum of five minutes. Handling shoots carefully, particularly when transferring them into and out of tubes for vacuum infiltration, meant considerable time consumption.

4. Survivability of tissue. It had to be experimentally determined how the shoots would fare after the relatively harsh vacuum infiltration treatment, additional manipulation steps transient removal from the nutrient medium. After the infiltration, water and minimal nutrient supply had to be provided. It was shown that the shoots stayed healthy on LPch agar and water agar, but not wet foam. There was a risk of tall shoots (over approx. 4 cm) falling over without support, which is why they were kept in glass jars (supported by the wall or other shoots).

5. Overall time consumption. Each shoot had to be handled separately for vacuum infiltration, so the other aspects of the protocols had to be carried out in a time-saving manner if possible. Collecting needles from shoots was considered unnecessarily laborious due to the fragile nature of the young tissue. Thus, whole shoots were preferable to detached needles.

6. Variation among pine genotypes. It was assumed that all shoots would be affected equally by each procedure and negative control. This was shown to be false: Some genotypes demonstrated drastically lower resilience to treatments than others, and could not be used for conclusions.

Appendix G.

Alternative protein delivery methods for pine

G.1. Hypodermic needles

Prior to the vacuum infiltration method, fluid injection by syringes with 29 gauge hypodermic needles (Terumo) was attempted. Pine needles were injected from the bottom third at an angle, with the needle fully inserted into the tissue. Fluid could not be injected into pine shoot stems.

G.2. Vacuum infiltration of older needles

The proteins CfNLP and DsEcp2-1 were generated using *Pichia pastoris* (as in subsection 2.5.2) using the transformants kindly provided by Y. Guo. Sterile culture filtrates were applied to detached pine needles from two approx. six month old clonal *P. radiata* trees, derived as cuttings from seedlings at Scion, with DNB-susceptible and resistant genotypes, respectively.

Fascicles (groups of three needles) were briefly dipped in 70% ethanol, wiped clean with a tissue and placed upright in 0.2 ml water prior to the experiment to increase stomata apertures. Fifteen ml plastic conical tubes (BD Falcon™, Bedford, MA, USA) were filled with each required infiltration solution and a corkscrew was used to make a small hole in the cap. The fascicles were then completely submerged in the liquid, each tube holding three of susceptible and resistant genotype, with fascicles of different

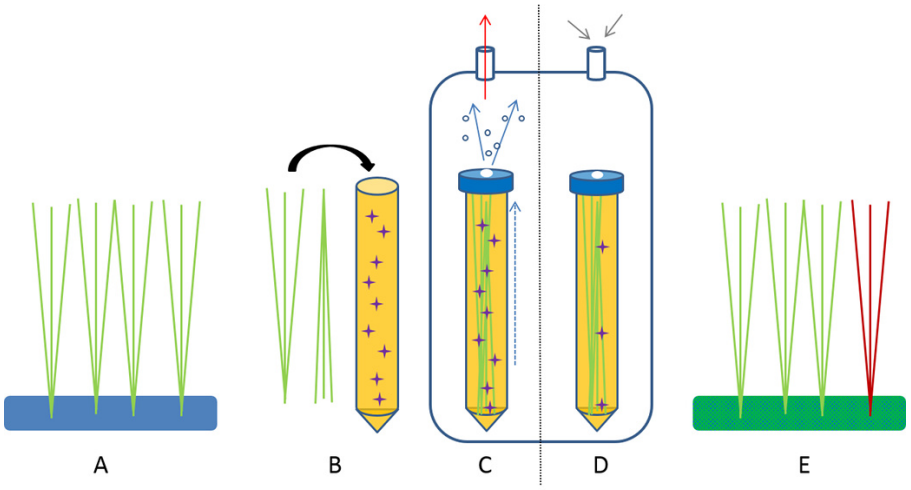

Figure G.1.: Pine needle vacuum infiltration scheme. A) Fascicles (normally three needles) were dipped in water to stimulate stomata aperture before the infiltration. B) Fascicles were then completely submerged in sterile filtrates of *Pichia pastoris* cultures transformed with either an empty vector, CfNLP- or DsEcp2-1-containing vector, or a control solution (water or 0.1% neutral red, NR). Star symbols represent proteins in solution. C) The tubes were closed with a cap with a hole and placed in the vacuum chamber. Vacuum (red arrow) was applied until gas bubbles rose from the needles for 2-3 minutes (circles represent gas). D) The vacuum pump was turned off and the air valve slowly opened to restore atmospheric pressure and allow the needles to take up proteins or neutral red solution via stomata. E) Fascicles were dried and placed in wet foam oasis for 7 d (red representing NR control).

genotypes facing opposite directions. Neutral red (0.1% in water) and the filtrate from a yeast transformant carrying an empty vector were used as negative controls.

The capped and vented tubes were placed in a glass vacuum jar attached to the in-house piped vacuum system (fixed strength). Vacuum was applied for approx. 5 min, so that gas bubbles would rise from the needles for 2-3 min. In later trials, this was changed to three shorter exposure periods to protect the tissue from collapse. After cutting off suction, the valve was slowly opened to bleed the vacuum and thus allow the needles take up the solutions surrounding them. As an additional negative control, needles were submerged in each solution for the same time period, but not exposed to vacuum.

After the vacuum treatment, the fascicles were wiped with a tissue and briefly left to air-dry. For symptom development, they were placed in a wet foam oasis (Zhangjiagang Assa Horticultural Products Co. Ltd, China) in a plastic chamber with a loose cover for up to seven days. They were monitored for necrotic lesions and other responses (e.g., desiccation). Untreated control needles were also included at this point. The process is illustrated in Fig. G.1.

Results and discussion: In a total of 113 vacuum-infiltrated susceptible-type needles (needles of the resistant clones never responded), 11 showed lesion-like symptoms. In 27 needles infiltrated with each, the negative control culture filtrate caused a lesion-like symptom once, CfNLP did five times and DsEcp2-1 also five times. Random chlorosis-like areas were also noted. Throughout the repeated assays, at least 1/4 of the distal part (towards tip) of a varying number of needles collapsed due to the treatment (estimated 40% of needles overall). This effect was reduced at least by half by altering the exposure to applying vacuum three times but for only one minute. Of the needles submerged in any of the liquids but not exposed to vacuum, less than 10% collapsed. Tip death was observed in many cases across all samples. Observations are collated in Fig. G.2.

Neutral red dye was found along needle surfaces in an overall random fashion, even with regard to stomata. In some needles red-purple dots within stomatal pores only were observed, but other areas of the same needle would be completely free of any stain, or completely covered in it. This was also shown in cross- and longitudinal sections in Fig. G.2 D, E. Migration of the dye within the tissue seemed to be limited, as shown by dissection of segments adjacent to stained surface. Needles submerged in neutral red solution without vacuum exhibited red patches, but these were easily removed by washing the needles in ethanol, indicating no uptake.

No injected needles exhibited specific responses. Desiccation/collapse occurred immediately distal of the injection site in general.

In summary, some responses to the necrosis-inducing CfNLP and the effector DsEcp2-1 were observed. These lesion-like responses could have been caused by the secreted proteins, however the consistency of the results was low. Neutral red application demonstrated the vacuum infiltration was working but also highlighted the random nature of uptake events. This made replication difficult and might account for the inconsistency in the results. Lack of necrotic lesions, especially in the last trial with no responses seen, could ultimately be due to insufficient protein concentration, failed delivery, or other reasons. For example, the proteins might not be in the correct location within the needle for interaction with defence proteins.

G.3. Meristematic tissue

The following high-throughput assay was developed and carried out by Cathy Hargreaves at Scion, Rotorua. Originally it was used to test cotyledons of different pine families for their viability and performance after cryopreservation (Hargreaves *et al.*, 2004). Later it was successfully tested for the screening of pine tissue with various fungal extracts alongside forest trials with the same pine genotypes (C. Hargreaves, personal communication). Swapping fungal extracts with putative *D. septosporum* effectors, the assay was then trialled as an alternative effector delivery system to the vacuum infiltration.

Fifty-four pine genotypes (confidential to Scion) were used for this experiment, representing a range of Dothistroma susceptible and resistant genotypes. Up to ten non-germinated cotyledons were dissected from each of the 54 pine embryos. Cotyledons were exposed to benzylaminopurine (BA; a cytokinin) to stimulate formation of meristematic tissue, and uptake of secreted effector protein candidates that had been added to the medium. The latter were added as *P. pastoris* sterilised culture filtrates, at either 1 or 5 ml per 100 ml of half-strength LPch medium (subsection 2.2.4; 1/2 LP5; Quoirin & Lepoivre, 1977; Hargreaves *et al.*, 2004). After 27 d, cotyledons were assessed for responses: colour of tissue, if grown into shoots, or 'no growth' was recorded. They were then transferred to a non-BA "elongation" LP5 medium in deep Petri dishes, leading to shoot formation (Hargreaves *et al.*, 2004). After a total nine weeks of culture, the status and growth of cotyledons was recorded and scored using five categories, 1 being white (dead), 5 being green shoots >5 mm in length (very healthy). An illustration of the workflow is given in Fig. G.3 and the full scoring system is described below and in Fig. G.4.

Results and discussion: A first trial of the assay exposing the pine cotyledons to sterile yeast culture filtrates representing a negative (empty vector, EV) and positive control (CfNLP) in their growth medium was carried out at Scion. Two different doses of each sample were mixed into the medium. The plants generally responded with impaired growth to both EV and CfNLP filtrates compared to the 'absolute' negative control (no filtrates), as shown in Fig. G.4. There was no clear difference between the negative effects of EV and CfNLP. This led to the conclusion that the culture filtrate itself affected the growth of the shoots. This could include components of the yeast induction buffer or

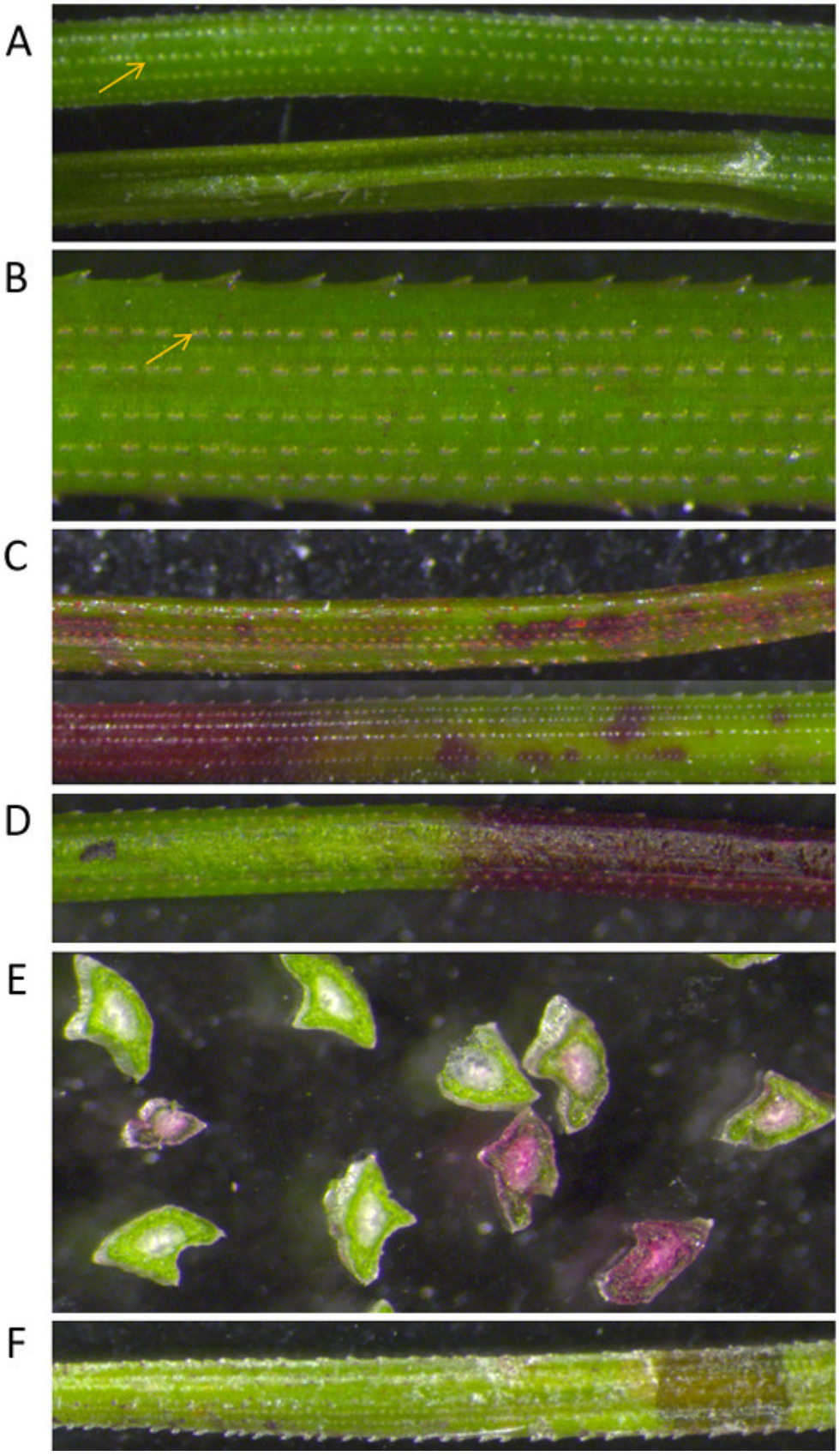

Figure G.2.: Needles after vacuum infiltration with culture filtrates or neutral red. A) Healthy state (top) and collapse (bottom) of needles on the same fascicle. B) In this section of the needle, neutral red (NR) spots were found in nearly every stomatal pore. The arrow indicates an example, compare to stomata appearing white in A. C) These samples illustrate the random uptake of neutral red with discrete spots seen where NR entered through stomata (top only) and blocks of colour where NR was probably taken up through damaged regions of the tissue, or migrated within the needle. D) Longitudinal section of an apparently densely stained needle confirms the saturation of the tissue with dye. E) Cross sections of densely stained and adjacent regions indicate limited migration of neutral red inside the needle. F) A necrosis-like lesion event obtained following infiltration with DsEcp2-1.

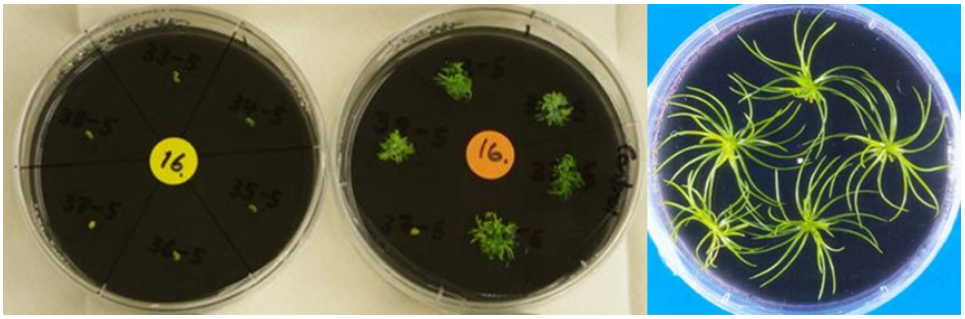

Figure G.3.: Representation of experimental setup of the meristematic tissue assay (courtesy of C. Hargreaves, Scion). Left and centre: Six pine genotypes on LP5 elongation medium after exposure to a fungal extract (left) and control (centre). Cotyledons were placed in the same section of each dish to for easy comparison. Right: Healthy (score 5) cotyledons. These images are *not* affiliated with this study (such were not available) and serve as illustration only.

possibly remainders of cell fractions such as fungal cell wall polysaccharides that could trigger PTI. Because of this, results of the treatments EV and CfNLP were also pooled by dose, 'low' and 'high', to determine if there was a dose-dependent effect of the filtrates. Indeed, cotyledons overall were more heavily impaired by the higher dose, with just 2.1% of them reaching the green stage (response 3, 4, or 5), compared to 54.4% with the lower dose and 95% for the untreated control.

Each of the 54 pine genotypes was also separately analysed to distinguish those with possible higher resilience to the treatment, however, the small sample size did not allow for stringent conclusions.

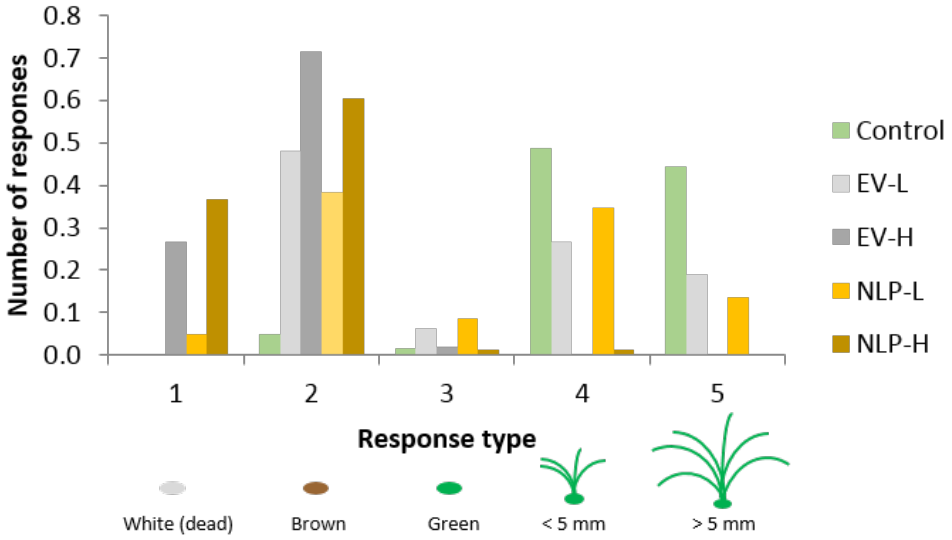

Figure G.4.: Number of cotyledons with one of five response types after being exposed to different treatments. Treatments were control (1/2 LP5 medium), Low dose of EV or CfNLP culture filtrate (1 ml per 100 ml 1/2 LP5), and High dose of EV or CfNLP culture filtrate (5 ml per 100 ml 1/2 LP5). Responses were scored using an arbitrary scale of 1 (dead) to 5 (healthy shoots >5 mm as illustrated below the chart. Response numbers were normalised by the number of cotyledons in each treatment as those were not equal.

Bibliography

Abramoff, M, Magalhaes, P, & Ram, S. 2004. Biophotonics international. *Biophotonics Int*, **11**, 36–42.

Aimanianda, V, Bayry, J, Bozza, S, Kniemeyer, O, Perruccio, K, Elluru, S. R, Clavaud, C, Paris, S, Brakhage, A. A, Kaveri, S. V, *et al.* 2009. Surface hydrophobin prevents immune recognition of airborne fungal spores. *Nature*, **460**(7259), 1117.

Allen, C. D, Macalady, A. K, Chenchouni, H, Bachelet, D, McDowell, N, Vennetier, M, Kitzberger, T, Rigling, A, Breshears, D. D, Hogg, E. T, *et al.* 2010. A global overview of drought and heat-induced tree mortality reveals emerging climate change risks for forests. *Forest Ecology and Management*, **259**(4), 660–684.

Altschul, S. F, Gish, W, Miller, W, Myers, E. W, & Lipman, D. J. 1990. Basic local alignment search tool. *Journal of Molecular Biology*, **215**(3), 403–410.

Altschul, S. F, Wootton, J. C, Gertz, E. M, Agarwala, R, Morgulis, A, Schäffer, A. A, & Yu, Y.-K. 2005. Protein database searches using compositionally adjusted substitution matrices. *The FEBS Journal*, **272**(20), 5101–5109.

Anderson, R. G, Casady, M. S, Fee, R. A, Vaughan, M. M, Deb, D, Fedkenheuer, K, Huffaker, A, Schmelz, E. A, Tyler, B. M, & McDowell, J. M. 2012. Homologous RXLR effectors from *Hyaloperonospora arabidopsidis* and *Phytophthora sojae* suppress immunity in distantly related plants. *The Plant Journal*, **72**(6), 882–893.

Armstrong, M. R, Whisson, S. C, Pritchard, L, Bos, J. I, Venter, E, Avrova, A. O, Rehmany, A. P, Böhme, U, Brooks, K, Cherevach, I, *et al.* 2005. An ancestral oomycete locus contains late blight avirulence gene *Avr3a*, encoding a protein that is recognized

in the host cytoplasm. *Proceedings of the National Academy of Sciences*, **102**(21), 7766–7771.

Asai, S, & Shirasu, K. 2015. Plant cells under siege: plant immune system versus pathogen effectors. *Current Opinion in Plant Biology*, **28**, 1–8.

Asai, S, Rallapalli, G, Piquerez, S. J, Caillaud, M.-C, Furzer, O. J, Ishaque, N, Wirthmueller, L, Fabro, G, Shirasu, K, & Jones, J. D. 2014. Expression profiling during *Arabidopsis*/downy mildew interaction reveals a highly-expressed effector that attenuates responses to salicylic acid. *PLoS Pathogens*, **10**(10), e1004443.

Baccelli, I, Lombardi, L, Luti, S, Bernardi, R, Picciarelli, P, Scala, A, & Pazzagli, L. 2014. Cerato-platanin induces resistance in *Arabidopsis* leaves through stomatal perception, overexpression of salicylic acid-and ethylene-signalling genes and camalexin biosynthesis. *PLoS ONE*, **9**(6), e100959.

Bailey, B. A, Dean, J. F, & Anderson, J. D. 1990. An ethylene biosynthesis-inducing endoxylanase elicits electrolyte leakage and necrosis in *Nicotiana tabacum* cv *Xanthi* leaves. *Plant Physiology*, **94**(4), 1849–1854.

Baker, S. E, Kroken, S, Inderbitzin, P, Asvarak, T, Li, B.-Y, Shi, L, Yoder, O. C, & Turgeon, B. G. 2006. Two polyketide synthase-encoding genes are required for biosynthesis of the polyketide virulence factor, T-toxin, by *Cochliobolus heterostrophus*. *Molecular plant-microbe interactions*, **19**(2), 139–149.

Barnes, I, Crous, P. W, Wingfield, B. D, & Wingfield, M. J. 2004. Multigene phylogenies reveal that red band needle blight of *Pinus* is caused by two distinct species of *Dothistroma*, *D. septosporum* and *D. pini*. *Studies in Mycology*, **50**(2), 551–566.

Barnes, I, Kirisits, T, Akulov, A, Chhetri, D, Wingfield, B. D, Bulgakov, T, & Wingfield, M. J. 2008. New host and country records of the Dothistroma needle blight pathogens from Europe and Asia. *Forest Pathology*, **38**(3), 178–195.

Barnes, I, Wingfield, M. J, Carbone, I, Kirisits, T, & Wingfield, B. D. 2014. Population structure and diversity of an invasive pine needle pathogen reflects anthropogenic activity. *Ecology and Evolution*, **4**(18), 3642–3661.

Battaglia, E, Griffiths, S, Visser, J, & de Wit, Pierre J. G. M. Mesarich, C. H. unpublished. A GH43 endo-arabinanase from the leaf mould fungus, *Cladosporium fulvum*, is an invasion pattern recognized by tomato.

Bebber, D. P, Ramotowski, M. A, & Gurr, S. J. 2013. Crop pests and pathogens move polewards in a warming world. *Nature Climate Change*, **3**(11), 985.

Bendtsen, J. D, Nielsen, H, von Heijne, G, & Brunak, S. 2004. Improved prediction of signal peptides: SignalP 3.0. *Journal of Molecular Biology*, **340**(4), 783–795.

Betts, M. J, & Russell, R. B. 2003. Amino acid properties and consequences of substitutions. *Bioinformatics for Geneticists*, **317**, 289.

Blodgett, J, & Stanosz, G. 1997. Differential inhibition of *Sphaeropsis sapinea* morphotypes by a phenolic compound and several monoterpenes of red pine. *Phytopathology*, **87**(6), 606–609.

Boivin, E. B, Lepage, É, Matton, D. P, de Crescenzo, G, & Jolicoeur, M. 2010. Transient expression of antibodies in suspension plant cell suspension cultures is enhanced when co-transformed with the tomato bushy stunt virus p19 viral suppressor of gene silencing. *Biotechnology Progress*, **26**(6), 1534–1543.

Bolton, M. D, van Esse, H. P, Vossen, J. H, de Jonge, R, Stergiopoulos, I, Stulemeijer, I. J. E, van den Berg, G. C. M, Borrás-Hidalgo, O, Dekker, H. L, de Koster, C. G, de Wit, P. J. G. M, Joosten, M. H. A. J, & Thomma, B. P. H. J. 2008. The novel *Cladosporium fulvum* lysin motif effector Ecp6 is a virulence factor with orthologues in other fungal species. *Molecular Microbiology*, **69**(1), 119–136.

Bos, J. I, Kanneganti, T.-D, Young, C, Cakir, C, Huitema, E, Win, J, Armstrong, M. R, Birch, P. R, & Kamoun, S. 2006. The C-terminal half of *Phytophthora infestans* RXLR effector AVR3a is sufficient to trigger R3a-mediated hypersensitivity and suppress INF1-induced cell death in *Nicotiana benthamiana*. *The Plant Journal*, **48**(2), 165–176.

Bos, J. I, Armstrong, M. R, Gilroy, E. M, Boevink, P. C, Hein, I, Taylor, R. M, Zhendong, T, Engelhardt, S, Vetukuri, R. R, Harrower, B, *et al.* 2010. *Phytophthora infestans*

effector AVR3a is essential for virulence and manipulates plant immunity by stabilizing host E3 ligase CMPG1. *Proceedings of the National Academy of Sciences*, **107**(21), 9909–9914.

Boutrot, F, & Zipfel, C. 2017. Function, discovery, and exploitation of plant pattern recognition receptors for broad-spectrum disease resistance. *Annual Review of Phytopathology*, **55**(1).

Bradshaw, R. E. 2004. Dothistroma (red-band) needle blight of pines and the dothistromin toxin: a review. *Forest Pathology*, **34**, 163–185.

Bradshaw, R. E, Feng, Z, Schwelm, A, Yang, Y, & Zhang, S. 2009. Functional analysis of a putative dothistromin toxin MFS transporter gene. *Toxins*, **1**(2), 173–187.

Bradshaw, R. E, Slot, J. C, Moore, G. G, Chettri, P, Wit, P. J. G. M, Ehrlich, K. C, Ganley, A. R. D, Olson, M. A, Rokas, A, & Carbone, I. 2013. Fragmentation of an aflatoxin-like gene cluster in a forest pathogen. *New Phytologist*, **198**(2), 525–535.

Bradshaw, R. E, Guo, Y, Sim, A. D, Kabir, M. S, Chettri, P, Ozturk, I. K, Hunziker, L, Ganley, R. J, & Cox, M. P. 2016. Genome-wide gene expression dynamics of the fungal pathogen *Dothistroma septosporum* throughout its infection cycle of the gymnosperm host *Pinus radiata*. *Molecular Plant Pathology*, **17**(2), 210–224.

Bradshaw, R. E, Sim, A. D, Chettri, P, Dupont, P.-Y, Guo, Y, Hunziker, L, McDougal, R. L, van der Nest, A, Fourie, A, Wheeler, D, Cox, M. P, & Barnes, I. submitted. Global population genomics of the forest pathogen *Dothistroma septosporum* suggest that chromosome duplications influence virulence factor levels.

Brar, S, Tabima, J, McDougal, R, Dupont, P.-Y, Feau, N, Hamelin, R, Panda, P, Le-Boldus, J, Grünwald, N, Hansen, E, *et al.* 2018. Genetic diversity of *Phytophthora pluvialis*, a pathogen of conifers, in New Zealand and the west coast of the United States of America. *Plant Pathology*, **67**(5), 1131–1139.

Brar, S. 2018. *Genetic diversity and gene expression analysis of Phytophthora pluvialis, a foliar pathogen of conifers*. Ph.D. thesis, Massey University, Palmerston North, New Zealand.

Breen, S, Williams, S. J, Winterberg, B, Kobe, B, & Solomon, P. S. 2016. Wheat PR-1 proteins are targeted by necrotrophic pathogen effector proteins. *The Plant Journal*, **88**(1), 13–25.

Brendolise, C, Montefiori, M, Dinis, R, Peeters, N, Storey, R. D, & Rikkerink, E. H. 2017. A novel hairpin library-based approach to identify NBS–LRR genes required for effector-triggered hypersensitive response in *Nicotiana benthamiana*. *Plant Methods*, **13**(1), 32.

Brown, A, & Webber, J. 2008. *Red band needle blight of conifers in Britain*. Forestry Commission.

Buchan, D. W, Minneci, F, Nugent, T. C, Bryson, K, & Jones, D. T. 2013. Scalable web services for the PSIPRED Protein Analysis Workbench. *Nucleic Acids Research*, **41**(W1), W349–W357.

Bulman, L. S, Dick, M. A, Ganley, R. J, McDougal, R. L, Schwelm, A, & Bradshaw, R. E. 2013. Dothistroma needle blight. *Pages 436–457 of:* Gonthier, P, & Nicolotti, G (eds), *Infectious Forest Diseases*. CAB International.

Bulman, L, Bradshaw, R, Fraser, S, Martín-García, J, Barnes, I, Musolin, D, La Porta, N, Woods, A, Diez, J, Koltay, A, *et al.* 2016. A worldwide perspective on the management and control of Dothistroma needle blight. *Forest Pathology*, **46**(5), 472–488.

Burgess, T. I, & Wingfield, M. J. 2016. Pathogens on the move: a 100-year global experiment with planted eucalypts. *Bioscience*, **67**(1), 14–25.

Burton, Z. F. 2018. Chapter 11—α/β Proteins. *Pages 33 – 43 of:* Burton, Z. F (ed), *Evolution Since Coding*. Academic Press.

Caillaud, M.-C, Asai, S, Rallapalli, G, Piquerez, S, Fabro, G, & Jones, J. D. 2013. A downy mildew effector attenuates salicylic acid–triggered immunity in *Arabidopsis* by interacting with the host mediator complex. *PLoS Biology*, **11**(12), e1001732.

Cantarel, B. L, Coutinho, P. M, Rancurel, C, Bernard, T, Lombard, V, & Henrissat, B.

2008. The Carbohydrate-Active EnZymes database (CAZy): an expert resource for glycogenomics. *Nucleic Acids Research*, **37**(suppl_1), D233–D238.

Cen, K, Li, B, Lu, Y, Zhang, S, & Wang, C. 2017. Divergent LysM effectors contribute to the virulence of *Beauveria bassiana* by evasion of insect immune defenses. *PLoS Pathogens*, **13**(9), e1006604.

Cerda, F, Aquea, F, Gebauer, M, Medina, C, & Arce-Johnson, P. 2002. Stable transformation of *Pinus radiata* embryogenic tissue by *Agrobacterium tumefaciens*. *Plant Cell, Tissue and Organ Culture*, **70**(3), 251–257.

Chang, T.-C, Salvucci, A, Crous, P. W, & Stergiopoulos, I. 2016. Comparative genomics of the Sigatoka disease complex on banana suggests a link between parallel evolutionary changes in *Pseudocercospora fijiensis* and *Pseudocercospora eumusae* and increased virulence on the banana host. *PLoS Genetics*, **12**(8), e1005904.

Charity, J, Holland, L, Grace, L, & Walter, C. 2005. Consistent and stable expression of the *nptI*I, *uid*A and *bar* genes in transgenic *Pinus radiata* after *Agrobacterium tumefaciens*-mediated transformation using nurse cultures. *Plant Cell Reports*, **23**(9), 606–616.

Chen, H, Kovalchuk, A, Keriö, S, & Asiegbu, F. O. 2013a. Distribution and bioinformatic analysis of the cerato-platanin protein family in Dikarya. *Mycologia*, **105**(6), 1479–1488.

Chen, H, Quintana, J, Kovalchuk, A, Ubhayasekera, W, & Asiegbu, F. O. 2015. A cerato-platanin-like protein HaCPL2 from *Heterobasidion annosum sensu stricto* induces cell death in *Nicotiana tabacum* and *Pinus sylvestris*. *Fungal Genetics and Biology*, **84**, 41–51.

Chen, S, Songkumarn, P, Venu, R, Gowda, M, Bellizzi, M, Hu, J, Liu, W, Ebbole, D, Meyers, B, Mitchell, T, *et al.* 2013b. Identification and characterization of *in planta*–expressed secreted effector proteins from *Magnaporthe oryzae* that induce cell death in rice. *Molecular Plant-Microbe Interactions*, **26**(2), 191–202.

Chettri, P, Ehrlich, K. C, Cary, J. W, Collemare, J, Cox, M. P, Griffiths, S. A, Olson,

M. A, de Wit, P. J, & Bradshaw, R. E. 2013. Dothistromin genes at multiple separate loci are regulated by AflR. *Fungal Genetics and Biology*, **51**, 12–20.

Chruszcz, M, Chapman, M. D, Osinski, T, Solberg, R, Demas, M, Porebski, P. J, Majorek, K. A, Pomés, A, & Minor, W. 2012. *Alternaria alternata* allergen Alt a 1: a unique β-barrel protein dimer found exclusively in fungi. *Journal of Allergy and Clinical Immunology*, **130**(1), 241–247.

Chuma, I, Isobe, C, Hotta, Y, Ibaragi, K, Futamata, N, Kusaba, M, Yoshida, K, Terauchi, R, Fujita, Y, Nakayashiki, H, *et al.* 2011. Multiple translocation of the *AVR-Pita* effector gene among chromosomes of the rice blast fungus *Magnaporthe oryzae* and related species. *PLoS Pathogens*, **7**(7), e1002147.

Cingolani, P, Platts, A, Wang, L. L, Coon, M, Nguyen, T, Wang, L, Land, S. J, Lu, X, & Ruden, D. M. 2012. A program for annotating and predicting the effects of single nucleotide polymorphisms, SnpEff: SNPs in the genome of Drosophila melanogaster strain w1118; iso-2; iso-3. *Fly*, **6**(2), 80–92.

Clarke, C. R, Studholme, D. J, Hayes, B, Runde, B, Weisberg, A, Cai, R, Wroblewski, T, Daunay, M.-C, Wicker, E, Castillo, J. A, *et al.* 2015. Genome-enabled phylogeographic investigation of the quarantine pathogen *Ralstonia solanacearum* race 3 biovar 2 and screening for sources of resistance against its core effectors. *Phytopathology*, **105**(5), 597–607.

Clarkson, J. J, Kelly, L. J, Leitch, A. R, Knapp, S, & Chase, M. W. 2010. Nuclear glutamine synthetase evolution in Nicotiana: phylogenetics and the origins of allotetraploid and homoploid (diploid) hybrids. *Molecular Phylogenetics and Evolution*, **55**(1), 99–112.

Cook, D. E, Mesarich, C. H, & Thomma, B. P. 2015. Understanding plant immunity as a surveillance system to detect invasion. *Phytopathology*, **53**(1), 541.

Couto, D, & Zipfel, C. 2016. Regulation of pattern recognition receptor signalling in plants. *Nature Reviews Immunology*, **16**(9), 537.

Cox, M. P, Peterson, D. A, & Biggs, P. J. 2010. SolexaQA: At-a-glance quality assessment of Illumina second-generation sequencing data. *BMC Bioinformatics*, **11**(1), 485.

Cruz, C. D, & Valent, B. 2017. Wheat blast disease: danger on the move. *Tropical Plant Pathology*, **42**(3), 210–222.

Cummings, R. D, & McEver, R. P. 2009. C-type lectins. *In: Essentials of Glycobiology. 2nd edition.* Cold Spring Harbor Laboratory Press.

Dagenais, T. R, Giles, S. S, Aimanianda, V, Latgé, J.-P, Hull, C. M, & Keller, N. P. 2010. *Aspergillus fumigatus* LaeA-mediated phagocytosis is associated with a decreased hydrophobin layer. *Infection and immunity*, **78**(2), 823–829.

Dalio, R, Fleischmann, F, Chambery, A, Eichmann, R, Massola Jr, N, Pascholati, S, & Osswald, W. 2017a. Immunodepletion of α-plurivorin effector leads to loss of virulence of *Phytophthora plurivora* towards *Fagus sylvatica*. *Forest Pathology*, **47**(5), e12362.

Dalio, R. J, Magalhães, D. M, Rodrigues, C. M, Arena, G. D, Oliveira, T. S, Souza-Neto, R. R, Picchi, S. C, Martins, P. M, Santos, P. J, Maximo, H. J, *et al.* 2017b. PAMPs, PRRs, effectors and R-genes associated with citrus–pathogen interactions. *Annals of botany*, **119**(5), 749–774.

Darwiche, R, Mène-Saffrané, L, Gfeller, D, Asojo, O. A, & Schneiter, R. 2017. The pathogen-related yeast protein Pry1, a member of the CAP protein superfamily, is a fatty acid-binding protein. *Journal of Biological Chemistry*, **292**(20), 8304–8314.

Dash, J. P, Watt, M. S, Pearse, G. D, Heaphy, M, & Dungey, H. S. 2017. Assessing very high resolution UAV imagery for monitoring forest health during a simulated disease outbreak. *ISPRS Journal of Photogrammetry and Remote Sensing*, **131**, 1–14.

de Guillen, K, Ortiz-Vallejo, D, Gracy, J, Fournier, E, Kroj, T, & Padilla, A. 2015. Structure analysis uncovers a highly diverse but structurally conserved effector family in phytopathogenic fungi. *PLoS Pathogens*, **11**(10), e1005228.

de Jonge, R, van Esse, P. H, Kombrink, A, Shinya, T, Desaki, Y, Bours, R, van der Krol, S, Shibuya, N, Joosten, M. H. A. J, & Thomma, B. P. H. J. 2010. Conserved fungal

LysM effector Ecp6 prevents chitin-triggered immunity in plants. *Science*, **329**(5994), 953–955.

de Jonge, R, Bolton, M. D, & Thomma, B. P. 2011. How filamentous pathogens co-opt plants: the ins and outs of fungal effectors. *Current Opinion in Plant Biology*, **14**(4), 400–406.

de O. Barsottini, M. R, de Oliveira, J. F, Adamoski, D, Teixeira, P. J, do Prado, P. F, Tiezzi, H. O, Sforça, M. L, Cassago, A, Portugal, R. V, de Oliveira, P. S, *et al.* 2013. Functional diversification of cerato-platanins in *Moniliophthora perniciosa* as seen by differential expression and protein function specialization. *Molecular Plant-Microbe Interactions*, **26**(11), 1281–1293.

de Oliveira, A. L, Gallo, M, Pazzagli, L, Benedetti, C. E, Cappugi, G, Scala, A, Pantera, B, Spisni, A, Pertinhez, T. A, & Cicero, D. O. 2011. The structure of the elicitor cerato-platanin (CP), the first member of the CP fungal protein family, reveals a double $\psi\beta$-barrel fold and carbohydrate binding. *Journal of Biological Chemistry*, **286**(20), 17560–17568.

de Silva, D. D, Crous, P. W, Ades, P. K, Hyde, K. D, & Taylor, P. W. 2017. Life styles of *Colletotrichum* species and implications for plant biosecurity. *Fungal Biology Reviews*, **31**(3), 155–168.

de Wit, P. J. G. M, van der Burgt, A, Okmen, B, Stergiopoulos, I, Abd-Elsalam, K. A, Aerts, A. L, Bahkali, A. H, Beenen, H. G, Chettri, P, Cox, M. P, *et al.* 2012. The genomes of the fungal plant pathogens *Cladosporium fulvum* and *Dothistroma septosporum* reveal adaptation to different hosts and lifestyles but also signatures of common ancestry. *PLoS Genetics*, **8**(11), e1003088.

de Wit, P. J, & Spikman, G. 1982. Evidence for the occurrence of race and cultivar-specific elicitors of necrosis in intercellular fluids of compatible interactions of *Cladosporium fulvum* and tomato. *Physiological Plant Pathology*, **21**(1), 1–11.

de Wit, P. J, Mehrabi, R, van den Burg, H. A, & Stergiopoulos, I. 2009a. Fungal effector proteins: past, present and future. *Molecular Plant Pathology*, **10**(6), 735–747.

de Wit, P. J, Joosten, M. H, Thomma, B. H, & Stergiopoulos, I. 2009b. Gene for gene models and beyond: the *Cladosporium fulvum*-Tomato pathosystem. *Pages 135–156 of: Plant Relationships*. Springer.

Deng, H, Gao, R, Liao, X, & Cai, Y. 2017. CRISPR system in filamentous fungi: Current achievements and future directions. *Gene*, **627**, 212–221.

Denton-Giles, M. 2014. *Characterization of incompatible and compatible Camellia–Ciborinia camelliae plant–pathogen interactions*. Ph.D. thesis, Massey University, Palmerston North, New Zealand.

Dereeper, A, Guignon, V, Blanc, G, Audic, S, Buffet, S, Chevenet, F, Dufayard, J.-F, Guindon, S, Lefort, V, Lescot, M, *et al.* 2008. Phylogeny. fr: robust phylogenetic analysis for the non-specialist. *Nucleic Acids Research*, **36**(suppl_2), W465–W469.

Desprez-Loustau, M.-L, Aguayo, J, Dutech, C, Hayden, K. J, Husson, C, Jakushkin, B, Marçais, B, Piou, D, Robin, C, & Vacher, C. 2016. An evolutionary ecology perspective to address forest pathology challenges of today and tomorrow. *Annals of Forest Science*, **73**(1), 45–67.

Di, X, Cao, L, Hughes, R. K, Tintor, N, Banfield, M. J, & Takken, F. L. 2017. Structure–function analysis of the *Fusarium oxysporum* Avr2 effector allows uncoupling of its immune-suppressing activity from recognition. *New Phytologist*, **216**(3), 897–914.

Dixon, M. S, Golstein, C, Thomas, C. M, van der Biezen, E. A, & Jones, J. D. 2000. Genetic complexity of pathogen perception by plants: the example of Rcr3, a tomato gene required specifically by Cf-2. *Proceedings of the National Academy of Sciences*, **97**(16), 8807–8814.

Dixon, R. A. 2001. Natural products and plant disease resistance. *Nature*, **411**(6839), 843.

Djamei, A, Schipper, K, Rabe, F, Ghosh, A, Vincon, V, Kahnt, J, Osorio, S, Tohge, T, Fernie, A. R, Feussner, I, *et al.* 2011. Metabolic priming by a secreted fungal effector. *Nature*, **478**(7369), 395–398.

do Amaral, A. M, Antoniw, J, Rudd, J. J, & Hammond-Kosack, K. E. 2012. Defining the predicted protein secretome of the fungal wheat leaf pathogen *Mycosphaerella graminicola*. *PLoS ONE*, **7**(12), e49904.

Donoso, A, Rodriguez, V, Carrasco, A, Ahumada, R, Sanfuentes, E, & Valenzuela, S. 2015. Relative expression of seven candidate genes for pathogen resistance on *Pinus radiata* infected with *Fusarium circinatum*. *Physiological and Molecular Plant Pathology*, **92**, 42–50.

Drenkhan, R, Tomešová-Haataja, V, Fraser, S, Bradshaw, R, Vahalik, P, Mullett, M, Martín-García, J, Bulman, L, Wingfield, M, Kirisits, T, *et al.* 2016. Global geographic distribution and host range of *Dothistroma* species: a comprehensive review. *Forest Pathology*.

Du, J, Guo, X, Chen, L, Xie, C, & Liu, J. 2017. Proteomic analysis of differentially expressed proteins of *Nicotiana benthamiana* triggered by INF1 elicitin from *Phytophthora infestans*. *Journal of General Plant Pathology*, **83**(2), 66–77.

Dutheil, J. Y, Mannhaupt, G, Schweizer, G, MK Sieber, C, Münsterkötter, M, Güldener, U, Schirawski, J, & Kahmann, R. 2016. A tale of genome compartmentalization: the evolution of virulence clusters in smut fungi. *Genome biology and evolution*, **8**(3), 681–704.

Dyson, H. J, & Wright, P. E. 2005. Intrinsically unstructured proteins and their functions. *Nature Reviews Molecular Cell Biology*, **6**(3), 197.

Eaton, C. J, Dupont, P.-Y, Solomon, P, Clayton, W, Scott, B, & Cox, M. P. 2015. A core gene set describes the molecular basis of mutualism and antagonism in *Epichloë* spp. *Molecular Plant-Microbe Interactions*, **28**(3), 218–231.

Eisenhaber, B, Schneider, G, Wildpaner, M, & Eisenhaber, F. 2004. A sensitive predictor for potential GPI lipid modification sites in fungal protein sequences and its application to genome-wide studies for *Aspergillus nidulans*, *Candida albicans*, *Neurospora crassa*, *Saccharomyces cerevisiae* and *Schizosaccharomyces pombe*. *Journal of Molecular Biology*, **337**(2), 243–253.

Emanuelsson, O, Nielsen, H, Brunak, S, & Von Heijne, G. 2000. Predicting subcellular localization of proteins based on their N-terminal amino acid sequence. *Journal of Molecular Biology*, **300**(4), 1005–1016.

Emanuelsson, O, Brunak, S, Von Heijne, G, & Nielsen, H. 2007. Locating proteins in the cell using TargetP, SignalP and related tools. *Nature Protocols*, **2**(4), 953.

Engler, C, Kandzia, R, & Marillonnet, S. 2008. A one pot, one step, precision cloning method with high throughput capability. *PLoS ONE*, **3**(11), e3647.

Engler, C, Gruetzner, R, Kandzia, R, & Marillonnet, S. 2009. Golden Gate shuffling: a one-pot DNA shuffling method based on type IIs restriction enzymes. *PLoS ONE*, **4**(5), e5553.

Evans, H. C. 1984. *The genus Mycosphaerella and its anamorphs Cercoseptoria, Dothistroma and Lecanosticta on pines*. 1st edn. Vol. No.153. Surrey: Commonwealth Agricultural Bureaux.

Feng, B.-Z, Zhu, X.-P, Fu, L, Lv, R.-F, Storey, D, Tooley, P, & Zhang, X.-G. 2014a. Characterization of necrosis-inducing NLP proteins in *Phytophthora capsici*. *BMC Plant Biology*, **14**(1), 126.

Feng, J, Zhang, H, Strelkov, S. E, & Hwang, S.-F. 2014b. The LmSNF1 gene is required for pathogenicity in the canola blackleg pathogen *Leptosphaeria maculans*. *PLoS ONE*, **9**(3), e92503.

Fesel, P. H, & Zuccaro, A. 2016. β-glucan: Crucial component of the fungal cell wall and elusive MAMP in plants. *Fungal Genetics and Biology*, **90**, 53–60.

Fisher, M. C, Henk, D. A, Briggs, C. J, Brownstein, J. S, Madoff, L. C, McCraw, S. L, & Gurr, S. J. 2012. Emerging fungal threats to animal, plant and ecosystem health. *Nature*, **484**(7393), 186.

Fisher, M. C, Gow, N. A, & Gurr, S. J. 2016. *Tackling emerging fungal threats to animal health, food security and ecosystem resilience*.

Flor, H. H. 1955. Host-parasite interaction in flax rust–its genetics and other implications. *Phytopathology*, **45**(12), 680–685.

Foster, A. J, Martin-Urdiroz, M, Yan, X, Wright, S, Soanes, D. M, & Talbot, N. J. 2018. CRISPR-Cas9 ribonucleoprotein-mediated co-editing and counterselection in the rice blast fungus. *bioRxiv*, 349134.

Franceschetti, M, Maqbool, A, Jiménez-Dalmaroni, M. J, Pennington, H. G, Kamoun, S, & Banfield, M. J. 2017. Effectors of filamentous plant pathogens: commonalities amid diversity. *Microbiology and Molecular Biology Reviews*, **81**(2), e00066–16.

Franco-Orozco, B, Berepiki, A, Ruiz, O, Gamble, L, Griffe, L. L, Wang, S, Birch, P. R, Kanyuka, K, & Avrova, A. 2017. A new proteinaceous pathogen-associated molecular pattern (PAMP) identified in Ascomycete fungi induces cell death in Solanaceae. *New Phytologist*, **214**(4), 1657–1672.

Franich, R, Gaskin, R, Wells, L, & Zabkiewicz, J. 1982. Effect of *Pinus radiata* needle monoterpenes on spore germination and mycelial growth of *Dothistroma pini in vitro* in relation to mature tree resistance. *Physiological Plant Pathology*, **21**(1), 55–63.

Franich, R. A, Carson, M. J, & Carson, S. D. 1986. Synthesis and accumulation of benzoic acid in *Pinus radiata* needles in response to tissue injury by dothistromin, and correlation with resistance of *P. radiata* families to *Dothistroma pini*. *Physiological and Molecular Plant Pathology*, **28**(2), 267–286.

Fraser, S, Martín-García, J, Perry, A, Kabir, M, Owen, T, Solla, A, Brown, A, Bulman, L, Barnes, I, Hale, M, *et al.* 2015. A review of Pinaceae resistance mechanisms against needle and shoot pathogens with a focus on the *Dothistroma–Pinus* interaction. *Forest Pathology*.

Frías, M, González, C, & Brito, N. 2011. BcSpl1, a cerato-platanin family protein, contributes to *Botrytis cinerea* virulence and elicits the hypersensitive response in the host. *New Phytologist*, **192**(2), 483–495.

Frías, M, Brito, N, González, M, & González, C. 2014. The phytotoxic activity of the

cerato-platanin BcSpl1 resides in a two-peptide motif on the protein surface. *Molecular Plant Pathology*, **15**(4), 342–351.

Friesen, T. L, Faris, J. D, Solomon, P. S, & Oliver, R. P. 2008. Hostspecific toxins: effectors of necrotrophic pathogenicity. *Cell Microbiol*, **10**, 1421–1428.

Frischmann, A, Neudl, S, Gaderer, R, Bonazza, K, Zach, S, Gruber, S, Spadiut, O, Friedbacher, G, Grothe, H, & Seidl-Seiboth, V. 2013. Self-assembly at air/water interfaces and carbohydrate binding properties of the small secreted protein EPL1 from the fungus *Trichoderma atroviride*. *Journal of Biological Chemistry*, **288**(6), 4278–4287.

Fry, W, Birch, P, Judelson, H, Grünwald, N, Danies, G, Everts, K, Gevens, A, Gugino, B, Johnson, D, Johnson, S, *et al.* 2015. Five reasons to consider *Phytophthora infestans* a reemerging pathogen. *Phytopathology*, **105**(7), 966–981.

Fry, W. 2008. *Phytophthora infestans*: the plant (and *R* gene) destroyer. *Molecular Plant Pathology*, **9**(3), 385–402.

Gadgil, P. D. 1967. Infection of *Pinus radiata* needles by *Dothistroma pini*. *New Zealand Journal of Botany*, **5**, 498–503.

Gadgil, P. 1970. Survival of *Dothistroma pini* on fallen needles of *Pinus radiata*. *New Zealand Journal of Botany*, **8**(3), 303–309.

Gamir, J, Darwiche, R, Hof, P, Choudhary, V, Stumpe, M, Schneiter, R, & Mauch, F. 2017. The sterol-binding activity of PATHOGENESIS-RELATED PROTEIN 1 reveals the mode of action of an antimicrobial protein. *The Plant Journal*, **89**(3), 502–509.

Garabagi, F, Gilbert, E, Loos, A, McLean, M. D, & Hall, J. C. 2012. Utility of the P19 suppressor of gene-silencing protein for production of therapeutic antibodies in *Nicotiana* expression hosts. *Plant Biotechnology Journal*, **10**(9), 1118–1128.

Garrison, E, & Marth, G. 2012. Haplotype-based variant detection from short-read sequencing. *arXiv preprint arXiv:1207.3907*.

Gawehns, F, Houterman, P, Ichou, F. A, Michielse, C, Hijdra, M, Cornelissen, B, Rep, M, & Takken, F. 2014. The *Fusarium oxysporum* effector Six6 contributes to virulence

and suppresses I-2-mediated cell death. *Molecular Plant-Microbe Interactions*, **27**(4), 336–348.

Gibson, I. 1972. Dothistroma blight of *Pinus radiata*. *Annual Review of Phytopathology*, **10**(1), 51–72.

Gilroy, E. M, Taylor, R. M, Hein, I, Boevink, P, Sadanandom, A, & Birch, P. R. 2011. CMPG1-dependent cell death follows perception of diverse pathogen elicitors at the host plasma membrane and is suppressed by *Phytophthora infestans* RXLR effector AVR3a. *New Phytologist*, **190**(3), 653–666.

Giraldo, M. C, & Valent, B. 2013. Filamentous plant pathogen effectors in action. *Nature Reviews Microbiology*, **11**(11), 800.

González-Lamothe, R, Tsitsigiannis, D. I, Ludwig, A. A, Panicot, M, Shirasu, K, & Jones, J. D. 2006. The U-box protein CMPG1 is required for efficient activation of defense mechanisms triggered by multiple resistance genes in tobacco and tomato. *The Plant Cell*, **18**(4), 1067–1083.

Grace, L. J, Charity, J. A, Gresham, B, Kay, N, & Walter, C. 2005. Insect-resistant transgenic *Pinus radiata*. *Plant Cell Reports*, **24**(2), 103–111.

Groenewald, M, Barnes, I, Bradshaw, R. E, Brown, A. V, Dale, A, Groenewald, J. Z, Lewis, K. J, Wingfield, B. D, Wingfield, M. J, & Crous, P. W. 2007. Characterization and distribution of mating type genes in the Dothistroma needle blight pathogens. *Phytopathology*, **97**(7), 825–834.

Gui, Y.-J, Chen, J.-Y, Zhang, D.-D, Li, N.-Y, Li, T.-G, Zhang, W.-Q, Wang, X.-Y, Short, D. P, Li, L, Guo, W, *et al.* 2017. *Verticillium dahliae* manipulates plant immunity by glycoside hydrolase 12 proteins in conjunction with carbohydrate-binding module 1. *Environmental Microbiology*, **19**(5), 1914–1932.

Guiguet, A, Dubreuil, G, Harris, M. O, Appel, H. M, Schultz, J. C, Pereira, M. H, & Giron, D. 2016. Shared weapons of blood-and plant-feeding insects: surprising commonalities for manipulating hosts. *Journal of Insect Physiology*, **84**, 4–21.

Guindon, S, Dufayard, J.-F, Lefort, V, Anisimova, M, Hordijk, W, & Gascuel, O. 2010. New algorithms and methods to estimate maximum-likelihood phylogenies: assessing the performance of PhyML 3.0. *Systematic Biology*, **59**(3), 307–321.

Guo, Y. 2015. *Identification and characterisation of Dothistroma septosporum effectors.* Ph.D. thesis, Massey University, Palmerston North, New Zealand.

Haas, H, Eisendle, M, & Turgeon, B. G. 2008. Siderophores in fungal physiology and virulence. *Annual Review of Phytopathology*, **46**, 149–187.

Haddadi, P, Ma, L, Wang, H, & Borhan, M. H. 2016. Genome-wide transcriptomic analyses provide insights into the lifestyle transition and effector repertoire of *Leptosphaeria maculans* during the colonization of *Brassica napus* seedlings. *Molecular Plant Pathology*, **17**(8), 1196–1210.

Hall, T, Biosciences, I, & Carlsbad, C. 2011. BioEdit: an important software for molecular biology. *GERF Bulletin of Biosciences*, **2**(1), 60–61.

Han, L, Liu, Z, Liu, X, & Qiu, D. 2012. Purification, crystallization and preliminary X-ray diffraction analysis of the effector protein PevD1 from *Verticillium dahliae*. *Acta Crystallographica Section F: Structural Biology and Crystallization Communications*, **68**(7), 802–805.

Hargreaves, C, Grace, L, van der Maas, S, Reeves, C, Holden, G, Menzies, M, Kumar, S, & Foggo, M. 2004. Cryopreservation of *Pinus radiata* zygotic embryo cotyledons: effect of storage duration on adventitious shoot formation and plant growth after 2 years in the field. *Canadian Journal of Forest Research*, **34**(3), 600–608.

Heath, M. C. 2000a. Hypersensitive response-related death. *Pages 77–90 of: Programmed cell death in higher plants.* Springer.

Heath, M. C. 2000b. Nonhost resistance and nonspecific plant defenses. *Current Opinion in Plant Biology*, **3**(4), 315–319.

Hellens, R, Mullineaux, P, & Klee, H. 2000. Technical focus: a guide to *Agrobacterium* binary Ti vectors. *Trends in Plant Science*, **5**(10), 446–451.

Hemetsberger, C, Herrberger, C, Zechmann, B, Hillmer, M, & Doehlemann, G. 2012. The *Ustilago maydis* effector Pep1 suppresses plant immunity by inhibition of host peroxidase activity. *PLoS Pathogens*, **8**(5), e1002684.

Hirst, P, Richardson, T, Carson, S, Bradshaw, R, *et al.* 1999. *Dothistroma pini* genetic diversity is low in New Zealand. *New Zealand Journal of Forestry Science*, **29**(3), 459–472.

Hotter, G. S. 1997. Elicitor-induced oxidative burst and phenylpropanoid metabolism in *Pinus radiata* cell suspension cultures. *Functional Plant Biology*, **24**(6), 797–804.

Huang, Y, Busk, P. K, & Lange, L. 2015. Cellulose and hemicellulose-degrading enzymes in *Fusarium commune* transcriptome and functional characterization of three identified xylanases. *Enzyme and Microbial Technology*, **73**, 9–19.

Hunziker, L, Mesarich, C. H, McDougal, R. L, & Bradshaw, R. E. 2016. Effector identification in the pine pathogen *Dothistroma septosporum*. *New Zealand Plant Protection*, **69**, 94–98.

Hurlburt, N. K, Chen, L.-H, Stergiopoulos, I, & Fisher, A. J. 2018. Structure of the *Cladosporium fulvum* Avr4 effector in complex with (GlcNAc) 6 reveals the ligand-binding mechanism and uncouples its intrinsic function from recognition by the Cf-4 resistance protein. *PLoS Pathogens*, **14**(8), e1007263.

Iida, Y, van't Hof, P, Beenen, H, Mesarich, C, Kubota, M, Stergiopoulos, I, Mehrabi, R, Notsu, A, Fujiwara, K, Bahkali, A, Abd-Elsalam, K, Collemare, J, & de Wit, P. J. G. M. 2015. Novel nutations detected in avirulence genes overcoming tomato *Cf* resistance genes in isolates of a japanese population of *Cladosporium fulvum*. *PLoS ONE*, **10**(4), e0123271.

Illergård, K, Ardell, D. H, & Elofsson, A. 2009. Structure is three to ten times more conserved than sequence—a study of structural response in protein cores. *Proteins: Structure, Function, and Bioinformatics*, **77**(3), 499–508.

Inoue, K, Kitaoka, H, Park, P, & Ikeda, K. 2016. Novel aspects of hydrophobins in wheat

isolate of *Magnaporthe oryzae*: Mpg1, but not Mhp1, is essential for adhesion and pathogenicity. *Journal of General Plant Pathology*, **82**(1), 18–28.

Isaza, R. E. A, Diaz-Trujillo, C, Dhillon, B, Aerts, A, Carlier, J, Crane, C. F, de Jong, T. V, de Vries, I, Dietrich, R, Farmer, A. D, *et al.* 2016. Combating a global threat to a clonal crop: banana black Sigatoka pathogen *Pseudocercospora fijiensis* (synonym *Mycosphaerella fijiensis*) genomes reveal clues for disease control. *PLoS Genetics*, **12**(8), e1005876.

Isik, F. 2014. Genomic selection in forest tree breeding: the concept and an outlook to the future. *New Forests*, **45**(3), 379–401.

Ivkovic, M, Baltunis, B, Gapare, W, Sasse, J, Dutkowski, G, Elms, S, & Wu, H. 2010. Breeding against Dothistroma needle blight of radiata pine in Australia. *Canadian Journal of Forest Research-Revue Canadienne De Recherche Forestiere*, **40**(8), 1653–1660.

Ivory, M. H. 1967. A new variety of *Dothistroma pini* in Kenya. *Transactions of the British Mycological Society*, **50**, 289–297.

Jayaraman, J, Choi, S, Prokchorchik, M, Choi, D. S, Spiandore, A, Rikkerink, E. H, Templeton, M. D, Segonzac, C, & Sohn, K. H. 2017. A bacterial acetyltransferase triggers immunity in *Arabidopsis thaliana* independent of hypersensitive response. *Scientific Reports*, **7**.

Jeong, J. S, Mitchell, T. K, & Dean, R. A. 2007. The *Magnaporthe grisea* snodprot1 homolog, MSP1, is required for virulence. *FEMS Microbiology Letters*, **273**(2), 157–165.

Johansen, L. K, & Carrington, J. C. 2001. Silencing on the spot. Induction and suppression of RNA silencing in the *Agrobacterium*-mediated transient expression system. *Plant Physiology*, **126**(3), 930–938.

Jones, D. T. 1999. Protein secondary structure prediction based on position-specific scoring matrices. *Journal of Molecular Biology*, **292**(2), 195–202.

Jones, J. D. G, & Dangl, J. L. 2006. The plant immune system. *Nature*, **444**(7117), 323–329.

Joosten, M. H, Cozijnsen, T. J, & de Wit, P. J. 1994. Host resistance to a fungal tomato pathogen lost by a single base-pair change in an avirulence gene. *Nature*, **367**(6461), 384.

Joosten, M, Vogelsang, R, Cozijnsen, T. J, Verberne, M. C, & de Wit, P. 1997. The biotrophic fungus *Cladosporium fulvum* circumvents *Cf-4*-mediated resistance by producing unstable AVR4 elicitors. *The Plant Cell*, **9**(3), 367–379.

Kabir, M. S, Ganley, R. J, & Bradshaw, R. E. 2015. Dothistromin toxin is a virulence factor in Dothistroma needle blight of pines. *Plant Pathology*, **64**(1), 225–234.

Kabir, M. S, Ganley, R. J, & Bradshaw, R. E. 2015. The hemibiotrophic lifestyle of the fungal pine pathogen *Dothistroma septosporum*. *Forest Pathology*, **45**(3), 190–202.

Kabir, M. S. 2014. *Investigation of Dothistroma needle blight development on Pinus radiata*. Ph.D. thesis, Massey University, Palmerston North, New Zealand.

Kabir, M, Ganley, R, & Bradshaw, R. 2013. An improved artificial pathogenicity assay for Dothistroma needle blight on *Pinus radiata*. *Australasian Plant Pathology*, **42**(4), 503–510.

Kamel, L, Tang, N, Malbreil, M, San Clemente, H, Le Marquer, M, Roux, C, & dit Frey, N. F. 2017. The comparison of expressed candidate secreted proteins from two arbuscular mycorrhizal fungi unravels common and specific molecular tools to invade different host plants. *Frontiers in Plant Science*, **8**.

Kamoun, S. 2006. A catalogue of the effector secretome of plant pathogenic oomycetes. *Annual Review of Phytopathology*, **44**.

Kamoun, S. 2007. Groovy times: filamentous pathogen effectors revealed. *Current Opinion in Plant Biology*, **10**(4), 358–365.

Kamoun, S, van West, P, Vleeshouwers, V. G, de Groot, K. E, & Govers, F. 1998.

Resistance of *Nicotiana benthamiana* to *Phytophthora infestans* is mediated by the recognition of the elicitor protein INF1. *The Plant Cell*, **10**(9), 1413–1425.

Katoh, K, Kuma, K.-i, Toh, H, & Miyata, T. 2005. MAFFT version 5: improvement in accuracy of multiple sequence alignment. *Nucleic Acids Research*, **33**(2), 511–518.

Kearse, M, Moir, R, Wilson, A, Stones-Havas, S, Cheung, M, Sturrock, S, Buxton, S, Cooper, A, Markowitz, S, Duran, C, *et al.* 2012. Geneious Basic: an integrated and extendable desktop software platform for the organization and analysis of sequence data. *Bioinformatics*, **28**(12), 1647–1649.

Kelly, L. J, Leitch, A. R, Clarkson, J. J, Knapp, S, & Chase, M. W. 2013. Reconstructing the complex evolutionary origin of wild allopolyploid tobaccos (*Nicotiana* section *Suaveolentes*). *Evolution: International Journal of Organic Evolution*, **67**(1), 80–94.

Kema, G. H, Yu, D, Rijkenberg, F. H, Shaw, M. W, & Baayen, R. P. 1996. Histology of the pathogenesis of *Mycosphaerella graminicola* in wheat. *Phytopathology*, **86**(7), 777–786.

Kennedy, S. G, Yanchuk, A. D, Stackpole, D. J, & Jefferson, P. A. 2014. Incorporating non-key traits in selecting the *Pinus radiata* production population. *New Zealand Journal of Forestry Science*, **44**(1), 12.

Keon, J, Antoniw, J, Carzaniga, R, Deller, S, Ward, J. L, Baker, J. M, Beale, M. H, Hammond-Kosack, K, & Rudd, J. J. 2007. Transcriptional adaptation of *Mycosphaerella graminicola* to programmed cell death (PCD) of its susceptible wheat host. *Molecular Plant-Microbe Interactions*, **20**(2), 178–193.

Kershaw, M. J, Wakley, G, & Talbot, N. J. 1998. Complementation of the Mpg1 mutant phenotype in *Magnaporthe grisea* reveals functional relationships between fungal hydrophobins. *The EMBO Journal*, **17**(14), 3838–3849.

Kershaw, M. J, Thornton, C. R, Wakley, G. E, & Talbot, N. J. 2005. Four conserved intramolecular disulphide linkages are required for secretion and cell wall localization of a hydrophobin during fungal morphogenesis. *Molecular microbiology*, **56**(1), 117–125.

Kettles, G. J, Bayon, C, Canning, G, Rudd, J. J, & Kanyuka, K. 2017. Apoplastic recognition of multiple candidate effectors from the wheat pathogen *Zymoseptoria tritici* in the nonhost plant *Nicotiana benthamiana*. *New Phytologist*, **213**(1), 338–350.

Kim, S, Ahn, I.-P, Rho, H.-S, & Lee, Y.-H. 2005. MHP1, a *Magnaporthe grisea* hydrophobin gene, is required for fungal development and plant colonization. *Molecular Microbiology*, **57**(5), 1224–1237.

King, S. R, McLellan, H, Boevink, P. C, Armstrong, M. R, Bukharova, T, Sukarta, O, Win, J, Kamoun, S, Birch, P. R, & Banfield, M. J. 2014. *Phytophthora infestans* RXLR effector PexRD2 interacts with host MAPKKKε to suppress plant immune signaling. *The Plant Cell*.

Kinloch Jr, B. B, & Dupper, G. E. 2002. Genetic specificity in the white pine-blister rust pathosystem. *Phytopathology*, **92**(3), 278–280.

Kinloch Jr, B. B, Sniezko, R. A, & Dupper, G. E. 2004. Virulence gene distribution and dynamics of the white pine blister rust pathogen in western North America. *Phytopathology*, **94**(7), 751–758.

Kloppholz, S, Kuhn, H, & Requena, N. 2011. A secreted fungal effector of *Glomus intraradices* promotes symbiotic biotrophy. *Current Biology*, **21**(14), 1204–1209.

Kombrink, A, & Thomma, B. P. 2013. LysM effectors: secreted proteins supporting fungal life. *PLoS Pathogens*, **9**(12), e1003769.

Koncz, C, & Schell, J. 1986. The promoter of T L-DNA gene 5 controls the tissue-specific expression of chimaeric genes carried by a novel type of *Agrobacterium* binary vector. *Molecular and General Genetics MGG*, **204**(3), 383–396.

Krogh, A, Larsson, B, Von Heijne, G, & Sonnhammer, E. L. 2001. Predicting transmembrane protein topology with a hidden Markov model: application to complete genomes. *Journal of Molecular Biology*, **305**(3), 567–580.

Krzywinski, M, Schein, J, Birol, I, Connors, J, Gascoyne, R, Horsman, D, Jones, S. J,

& Marra, M. A. 2009. Circos: an information aesthetic for comparative genomics. *Genome research*, **19**(9), 1639–1645.

Lacroix, H, Whiteford, J. R, & Spanu, P. D. 2008. Localization of *Cladosporium fulvum* hydrophobins reveals a role for HCf-6 in adhesion. *FEMS Microbiology Letters*, **286**(1), 136–144.

Laemmli, U. K. 1970. Cleavage of structural proteins during the assembly of the head of bacteriophage T4. *Nature*, **227**(5259), 680–685.

Langmead, B, & Salzberg, S. L. 2012. Fast gapped-read alignment with Bowtie 2. *Nature Methods*, **9**(4), 357–359.

Lannoo, N, & Van Damme, E. J. 2014. Lectin domains at the frontiers of plant defense. *Frontiers in Plant Science*, **5**, 397.

Laugé, R, Joosten, M. H, van den Ackerveken, G. F, van den Broek, H. W, & de Wit, P. J. 1997. The *in planta*-produced extracellular proteins ECP1 and ECP2 of *Cladosporium fulvum* are virulence factors. *Molecular plant-microbe interactions*, **10**(6), 725–734.

Li, B, Ravnskov, S, Xie, G, & Larsen, J. 2008. Differential effects of *Paenibacillus* spp. on cucumber mycorrhizas. *Mycological progress*, **7**(4), 277–284.

Li, Y, Suontama, M, Burdon, R. D, & Dungey, H. S. 2017. Genotype by environment interactions in forest tree breeding: review of methodology and perspectives on research and application. *Tree Genetics & Genomes*, **13**(3), 60.

Li, Y, Dungey, H. S, Carson, M, & Carson, S. 2018. Genotype by environment interaction for growth and *Dothistroma* resistance and clonal connectivity between environments in radiata pine in New Zealand and Australia. *PloS one*, **13**(10), e0205402.

Liebhold, A. M, Brockerhoff, E. G, Kalisz, S, Nuñez, M. A, Wardle, D. A, & Wingfield, M. J. 2017. Biological invasions in forest ecosystems. *Biological Invasions*, **19**(11), 3437–3458.

Liebrand, T. W, van den Burg, H. A, & Joosten, M. H. 2014. Two for all: receptor-associated kinases SOBIR1 and BAK1. *Trends in Plant Science*, **19**(2), 123–132.

Liu, J.-J, Sturrock, R. N, Sniezko, R. A, Williams, H, Benton, R, & Zamany, A. 2015. Transcriptome analysis of the white pine blister rust pathogen *Cronartium ribicola*: *de novo* assembly, expression profiling, and identification of candidate effectors. *BMC Genomics*, **16**(1), 678.

Liu, M, Duan, L, Wang, M, Zeng, H, Liu, X, & Qiu, D. 2016. Crystal structure analysis and the identification of distinctive functional regions of the protein elicitor Mohrip2. *Frontiers in Plant Science*, **7**, 1103.

Liu, T, Song, T, Zhang, X, Yuan, H, Su, L, Li, W, Xu, J, Liu, S, Chen, L, Chen, T, *et al.* 2014. Unconventionally secreted effectors of two filamentous pathogens target plant salicylate biosynthesis. *Nature Communications*, **5**, 4686.

Liu, Z, Faris, J. D, Oliver, R. P, Tan, K.-C, Solomon, P. S, McDonald, M. C, McDonald, B. A, Nunez, A, Lu, S, Rasmussen, J. B, & Friesen, T. L. 2009. SnTox3 acts in effector triggered susceptibility to induce disease on wheat carrying the *Snn3* gene. *PLoS Pathogens*, **5**(9), e1000581.

Liu, Z, Zhang, Z, Faris, J. D, Oliver, R. P, Syme, R, McDonald, M. C, McDonald, B. A, Solomon, P. S, Lu, S, Shelver, W. L, *et al.* 2012. The cysteine rich necrotrophic effector SnTox1 produced by *Stagonospora nodorum* triggers susceptibility of wheat lines harboring Snn1. *PLoS Pathogens*, **8**(1), e1002467.

Lo Presti, L, Lanver, D, Schweizer, G, Tanaka, S, Liang, L, Tollot, M, Zuccaro, A, Reissmann, S, & Kahmann, R. 2015. Fungal effectors and plant susceptibility. *Annual Review of Plant Biology*, **66**, 513–545.

Lobley, A, Sadowski, M. I, & Jones, D. T. 2009. pGenTHREADER and pDomTHREADER: new methods for improved protein fold recognition and superfamily discrimination. *Bioinformatics*, **25**(14), 1761–1767.

Lombard, V, Golaconda Ramulu, H, Drula, E, Coutinho, P. M, & Henrissat, B. 2013. The carbohydrate-active enzymes database (CAZy) in 2013. *Nucleic Acids Research*, **42**(D1), D490–D495.

Lombardi, L, Faoro, F, Luti, S, Baccelli, I, Martellini, F, Bernardi, R, Picciarelli, P, Scala, A, & Pazzagli, L. 2013. Differential timing of defense-related responses induced by cerato-platanin and cerato-populin, two non-catalytic fungal elicitors. *Physiologia Plantarum*, **149**(3), 408–421.

Lombardi, R, Circelli, P, Villani, M. E, Buriani, G, Nardi, L, Coppola, V, Bianco, L, Benvenuto, E, Donini, M, & Marusic, C. 2009. High-level HIV-1 Nef transient expression in *Nicotiana benthamiana* using the P19 gene silencing suppressor protein of Artichoke Mottled Crinckle Virus. *BMC Biotechnology*, **9**(1), 96.

Longmuir, A. L, Beech, P. L, & Richardson, M. F. 2017. Draft genomes of two Australian strains of the plant pathogen, *Phytophthora cinnamomi*. *F1000Research*, **6**.

Lozano-Torres, J. L, Wilbers, R. H, Gawronski, P, Boshoven, J. C, Finkers-Tomczak, A, Cordewener, J. H, America, A. H, Overmars, H. A, Van't Klooster, J. W, Baranowski, L, *et al.* 2012. Dual disease resistance mediated by the immune receptor Cf-2 in tomato requires a common virulence target of a fungus and a nematode. *Proceedings of the National Academy of Sciences*, **109**(25), 10119–10124.

Lu, S, Faris, J. D, Sherwood, R, Friesen, T. L, & Edwards, M. C. 2014. A dimeric PR-1-type pathogenesis-related protein interacts with ToxA and potentially mediates ToxA-induced necrosis in sensitive wheat. *Molecular Plant Pathology*, **15**(7), 650–663.

Luderer, R, de Kock, M. J, Dees, R. H, de Wit, P. J, & Joosten, M. H. 2002a. Functional analysis of cysteine residues of ECP elicitor proteins of the fungal tomato pathogen *Cladosporium fulvum*. *Molecular Plant Pathology*, **3**(2), 91–95.

Luderer, R, Takken, F. L, Wit, P. J. d, & Joosten, M. H. 2002b. *Cladosporium fulvum* overcomes Cf-2-mediated resistance by producing truncated AVR2 elicitor proteins. *Molecular microbiology*, **45**(3), 875–884.

Lyu, X, Shen, C, Fu, Y, Xie, J, Jiang, D, Li, G, & Cheng, J. 2015. Comparative genomic and transcriptional analyses of the carbohydrate-active enzymes and secretomes of phytopathogenic fungi reveal their significant roles during infection and development. *Scientific Reports*, **5**, 15565.

Ma, L, Lukasik, E, Gawehns, F, & Takken, F. L. 2012. The use of agroinfiltration for transient expression of plant resistance and fungal effector proteins in *Nicotiana benthamiana* leaves. *Plant Fungal Pathogens: Methods and Protocols*, 61–74.

Ma, Z, Song, T, Zhu, L, Ye, W, Wang, Y, Shao, Y, Dong, S, Zhang, Z, Dou, D, Zheng, X, *et al.* 2015. A *Phytophthora sojae* glycoside hydrolase 12 protein is a major virulence factor during soybean infection and is recognized as a PAMP. *The Plant Cell*, **27**(7), 2057–2072.

Ma, Z, Zhu, L, Song, T, Wang, Y, Zhang, Q, Xia, Y, Qiu, M, Lin, Y, Li, H, Kong, L, *et al.* 2017. A paralogous decoy protects *Phytophthora sojae* apoplastic effector PsXEG1 from a host inhibitor. *Science*, **355**(6326), 710–714.

Maleki, S. S, Mohammadi, K, & Ji, K. S. 2018. Study on factors influencing transformation efficiency in *Pinus massoniana* using *Agrobacterium tumefaciens*. *Plant Cell, Tissue and Organ Culture*, **133**(3), 437–445.

Manning, V. A, Chu, A. L, Steeves, J. E, Wolpert, T. J, & Ciuffetti, L. M. 2009. A host-selective toxin of *Pyrenophora tritici-repentis*, Ptr ToxA, induces photosystem changes and reactive oxygen species accumulation in sensitive wheat. *Molecular Plant-Microbe Interactions*, **22**(6), 665–676.

Marks, C. E, Newbigin, E, & Ladiges, P. Y. 2011. Comparative morphology and phylogeny of *Nicotiana* section *Suaveolentes* (Solanaceae) in Australia and the South Pacific. *Australian Systematic Botany*, **24**(2), 61–86.

Marshall, R, Kombrink, A, Motteram, J, Loza-Reyes, E, Lucas, J, Hammond-Kosack, K. E, Thomma, B. P, & Rudd, J. J. 2011. Analysis of two *in planta* expressed LysM effector homologs from the fungus *Mycosphaerella graminicola* reveals novel functional properties and varying contributions to virulence on wheat. *Plant Physiology*, **156**(2), 756–769.

Massingham, T, & Goldman, N. 2005. Detecting amino acid sites under positive selection and purifying selection. *Genetics*, **169**(3), 1753–1762.

McDonald, B. A, & Linde, C. 2002. Pathogen population genetics, evolutionary potential, and durable resistance. *Annual Review of Phytopathology*, **40**(1), 349–379.

McDonald, M. C, Williams, A. H, Milgate, A, Pattemore, J. A, Solomon, P. S, & Hane, J. K. 2015. Next-generation re-sequencing as a tool for rapid bioinformatic screening of presence and absence of genes and accessory chromosomes across isolates of *Zymoseptoria tritici*. *Fungal Genetics and Biology*, **79**, 71 – 75. *Septoria tritici* blotch disease of wheat: Tools and techniques to study the pathogen *Zymoseptoria tritici*.

McDonald, M. C, Ahren, D, Simpfendorfer, S, Milgate, A, & Solomon, P. S. 2018. The discovery of the virulence gene ToxA in the wheat and barley pathogen *Bipolaris sorokiniana*. *Molecular Plant Pathology*, **19**(2), 432–439.

McDougal, R, Yang, S, Schwelm, A, Stewart, A, & Bradshaw, R. 2011. A novel GFP-based approach for screening biocontrol microorganisms in vitro against *Dothistroma septosporum*. *Journal of Microbiological Methods*, **87**(1), 32–37.

McDowell, J. M. 2013. Genomic and transcriptomic insights into lifestyle transitions of a hemi-biotrophic fungal pathogen. *New Phytologist*, **197**(4), 1032–1034.

Melin, P, Schnürer, J, & Wagner, E. G. H. 2003. Characterization of phiA, a gene essential for phialide development in *Aspergillus nidulans*. *Fungal Genetics and Biology*, **40**(3), 234–241.

Mentlak, T. A, Kombrink, A, Shinya, T, Ryder, L. S, Otomo, I, Saitoh, H, Terauchi, R, Nishizawa, Y, Shibuya, N, Thomma, B. P, *et al.* 2012. Effector-mediated suppression of chitin-triggered immunity by *Magnaporthe oryzae* is necessary for rice blast disease. *The Plant Cell*.

Mesarich, C. H, Griffiths, S. A, van der Burgt, A, Ökmen, B, Beenen, H. G, Etalo, D. W, Joosten, M. H. A. J, & de Wit, P. J. G. M. 2014. Transcriptome sequencing uncovers the *Avr5* avirulence gene of the tomato leaf mold pathogen *Cladosporium fulvum*. *Molecular Plant-Microbe Interactions*, **27**(8), 846–857.

Mesarich, C. H, Stergiopoulos, I, Beenen, H. G, Cordovez, V, Guo, Y, Karimi Jashni, M, Bradshaw, R. E, & Wit, P. J. 2016. A conserved proline residue in Dothideomycete

Avr4 effector proteins is required to trigger a Cf-4-dependent hypersensitive response. *Molecular Plant Pathology*, **17**(1), 84–95.

Mesarich, C. H, Ökmen, B, Rovenich, H, Griffiths, S. A, Wang, C, Karimi Jashni, M, Mihajlovski, A, Collemare, J, Hunziker, L, Deng, C. H, *et al.* 2017. Specific hypersensitive response–associated recognition of new apoplastic effectors from *Cladosporium fulvum* in wild tomato. *Molecular Plant-Microbe Interactions*, **31**(1), 145–162.

Mirzadi Gohari, A, Ware, S. B, Wittenberg, A. H, Mehrabi, R, Ben M'Barek, S, Verstappen, E. C, van der Lee, T. A, Robert, O, Schouten, H. J, de Wit, P. P, *et al.* 2015. Effector discovery in the fungal wheat pathogen *Zymoseptoria tritici*. *Molecular Plant Pathology*, **16**(9), 931–945.

Möller, E, Bahnweg, G, Sandermann, H, & Geiger, H. 1992. A simple and efficient protocol for isolation of high molecular weight DNA from filamentous fungi, fruit bodies, and infected plant tissues. *Nucleic Acids Research*, **20**(22), 6115.

Morin, L, Aveyard, R, Lidbetter, J. R, & Wilson, P. G. 2012. Investigating the host-range of the rust fungus *Puccinia psidii sensu lato* across tribes of the family Myrtaceae present in Australia. *PLoS ONE*, **7**(4), e35434.

Motteram, J, Küfner, I, Deller, S, Brunner, F, Hammond-Kosack, K. E, Nürnberger, T, & Rudd, J. J. 2009. Molecular characterization and functional analysis of MgNLP, the sole NPP1 domain-containing protein, from the fungal wheat leaf pathogen *Mycosphaerella graminicola*. *Molecular Plant-Microbe Interactions*, **22**(7), 790–799.

Mueller, A. N, Ziemann, S, Treitschke, S, Aßmann, D, & Doehlemann, G. 2013. Compatibility in the *Ustilago maydis*–maize interaction requires inhibition of host cysteine proteases by the fungal effector Pit2. *PLoS Pathogens*, **9**(2), e1003177.

Muir, J. A, & Cobb, Jr, F. W. 2005. Infection of radiata and bishop pine by *Mycosphaerella pini* in California. *Canadian Journal of Forest Research*, **35**, 2529–2538.

Mukhtar, M. S, Carvunis, A.-R, Dreze, M, Epple, P, Steinbrenner, J, Moore, J, Tasan, M, Galli, M, Hao, T, Nishimura, M. T, *et al.* 2011. Independently evolved virulence

effectors converge onto hubs in a plant immune system network. *science*, **333**(6042), 596–601.

Nimchuk, Z, Eulgem, T, Holt Iii, B. F, & Dangl, J. L. 2003. Recognition and response in the plant immune system. *Annual Review of genetics*, **37**(1), 579–609.

Noar, R. D, & Daub, M. E. 2016. Transcriptome sequencing of *Mycosphaerella fijiensis* during association with *Musa acuminata* reveals candidate pathogenicity genes. *BMC Genomics*, **17**(1), 690.

Nováková, M, Šašek, V, Trdá, L, Krutinová, H, Mongin, T, Valentová, O, Balesdent, M.-H, Rouxel, T, & Burketová, L. 2016. *Leptosphaeria maculans* effector AvrLm4-7 affects SA-and ET-signalling and H_2O_2 accumulation in *Brassica napus*. *Molecular Plant Pathology*, **17**(6), 818–831.

O'Connell, R. J, Thon, M. R, Hacquard, S, Amyotte, S. G, Kleemann, J, Torres, M. F, Damm, U, Buiate, E. A, Epstein, L, Alkan, N, *et al.* 2012. Lifestyle transitions in plant pathogenic *Colletotrichum* fungi deciphered by genome and transcriptome analyses. *Nature Genetics*, **44**(9), 1060.

Oh, C.-S, Pedley, K. F, & Martin, G. B. 2010. Tomato 14-3-3 protein 7 positively regulates immunity-associated programmed cell death by enhancing protein abundance and signaling ability of MAPKKK α. *The Plant Cell*, **22**(1), 260–272.

Ohm, R. A, Feau, N, Henrissat, B, Schoch, C. L, Horwitz, B. A, Barry, K. W, Condon, B. J, Copeland, A. C, Dhillon, B, Glaser, F, *et al.* 2012. Diverse lifestyles and strategies of plant pathogenesis encoded in the genomes of eighteen Dothideomycetes fungi. *PLoS Pathogens*, **8**(12), e1003037.

Ökmen, B, & Doehlemann, G. 2014. Inside plant: biotrophic strategies to modulate host immunity and metabolism. *Current Opinion in Plant Biology*, **20**, 19–25.

Ökmen, B, Etalo, D. W, Joosten, M. H, Bouwmeester, H. J, Vos, R. C, Collemare, J, & de Wit, P. J. 2013. Detoxification of α-tomatine by *Cladosporium fulvum* is required for full virulence on tomato. *New Phytologist*, **198**(4), 1203–1214.

O'Leary, B. M, Rico, A, McCraw, S, Fones, H. N, & Preston, G. M. 2014. The infiltration-centrifugation technique for extraction of apoplastic fluid from plant leaves using *Phaseolus vulgaris* as an example. *Journal of Visualized Experiments: JoVE*.

Oliver, R. P, & Solomon, P. S. 2010. New developments in pathogenicity and virulence of necrotrophs. *Current Opinion in Plant Biology*, **13**(4), 415–419.

Oliver, R. P, Friesen, T. L, Faris, J. D, & Solomon, P. S. 2012. Stagonospora nodorum: from pathology to genomics and host resistance. *Annual Review of Phytopathology*, **50**, 23–43.

Olmstead, R. G, Bohs, L, Migid, H. A, Santiago-Valentin, E, Garcia, V. F, & Collier, S. M. 2008. A molecular phylogeny of the Solanaceae. *Taxon*, **57**(4), 1159–1181.

Oome, S, Raaymakers, T. M, Cabral, A, Samwel, S, Böhm, H, Albert, I, Nürnberger, T, & van den Ackerveken, G. 2014. Nep1-like proteins from three kingdoms of life act as a microbe-associated molecular pattern in *Arabidopsis*. *Proceedings of the National Academy of Sciences*, **111**(47), 16955–16960.

Opabode, J. T. 2006. *Agrobacterium*-mediated transformation of plants: emerging factors that influence efficiency. *Biotechnology and Molecular Biology Reviews*, **1**(1), 12–20.

Ottmann, C, Luberacki, B, Küfner, I, Koch, W, Brunner, F, Weyand, M, Mattinen, L, Pirhonen, M, Anderluh, G, Seitz, H. U, *et al.* 2009. A common toxin fold mediates microbial attack and plant defense. *Proceedings of the National Academy of Sciences*, **106**(25), 10359–10364.

Ozturk, I. K. 2016. *Secondary metabolism of the forest pathogen Dothistroma septosporum*. Ph.D. thesis, Massey University, Palmerston North, New Zealand.

Park, C.-H, Chen, S, Shirsekar, G, Zhou, B, Khang, C. H, Songkumarn, P, Afzal, A. J, Ning, Y, Wang, R, Bellizzi, M, *et al.* 2012. The *Magnaporthe oryzae* effector AvrPiz-t targets the RING E3 Ubiquitin Ligase APIP6 to suppress pathogen-associated molecular pattern–triggered immunity in rice. *The Plant Cell*, **24**(11), 4748–4762.

Paulus, J. K, Kourelis, J, & van der Hoorn, R. A. 2017. Bodyguards: pathogen-derived decoys that protect virulence factors. *Trends in Plant Science*, **22**(5), 355–357.

Pazzagli, L, Cappugi, G, Manao, G, Camici, G, Santini, A, & Scala, A. 1999. Purification, characterization, and amino acid sequence of cerato-platanin, a new phytotoxic protein from *Ceratocystis fimbriata f. sp. platani*. *Journal of Biological Chemistry*, **274**(35), 24959–24964.

Pazzagli, L, Seidl-Seiboth, V, Barsottini, M, Vargas, W. A, Scala, A, & Mukherjee, P. K. 2014. Cerato-platanins: elicitors and effectors. *Plant Science*, **228**, 79–87.

Peterson, G. W, Walla, J. A, *et al.* 1978. Development of *Dothistroma pini* upon and within needles of Austrian and ponderosa pines in eastern Nebraska. *Phytopathology*, **68**(10), 1422–1430.

Petre, B, & Kamoun, S. 2014. How do filamentous pathogens deliver effector proteins into plant cells? *PLoS Biology*, **12**(2), e1001801.

Piou, D, & Ioos, R. 2013. First report of *Dothistroma pini*, a recent agent of the Dothistroma needle blight, on *Pinus radiata* in France. *Plant Disease*, **98**(6), 841.

Plett, J. M, & Martin, F. M. 2018. Know your enemy, embrace your friend: using omics to understand how plants respond differently to pathogenic and mutualistic microorganisms. *The Plant Journal*.

Plett, J. M, Daguerre, Y, Wittulsky, S, Vayssières, A, Deveau, A, Melton, S. J, Kohler, A, Morrell-Falvey, J. L, Brun, A, Veneault-Fourrey, C, *et al.* 2014. Effector MiSSP7 of the mutualistic fungus *Laccaria bicolor* stabilizes the Populus JAZ6 protein and represses jasmonic acid (JA) responsive genes. *Proceedings of the National Academy of Sciences*, 201322671.

Polyakova, G, Pashenova, N, Polyakov, V, & Zrazhevskaya, G. 2008. Induction of conifer immune responses by phytopathogenic fungus metabolites. *Russian Journal of Plant Physiology*, **55**(4), 496–502.

Postma, J, Liebrand, T. W, Bi, G, Evrard, A, Bye, R. R, Mbengue, M, Kuhn, H, Joosten, M. H, & Robatzek, S. 2016. Avr4 promotes Cf-4 receptor-like protein association with the BAK1/SERK3 receptor-like kinase to initiate receptor endocytosis and plant immunity. *New Phytologist*, **210**(2), 627–642.

Prokchorchik, M. 2017. *Molecular analysis of plant innate immunity triggered by secreted effectors from bacterial and fungal pathogens of apple.* Ph.D. thesis, Massey University, Palmerston North, New Zealand.

Qu, F, & Morris, T. J. 2002. Efficient infection of *Nicotiana benthamiana* by Tomato bushy stunt virus is facilitated by the coat protein and maintained by p19 through suppression of gene silencing. *Molecular Plant-Microbe Interactions*, **15**(3), 193–202.

Quarantin, A, Glasenapp, A, Schäfer, W, Favaron, F, & Sella, L. 2016. Involvement of the *Fusarium graminearum* cerato-platanin proteins in fungal growth and plant infection. *Plant Physiology and Biochemistry*, **109**, 220–229.

Quinlan, A. R. 2014. BEDTools: the Swiss-army tool for genome feature analysis. *Current Protocols in Bioinformatics*, 11–12.

Quinlan, A. R, & Hall, I. M. 2010. BEDTools: a flexible suite of utilities for comparing genomic features. *Bioinformatics*, **26**(6), 841–842.

Quoirin, M, & Lepoivre, P. 1977. Improved media for in vitro culture of *Prunus* sp. *Pages 437–442 of: Symposium on Tissue Culture for Horticultural Purposes 78.*

Raffaello, T, & Asiegbu, F. O. 2017. Small secreted proteins from the necrotrophic conifer pathogen *Heterobasidion annosum sl* (HaSSPs) induce cell death in *Nicotiana benthamiana*. *Scientific Reports*, **7**.

Ravensdale, M, Nemri, A, Thrall, P. H, Ellis, J. G, & Dodds, P. N. 2011. Co-evolutionary interactions between host resistance and pathogen effector genes in flax rust disease. *Molecular Plant Pathology*, **12**(1), 93–102.

Rep, M. 2005. Small proteins of plant-pathogenic fungi secreted during host colonization. *FEMS Microbiology Letters*, **253**(1), 19–27.

Robin, G. P, Kleemann, J, Neumann, U, Cabre, L, Dallery, J.-F, Lapalu, N, & O'Connell, R. J. 2018. Subcellular localization screening of *Colletotrichum higginsianum* effector candidates identifies fungal proteins targeted to plant peroxisomes, Golgi bodies and microtubules. *Frontiers in Plant Science*, **9**, 562.

Rooney, H. C. E, van't Klooster, J. W, van der Hoorn, R. A. L, Joosten, M. H. A. J, Jones, J. D. G, & de Wit, P. J. G. M. 2005. *Cladosporium* Avr2 inhibits tomato Rcr3 protease required for Cf-2-dependent disease resistance. *Science*, **308**(5729), 1783–1786.

Rose, J. K, Ham, K.-S, Darvill, A. G, & Albersheim, P. 2002. Molecular cloning and characterization of glucanase inhibitor proteins: coevolution of a counterdefense mechanism by plant pathogens. *The Plant Cell*, **14**(6), 1329–1345.

RStudio Team. 2016. *RStudio: Integrated Development Environment for R.* RStudio, Inc., Boston, MA.

Ruocco, M, Lanzuise, S, Lombardi, N, Woo, S. L, Vinale, F, Marra, R, Varlese, R, Manganiello, G, Pascale, A, Scala, V, *et al.* 2015. Multiple roles and effects of a novel *Trichoderma* hydrophobin. *Molecular Plant-Microbe Interactions*, **28**(2), 167–179.

Ryals, J. A, Neuenschwander, U. H, Willits, M. G, Molina, A, Steiner, H.-Y, & Hunt, M. D. 1996. Systemic acquired resistance. *The Plant Cell*, **8**(10), 1809.

Sambrook, J, Fritsch, E. F, Maniatis, T, *et al.* 1989. *Molecular cloning: a laboratory manual.* Cold spring harbor laboratory press.

Sánchez-Rangel, D, Sánchez-Nieto, S, & Plasencia, J. 2012. Fumonisin B1, a toxin produced by *Fusarium verticillioides*, modulates maize β-1, 3-glucanase activities involved in defense response. *Planta*, **235**(5), 965–978.

Sánchez-Vallet, A, Saleem-Batcha, R, Kombrink, A, Hansen, G, Valkenburg, D.-J, Thomma, B. P, & Mesters, J. R. 2013. Fungal effector Ecp6 outcompetes host immune receptor for chitin binding through intrachain LysM dimerization. *elife*, **2**, e00790.

Schneider, C. A, Rasband, W. S, & Eliceiri, K. W. 2012. NIH Image to ImageJ: 25 years of image analysis. *Nature Methods*, **9**(7), 671.

Schoettle, A, Sniezko, R, Kegley, A, & Burns, K. 2014. White pine blister rust resistance in limber pine: evidence for a major gene. *Phytopathology*, **104**(2), 163–173.

Schwelm, A, Barron, N, Baker, J, Dick, M, Long, P, Zhang, S, & Bradshaw, R. 2009. Dothistromin toxin is not required for Dothistroma needle blight in *Pinus radiata*. *Plant pathology*, **58**(2), 293–304.

Scott, B, Green, K, & Berry, D. 2018. The fine balance between mutualism and antagonism in the *Epichloë festucae*–grass symbiotic interaction. *Current Opinion in Plant Biology*, **44**, 32–38.

Scott, P, & Williams, N. 2014. Phytophthora diseases in New Zealand forests. *NZ Journal of Forestry*, **59**(2), 15.

Shabab, M, Shindo, T, Gu, C, Kaschani, F, Pansuriya, T, Chintha, R, Harzen, A, Colby, T, Kamoun, S, & van der Hoorn, R. A. 2008. Fungal effector protein AVR2 targets diversifying defense-related cys proteases of tomato. *The Plant Cell*, **20**(4), 1169–1183.

Shain, L, & Franich, R. A. 1981. Induction of Dothistroma blight symptoms with dothistromin. *Physiological Plant Pathology*, **19**, 49–55.

Sharpee, W, Oh, Y, Yi, M, Franck, W, Eyre, A, Okagaki, L. H, Valent, B, & Dean, R. A. 2017. Identification and characterization of suppressors of plant cell death (SPD) effectors from *Magnaporthe oryzae*. *Molecular Plant Pathology*, **18**(6), 850–863.

Sievers, F, Wilm, A, Dineen, D, Gibson, T. J, Karplus, K, Li, W, Lopez, R, McWilliam, H, Remmert, M, Söding, J, *et al.* 2011. Fast, scalable generation of high-quality protein multiple sequence alignments using Clustal Omega. *Molecular Systems Biology*, **7**(1), 539.

Sniezko, R. A, Smith, J, Liu, J.-J, & Hamelin, R. C. 2014. Genetic resistance to fusiform rust in southern pines and white pine blister rust in white pines—a contrasting tale of two rust pathosystems—current status and future prospects. *Forests*, **5**(9), 2050–2083.

Söding, J. 2004. Protein homology detection by HMM–HMM comparison. *Bioinformatics*, **21**(7), 951–960.

Song, J, Win, J, Tian, M, Schornack, S, Kaschani, F, Ilyas, M, van der Hoorn, R. A, & Kamoun, S. 2009. Apoplastic effectors secreted by two unrelated eukaryotic plant pathogens target the tomato defense protease Rcr3. *Proceedings of the National Academy of Sciences*, **106**(5), 1654–1659.

Sperschneider, J, Dodds, P. N, Gardiner, D. M, Manners, J. M, Singh, K. B, & Taylor, J. M. 2015. Advances and challenges in computational prediction of effectors from plant pathogenic fungi. *PLoS Pathogens*, **11**(5), e1004806.

Sperschneider, J, Gardiner, D. M, Dodds, P. N, Tini, F, Covarelli, L, Singh, K. B, Manners, J. M, & Taylor, J. M. 2016. EffectorP: predicting fungal effector proteins from secretomes using machine learning. *New Phytologist*, **210**(2), 743–761.

Sperschneider, J, Dodds, P. N, Singh, K. B, & Taylor, J. M. 2017. ApoplastP: prediction of effectors and plant proteins in the apoplast using machine learning. *bioRxiv*, 182428.

Sperschneider, J, Dodds, P. N, Gardiner, D. M, Singh, K. B, & Taylor, J. M. 2018. Improved prediction of fungal effector proteins from secretomes with EffectorP 2.0. *Molecular Plant Pathology*, **19**(9), 2094–2110.

Spoel, S. H, & Dong, X. 2012. How do plants achieve immunity? Defence without specialized immune cells. *Nature Reviews Immunology*, **12**(2), 89.

Stergiopoulos, I, de Kock, M. J, Lindhout, P, & de Wit, P. J. 2007. Allelic variation in the effector genes of the tomato pathogen *Cladosporium fulvum* reveals different modes of adaptive evolution. *Molecular Plant-Microbe Interactions*, **20**(10), 1271–1283.

Stergiopoulos, I, van den Burg, H. A, Ökmen, B, Beenen, H. G, van Liere, S, Kema, G. H, & de Wit, P. J. 2010. Tomato Cf resistance proteins mediate recognition of cognate homologous effectors from fungi pathogenic on dicots and monocots. *Proceedings of the National Academy of Sciences*, **107**(16), 7610–7615.

Stergiopoulos, I, Cordovez, V, Ökmen, B, Beenen, H. G, Kema, G. H, & de Wit, P. J. 2014. Positive selection and intragenic recombination contribute to high allelic diversity in effector genes of *Mycosphaerella fijiensis*, causal agent of the black leaf streak disease of banana. *Molecular Plant Pathology*, **15**(5), 447–460.

Stewart, J. E, Kim, M.-S, & Klopfenstein, N. B. 2018. Molecular genetic approaches toward understanding forest-associated fungi and their interactive roles within forest ecosystems. *Current Forestry Reports*, **4**(2), 72–84.

Storey, J. D, *et al.* 2003. The positive false discovery rate: a Bayesian interpretation and the q-value. *The Annals of Statistics*, **31**(6), 2013–2035.

Sunde, M, Pham, C. L, & Kwan, A. H. 2017. Molecular characteristics and biological functions of surface-active and surfactant proteins. *Annual Review of biochemistry*, **86**, 585–608.

Talbot, N. J, Ebbole, D. J, & Hamer, J. E. 1993. Identification and characterization of MPG1, a gene involved in pathogenicity from the rice blast fungus *Magnaporthe grisea*. *The Plant Cell*, **5**(11), 1575–1590.

Tanaka, S, Brefort, T, Neidig, N, Djamei, A, Kahnt, J, Vermerris, W, Koenig, S, Feussner, K, Feussner, I, & Kahmann, R. 2014. A secreted *Ustilago maydis* effector promotes virulence by targeting anthocyanin biosynthesis in maize. *Elife*, **3**, e01355.

Tang, W, & Newton, R. 2003. Genetic transformation of conifers and its application in forest biotechnology. *Plant Cell Reports*, **22**(1), 1–15.

Tang, W, Xiao, B, & Fei, Y. 2014. Slash pine genetic transformation through embryo cocultivation with *A. tumefaciens* and transgenic plant regeneration. *In Vitro Cellular & Developmental Biology-Plant*, **50**(2), 199–209.

Taylor, R. G, Walker, D. C, & McInnes, R. 1993. *E. coli* host strains significantly affect the quality of small scale plasmid DNA preparations used for sequencing. *Nucleic Acids Research*, **21**(7), 1677.

Thomma, B. P. H. J, Nürnberger, T, & Joosten, M. H. A. J. 2011. Of PAMPs and effectors: the blurred PTI-ETI dichotomy. *The Plant Cell Online*, **23**(1), 4–15.

Thomma, B. P, van Esse, H. P, Crous, P. W, & de Wit, P. J. 2005. *Cladosporium fulvum* (syn. *Passalora fulva*), a highly specialized plant pathogen as a model for functional

studies on plant pathogenic Mycosphaerellaceae. *Molecular Plant Pathology*, **6**(4), 379–393.

Tian, M, Win, J, Song, J, van der Hoorn, R, van der Knaap, E, & Kamoun, S. 2007. A *Phytophthora infestans* cystatin-like protein targets a novel tomato papain-like apoplastic protease. *Plant Physiology*, **143**(1), 364–377.

Torres, M. A, Jones, J. D, & Dangl, J. L. 2005. Pathogen-induced, NADPH oxidase–derived reactive oxygen intermediates suppress spread of cell death in *Arabidopsis thaliana*. *Nature Genetics*, **37**(10), 1130.

Tsuge, T, Harimoto, Y, Akimitsu, K, Ohtani, K, Kodama, M, Akagi, Y, Egusa, M, Yamamoto, M, & Otani, H. 2012. Host-selective toxins produced by the plant pathogenic fungus *Alternaria alternata*. *FEMS Microbiology Reviews*, **37**(1), 44–66.

Untergasser, A, Cutcutache, I, Koressaar, T, Ye, J, Faircloth, B. C, Remm, M, & Rozen, S. G. 2012. Primer3—new capabilities and interfaces. *Nucleic Acids Research*, **40**(15), e115–e115.

van den Burg, H. A, Westerink, N, Francoijs, K.-J, Roth, R, Woestenenk, E, Boeren, S, de Wit, P. J, Joosten, M. H, & Vervoort, J. 2003. Natural disulfide bond-disrupted mutants of AVR4 of the tomato pathogen *Cladosporium fulvum* are sensitive to proteolysis, circumvent Cf-4-mediated resistance, but retain their chitin binding ability. *Journal of Biological Chemistry*, **278**(30), 27340–27346.

van den Burg, H. A, Harrison, S. J, Joosten, M. H, Vervoort, J, & de Wit, P. J. 2006. *Cladosporium fulvum* Avr4 protects fungal cell walls against hydrolysis by plant chitinases accumulating during infection. *Molecular Plant-Microbe Interactions*, **19**(12), 1420–1430.

van der Hoorn, R. A. L, & Kamoun, S. 2008. From guard to decoy: a new model for perception of plant pathogen effectors. *The Plant Cell Online*, **20**(8), 2009–2017.

van der Hoorn, R. A. L, Laurent, F, Roth, R, & de Wit, P. J. G. M. 2000. Agroinfiltration is a versatile tool that facilitates comparative analyses of Avr9/Cf-9-induced and Avr4/Cf-4-induced necrosis. *Molecular Plant-Microbe Interactions*, **13**(4), 439–446.

van Esse, H. P, Bolton, M. D, Stergiopoulos, I, de Wit, P. J, & Thomma, B. P. 2007. The chitin-binding *Cladosporium fulvum* effector protein Avr4 is a virulence factor. *Molecular Plant-Microbe Interactions*, **20**(9), 1092–1101.

Vargas, W. A, Djonović, S, Sukno, S. A, & Kenerley, C. M. 2008. Dimerization controls the activity of fungal elicitors that trigger systemic resistance in plants. *Journal of Biological Chemistry*, **283**(28), 19804–19815.

Veena, Jiang, H, Doerge, R, & Gelvin, S. B. 2003. Transfer of T-DNA and Vir proteins to plant cells by *Agrobacterium tumefaciens* induces expression of host genes involved in mediating transformation and suppresses host defense gene expression. *The Plant Journal*, **35**(2), 219–236.

Veluthakkal, R, & Dasgupta, M. G. 2010. Pathogenesis-related genes and proteins in forest tree species. *Trees*, **24**(6), 993–1006.

Videira, S, Groenewald, J, Nakashima, C, Braun, U, Barreto, R. W, de Wit, P. J, & Crous, P. 2017. Mycosphaerellaceae–Chaos or clarity? *Studies in mycology*, **87**, 257–421.

Vleeshouwers, V. G. A. A, & Oliver, R. P. 2014. Effectors as tools in disease resistance breeding against biotrophic, hemibiotrophic, and necrotrophic plant pathogens. *Molecular Plant-Microbe Interactions*, **27**(3), 196–206.

Wahl, R, Wippel, K, Goos, S, Kämper, J, & Sauer, N. 2010. A novel high-affinity sucrose transporter is required for virulence of the plant pathogen *Ustilago maydis*. *PLoS Biology*, **8**(2), e1000303.

Wallis, C, Eyles, A, Chorbadjian, R, Gardener, B. M, Hansen, R, Cipollini, D, Herms, D, & Bonello, P. 2008. Systemic induction of phloem secondary metabolism and its relationship to resistance to a canker pathogen in Austrian pine. *New Phytologist*, **177**(3), 767–778.

Wang, B, Yang, X, Zeng, H, Liu, H, Zhou, T, Tan, B, Yuan, J, Guo, L, & Qiu, D. 2012. The purification and characterization of a novel hypersensitive-like response-inducing elicitor from *Verticillium dahliae* that induces resistance responses in tobacco. *Applied Microbiology and Biotechnology*, **93**(1), 191–201.

Wang, M, Weiberg, A, & Jin, H. 2015. Pathogen small RNAs: a new class of effectors for pathogen attacks. *Molecular Plant Pathology*, **16**(3), 219–223.

Wang, M, Weiberg, A, Dellota Jr, E, Yamane, D, & Jin, H. 2017a. *Botrytis* small RNA Bc-siR37 suppresses plant defense genes by cross-kingdom RNAi. *RNA Biology*, **14**(4), 421–428.

Wang, X, & Bennetzen, J. L. 2015. Current status and prospects for the study of *Nicotiana* genomics, genetics, and nicotine biosynthesis genes. *Molecular Genetics and Genomics*, **290**(1), 11–21.

Wang, Y, Xu, Y, Sun, Y, Wang, H, Qi, J, Wan, B, Ye, W, Lin, Y, Shao, Y, Dong, S, *et al.* 2018. Leucine-rich repeat receptor-like gene screen reveals that *Nicotiana* RXEG1 regulates glycoside hydrolase 12 MAMP detection. *Nature Communications*, **9**(1), 594.

Wang, Z, Han, Q, Zi, Q, Lv, S, Qiu, D, & Zeng, H. 2017b. Enhanced disease resistance and drought tolerance in transgenic rice plants overexpressing protein elicitors from *Magnaporthe oryzae*. *PLoS ONE*, **12**(4), e0175734.

Watt, M. S, Kriticos, D. J, Alcaraz, S, Brown, A. V, & Leriche, A. 2009. The hosts and potential geographic range of Dothistroma needle blight. *Forest Ecology and Management*, **257**(6), 1505–1519.

Watt, M. S, Palmer, D. J, & Bulman, L. S. 2011. Predicting the severity of *Dothistroma* on *Pinus radiata* under current climate in New Zealand. *Forest Ecology and Management*, **261**(11), 1792–1798.

Wawra, S, Fesel, P, Widmer, H, Timm, M, Seibel, J, Leson, L, Kesseler, L, Nostadt, R, Hilbert, M, Langen, G, *et al.* 2016. The fungal-specific β-glucan-binding lectin FGB1 alters cell-wall composition and suppresses glucan-triggered immunity in plants. *Nature Communications*, **7**, 13188.

Wei, C.-F, Kvitko, B. H, Shimizu, R, Crabill, E, Alfano, J. R, Lin, N.-C, Martin, G. B, Huang, H.-C, & Collmer, A. 2007. A *Pseudomonas syringae* pv. *tomato* DC3000 mutant lacking the type III effector HopQ1-1 is able to cause disease in the model plant *Nicotiana benthamiana*. *The Plant Journal*, **51**(1), 32–46.

Weiberg, A, Bellinger, M, & Jin, H. 2015. Conversations between kingdoms: small RNAs. *Current Opinion In Biotechnology*, **32C**(Jan.), 207–215.

Welsh, C, Lewis, K, & Woods, A. 2009. The outbreak history of Dothistroma needle blight: an emerging forest disease in northwestern British Columbia, Canada. *Canadian Journal of Forest Research*, **39**(12), 2505–2519.

Welsh, C, Lewis, K. J, & Woods, A. J. 2014. Regional outbreak dynamics of Dothistroma needle blight linked to weather patterns in British Columbia, Canada. *Canadian Journal of Forest Research*, **44**, 212–219.

Wessels, J. 1994. Developmental regulation of fungal cell wall formation. *Annual Review of Phytopathology*, **32**(1), 413–437.

Wingfield, M, Brockerhoff, E, Wingfield, B. D, & Slippers, B. 2015. Planted forest health: the need for a global strategy. *Science*, **349**(6250), 832–836.

Woods, A, Martín-García, J, Bulman, L, Vasconcelos, M. W, Boberg, J, La Porta, N, Peredo, H, Vergara, G, Ahumada, R, Brown, A, *et al.* 2016. Dothistroma needle blight, weather and possible climatic triggers for the disease's recent emergence. *Forest Pathology*, **46**(5), 443–452.

Wösten, H, Schuren, F, & Wessels, J. 1994. Interfacial self-assembly of a hydrophobin into an amphipathic protein membrane mediates fungal attachment to hydrophobic surfaces. *The EMBO Journal*, **13**(24), 5848–5854.

Wösten, H. A, & Scholtmeijer, K. 2015. Applications of hydrophobins: current state and perspectives. *Applied Microbiology and Biotechnology*, **99**(4), 1587–1597.

Wösten, H. A, van Wetter, M.-A, Lugones, L. G, van der Mei, H. C, Busscher, H. J, & Wessels, J. G. 1999. How a fungus escapes the water to grow into the air. *Current Biology*, **9**(2), 85–88.

Wu, C.-H, Derevnina, L, & Kamoun, S. 2018. Receptor networks underpin plant immunity. *Science*, **360**(6395), 1300–1301.

Xiang, C, Han, P, Lutziger, I, Wang, K, & Oliver, D. J. 1999. A mini binary vector series for plant transformation. *Plant Molecular Biology*, **40**(4), 711–717.

Xue, B, Dunker, A. K, & Uversky, V. N. 2012. Orderly order in protein intrinsic disorder distribution: disorder in 3500 proteomes from viruses and the three domains of life. *Journal of Biomolecular Structure and Dynamics*, **30**(2), 137–149.

Yang, G, Tang, L, Gong, Y, Xie, J, Fu, Y, Jiang, D, Li, G, Collinge, D. B, Chen, W, & Cheng, J. 2018. A cerato-platanin protein SsCP1 targets plant PR1 and contributes to virulence of *Sclerotinia sclerotiorum*. *New Phytologist*, **217**(2), 739–755.

Yang, J, Yan, R, Roy, A, Xu, D, Poisson, J, & Zhang, Y. 2015. The I-TASSER Suite: protein structure and function prediction. *Nature Methods*, **12**(1), 7.

Yang, Y, Zhang, H, Li, G, Li, W, Wang, X, & Song, F. 2009. Ectopic expression of MgSM1, a Cerato-platanin family protein from *Magnaporthe grisea*, confers broad-spectrum disease resistance in *Arabidopsis*. *Plant Biotechnology Journal*, **7**(8), 763–777.

Yang, Z. 2007. PAML 4: phylogenetic analysis by maximum likelihood. *Molecular Biology and Evolution*, **24**(8), 1586–1591.

Yoshino, K, Irieda, H, Sugimoto, F, Yoshioka, H, Okuno, T, & Takano, Y. 2012. Cell death of *Nicotiana benthamiana* is induced by secreted protein NIS1 of *Colletotrichum orbiculare* and is suppressed by a homologue of CgDN3. *Molecular Plant-Microbe Interactions*, **25**(5), 625–636.

Youngman, R. J, & Elstner, E. 1984. Photodynamic and reductive mechanisms of oxygen activation by the fungal phytotoxins, cercosporin and dothistromin. *In: Oxygen radicals in chemistry and biology: proceedings/third international conference, Neuherberg, Federal Republic of Germany, July 10-15, 1983; editors, W. Bors, M. Saran, D. Tait.* Berlin [W. Ger.]: W. de Gruyter, c1984.

Zhang, W.-J, Pedersen, C, Kwaaitaal, M, Gregersen, P. L, Mørch, S. M, Hanisch, S, Kristensen, A, Fuglsang, A. T, Collinge, D. B, & Thordal-Christensen, H. 2012. Interaction of barley powdery mildew effector candidate CSEP0055 with the defence protein PR17c. *Molecular Plant Pathology*, **13**(9), 1110–1119.

Zhang, Y, Liang, Y, Dong, Y, Gao, Y, Yang, X, Yuan, J, & Qiu, D. 2017a. The *Magnaporthe oryzae* Alt A 1-like protein MoHrip1 binds to the plant plasma membrane. *Biochemical and biophysical research communications*, **492**(1), 55–60.

Zhang, Y, Gao, Y, Liang, Y, Dong, Y, Yang, X, Yuan, J, & Qiu, D. 2017b. The *Verticillium dahliae* SnodProt1-like protein VdCP1 contributes to virulence and triggers the plant immune system. *Frontiers in Plant Science*, **8**, 1880.

Zhou, R, Zhu, T, Han, L, Liu, M, Xu, M, Liu, Y, Han, D, Qiu, D, Gong, Q, & Liu, X. 2017. The asparagine-rich protein NRP interacts with the *Verticillium* effector PevD1 and regulates the subcellular localization of cryptochrome 2. *Journal of Experimental Botany*, **68**(13), 3427–3440.

Ziemienowicz, A. 2014. Agrobacterium-mediated plant transformation: factors, applications and recent advances. *Biocatalysis and Agricultural Biotechnology*, **3**(4), 95–102.

Zimmermann, L, Stephens, A, Nam, S.-Z, Rau, D, Kübler, J, Lozajic, M, Gabler, F, Söding, J, Lupas, A. N, & Alva, V. 2018. A completely reimplemented mPI bioinformatics toolkit with a new HHpred server at its core. *Journal of molecular biology*, **430**(15), 2237–2243.